

Metallurgy of Welding

Third Edition

J. F. Lancaster

METALLURGY OF WELDING

Metallurgy of Welding

J. F. LANCASTER

London

GEORGE ALLEN & UNWIN

Boston

Sydney

First published as Metallurgy of welding, brazing and soldering
in 1965

Third edition 1980

This book is copyright under the Berne Convention. All rights are reserved. Apart from any fair dealing for the purpose of private study, research, criticism or review, as permitted under the Copyright Act, 1956, no part of this publication may be reproduced, stored in a retrieval system, or transmitted, in any form or by any means, electronic, electrical, chemical, mechanical, optical, photocopying, recording or otherwise, without the prior permission of the copyright owner. Enquiries should be sent to the publishers at the undermentioned address:

GEORGE ALLEN & UNWIN LTD
40 Museum Street, London WC1A 1LU

© J. F. Lancaster, 1980

Softcover reprint of the hardcover 1st edition 1980

British Library Cataloguing in Publication Data

Lancaster, John Frederick

Metallurgy of welding. — 2nd ed.

1. Welding

2. Solder and soldering

3. Brazing

**I. Title II. Metallurgy of welding, brazing
and soldering**

671.5

TS227

ISBN 978-94-010-9508-2

ISBN 978-94-010-9506-8 (eBook)

DOI 10.1007/978-94-010-9506-8

Typeset in 10 on 12 point Times by Alden Press Ltd.

Preface

This book is intended, like its predecessor (*The metallurgy of welding, brazing and soldering*), to provide a textbook for undergraduate and postgraduate students concerned with welding, and for candidates taking the Welding Institute examinations. At the same time, it may prove useful to practising engineers, metallurgists and welding engineers in that it offers a resumé of information on welding metallurgy together with some material on the engineering problems associated with welding such as reliability and risk analysis.

In certain areas there have been developments that necessitated complete re-writing of the previous text. Thanks to the author's colleagues in Study Group 212 of the International Institute of Welding, understanding of mass flow in fusion welding has been radically transformed. Knowledge of the metallurgy of carbon and ferritic alloy steel, as applied to welding, has continued to advance at a rapid pace, while the literature on fracture mechanics accumulates at an even greater rate. In other areas, the welding of non-ferrous metals for example, there is little change to report over the last decade, and the original text of the book is only slightly modified. In those fields where there has been significant advance, the subject has become more quantitative and the standard of mathematics required for a proper understanding has been raised. Mass flow in welding, for example, is not comprehensible without some knowledge of fluid dynamics, and fluid dynamics in turn is not comprehensible without a knowledge of vector analysis. In this and in other ways, welding technology will in the future, as it advances from a workshop subject to a full-fledged branch of engineering, demand higher standards of academic achievement from its students.

SI units are used throughout the book and a list of conversion factors is to be found in Appendix 2. Symbols are standardised so far as practicable and are listed in Appendix 1. The American Welding Society designations for welding processes have been used, although it is realised that in Europe (including the United Kingdom) there is a general preference for the older terms, TIG as opposed to GTA, for example. The AWS terms have been employed because they are more precise, have been standardised for a wider range of processes, and because AWS practice finds increasing acceptance internationally, particularly in the oil, gas, petroleum and petrochemical industries, where welding is a key process in the manufacture of plant and equipment.

The author is glad to have the opportunity to thank Professor R. L. Apps, Professor C. E. Jackson and Dr. M. F. Jordan, for undertaking the onerous task

of reading and commenting on the first draft of this book. The majority of the comments thus received were incorporated into the final text, thereby much improving its quality.

J. F. Lancaster

Contents

<i>PREFACE</i>	<i>Page vii</i>
CHAPTER 1 <i>INTRODUCTORY</i>	1
1.1 Welding in ancient and medieval times	1
1.2 The advent of fusion welding	2
1.3 The theory of metal joining techniques	4
1.4 Welding engineering	4
CHAPTER 2 <i>PROCESSES AND TYPES OF JOINT</i>	6
2.1 The general character of welding, brazing, soldering and adhesive jointing	6
2.2 The nature of welding processes	6
2.2.1 The classification of fusion welding processes	7
2.2.2 Heat source intensity	7
2.2.3 Heat input rate	13
2.2.4 Shielding methods	14
2.3 Types of fusion welded joint	16
CHAPTER 3 <i>MASS AND HEAT FLOW IN WELDING</i>	19
3.1 General	19
3.2 Mass flow: general	20
3.3 Mass flow from the electrode to the workpiece	21
3.3.1 The pinch instability	22
3.3.2 Other modes of instability	26
3.4 Mass flow in the weld pool	29
3.5 Heat flow: general	31
3.5.1 Heat sources	31
3.5.2 The welding arc	32
3.5.2.1 Electrode interactions	33
3.5.2.2 The arc column	35
3.5.3 Heat flow in the electrode	39
3.5.3.1 Time-dependent heat flow	39
3.5.4 Heat flow in the weld pool	41
3.5.5 Heat flow in the solid workpiece: theory	41
3.5.6 Heat flow in the solid workpiece: experimental	45
CHAPTER 4 <i>METALLURGICAL EFFECTS OF THE WELD THERMAL CYCLE</i>	51
4.1 Metallurgical effects in the weld metal	51
4.1.1 Gas-metal reactions	51
4.1.1.1 Absorption	52
4.1.1.2 Reaction	53
4.1.1.3 Evolution	55

4.1.2	Dilution and uniformity of the weld deposit	58
4.1.3	Weld pool solidification	59
4.1.4	Weld cracking	63
4.1.4.1	Supersolidus cracking	64
4.1.4.2	Subsolidus cracking	67
4.2	Metallurgical effects in the parent metal and solidified weld metal	67
4.2.1	Microstructural changes in the heat-affected zone	67
4.2.2	Precipitation and embrittlement in the heat-affected zone	68
4.2.3	Contraction and residual stress	70
CHAPTER 5	<i>SOLID-PHASE WELDING</i>	74
5.1	Fundamentals	74
5.1.1	The cohesion and strength of metals	74
5.1.2	Surface deformation	76
5.1.3	Surface films	77
5.1.4	Recrystallisation	78
5.1.5	Diffusion	78
5.2	Processes	79
5.2.1	Pressure welding at elevated temperature	79
5.2.2	Diffusion bonding	82
5.2.3	Cold pressure welding	83
5.2.4	Friction welding	83
5.2.5	Explosive welding	84
CHAPTER 6	<i>BRAZING, SOLDERING AND ADHESIVE BONDING</i>	87
6.1	Physical aspects	87
6.1.1	Bonding	87
6.1.2	Surface energy and contact angle	88
6.1.3	Capillary action	91
6.2	Soldering and brazing	93
6.2.1	Wetting and spreading	93
6.2.2	Filling the joint	95
6.2.3	Solidification range	95
6.3	Soldering	95
6.3.1	Joint design	95
6.3.2	Solders	96
6.3.3	Fluxes	96
6.3.4	Soldering methods	97
6.3.5	Application to various metals	97
6.4	Brazing	97
6.4.1	Joint design	97
6.4.2	Brazing solders	98
6.4.3	Fluxes and protective atmospheres	98
6.4.4	Brazing methods	101
6.4.5	Bronze welding	102
6.4.6	Application to various metals	102
6.5	Adhesive bonding	103
6.5.1	Mechanical strength	104
6.5.1.1	Contact angle	104
6.5.1.2	Residual stress and stress concentration factors	105
6.5.2	Bonding methods	106
6.5.2.1	Preparing the surface	106
6.5.2.2	Types of adhesive and the mode of application	107
6.5.2.3	Curing the joint	107

6.5.2.4	Testing	108
6.5.3	Applications	108
CHAPTER 7	<i>CARBON AND FERRITIC-ALLOY STEELS</i>	110
7.1	Scope	110
7.2	Metallurgy of the liquid weld metal	110
7.2.1	Gas-metal reactions	110
7.2.1.1	Reactions in the transferring drop	111
7.2.1.2	Reactions in the weld pool	111
7.2.2	Slag-metal reactions	112
7.2.2.1	The mechanics of slag-metal interaction	112
7.2.2.2	The chemistry of slag-metal interaction	114
7.2.3	Solidification and solidification cracking	116
7.3	Transformation and microstructure of steel	118
7.3.1	Transformation and microstructure of weld metal	120
7.3.2	Transformation and microstructure in the heat-affected zone	121
7.4	The mechanical properties of the welded joint	126
7.4.1	The mechanical properties of weld metals	127
7.4.2	The mechanical properties of the heat-affected zone	129
7.4.2.1	The hardness of the HAZ	129
7.4.2.2	The fracture toughness of the HAZ	131
7.5	Stress intensification, embrittlement, and cracking of fusion welds below the solidus	134
7.5.1	Stress concentration	134
7.5.2	Embrittlement of fusion welds	134
7.5.3	The hydrogen embrittlement and cracking of welds in steel	135
7.5.3.1	Hydrogen attack	136
7.5.3.2	Hydrogen embrittlement	136
7.5.3.3	The solution of hydrogen	136
7.5.3.4	Cracking due to dissolved hydrogen	138
7.5.3.5	Hydrogen-induced cold cracking in welds	139
7.5.3.6	Testing for hydrogen-induced cold cracking	147
7.5.3.7	Measures to avoid hydrogen-induced cold cracking	150
7.5.4	Chevron cracking	152
7.5.5	Lamellar tearing	155
7.5.6	Reheat cracking	156
7.6	Welding problems with iron and steel products	160
7.6.1	Cast iron	160
7.6.2	Steels used primarily for their mechanical properties	162
7.6.2.1	Carbon and carbon-manganese steels	163
7.6.2.2	Microalloyed steels	164
7.6.2.3	Low-alloy normalised and tempered (NT) steels	167
7.6.2.4	Low-alloy quenched and tempered (QT) steels	170
7.6.3	Steels for subzero temperature use	172
7.6.4	Low-alloy corrosion- and heat-resisting steels	172
7.6.5	Ferritic and austenitic/ferritic chromium stainless steels	173
CHAPTER 8	<i>AUSTENITIC AND HIGH-ALLOY STEELS</i>	178
8.1	Scope	178
8.2	Metallurgy of the weld metal and heat-affected zone	178
8.2.1	Alloy constitution	178
8.2.2	Carbide precipitation	180
8.2.3	Solidification cracking in the weld deposit	182

8.2.4	Hot cracking in the heat-affected zone during welding	185
8.2.5	Reheat cracking	186
8.3	Corrosion	187
8.3.1	Intergranular corrosion	187
8.3.2	Stress corrosion cracking	190
8.3.3	Preferential corrosion of welds	191
8.4	Corrosion-resistant steels: alloys and welding procedures	192
8.5	Weld overlay cladding and dissimilar metal joints	193
8.6	Heat-resisting steels: alloys and welding procedures	194
8.7	Hardenable high-alloy steels	195
CHAPTER 9 NON-FERROUS METALS		197
9.1	Aluminium and its alloys	197
9.1.1	Processes and materials	197
9.1.2	Porosity	198
9.1.3	Cracking	199
9.1.4	Mechanical properties	202
9.1.5	Alloys and welding procedures	204
9.2	Magnesium and its alloys	205
9.2.1	Alloys and welding procedures	205
9.2.2	Oxide film removal	206
9.2.3	Cracking	206
9.2.4	Mechanical properties	206
9.2.5	Corrosion resistance and fire risk	206
9.3	Copper and its alloys	207
9.3.1	Processes and materials	207
9.3.2	Heat input	207
9.3.3	Porosity	208
9.3.4	Cracking	209
9.3.5	Mechanical properties	209
9.3.6	Alloys and welding procedures	209
9.4	Nickel and its alloys	211
9.4.1	Cracking	211
9.4.2	Porosity	212
9.4.3	Mechanical properties	213
9.4.4	Corrosion resistance	213
9.4.5	Oxidation and creep resistance	216
9.4.6	Alloys and welding procedures	216
9.5	The reactive and refractory metals – beryllium, titanium, zirconium, niobium, molybdenum, tantalum and tungsten	216
9.5.1	Embrittlement due to gas absorption	217
9.5.2	Embrittlement due to recrystallisation	218
9.5.3	Porosity	219
9.5.4	Cracking	219
9.5.5	Tensile properties	219
9.5.6	Alloys and welding procedures	220
9.6	The low-melting metals: lead and zinc	221
9.6.1	Lead	221
9.6.2	Zinc	221
9.7	The precious metals: silver, gold, platinum	222
9.7.1	Silver	222
9.7.2	Gold	222
9.7.3	Platinum	222
9.7.4	Other platinum-group metals	222

CHAPTER 10	<i>THE BEHAVIOUR OF WELDS IN SERVICE</i>	224
10.1	Reliability	224
10.2	Service problems associated with welding	226
10.3	Fast crack growth	226
	10.3.1 General	226
	10.3.2 Linear elastic-fracture mechanics (LEFM)	228
	10.3.3 Alternative means of estimating or measuring fracture toughness	233
10.4	Slow crack propagation	236
10.5	Corrosion of welds	239
10.6	Risk analysis	242
APPENDIX 1	<i>SYMBOLS</i>	244
APPENDIX 2	<i>CONVERSION FACTORS</i>	247
INDEX		249

List of tables

2.1	Fusion welding and cutting processes	page 8
2.2	Heat source intensities and type of penetration	12
3.1	IIW classification of metal transfer	21
3.2	Dominant forces in metal transfer	29
3.3	Electron work function and ionisation potential of pure metals	33
3.4	Temperature of the arc column in various gases	36
3.5	Dissociation of gases in the arc	37
5.1	Solid-phase welding processes	80
6.1	Surface free energy and surface tension of metals and adhesives	90
6.2	Furnace atmospheres for brazing	100
6.3	Shear strength of 12.5 mm redux bonded lap joints at room temperature. Mechanical properties of redux (20 °C)	105
7.1	Fracture toughness ($\text{MN}/\text{m}^{3/2}$) of weld HAZ in ASTM A533 (Mn–Mo) steel at -196°C	133
7.2	AWS requirements for moisture content of hydrogen-controlled electrode coatings	142
7.3	High-strength line pipe steel	166
7.4	Typical compositions of pearlite-reduced X 70 line pipe steel	167
7.5	Low-alloy high-tensile NT steels for welded fabrication	168
7.6	Low-alloy high-strength QT steels for welded fabrication	169
7.7	Ultra high-strength maraging and QT steels for welded fabrication	171
7.8	Heat-resistant and corrosion-resistant chromium–molybdenum steels	173
7.9	Chemical composition of ferritic and ferritic/austenitic stainless steels	175
8.1	Standard intergranular corrosion tests for stainless steels	189
8.2	Corrosion-resistant austenitic Cr–Ni steels	192
8.3	Heat-resistant austenitic Cr–Ni alloys	194
9.1	Nickel and nickel alloys	214
10.1	Alloy systems subject to stress corrosion cracking	240

METALLURGY OF WELDING

1 Introductory

1.1 WELDING IN ANCIENT AND MEDIEVAL TIMES

The great majority of metal-joining processes have been invented in recent years but some, notably the **forge welding** of iron, **brazing** and **soldering**, have a very long history. Soldering and the hammer welding of gold appear to have been known during the Bronze Age, but they were mainly used for making ornaments. Welding first evolved as a technique of primary economic importance when the use of iron became widespread, it being required not only in order to make finished products, but also as part of the iron-making process itself. The method of smelting ironstone in ancient and medieval times was to heat a mixture of ore and charcoal in a blast of air, so regulating the heat that a proportion of the ore was reduced to iron without melting. The mass of iron particles and slag so formed was then removed from the furnace, cleaned, reheated, and then hammered in order to consolidate the metal. The **blooms** produced in this way were small, and, as a rule, a number had to be welded together in order to form a piece of workable size. Special welding furnaces were constructed for this purpose in some localities.

The carbon content of the metal obtained by direct reduction lay generally between 0.02% and 0.10%, so that it lacked the hardenability required for cutting tools and swords. Steel, however, was a relatively costly material throughout the Roman era and the Middle Ages. Therefore tools for which a keen or hard edge was essential were frequently made by **steeling** — welding a thin strip of steel to the edge of the tool, and then hardening and tempering to the appropriate degree.

Swords were also manufactured by welding. Viking smiths made strong, tough sword-blades by **carburising** thin strips of iron and then welding them together lengthwise, thus obtaining a much better carbon distribution than could be achieved by **cementation** of a completed iron blade. Later this technique was superseded by the **Damascening** process which is similar in principle, but results in a finer pattern and therefore an even better mixing of high-carbon and low-carbon regions.

Other armaments produced during the Middle Ages were also fabricated by welding. The bolts shot from crossbows were tipped with steel, the tips being attached by welding. Cannon were either cast in bronze, or were fabricated by welding together a number of iron bands, and, in defence, welding was employed in making armour (particularly chain mail) and in the ironwork used for reinforcing strongpoints.

The relative importance of welding in iron-making and as a metal fabrication technique during the Middle Ages resulted from two main causes: the high cost of steel and the fact that blooms could only be produced in small sizes. The shortage of steel continued throughout the medieval period but, following the introduction of water power in the twelfth or thirteenth century, the bloom size increased substantially — up to a hundredweight or more, as compared with a few pounds in Roman and Anglo-Saxon times. There was no longer any need, therefore, to weld blooms together in order to make a piece of useful size. Later still, in the fifteenth century, came the invention of the blast furnace and of the indirect process of making steel. One result of this development was the availability of a cheap casting material. Iron castings were used for a number of products previously made from welded wrought iron, an important example being the cannon which were so successfully produced by the foundries of that period.

Thus, with the improvement of iron-making techniques during the later Middle Ages, the importance of welding in metal production and fabrication diminished. Further development reinforced this trend. Forge welding is ill-adapted to joining the edges of large plates; consequently, iron plates and later steel plates (when they became available) were joined by riveting or bolting. Welding continued to be used by blacksmiths, but was no longer of central importance to metals' technology as a whole, and, before it could become effective as a means of joining the metal products developed during the industrial revolution, new and radically different processes were required.

1.2 THE ADVENT OF FUSION WELDING

The welding process in use during the period so far considered is a solid-phase process. The two iron or steel parts to be joined are raised to a white heat in the forge fire and, if necessary, fluxed by means of sand. Hammering the joint then extrudes the liquid oxide or slag and brings the clean metal surfaces close enough together to form a metallic bond. It will be obvious that the success of such an operation depends upon the smith's ability to maintain the joint surfaces at a reasonably uniform temperature before and during the hammering operation, and for the most part this limits the size of objects that can be forge welded. A forge-welding process, **hammer welding**, was used on a limited scale for manufacturing aluminium and steel vessels from plate prior to about 1930, but the process was costly and required great skill.

The problem of welding plate was overcome by **fusion welding**, in which a heat source intense enough to melt the edges is traversed along the joint. Heat sources of sufficient intensity first became available on an industrial scale at the end of the nineteenth century, when **gas welding**, **arc welding** and **resistance welding** all made their appearance. Gas welding was made possible by the supply of oxygen, hydrogen and acetylene at an economic price, and by the invention of suitable torches and gas storage techniques. By 1916 **oxy-acetylene welding**

was a fully developed process capable of producing good-quality fusion welds in thin steel plates, aluminium and deoxidised copper, and differing only in detail from the process as it is known today. Arc welding with a fusible electrode — the most important of the fusion processes — is more complex in character and developed more slowly. Initially bare wire electrodes were used, but the resultant weld metal was high in nitrogen content and therefore brittle. Wrapping the wire with asbestos or paper improved the properties of weld deposits, and led eventually to the modern type of arc-welding electrode, which is coated with a mixture of minerals, ferro-alloys and in some cases organic materials, bonded with sodium or potassium silicate.

In the early stages of this development fusion welding was used primarily as a means of repairing worn or damaged metal parts, but during World War 1 Government departments and inspection agencies such as Lloyds Register of Shipping initiated research into the acceptability of the technique as a primary means of joining metals, and prototype welded structures were made. Nevertheless, riveting remained the predominant method of joining steel plate and sections until World War 2. During and after this war the use of fusion welding for shipbuilding, for chemical, petroleum and steam power plant, and for structural steelwork, became widespread and replaced riveting for the majority of fabrications.

Largely because the metallurgical problems which beset fusion welding do not arise to the same degree in resistance welding (at least so far as carbon steel is concerned), this latter group of processes was established in production long before arc welding was generally accepted. **Spot and seam welding**, which are used for making lap joints in thin sheet, and **butt welding**, used for chainmaking and for joining bar and sections, were well established by 1920. Subsequent development of resistance welding has been mainly concerned with improvement of the welding machines — better timing controls for spot welders, for example — and its application to alloy steels and non-ferrous metals.

Thus, welding once again acquired a position of central importance in the fabrication of engineering structures. This trend has continued. Since the invention of inert-gas shielded welding in 1943, welding processes have developed and multiplied at a most remarkable rate, and as a result the great majority of metals currently used in industry can be welded by one means or another. Moreover, the productivity of welding processes has increased rapidly, and is in most cases higher than alternative techniques such as bolting or riveting. Consequently, there is an incentive to develop alloys which, besides having other desirable characteristics, are readily weldable. Low-carbon low-alloy steel, titanium-stabilised austenitic stainless steel, and phosphorus-deoxidised copper are examples of alloys that have been developed for improved weldability. In this way welding has come to influence not only fabrication methods, but metals technology as a whole.

1.3 THE THEORY OF METAL JOINING TECHNIQUES

Parallel with the development of metal-joining processes, understanding of the relevant physical and metallurgical processes has grown at an accelerating pace. Fusion welding, and metal arc welding with coated electrodes in particular, has generated a number of important metallurgical problems. By about 1930 the basic requirements for producing carbon steel weld metal of adequate quality – in particular, effective deoxidation, low sulphur and phosphorus content, and a high manganese–sulphur ratio – were understood. This was undoubtedly one of the factors which made possible the subsequent application of welding to large steel structures. During World War 2 it was realised that hydrogen dissolved in the weld metal was one of the causes of cracking in low-alloy steel-welded joints, and the research which followed up this idea, together with the development of low hydrogen electrodes, made possible the extension of welding to the low-alloy steel field. The spectacular failures of some welded ships during and after World War 2 led to extensive research into the phenomenon of **brittle fracture**, and more recently the development of **fracture mechanics** has made it possible to deal with this type of problem in a quantitative manner.

These and many other investigations into welding problems have produced a very considerable body of knowledge, and an acquaintance with at least the broad outlines of this branch of applied metallurgy is becoming more and more essential to those concerned with the development of alloys and the industrial use of metals.

Knowledge of welding physics has been acquired more slowly. The theory of heat flow is well developed, and there have been some useful investigations in this field, but it is only recently that significant progress has been made in the study of those physical phenomena which are specifically associated with arc welding, such as metal transfer and mass flow in welding arcs. The investigation of such problems is producing information and ideas that have particular value in the development of welding processes.

1.4 WELDING ENGINEERING

There remains a third domain of welding knowledge which will not be dealt with in this book, namely the mechanics of applying the various processes – the design of edge preparations, methods of applying preheat and postwelding heat treatment, the sequence and number of runs and so forth. These matters are primarily the function of the welding engineer rather than the metallurgist. Nevertheless, it must not be forgotten that the successful completion of a weld requires not only the correct prescription of metallurgical requirements such as preheat, type of filler alloy or electrode coating, but also proper execution; and that sound practical application is just as important as well founded theory.

FURTHER READING

- Schubert, H. R. 1957. *History of the British iron and steel industry to 1775*.
London: Routledge and Kegan Paul.
- Tylecote, R. F. 1962. *Metallurgy in archaeology*, London.
- Tylecote, R. F. 'A History of Metallurgy', The Metals Society, London, 1976.
- Winterton, K. *Welding and Metal Fab.*, 1962, **30**, 438–42 and 488–92.
- Winterton, K. *Welding and Metal Fab.*, 1963, **31**, 71–6.

2 Processes and types of joint

2.1 THE GENERAL CHARACTER OF WELDING, BRAZING, SOLDERING AND ADHESIVE JOINTING

The methods of joining metals may be divided into two main categories: those which rely on macroscopic mechanical forces, on the one hand, and those that depend on interatomic or intermolecular forces on the other. The first category is typified by bolting. The joint strength is obtained from the shear strength of the bolts and the frictional forces that keep the nuts in place. In the second group of joining methods, with which this book is concerned, the surfaces to be joined are brought closely enough together for either the metallic bond or, alternatively, van der Waals or other intermolecular forces to become effective. Welding, brazing, soldering and adhesive jointing *processes* are the means by which the required degree of proximity may be achieved.

The non-mechanical joining techniques may be further divided into three sub-categories: welding, brazing and soldering, and adhesive bonding. In welding the joint has more or less the same composition throughout, or if there is a bridging material of different composition it has a similar melting point to that of the metals being joined. In brazing and soldering the joint is made using a metal of different composition and lower melting point, while in adhesive bonding the jointing substance is a non-metal and no attempt is made to form a metallic bond. Brazing, soldering and adhesive joining will be considered in Chapter 6.

2.2 THE NATURE OF WELDING PROCESSES

From a metallurgical viewpoint welding processes may be divided into two main categories: fusion-welding processes and solid-phase welding processes. In **fusion welding** the two edges or surfaces to be joined are heated to the melting point and, where necessary, molten **filler metal** is added to fill the joint gap. Such welds comprise three metallurgical zones; the **fusion zone**, the unmelted **heat-affected zone (HAZ)** adjacent to the fusion zone, and the unaffected **parent plate** (Fig. 2.1). **Solid-phase** welds, on the other hand, are made by bringing two clean, solid metal surfaces into sufficiently close contact for a metallic bond to be formed between them (Fig. 2.2). Whereas fusion welding necessarily requires part of the metal to be heated above the melting

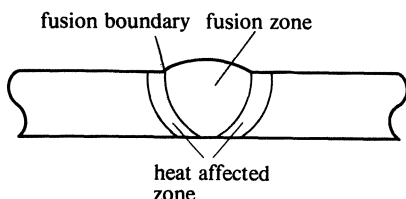


Figure 2.1 Fusion weld.

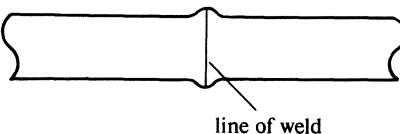


Figure 2.2 Solid phase weld.

point, solid-phase welding may be accomplished at temperatures as low as normal room temperature. Solid-phase welding will be considered in detail in Chapter 5.

2.2.1 The classification of fusion welding processes

The way in which a fusion weld is made may have a profound effect on the properties of the joint. The three most important characteristics of a fusion-welding process in this respect are the *intensity of the heat source*, the *heat input rate per unit length of weld* and the type and effectiveness of the method used to *shield* the weld from the atmosphere. In Table 2.1, which sets out the characteristics of the more important fusion welding processes, the method of shielding has been used (arbitrarily) as a means of grouping the different methods. Fusion welding is in a state of rapid development and it is not practicable to give figures for the relative use of individual processes. Until recent years, the bulk of welding was done by the **shielded metal arc (SMA)** process, but the present trend is for automatic and semi-automatic processes to be used to an increasing extent. In particular, the **gas metal arc (GMA)** processes, which are characterised by high productivity combined with flexibility in use, are gaining at the expense of SMA welding. In terms of bulk use, the most important processes are SMA, **submerged arc-welding (SAW)**, GMA and resistance welding.

The means of adding filler metal may affect the characteristics of the arc-welding process. In **gas tungsten arc (GTA)** welding, the filler material is fed separately by hand and this gives a higher degree of control than is usually obtainable with those processes where the electrode itself melts and provides the filler (see Section 2.2.4). For details of the equipment used, reference should be made to 'Further Reading' at the end of this chapter.

2.2.2 Heat source intensity

A minimum **heat source intensity** is required before it is possible for a fusion weld to be made. It will be evident that if the total heat flux across the **fusion boundary** is q , then as a minimum there must be heat liberation at an equal rate within the area of the molten weld pool. As the heat source intensity increases a point is reached (at about 10^9 W/m^2) where the source is capable of vaporising

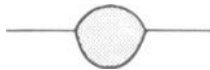






	Arc	Direct current, electrode positive	As above, but using solid wire. Free flight metal transfer	Argon or Helium. Argon/O ₂ or Argon/CO ₂	Non-ferrous metal. Carbon, low-alloy or high-alloy steel	2 mm upwards	Welding of high-alloy and non-ferrous metals. Pipe welding. General engineering
Gas metal arc (GMA) solid wire	Arc	Direct current, electrode positive	As above, but in short-circuiting metal transfer mode	Argon/O ₂ Argon/CO ₂ CO ₂	Carbon and low alloy steel	1 mm upwards	Sheet metal, root pass in pipe welding positional welding
	Pulsed arc	Direct current, electrode positive. 50–100 Hz pulse superposed on low background current	Pulse detaches drop at electrode tip and permits free flight transfer at low current	Argon Argon/O ₂ Argon/CO ₂	Non-ferrous metals. Carbon, low-alloy and high-alloy steels	1 mm upwards	Positional welding of relatively thin carbon or alloy steel
Gas welding (OAW)	Oxyacetylene flame		Manual. Metal melted by flame and filler wire fed in separately	Gas (CO, H ₂ , CO ₂ , H ₂ O)	Carbon steel, copper, aluminium, zinc and lead. Bronze welding	Sheet metal and pipe up to about 6 mm	Sheet metal welding small diameter pipe
Gas cutting (OFC–A)	Oxyacetylene/Oxygen flame		Oxygen jet injected through flame oxidises and ejects metal along the cutting line	Oxygen	Carbon and low-alloy steel		Cutting and bevelling plate for welding. General engineering applications
Gas tungsten arc (GTA) welding	Arc	Alternating current with stabilisation for aluminium, magnesium and alloys, direct current electrode negative for other metals	Manual or automatic arc maintained between non-consumable tungsten electrode and work. Filler wire fed in separately	Argon, Helium or Argon/Helium mixtures	All engineering metals except Zn and Be and their alloys	1 mm to about 6 mm	Non-ferrous and alloy steel welding in all engineering fields. Root pass in pipe welds

Process	Heat source	Power source and polarity	Mechanics	Shielding or cutting agent	Typical applications	
					Metals	Thickness range
Pulsed gas tungsten arc (GTA) welding	Arc	Direct current, electrode negative with low frequency (1 Hz) or high-frequency (1 kHz) current modulation	Low-frequency pulse allows better control over weld pool behaviour. High frequency pulse improves arc stiffness	Argon	As above	1 mm to about 6 mm Automatic GTA welding of tubes or tube-to-tube sheet, to improve consistency of penetration or (high frequency) prevent arc wander
Plasma welding (PAW)	Arc	Direct current, electrode negative	As for gas tungsten arc, except that arc forms in a chamber from which plasma is ejected through a nozzle. Improved stiffness and less power variation than GTA	Argon, Helium, Argon/Hydrogen mixtures	As above	Usually up to about 1.5 mm Normally low-current application where gas tungsten arc lacks stiffness. Also used at higher currents in keyholing mode for root runs
Plasma cutting (PAC)	Arc	Direct current, electrode negative	As for welding, but higher current and gas flow rates	Argon/H ₂	All engineering metals	1 mm upwards Used particularly for stainless and non-ferrous metals but also carbon and low-alloy steel
Stud (SW)	Arc	Direct current, electrode negative for steel, positive for non-ferrous	Semi-automatic or automatic. Arc drawn between tip of stud and work until melting occurs and stud then pressed on to surface. Weld cycle controlled by timer	Self-generated gas + ceramic ferrule around weld zone	Carbon, low-alloy and high-alloy steel Aluminium Nickel and copper alloys require individual study	Stud diameters up to about 25 mm Shipbuilding, railway and automotive industries. Pressure vessels (for attaching insulation) furnace tubes and general engineering

Spot, seam and projection (RSW, RSEW, RPW)	Resistance heating at interface of lapped joint	Alternating current. Transformer with low voltage, high current output	Lapped sheet clamped between two copper electrodes and welded by means of high current pulses. Weld may be continuous (seam) or intermittent (spot and projection)	Self-shielded + water for resistance welding Mo, Ta and W	All engineering metals except Cu and Ag. Al requires special treatment	Sheet metal up to about 6 mm	Automobile and aircraft industries. Sheet metal fabrication in general engineering
Electron beam (EBW)	Electron beam	Direct current, 10–200 kV, power generally in range $\frac{1}{2}$ –10 kW. Workpiece positive	Automatic welding carried out in vacuum. Beam of electrons emitted by cathode focused on joint. No metal transfer	Vacuum ($\sim 10^{-4}$ mm Hg)	All metals except where excessive gas evolution and/or vaporisation occurs	Up to about 25 mm normally but may go to 100 mm	Nuclear and aerospace industries. Welding and repair of machinery components such as gears
Laser (LBW)	Light beam	None	As for electron beam except different energy source	Helium	As for electron beam	Up to 10 mm	Potentially as for electron beam. Cutting non-metallic materials
Thermit (TW)	Chemical reaction	None	A mixture of metal oxide and aluminium is ignited, forming a pool of superheated liquid metal, which then flows into and fuses with the joint faces	None	Steel, austenitic CrNi steel, copper, copper alloys, steel/copper joints	Normally up to 100 mm	Welding rails copper conductors to each other and to steel

the metal as well as melting it. The pressure generated by the emergent metal vapour then depresses the weld pool until this pressure is balanced by hydrostatic pressure and surface tension forces. In this way a *penetrating* heat source may be generated which gives a deep finger-like penetration. This type of penetration is also known as a 'keyhole'. Table 2.2 shows typical heat source intensities for various processes and the corresponding type of penetration. If the current is sufficiently high, both the GTA and GMA processes may generate a deep, narrow penetration at the centre of a weld pool that is otherwise roughly semicircular in section. In the case of the plasma (high current), electron-beam and laser processes, it is possible to restrict the heated area and limit the spread of the weld pool at the surface.

Table 2.2 Heat source intensities and type of penetration

<i>Process</i>	<i>Heat source intensity W/m^2</i>		<i>Fused zone profile</i>
Flux-shielded arc welding	5×10^6 to 5×10^8		
Gas-shielded arc welding	5×10^6 to 5×10^8	Normal current	
		High current	
Plasma	5×10^6 to 5×10^{10}	Low current	
		High current	
Electron beam and laser	10^{10} to 10^{12}	Defocused beam	
		Focused beam	

In principle, the use of a penetrating heat source in fusion welding is attractive since the fused and heat-affected zones are narrow and this minimises both metallurgical damage and distortion. On the other hand, the joint fit-up prior to welding must be accurate and the motion of the torch relative to the joint must be equally accurate. Even so, such deep penetration welds may be subject to defects such as **cold shuts** or **lack of fusion**, **porosity** and **hot cracking** if correct procedures are not followed. Plasma keyhole welding is more tolerant in this respect than electron beam or laser. Because of the requirement for high precision and because of the high cost of equipment, this type of welding is used mainly for joining premachined components and in capital-intensive industries such as automobiles and aerospace.

Most welding is carried out using processes that generate a *surface* weld pool of roughly semicircular cross section. When it is required to fill a joint that is deeper than the penetration of such a source, it is necessary to make a number of successive passes or runs. This technique is known as **multi-pass** or **multi-run** welding (Fig. 2.3).

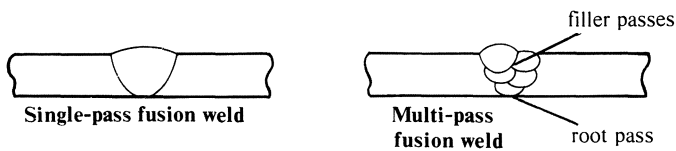


Figure 2.3 Single- and multi-pass welds.

2.2.3 Heat input rate

If V represents arc voltage, I arc current and η is the proportion of arc energy that is transferred as heat to the workpiece, then the heat input rate q per unit length of weld is:

$$\frac{\eta VI}{v} = q/v$$

where v is the welding speed. The heat input rate is one of the most important variables in fusion welding since it governs heating rates, cooling rates and weld pool size. Generally speaking, the higher the heat input rate the *lower* the cooling rate and *larger* the weld pool. As will be seen later (Ch. 3) there is an *inverse* relationship between weld pool size and cooling rate. In the welding of steel this is an important relationship since increased cooling rates increase the risk of hydrogen-induced cracking. Experience indicates that a **high heat input rate process** like submerged arc welding gives less HAZ cracking in the welding of alloy steel than does SMA welding, where heat input rates are lower (but note that there may be other variables that contribute to this difference in behaviour).

The other metallurgical feature that is directly affected by heat input rate is the grain size in the heat-affected zone and in the weld metal. Grains in the

solidifying weld metal grow coherently with grains in the solid metal at the fusion boundary. Therefore, the longer the time spent above the grain-coarsening temperature of the alloy in question, the coarser the structure in the heat-affected zone and in the weld metal. In face-centred cubic metals and alloys, coarse grain size may not have much effect on weld behaviour but in the case of ferritic steels various properties, particularly notch-ductility, deteriorate as the grain size increases. A high heat input rate process will, in general, give a longer thermal cycle and tend to generate a coarser structure. In the case of steel welding, it is therefore necessary to seek a heat input rate that gives the optimum combination of grain size and cooling rate.

The term 'high heat input rate process' must be qualified by saying that this quality is determined primarily by the welding current range over which it is practicable or economic to use the process. SMA welding is normally applied manually for all position welding, when the current range is 50–350 A. However, there is an automatic process (Fusarc welding) which employs a flux-coated wire as in SMA welding and where the current range (200–750 A) and heat input rate is similar to that for SAW. This is possible because the process is operated automatically in the flat position: with high currents the weld pool becomes difficult to control in manual operation, particularly in positional welding. Other physical limitations to heat input rate are excessive spatter (in GMA welding with Ar/O₂ mixtures) or instability due to the formation of a deep-penetration weld pool, or due to the development of an unfavourable mode of metal transfer (inert gas shielded GMA welding).

Processes may also become unstable or ineffective at some lower current level, due to inadequate heat input or to an unsuitable mode of metal transfer and it may be desirable to lower this current level in order to permit the welding of thin material, positional welding, and the like. In GMA welding this has been accomplished by using a short-circuiting mode of metal transfer or by using a pulsed current. Both techniques stabilise metal transfer in a current range where it would normally be hard to control. Low frequency pulsed current may also be applied to GTA welding for thin material. Other means of stabilising GTA welding at low current include the use of high frequency (~ 10 kHz) pulses or directing the arc column through an orifice (low current plasma welding).

2.2.4 Shielding methods

The drop at the tip of a fusible electrode may reach boiling point while the centre of the weld pool, although much cooler, is substantially above the melting point. At such temperatures reaction with oxygen and nitrogen from the atmosphere is rapid and, to avoid embrittlement by these elements, some form of **shielding** is required. This protection may be obtained by means of flux, gas, or a combination of the two, or it may result from physical shielding (as in spot welding) or from evacuation of the atmosphere, as in electron-beam welding. The only process in which flux alone provides the shield is electroslag welding.

In SMA and SAW flux is provided, but the gases generated by vaporisation and chemical reaction at the electrode tip are also protective.

In SMA welding the electrode coating is composed of a mixture of minerals, organic material, ferro-alloys and iron powder bonded with sodium or potassium silicate. **Cellulosic** (BS Class C or AWS 6010) electrodes contain cellulose, rutile and magnesium silicate, while **rutile** (BS Class R or AWS 6013) electrodes contain a small amount of cellulose with rutile and calcium carbonate. Because of the organic content these types of coating are baked after application at 100–150 °C and a substantial amount of moisture is retained. Consequently, the gas that is generated during welding by decomposition of the coating contains a high proportion (about 40%) of hydrogen. Basic (BS Class B AWS 7015, 7016 and 7018) electrode coatings, on the other hand, contain no organic matter, and therefore are baked at 400–450 °C, which drives off the bulk of the moisture content. The mineral content of such coating is largely calcium carbonate, which breaks down during welding to provide a CO/CO₂ shield. The volume of gas so generated is lower than with cellulosic or rutile coatings and this is one reason why it is necessary to use a shorter arc with basic electrodes than with other types. Other effects of gas composition will be discussed in Sections 4.1.1 and 7.5.

In SMA welding the drops that transfer from the electrode to the weld pool are coated with slag and the weld pool itself has a slag coating. The self-generated gas is the main protective agent during metal transfer while the slag protects the solidifying and cooling weld metal.

In SAW the flux is a coarse granular powder that is dispensed on to the workpiece immediately ahead of the arc. This flux melts around the arc to form a bubble, which bursts periodically and re-forms. Metal may be transferred directly across the cavity so formed or it may transfer through the wall of molten flux. The shield in this case consists of gas generated from the electrode plus molten flux, plus the unmelted granular layer around the molten flux. The granular flux may be made by agglomeration, sintering or fusing and may be chemically basic, neutral or acid. It may also contain ferro-alloys as deoxidants or additive elements.

Shielding by means of an external gas supply is used in GMA, GTA and plasma welding. The gas is dispensed through a nozzle surrounding the electrode, although in the welding of reactive metals an extended shield, or a gas-filled box, may be required. For non-ferrous metals and GTA welding, the inert gases argon or helium are used. Argon/hydrogen mixtures may be used for GTA welding of nickel and for plasma torches, where the hydrogen increases the arc power. In the case of GMA welding of steel, the pure inert gases are not suitable because cathode spots wander over the surface of the workpiece, resulting in irregular weld pool formation. Additions of oxygen or carbon dioxide inhibit cathode spot wander and promote regularity of operation. Typical mixtures are 98% Ar, 2% O₂ and 80% Ar, 20% CO₂. Spatter increases with increasing CO₂ addition and above 20% CO₂ it is necessary to use short-circuiting metal transfer to avoid excessive spatter. Pure CO₂ may be used for such **short-circuiting** or **dip-transfer** welding techniques.

In resistance welding, the weld pool is generated internally and is protected by the surrounding solid metal. Stud welding relies partly on physical shielding, but the stud tip may be coated with deoxidant. The vacuum in which electron-beam welding is carried out provides complete protection against the external atmosphere, but if the metals being welded contain dissolved gas, this may be evolved, causing porosity. These three processes, which in other respects are very different, all rely to some degree on a mechanical rather than a chemical shield.

2.3 TYPES OF FUSION WELDED JOINT

Fusion welds may be made in a variety of forms. The joint illustrated in Figure 2.1 is a **butt weld** and in this instance the metal is fused to the full thickness of the plates being joined; it is therefore a **full penetration weld**. **Partial penetration welds** are also used for some engineering purposes. These and other types of joint that are made by fusion welding are illustrated in Figure 2.4.

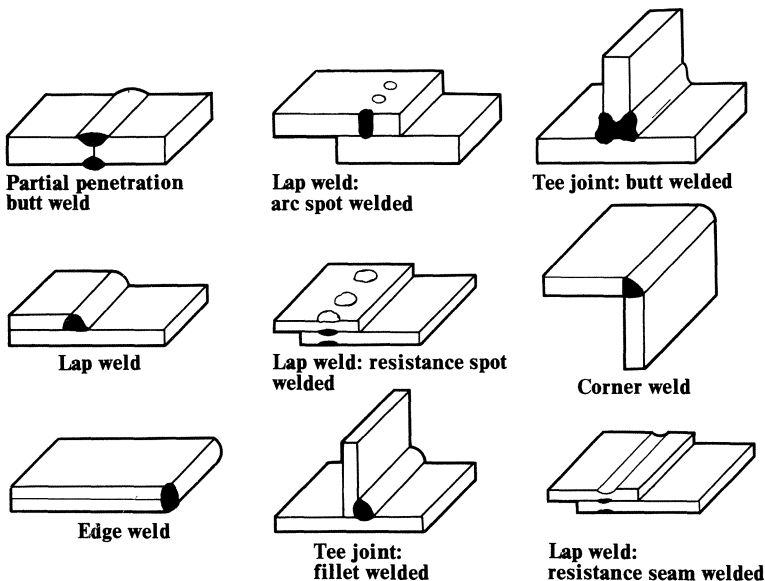


Figure 2.4 Types of fusion-welded joints.

Note that a **spot welded lap joint** may be made by resistance welding, in which case the fused zone is formed at the joint interface, or by arc welding, when the fused zone penetrates from the surface of the top sheet to the underlying sheet. Resistance welding may also be used to make a continuous weld (known as a **seam weld**) by forming a series of overlapping spot welds.

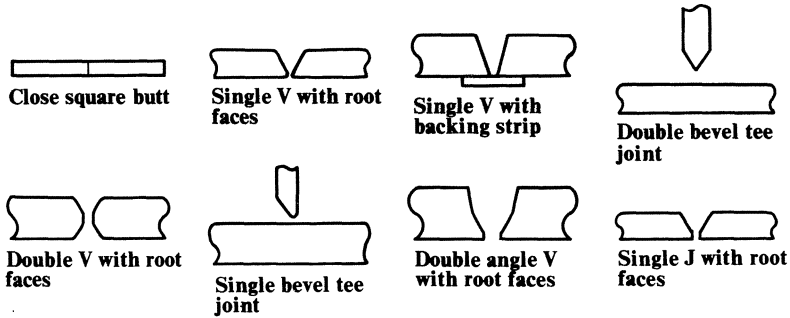


Figure 2.5 Typical edge preparations for welding.

In order to achieve the required degree of penetration, it is usually necessary to shape the edges of plates which are to be butt welded, and sometimes to leave a gap between them (Figure 2.5). In principle it is possible, by using a heat source of sufficient power, to fuse through the complete section even of very thick plate. However, the large weld pool so produced is difficult to control unless, as in electroslag welding, special equipment is available for this purpose. Also the weld metal and heat-affected zone of such welds have a relatively coarse grain and their mechanical properties may be adversely affected. Therefore it is normal practice to make multi-run welds in all but the thinnest material. Edge preparation is required in multi-run welds so as to give access to the root and all other parts of the joint, thereby ensuring that each run may be properly fused to the parent metal and to the run below. The metal required to fill the groove so formed is supplied either by **filler rod** which is added independently of the heat source, as in oxy-acetylene and GTA welding, or by the melting of an electrode in the case of GMA, SMA, SAW and electroslag welding. A fusion weld is most readily made when the plate lies in a horizontal plane and the welding is carried out from the top side (**flat welding**). Quite frequently, however, it is necessary to make the joint when the two members are set up vertically or at an angle to the horizontal, or it may be required to weld horizontal plates from the underside. The operation is then known as **positional welding** and the nomenclature of the various positions is indicated in Figure 2.6.

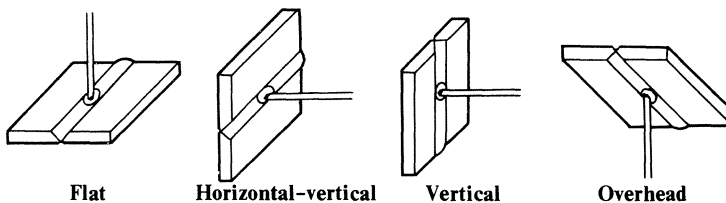


Figure 2.6 Welding positions.

FURTHER READING

American Welding Society 1976. *Welding handbook*, 7th edn, Sections 2 and 3. Miami: AWS; London: Macmillan.

Houldcroft, P. T. 1977. *Welding process technology*. Cambridge: Cambridge University Press.

American Society for Metals 1971. *Metals handbook*, 8th edn, vol. 6.

3 Mass and heat flow in welding

3.1 GENERAL

The character of heat flow in welding determines the nature of the **weld thermal cycle** and hence, in the case of transformable alloys, the microstructure of the weld metal and heat-affected zone. Mass flow, which encompasses the flow of plasma in the arc column, the flow of metal from electrode to weld pool, and the flow of metal in the weld pool itself, has less influence on the metallurgy of the joint. Irregularities or instabilities in mass flow may, however, limit the usefulness and range of application of specific processes and may cause irregularities in the heat-flow pattern.

Three laws govern mass and heat flow: the laws of conservation of mass, of conservation of momentum and of conservation of energy. The conservation of mass is expressed by the **equation of continuity** which, for steady incompressible flow, is:

$$\nabla \cdot \mathbf{v} = 0 \quad (3.1)$$

where \mathbf{v} is the velocity of the fluid.* Conservation of momentum is expressed by the **momentum equation**, which for the same conditions, and assuming constant physical properties is

$$\rho \frac{d\mathbf{v}}{dt} = -\nabla p + \eta \nabla^2 \mathbf{v} + \mathbf{J} \times \mathbf{B} + \rho \mathbf{g} \quad (3.2)$$

The term on the left-hand side of the equation represents inertia forces, while on the right-hand side the terms are respectively forces due to pressure gradients and viscosity, the Lorentz force, and the gravitation force.

Conservation of energy is expressed by the **energy equation**, which is

$$\rho C_p \frac{\partial T}{\partial t} = \kappa \nabla^2 T - \rho C_p (\mathbf{v} \cdot \nabla) T - \nabla \cdot \mathbf{q}_r + \frac{J^2}{\sigma} + \Phi \quad (3.3)$$

Equation 3.3 determines the temperature distribution in a flowing medium, and, if the pattern of flow is known (say, by solving the momentum equation) it is in principle also possible to obtain the temperature at any point. If we ignore the last three terms on the right-hand side of Equation 3.3, which represent radiation, joule heating and viscous energy dissipation respectively, and assume

* Symbols, including the vector notation used here, are defined in the Appendix.

steady conditions, $(\partial T / \partial t = 0)$ we obtain:

$$\kappa \nabla^2 T - \rho C_p (\mathbf{v} \cdot \nabla) T = 0 \quad (3.4)$$

in which the first term represents the rate of heat loss by conduction and the second the rate of heat loss by convection. Equation 3.4 governs for heat flow in all welding processes that employ a moving source of heat. However, in the solid phase region of the workpiece, the mass flow is uniform and regular whereas at the electrode tip, in the arc and in the weld pool, velocities are non-uniform and the flow may or may not be steady.

In all cases a formal analysis is only possible if the geometry of the system is simple, and, in general, axisymmetric. These conditions are realised to a fair degree in GTA and GMA welding with inert gas shielding. With active gas or flux shielding the heat and current flows in the electrode and in the arc column are irregular and the material presented below is only applicable to a limited extent. Heat flow in the workpiece is less affected by asymmetry in the behaviour of the arc, particularly in regions that are remote from the heat source. In the following sections mass flow phenomena will be reviewed first. Mass flow is considered before heat flow since for any given geometry the velocity distribution must be known before the temperature distribution may be obtained.

In developing solutions to the relevant flow equations it is necessary to select the most appropriate co-ordinate system. In the case of heat flow in solids (Section 3.5.5) the rectangular co-ordinate system (x, y, z) will be used, but for systems in which there is mass flow, the spherical co-ordinate system (r, θ, ϕ) may be more appropriate. Where spherical co-ordinates are used, this is indicated in the text.

3.2 MASS FLOW: GENERAL

It is customary to obtain solutions to the flow Equations 3.1 and 3.2 in terms of a **stream function** ψ . This quantity is such that **streamlines** of the flow are represented by:

$$\psi = \text{constant} \quad (3.5)$$

while velocities (for the spherical co-ordinate system) are

$$v_r = \frac{1}{r^2 \sin \theta} \frac{\partial \psi}{\partial \theta}; \quad v_\theta = -\frac{1}{r \sin \theta} \frac{\partial \psi}{\partial r} \quad (3.6)$$

The geometries with which we will be concerned are (in the case of mass flow) all axisymmetric, so that $v_\phi = 0$. Although the momentum equation (Equation 3.2) is non-linear, it is possible to obtain analytical solutions for the flow in an infinite or semi-infinite medium provided that $\mathbf{J} \times \mathbf{B} = 0$. When an electric current is present ($\mathbf{J} \times \mathbf{B} \neq 0$) it is possible to obtain a numerical solution for certain geometries, but this solution breaks down at values of current well

below those used in welding. Therefore, it is necessary to approximate, either by assuming that the electromagnetic force is concentrated at a point, or by ignoring the inertia force $\rho \, dv/dt$ in Equation 3.2. Analytical solutions to the flow equations are then possible, and, in spite of the approximation, they give a good qualitative, and sometimes a good quantitative, representation of real flow.

3.3 MASS FLOW FROM THE ELECTRODE TO THE WORKPIECE

In this section we shall be concerned with the manner in which liquid metal flows from the electrode tip into the weld pool or to use the normal welding terminology, with **metal transfer**. Gas flow in the arc column, which usually goes in the same direction, will be considered in Section 3.5.2.2.

The International Institute of Welding (IIW) classification of metal transfer is given in Table 3.1. This classification is phenomenological and does not attempt to define the mechanics of transfer. It is probable that in most cases a number of factors contribute to the transfer mechanism. Forces that have a significant effect in metal transfer are surface tension, gravity, electromagnetic forces, and forces due to vaporisation or chemical reaction. At the end of this section the probable mechanism of the various transfer modes will be reviewed.

Table 3.1 IIW classification of metal transfer

<i>Designation of transfer type</i>	<i>Welding processes (examples)</i>
1 Free flight transfer	
1.1 Globular	
1.1.1 Drop	Low-current GMA
1.1.2 Repelled	CO ₂ shielded GMA
1.2 Spray	
1.2.1 Projected	Intermediate-current GMA
1.2.2 Streaming	Medium-current GMA
1.2.3 Rotating	High-current GMA
1.3 Explosive	SMA (coated electrodes)
2 Bridging transfer	
2.1 Short-circuiting	Short-arc GMA, SMA
2.2 Bridging without interruption	Welding with filler wire addition
3 Slag-protected transfer	
3.1 Flux-wall guided	SAW
3.2 Other modes	SMA, cored wire, electroslog

In SMA welding there are a number of possible transfer mechanisms. One of these is explosive transfer. A bubble of CO forms in the drop at the electrode tip and grows at the same time as the drop itself grows. Eventually the bubble of CO bursts and a shower of small droplets is formed. In fully deoxidised electrodes such drops only form occasionally, and one of the primary modes of

transfer appears to be due to pressure at the arc root, which causes a local depression in the drop. The arc is in constant movement and as a result the part of the drop away from the arc root is likewise constantly in motion and is progressively forced towards the weld pool. Eventually it is detached either by inertia or by the pinch force, or it makes a short-circuit and is drawn into the pool by electromagnetic and surface-tension forces. Transfer of metal from coated electrodes is a complex phenomenon and other mechanisms may also play a part.

In GMA welding explosive transfer due to the formation of a CO bubble may occur but is exceptional with the deoxidised wires normally employed. Transfer may be of the short-circuiting type (in **dip transfer** or **short-arc** welding) or it may be in the projected mode. Combinations of these two transfer modes are also possible. The character of free-flight transfer depends on the current density in the electrode and on the strength of any imposed magnetic field. At low current densities large drops form at the electrode tip and detach with an initial acceleration lower than that due to gravity. As the current density J increases the drops become smaller and the initial acceleration increases up to a level above which a conical tip forms and the drops detach from the tip of the cone. At still higher values of J the cone transforms into a more or less cylindrical stream of liquid which breaks up into drops at its tip (streaming transfer). At still higher currents the cylindrical stream of liquid collapses into a rotating spiral (rotating transfer). Application of a longitudinal magnetic field causes the spiral to form at lower current densities.

It is found experimentally for steel that immediately prior to detachment the displacement δ of the centre of gravity of the drop is an exponential function of time:

$$\delta = \delta_0 e^{\omega t} \quad (3.7)$$

where δ_0 is an initial displacement and ω is a time constant, with dimensions $1/t$. The velocity v and acceleration a at any displacement δ are:

$$v = \frac{\partial \delta}{\partial t} = \omega \delta \quad (3.8)$$

and

$$a = \frac{\partial^2 \delta}{\partial t^2} = \omega^2 \delta \quad (3.9)$$

3.3.1 The pinch instability

In previous editions of this book, and in much of the welding literature on the subject, metal transfer in GMA welding has been considered in terms of the balance of forces on the drop at the electrode tip, so that the drop detaches when, for example, drag due to plasma flow, gravitational and electromagnetic forces exceed the retaining force due to surface tension. It has been shown experimentally that such an approach gives results that are quantitatively correct for the plasma-MIG and GMA processes in the range of large drop transfer, up

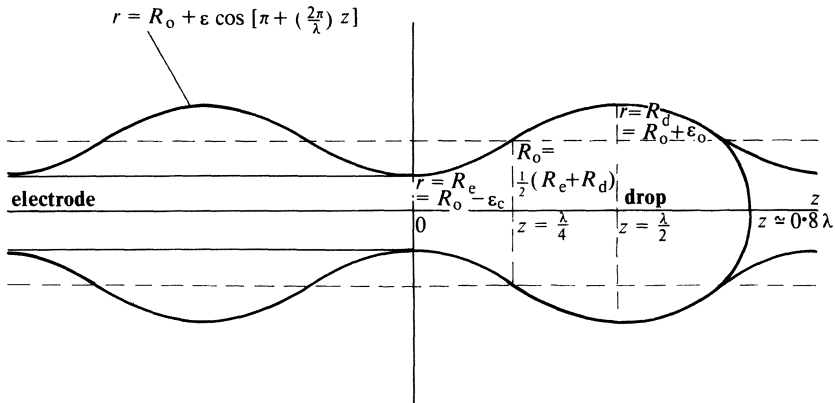


Figure 3.1 Assumed geometry of drop at the tip of an electrode as related to the sinusoidal perturbation of a liquid cylinder. For convenience the origin has been shifted to the solid/liquid boundary. This does not affect the argument given in the text.

to about 200 A. However it is implied that in its response to electromagnetic forces, the liquid drop at the tip of the electrode behaves as a solid body, and this is difficult to justify on theoretical grounds.

More recently consideration has been given to the possibility that drop transfer is due to an **instability**. Generally speaking, a system is stable if all types of infinitesimal perturbations lead to damped oscillations about the equilibrium state, and unstable if one or more types of perturbation grow exponentially, in the manner which has been observed experimentally for drops in GMA welding. In order to analyse the effect of perturbations on the drop at the electrode tip we will begin by considering instability in a cylindrical column of liquid, and then relate the geometry of a perturbed cylinder to that of the drop.

Consider first a cylinder in which no electric current is flowing. If the surface is deformed in a sinusoidal manner of the type shown in Figure 3.1, the pressure in the liquid due to surface tension is modified. When the pressure in the bulged regions exceeds that in the pinched regions, liquid will flow from bulge to pinch and the system is stable, while if the pressure gradient is in the opposite sense, the system is unstable and the cylinder disperses into droplets. The direction of the pressure gradient depends upon the **wavelength** λ of the surface deformation, and it may readily be shown that the system becomes unstable when the wavelength **exceeds** $2\pi R_0$, where R_0 is the initial outer radius of the cylinder.

The presence of an axial electric current in the cylinder reduces its stability; that is to say, it is unstable at wavelengths that become progressively shorter as the current increases. This is because the fluid pressure generated by the electromagnetic force increases with the current density, and is therefore higher in the pinched than in the bulged regions. There is a critical wavelength λ_c at which the system is **neutral**, i.e. neither stable nor unstable. At shorter wavelengths

surface tension acts to stabilise the cylinder and inhibits the destabilising effect of the axial current.

To obtain a quantitative result, and in particular to calculate the critical wavelength and the time constant for the instability, it is necessary to carry out a **dispersion analysis**. A sinusoidal perturbation of small amplitude ϵ is applied to the cylindrical surface:

$$r = R_0 + \epsilon \cos \left(\frac{2\pi R_0}{\lambda} \right) \quad (3.10)$$

It is further assumed that the perturbation is periodic in time, so that

$$\epsilon = \epsilon_0 \cos(\omega t) \quad (3.11)$$

The distributions of current density, of the self-induced magnetic field and of fluid pressure are now calculated. These quantities are inserted in the momentum equation (Equation 3.2), which leads to the **dispersion equation** and hence to a value of ω^2 . In obtaining this result the terms representing viscosity and gravitational force in the momentum equation are ignored, as are higher-order terms. The validity of these approximations can be determined only by experiment.

In the case of the cylindrical pinch mode (it will be seen later that there are other modes of instability) the instability may be generated by oscillations in either the radial or in the axial direction, and in the presence of an electric current the axial mode dominates. The dispersion equation in this case is:

$$\omega^2 = \frac{\gamma}{\rho R_0^3} \frac{x^2}{2I_0(x)} \left[(x^2 - 1) - \frac{\mu_0 I^2}{2\pi^2 R_0 \gamma} \right] \quad (3.12)$$

where $x = 2\pi R_0/\lambda$ and $I_0(x)$ is the modified Bessel function of the first kind of order zero. When ω^2 is positive the forces generated during the oscillation act towards the centre and the system is stable; if ω^2 is negative it is unstable. The way in which ω^2 varies with x is shown in Figure 3.2. For high values of x (small wavelengths) ω^2 is positive, but as x falls ω^2 becomes zero (the neutral point) and then falls to a minimum value where the wavelength is λ_m and the growth rate of the instability is a maximum. Thus, in a molten fuse wire it is predicted that the cylinder will disintegrate into drops whose centres of gravities are separated by a distance equal to λ_m , corresponding to x_m and the maximum growth rate. In a falling column of liquid the point at which it disintegrates will depend on the rate of fall as well as the maximum growth rate. In the case of a drop forming at an orifice, or a melting drop, the geometry is no longer cylindrical, and it is necessary to set up a model to relate the form of the drop to that of a deforming cylinder. Such a model is shown in Figure 3.1. The profile of the drop is assumed to follow a sinusoidal form, with the orifice or solid/liquid interface at $z = 0$ and the tip at about 0.8λ . The maximum radius R_d is at $z = \lambda/2$. The supposed initial radius of the deformed cylinder R_0 is, to a good approximation, $\frac{1}{2}(R_d + R_e)$ where R_e is the electrode radius. It is then assumed that the model will behave in the same way as an undeformed cylinder of

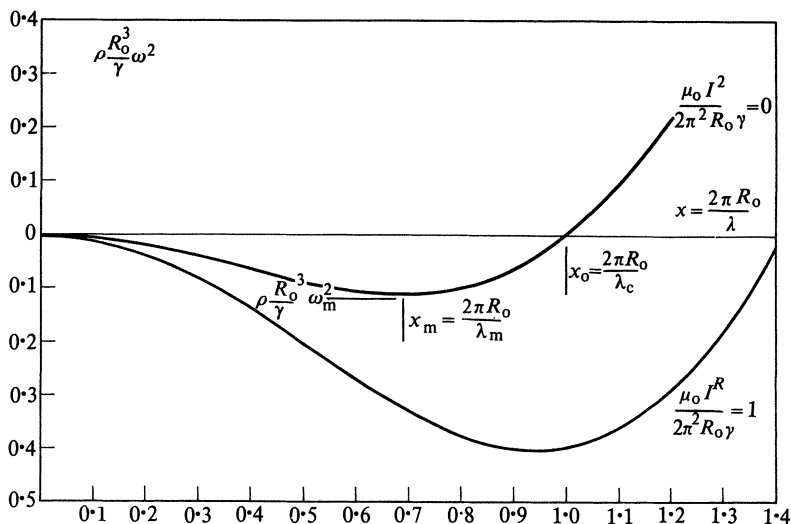


Figure 3.2 Non-dimensional growth rate constant for axial pinch instability as a function of $x = 2\pi R_0/\lambda$.

radius R_0 . Now initially the value of λ is small because the drop is short in length. As the drop grows, its length grows faster than $\frac{1}{2}(R_d + R_e)$ and therefore the value of x falls until it reaches the critical value x_c . Any further growth or oscillation permits an instability to initiate and the drop will detach, having reached a length somewhere between $0.8\lambda_c$ and $0.8\lambda_m$. In practice the instability grows faster than the drop grows in length so that it probably detaches close to λ_c . To quantify this model still further it will be assumed that the drop detaches when its forward displacement is R_0 . The displacement is exponential and therefore the initial velocity and acceleration may be found by substituting R_0 for δ in Equations 3.8 and 3.9. The value of ω must lie between zero and ω_m , corresponding to the maximum growth rate, and it seems reasonable that the actual value of ω will be somewhere between $\omega/10$ and ω_m . From observed values of drop radius for various currents it is then possible to calculate ω_m , λ_c and λ_m using Equations 3.8, 3.9 and 3.12. Note that instability requires ω^2 to be negative. This means that the expression within the square brackets in Equation 3.12 must be negative for instability and zero at the neutral point. Hence,

$$\lambda_c = \frac{2\pi R_0}{\left[1 + \frac{\mu_0 I^2}{2\pi R_0 \gamma}\right]^{1/2}} \quad (3.13)$$

and the calculated drop length at the neutral point is $0.8\lambda_c$ from Figure 3.1. Measured values of initial velocity, initial acceleration and drop length are compared with the limits calculated as indicated above and are shown in Figures 3.3, 3.4 and 3.5. It would appear that the model is at least self-consistent.

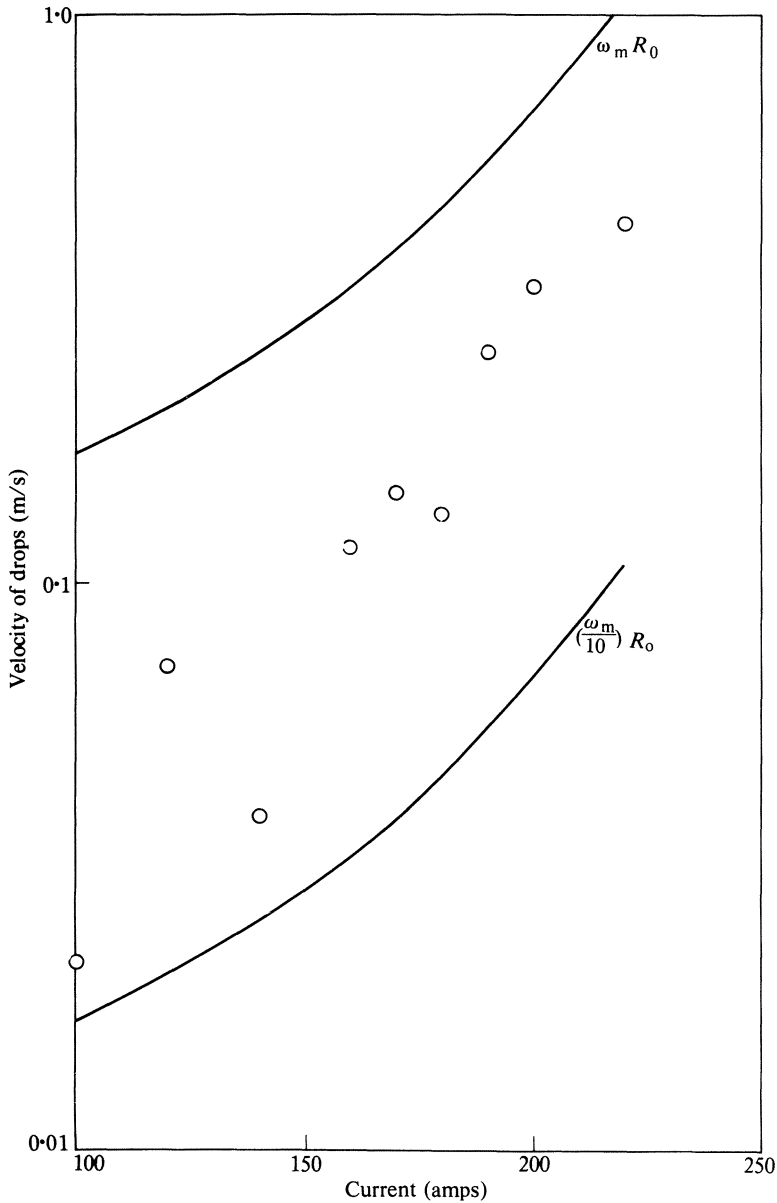


Figure 3.3 Initial velocity of drops in GMA welding using 1.2 mm diameter steel wire. ○ Measured values (J. Pintard, IIW document 212-89-66).

3.3.2 Other modes of instability

The pinch is not the only mode of instability promoted by the presence of an axial electric current in a cylindrical conductor. Suppose that the cylinder is perturbed in the radial as well as in the axial direction, such that:

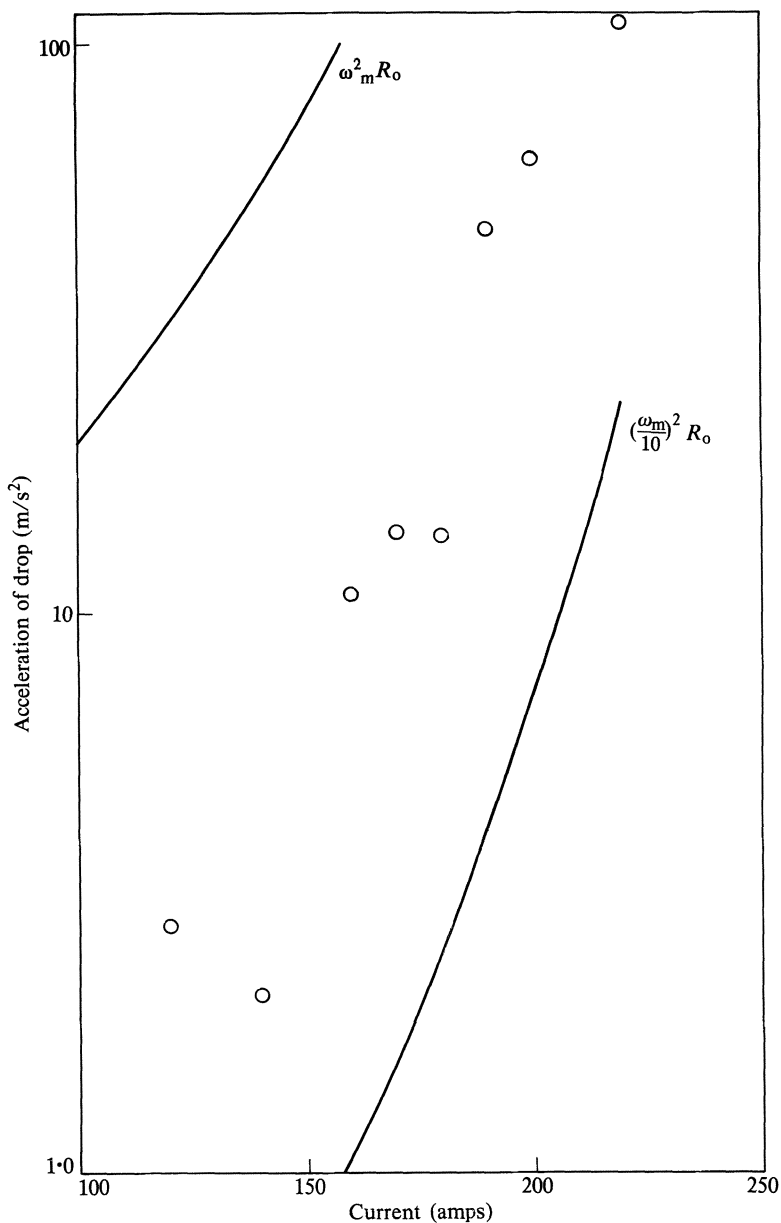


Figure 3.4 Initial acceleration of drops in GMA welding using 1.2 mm diameter steel wire. ○ Measured values (J. Pintard, IIW document 212-89-66).

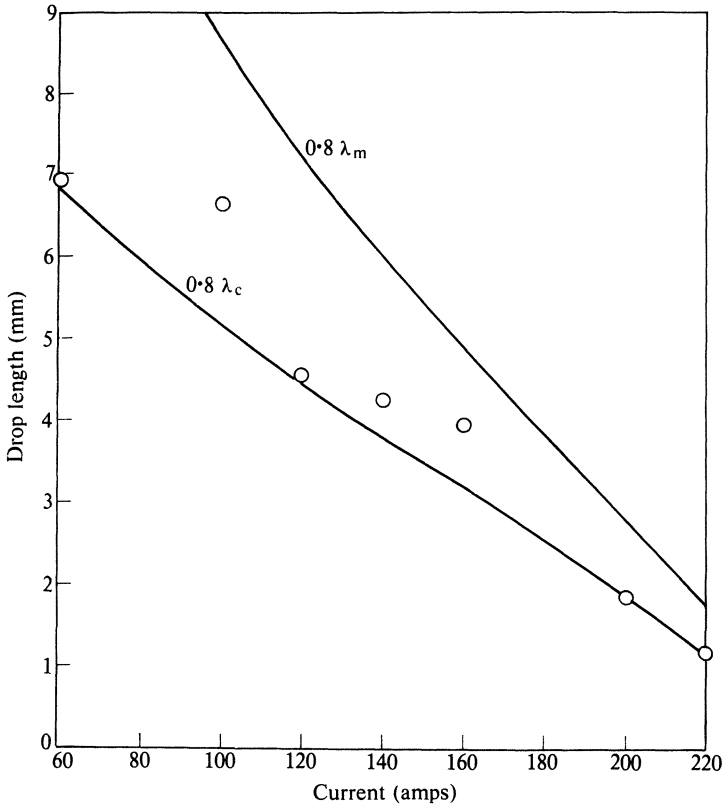


Figure 3.5 Drop length as a function of welding current.

$$r = R_0 + \epsilon \cos \left(m\theta + \frac{2\pi z}{\lambda} \right) \quad (3.14)$$

For $m = 0$, this reduces to Equation 3.10, corresponding to the **pinch** instability (physicists sometimes refer to this as the '**sausage-mode**' or **varicose** instability). When $m = 1$ the radial cross section is asymmetrical and the asymmetric hump spirals along the cylinder. In this mode, known as the **kink** instability, the cylinder collapses into a rotating spiral. If $m = 2$ a pair of spiral **flutes** (like the flutes of a column) appear in the cylinder and when it becomes unstable it splits longitudinally into two parts. Normally the lower unstable modes (i.e., lower values of m) develop in preference to higher modes. However, in the presence of a longitudinal magnetic field these positions may be reversed and, for example, the kink instability may dominate instead of the pinch. With still higher currents and magnetic fields the flute instability will, in theory, dominate over the other two. In GMA welding these predictions are generally borne out, except that the kink instability develops spontaneously at high currents (possibly because it generates its own longitudinal magnetic field). For a more detailed exposition of electromagnetically induced instabilities the reader should consult

the papers by Murty referenced under 'Further Reading' at the end of this chapter.

In argon-shielded GMA welding and GTA welding the current flow is usually axisymmetric so that it is possible for electromagnetic forces to be operative. Where the shield is chemically active, for example with CO_2 gas shielding or flux shielding, forces due to chemical reaction or vaporisation disturb the axial symmetry and may partially or completely inhibit the action of electromagnetic forces. In general, electromagnetic forces become relatively more important as the current density at the wire tip increases and as the chemical activity of the shield decreases, and vice versa.

Table 3.2 summarises the forces thought to be dominant in the various modes of metal transfer, and the mode of instability, where appropriate. Note that in globular transfer the effect of gravity is to elongate the drop, and to promote instability by increasing the wavelength λ for any given drop volume.

Table 3.2 Dominant forces in metal transfer

<i>Transfer type</i>	<i>Dominant force or mechanism</i>
1 Free flight	
1.1 Globular	
1.1.1 Drop	Gravity and electromagnetic pinch
1.1.2 Repelled	Chemical reaction generating vapour
1.2 Spray	
1.2.1 Projected	Electromagnetic pinch instability
1.2.2 Streaming	Electromagnetic
1.2.3 Rotating	Electromagnetic kink instability
1.3 Explosive	Chemical reaction to form a gas bubble
2 Bridging transfer	
2.1 Short-circuiting	Surface tension + electromagnetic forces
2.2 Bridging transfer without interruption	Surface tension + (hot wire) electromagnetic forces
3 Slag-protected transfer	
3.1 Flux-wall guided	Chemical and electromagnetic
3.2 Other modes	Chemical and electromagnetic

3.4 MASS FLOW IN THE WELD POOL

Assuming that the weld pool is a hemisphere of radius a , that the current enters at the central point and spreads uniformly into the liquid, it is possible to obtain an analytical solution for the flow provided that inertia effects are ignored. In the spherical co-ordinate system the stream function is

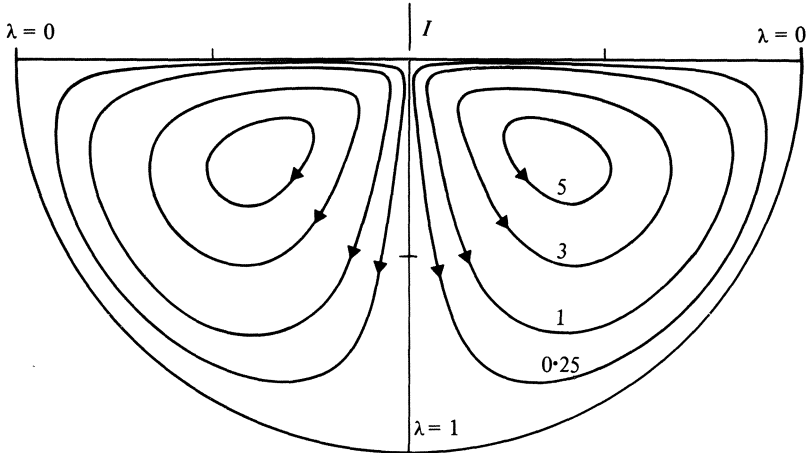


Figure 3.6 Streamlines for current-induced flow in a hemisphere. Numbers on curves are values of $2000\pi^2\eta\psi/\mu_0I^2$.

$$\psi \simeq \frac{\mu_0 I^2 r}{4\pi^2 \eta} (1 - \lambda^2) \lambda \left[1 - \left(\frac{r}{a} \right)^2 \right]^2 \left\{ \frac{5}{48} - \frac{3}{1280} \left[2 \left(\frac{r}{a} \right)^2 + 1 \right] (7\lambda^2 - 3) \right. \\ \left. + \frac{13}{43008} \left[3 \left(\frac{r}{a} \right)^4 + 2 \left(\frac{r}{a} \right)^2 + 1 \right] (33\lambda^4 - 30\lambda^2 + 5) \right\} \quad (3.15)$$

where $\lambda = \cos \theta$ and streamlines are as shown in Figure 3.6. This type of flow is designated **toroidal** and it has been reproduced experimentally using low melting-point metals contained in a bowl-shaped dish.

It may be shown that a toroidal flow will cause distortion of the liquid surface, such that the surface is depressed around the point of entry of the current. Such distortion has been observed experimentally.

Note that both theory and experiment here relate to a static pool whereas in welding practice (other than spot welding) the pool moves relative to the surrounding solid metal. Note also that in reality the current source is not point-like but is distributed. These factors would tend to weaken the toroidal flow. Indeed, the observed flow on the surface of a GTA weld pool is usually rotational with the direction of rotation being affected by the direction of current flow through the workpiece. It is quite possible, of course, that the rotational motion is superimposed on toroidal flow.

The pattern of flow in submerged arc welding has been well established by experimental work and is illustrated in Figure 3.7. There is a relatively deep depression in the weld pool surface below the arc. The liquid metal flows rapidly around and under this depression, and then runs backwards along the solid/liquid interface and reverses to produce a forward flow on the weld pool surface. Similar depressions are observed below the arc in SMA and GMA welding and it is probable that a similar flow pattern occurs with these processes also. The flow in such cases is largely determined by the forward motion of the arc

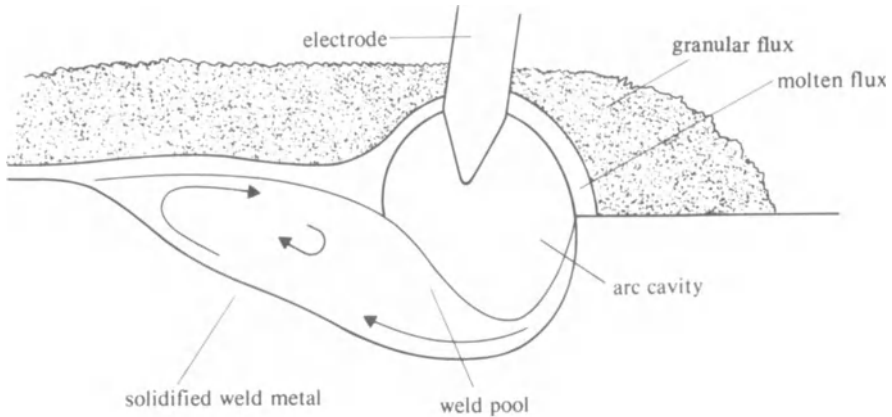


Figure 3.7 Typical form of weld pool in SA welding.

combined with the depression in the weld pool, which imposes a rearward acceleration on the liquid metal (see also Section 3.5.4).

3.5 HEAT FLOW: GENERAL

In the case of a solid moving with velocity v in the direction of the x axis, Equation 3.4 reduces to

$$\alpha \nabla^2 T - v \frac{\partial T}{\partial x} = 0 \quad (3.16)$$

where $\alpha = \kappa / \rho C_p$ is the **diffusivity of heat**. Solutions to this equation are usually obtained assuming a **point heat source** and the temperature distribution is calculated relative to the source as origin. In practice, heat sources are finite, and in many cases convection in the weld pool is strong enough to distort the temperature distribution in the surrounding solid metal. Nevertheless, the simple point source solutions give a sufficiently good approximation for many purposes.

Before proceeding to a discussion of heat flow, it is necessary to consider the nature of heat sources and, in particular, the electric arc.

3.5.1 Heat sources

In the mathematical treatment of heat flow there are three geometrical forms of heat source: a point source, a line source and a plane source. The distinction between a penetrating and a surface-welding heat source has already been made in Chapter 2. The medium-current welding arc is usually considered a surface heat source and is treated mathematically as a point, while penetrating sources such as electron-beams and lasers are treated as line heat sources. Heat flow in the electrode may under certain conditions approximate to that of a plane

heat source. The corresponding heat-flow regimes are **three-dimensional**, **two-dimensional** and **unidimensional** or **linear**. In welding it is also necessary to take account of the thickness of the material. For example, in fusion welding steel of 12 mm thickness or less, the heat source is best treated as a line, whereas with thicknesses above 25 mm it may be assumed to act as a point source. At intermediate thicknesses the temperature distribution is similar to that produced by a combination of point and line sources.

It is also necessary to distinguish between an **instantaneous** and a **continuous** source. Spot welding approximates to an instantaneous source in that the heat is liberated during a very short period of time, while arc welds are normally made with continuous sources. There may also be **periodic** heat sources, as in resistance seam welding and pulsed arc welding.

3.5.2 The welding arc

The electric arc that is used in welding is a high-current, low-voltage discharge, operating generally in the range 10–2000 amperes and at 10–50 volts. Broadly speaking, the arc constitutes a mechanism whereby electrons are evaporated from the **cathode**, transferred through a region of hot, ionised gas to the **anode** and there condensed. Structurally the arc may be divided into five parts (Fig. 3.8):

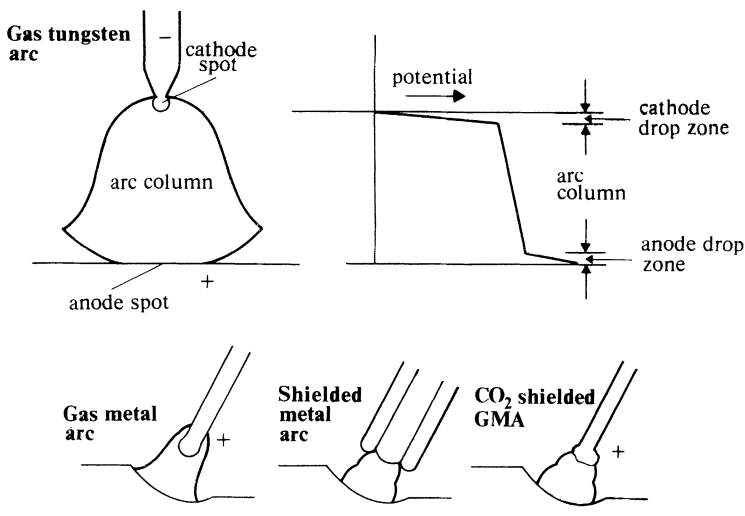


Fig. 3.8 Arc appearance and structure

- The **cathode spot**: that part of the negative electrode from which the electrons are emitted.
- The **cathode drop zone**: the gaseous region immediately adjacent to the cathode in which a sharp drop of potential occurs.

- (c) The **arc column**: the bright, visible portion of the arc, characterised by high temperature and a low potential gradient. (The column consists of **plasma**, highly ionised gas which is electrically conductive.)
- (d) The **anode drop zone**: the gaseous region immediately adjacent to the anode in which a further sharp drop of potential takes place.
- (e) The **anode spot**: the portion of the positive electrode within which the electrons are absorbed.

3.5.2.1 Electrode interactions

The energy required to evaporate one electron from a metal surface to the surrounding space is known as the **work function** ϕ_e (Table 3.3).

Table 3.3 Electron work function and ionisation potential of pure metals

<i>Metal</i>	<i>Work function electron-volts</i>	<i>First ionisation potential, V</i>
Aluminium	4.0	5.96
Barium	2.1	5.19
Calcium	2.2	6.09
Copper	4.3	7.68
Iron	4.5	7.83
Nickel	5.0	7.61
Potassium	2.2	4.3
Sodium	2.3	5.12
Tungsten	4.5	8.1

At the arc cathode this energy is derived from incoming positive ions that are accelerated through the cathode drop zone. If the cathode spot temperature is higher than that of the surrounding metal, heat is lost through the electrode at a rate q_e , and the overall energy balance is approximately

$$V_c I = \left(\phi_e + \frac{3}{2} \frac{kT}{e} \right) I + q_e \quad (3.17)$$

where V_c is the cathode drop and $3/2(kT/e)$ the thermal energy of the electrons. At the anode the electrons condense and give up energy to the electrode equal to the work function plus the thermal energy plus that gained in passing through the anode fall of potential V_a :

$$q_a = \left(\phi_e + \frac{3}{2} \frac{kT}{e} + V_a \right) I \quad (3.18)$$

In the arc column energy is lost mainly by convection (see Section 3.5.2.2);

$$q_p = V_p I \quad (3.19)$$

In the case of GTA welding the tungsten electrode is the cathode and the

workpiece is the anode. Assuming that a proportion of the arc column loss n is absorbed by the anode, the total rate of heat input to the anode is

$$\begin{aligned} h_a &= q_a + nq_p \\ &\simeq VI - [q_c + (1 - n)V_p I] \end{aligned} \quad (3.20)$$

where V , the total arc voltage, is equal to $V_a + V_p + V_c$. The arc efficiency is $\eta = h_a/VI$ and therefore

$$\eta = 1 - \frac{[q_c + (1 - n)V_p I]}{VI} \quad (3.21)$$

q_c is substantial in GTA welding and, hence, the efficiency of the process is relatively low. Where a consumable electrode is used, as in GMA, SMA and SA welding, most of the electrode heat passes over to the workpiece and the arc efficiency is high. This is particularly the case in SAW where the arc is surrounded by an insulating blanket of molten and granular flux.

Arc efficiency is not an important factor in the economics of welding processes, but it must be known for calculations of heat input rate. Figure 3.9 shows arc efficiencies for a number of processes operating in a three-dimensional (bead-on-plate) heat flow regime.

When the GTA process is used with electrode negative, the cathode spot that forms on the tungsten electrode is of a **thermionic** type. In a thermionic cathode the temperature is high enough for a proportion of the electrons to be able to jump the potential barrier at the metal surface. Such cathodes have a current density in the range 10^7 – 10^8 A/m² and are characteristically static and stable. Most engineering metals, however, boil at a temperature below that required for thermionic emission of electrons (see Fig. 3.10). The type of cathode spot that forms on these metals is designated **non-thermionic** or **mobile**.

Non-thermionic cathodes have a current density of 10^9 to 10^{10} A/m² and move over the metal surface, removing oxide films that may be in their track. The velocity of movement is reduced as the thickness of the oxide film increases. Multiple cathode spots may form, and individual spots may have a limited, and sometimes very short, lifetime. While there is no general agreement about the mechanism of the non-thermionic cathode, it is evident that oxide films play a significant role in their operation. One interpretation of this fact is that positive ions condense on the surface of the oxide and thereby set up a sufficiently high potential gradient to vaporise the film and either draw electrons out of the metal or generate them by ionisation of the vapour.

Non-thermionic cathodes play a useful role in welding metals like aluminium, where the oxide film may interfere with the formation of a sound fusion joint. In other cases the mobility of the cathode spot may cause instability. In the GMA welding of steel with electrode negative there is excessive arc movement unless the wire is coated with a substance that restricts the arc root to the electrode tip. Likewise it may be necessary to use an oxidising gas for GMA

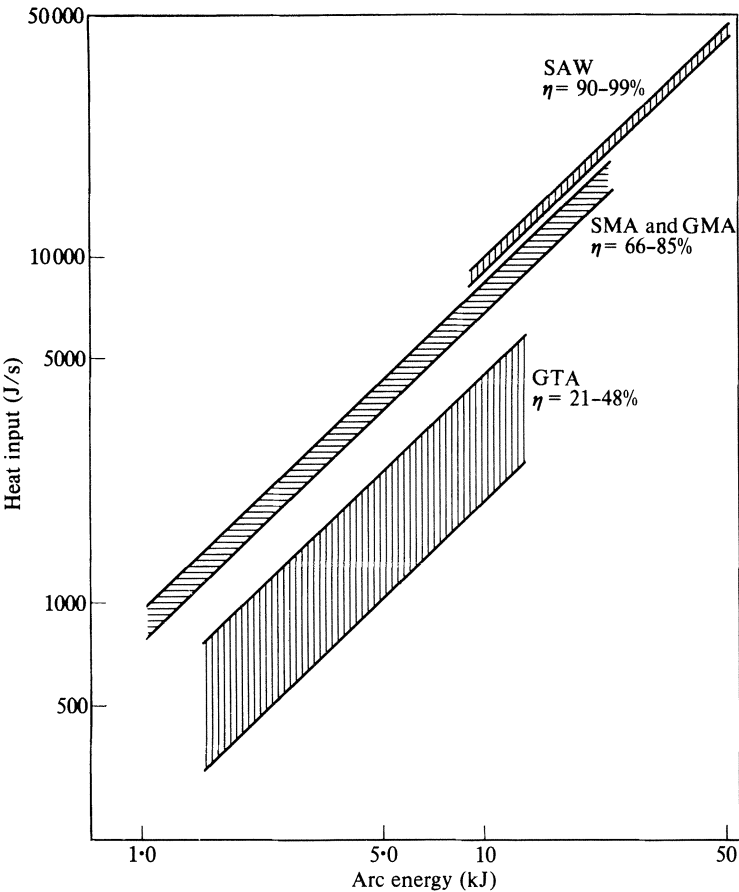


Figure 3.9 Measured arc efficiency η (after Christensen *et al.*).

electrode positive welding of steel (Section 2.2.4) to avoid excessive arc wander over the plate surface.

The anode appears to play a more passive role than the cathode in arc welding; for example, the current density depends on external factors such as gas temperature and the form of the electrode. In GMA welding with electrode positive, the anodic arc root on the electrode increases in size with increasing current, as does the anode on the workpiece in GTA welding, the current density being of the order 10^7 A/m^2 for GTA welding.

3.5.2.2 The arc column

The gas in the space between the cathode and anode is at a temperature sufficient for it to be electrically conductive (Table 3.4). At such temperatures any molecules present in the arc are dissociated wholly or partially into their constituent atoms, and the atoms themselves are ionised. The arc column is

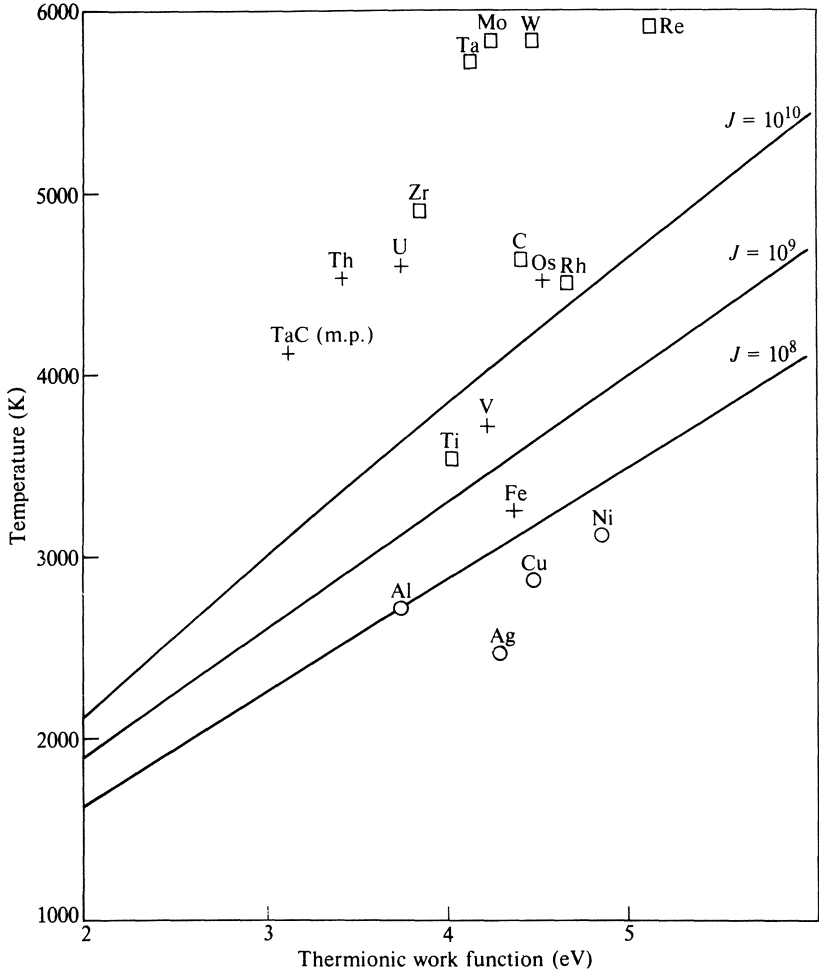


Figure 3.10 Temperature for thermionic emission at various current-density levels. Individual points show boiling point of pure elements versus work function. Elements known to produce thermionic type arcs in argon: □ Elements for which thermionic type emission has not been observed: ○ Elements for which information is lacking: + J is in A/m².

Table 3.4 Temperature of the arc column in various gases

Gas	Temperature of arc column close to cathode (K)
Alkali metal vapour	4000
Alkaline earth vapour	5000
Iron vapour	6000
Argon (200 amp)	10000–15000

Table 3.5 Dissociation of gases in the arc

<i>Gas</i>	<i>Temperature for 90% dissociation (K)</i>
CO ₂	3800
H ₂	4575
O ₂	5100
N ₂	8300

substantially in thermal equilibrium, so that a good estimate of the degree of dissociation and ionisation may be obtained using the relevant thermochemical data (Table 3.5). The arc column is **electrically neutral**, that is to say the number of electrons and positive ions present in any given volume is equal. However, because the mass of the electron is about one-thousandth of that of the lightest positive ion, its mobility is much higher. Consequently, most of the current is carried by electrons. The potential gradient in the column is low relative to that in the anode and cathode drop regions, in the range 5×10^2 to 5×10^3 V/m.

The existence of a jet-like flow in the arc column has been known for numbers of years and was first examined theoretically by Maecker. In a static conducting fluid cylinder the radial distribution of pressure due to the interaction between the current and its self-induced magnetic field is:

$$p = \frac{\mu_0 I J}{4\pi} \left[1 - \left(\frac{r}{R_0} \right)^2 \right] \quad (3.22)$$

and the pressure along the axis ($r = 0$) is $\mu_0 I J / 4\pi$. Maecker suggested that at points of maximum constriction in the column (for example at the cathode spot of a tungsten/argon arc) this would be the stagnation pressure, but away from the stagnation point there would be a corresponding velocity v :

$$\frac{1}{2} \rho v^2 = \frac{\mu_0 I J}{4\pi} \quad (3.23)$$

A better approximation to the flow is obtained using a solution to the momentum equation due to Squire. This gives the flow in an infinite medium resulting from the application of a force F at the origin. Return to Equation 3.22, we note that the electromagnetically-induced pressure exerts a longitudinal force:

$$F = \int_0^{R_0} 2\pi r p dr = \frac{\mu_0 I^2}{8\pi} \quad (3.24)$$

independent of the radius of the conductor. Supposing this to be the force exerted at the origin, the Squire solution may be related (somewhat arbitrarily) to arc current. The relevant stream function is, in spherical co-ordinates:

$$\psi = \frac{2\nu r(1 - \lambda^2)}{1 + C - \lambda^2} \quad (3.25)$$

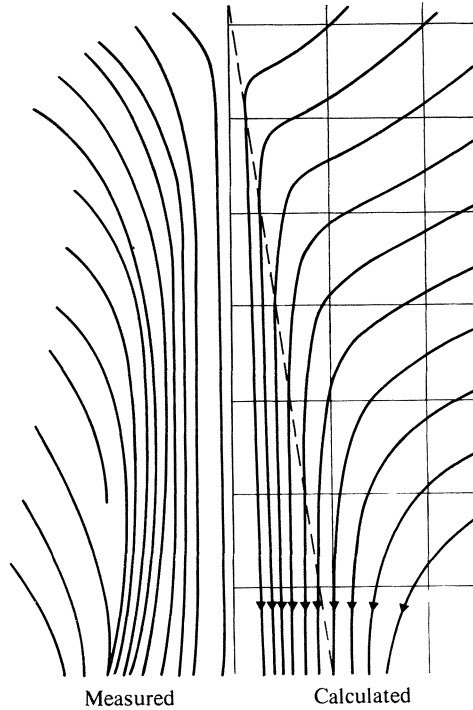


Figure 3.11 Measured and calculated streamlines for a 200 A carbon arc (Wienecke, R, 1955, *Z. Physik* 143, 135).

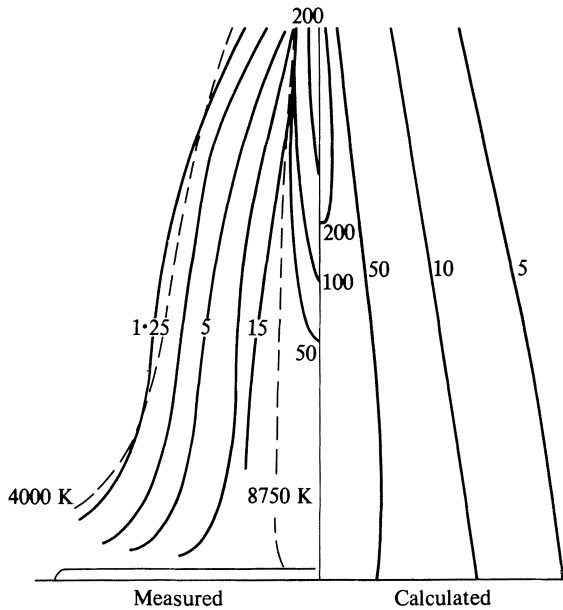


Figure 3.12 Measured and calculated velocity field for a 200 A carbon arc. Numbers on the curves are velocity in m/s (Wienecke, R, 1955, *Z. Physik* 143, 135).

where $\lambda = \cos \theta$ and C is a constant of integration which, at high flow rates, is

$$C = \frac{256\pi^2 \rho v^2}{3\mu_0 I^2} \quad (3.26)$$

Streamlines and constant velocity envelopes calculated from Equations 3.25 and 3.26 are compared with measured values for a 200 A carbon arc in Figures 3.11 and 3.12.

If it is assumed that at the same time as the force F there is a heat source of strength q at the origin, a solution of Equation 3.4 gives the temperature distribution as

$$T = \frac{A}{r} \left(\frac{C}{C+1-\lambda} \right)^{2P_r} \quad (3.27)$$

$$\frac{q}{4\pi\eta C_P} = A \left[\left(\frac{C+2}{2P_r+1} \right) \left\{ 1 - \left(\frac{C}{C+2} \right)^{2P_r+1} \right\} - \left(\frac{C}{2P_r-1} \right) \left\{ 1 - \left(\frac{C}{C+2} \right)^{2P_r-1} \right\} \right] \quad (3.28)$$

where $P_r = \rho\eta/\kappa$ the Prandtl number of the gas. Isotherms for argon with $C = 0.01$ (equivalent to about 100 A) and $P_r = 0.72$ (temperature 12 500 K) are shown in Figure 3.13. The numbers on the curves indicate relative temperatures. The form of the isotherms is similar to the profile of argon/tungsten arcs where the anode has been displaced to one side, giving unimpeded flow to the plasma. There are, however, more uncertainties in obtaining a quantitative result than in the case of mass flow because the physical properties and particularly the Prandtl number vary over a wide range depending on the assumed temperature.

One of the useful effects of axial flow in the arc column is to generate **stiffness**. A column of gas cannot, in the nature of things, possess the quality of rigidity. A jet, however, will resist lateral deflection and the higher its velocity the higher such resistance will be. The arc column may be deflected laterally by a wind or by a transverse magnetic field. Magnetic fields may be set up as a result of anisotropic current flow in the workpiece, generally due to the placing of the earth return, or they may result from magnetisation of plate material, particularly in the case of nickel alloy steels. Such fields impose a transverse $\mathbf{J} \times \mathbf{B}$ force on the column and cause **arc blow**: i.e. deflection of the column resulting in loss of control of the welding operation. The column may be stabilised against arc blow by imposing a longitudinal magnetic field (which also causes the plasma to spin), and in GTA welding by tapering the tungsten electrode more sharply or by imposing a medium-frequency pulse on the arc current.

3.5.3 Heat flow in the electrode

3.5.3.1 Time-dependent heat flow

For the linear flow of heat in a solid rod heated at the tip Equation 3.3 reduces to

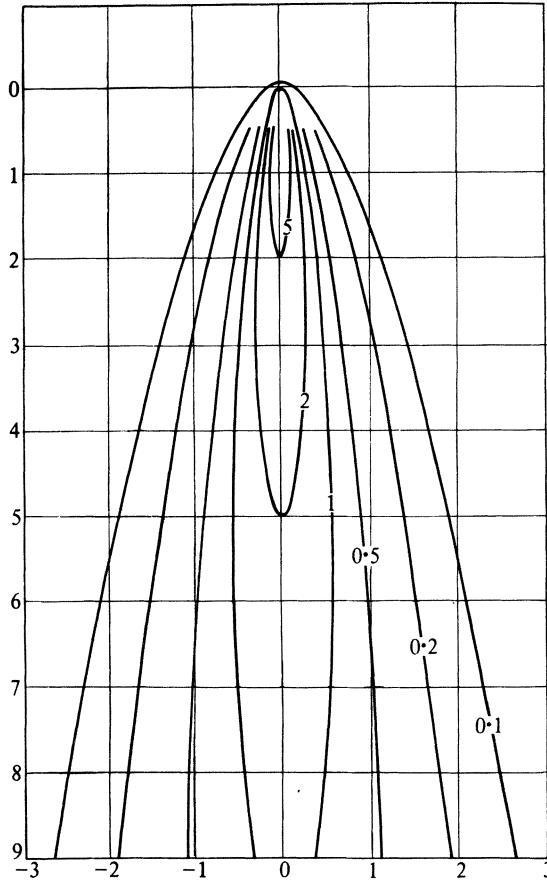


Figure 3.13 Calculated isotherms for a heated jet. $C = 0.01$, $Pr = 0.72$, $A = 10$ (Squire, H. B, 1951, *Quart. J. Mech. Appl. Math.* IV, 321).

$$\kappa \frac{\partial^2 T}{\partial z^2} = \frac{\partial T}{\partial t} \quad (3.29)$$

where z is axial distance. In the case of a constant heat flux across the end of the rod the solution to Equation 3.29 is

$$T = \frac{2q(\alpha t)^{1/2}}{\kappa} \operatorname{ierfc} \frac{z}{2(\alpha t)^{1/2}} \quad (3.30)$$

ierfc is tabulated in Carslaw and Jaeger (see 'Further Reading'). The temperature at the tip $z = 0$ is

$$T = \frac{2q}{\kappa} \left(\frac{\alpha t}{\pi} \right)^{1/2} \quad (3.31)$$

In the case of a welding electrode the linear geometry is modified by the shape of the liquid drop and the effective conductivity is increased by convection. In using Equation 3.30 and 3.31 due allowance must be made for these factors.

The equation for time-dependent linear heat flow is also used in theoretical models of resistance welding, particularly spot welding.

3.5.4 Heat flow in the weld pool

In static weld pools the heat flow is due to conduction and theoretical temperature distributions are no different to those calculated for solid metal. In the normal case, however, the mass flow rate is sufficient to generate convective heat flow. If the mass flow is isotropic, as in the ideal case of toroidal flow, then the temperature gradient across the weld pool will fall but the temperature distribution beyond the weld pool boundary will be the same as for pure conduction. When flow in the weld pool is anisotropic (as it normally is) the shape of the weld pool is modified. For example, if there is a strong flow of metal from front to rear the effect will be to elongate the weld pool. The thermal cycle in the solid metal will likewise be affected.

In GTA welding a spinning weld pool results in a displacement of the pool relative to the weld centreline. In submerged-arc and GMA welding the longitudinal flow of metal is associated with an increase in length of the weld pool, which averages 60% longer than the value calculated from the point source equation. In cross section such weld deposits may show a double profile which is probably associated with the reversal of flow at the rear of the weld pool. In extreme cases, hot tears may be generated at the junction of the two solidification patterns.

The temperature of the weld pool has been measured by a number of investigators. For steel the temperature may be expected to vary from the melting point up to 2100 °C and for aluminium up to 1000 °C. In the case of high energy density welding the surface temperature rises to the boiling point, and it is possible that such temperatures are also obtained in plasma and high-current GTA welding.

3.5.5 Heat flow in the solid workpiece: theory

It will be evident that convective effects in the weld pool will modify the temperature distribution in the solid plate as compared with that obtained in an isotropic medium. In addition, it must be borne in mind that latent heat is absorbed at the forward edge of the weld pool and liberated at the rear, and that the physical properties governing heat flow, thermal conductivity and diffusivity, vary with temperature. Thus, analytical solutions of the energy equation assuming a point or line heat source will only give an approximation to the actual temperature distribution. Nevertheless, these solutions are valuable in developing an overall picture of the character of heat flow in welding and the nature of the thermal cycle.

Assuming that joule heating can be neglected, Equation 3.3 reduces, for a solid material, to

$$\kappa \nabla^2 T - \rho C_P (\mathbf{v} \cdot \nabla) T = \frac{\partial T}{\partial t} \quad (3.32)$$

In the steady state $\partial T / \partial t = 0$. Also, for a solid \mathbf{v} is uniform and if its direction coincides with the x axis $(\mathbf{v} \cdot \nabla) T$ becomes $v(\partial T / \partial x)$. Putting $\kappa / \rho C_P = \alpha$ (the thermal diffusivity) gives the equation for steady heat flow in a moving solid:

$$\alpha \nabla^2 T - v \frac{\partial T}{\partial x} = 0 \quad (3.33)$$

When there is no relative movement between the body and the heat source Equation 3.33 reduces to the Laplace equation

$$\nabla^2 T = 0 \quad (3.34)$$

The equation for the diffusion of heat is linear and analytical solutions are available for many boundary conditions. Those most relevant to fusion welding are, in rectangular co-ordinates (x, y, z) .

- (a) A point heat source strength q moving with velocity v relative to a semi-infinite plate

$$T = \frac{q}{2\pi\kappa r} e^{-v(r-x)/2\alpha} \quad (3.35)$$

where $r^2 = x^2 + y^2 + z^2$

- (b) A line source strength q' per unit length moving with velocity v relative to an infinite plate of any thickness

$$T = \frac{q'}{2\pi\kappa} e^{vx/2\alpha} K_0\left(\frac{vr}{2\alpha}\right) \quad (3.36)$$

where $r^2 = x^2 + y^2$

- (c) A plane heat source of strength q'' per unit area moving with velocity v relative to a semi-infinite rod, or other regular section.

$$T = \frac{q''}{\rho C_P v} \quad \text{if } x > 0$$

$$T = \frac{q''}{\rho C_P v} e^{vx/\alpha} \quad \text{if } x < 0 \quad (3.37)$$

(a) represents an approximation to the conditions in multi-pass welding on thick plate; (b) approximates to single-pass welding of thin sheet or welding with a penetrating heat source such as an electron beam or a laser beam; (c) gives the temperature distribution in the solid portion of a welding electrode where circulation in the liquid portion is such as to make it more or less transparent to heat.

The point and line source solutions are those relevant to the temperature distribution in fusion welding. The **thermal cycle** is obtained by plotting T as a function of t (equal to x/v) for a fixed distance from the centre line $y = 0$.

One of the most important variables in fusion welding is the **cooling rate** in the weld and heat-affected zone. The theoretical cooling rate for any point (x, y, z) relative to the source as origin may be obtained by differentiation of Equations 3.35 and 3.36 to give, for the three-dimensional case

$$\frac{\partial T}{\partial t} = -\frac{vT}{r} \left[\frac{x}{r} - \frac{vr}{2\alpha} \left(1 - \frac{x}{r} \right) \right] \quad (3.38)$$

and for the two-dimensional case

$$\frac{\partial T}{\partial t} = -\frac{v^2 T}{2\alpha} \left[\frac{\frac{x}{r} K_1 \left(\frac{vr}{2\alpha} \right)}{K_0 \left(\frac{vr}{2\alpha} \right)} - 1 \right] \quad (3.39)$$

where $K_n(z)$ is a tabulated function (see references in Further Reading, p. 49).

For simplicity, consider a point along the central axis of the weld at the rear boundary of the weld pool where $r = x = x_1$ and $T = T_m$ the melting temperature. Then in the case of three-dimensional flow

$$\frac{\partial T}{\partial t} = -\frac{vT_m}{x_1} \quad (3.40)$$

while for two-dimensional flow

$$\frac{\partial T}{\partial t} = -\frac{v^2 T_m}{2\alpha} \left[\frac{K_1 \left(\frac{vx_1}{2\alpha} \right)}{K_0 \left(\frac{vx_1}{2\alpha} \right)} - 1 \right] \quad (3.41)$$

Equation 3.40 predicts that the cooling rate at the downstream edge of the weld pool will increase as the welding speed increases, and for similar welding speeds will be higher for small weld pools than for large. The cooling rates for two-dimensional flow follow a similar trend but are generally about half those for similar condition in three-dimensional flow (Figures 3.14 and 3.15). Equation 3.40 may also be expressed as follows:

$$\frac{\partial T}{\partial t} = -\frac{2\pi\kappa T_m^2}{(q/v)} \quad (3.42)$$

Thus, the cooling rate along the axis at the rear of the weld pool is inversely proportional to the parameter q/v . This quantity is known as the **heat input rate** (expressed in joules per unit length) and may be used as a means of standardising or comparing the heat flow conditions of welds. Both weld pool size and heat input rate are readily observable indicators of cooling rate, and their significance will be discussed in a later section. Note that in all cases the

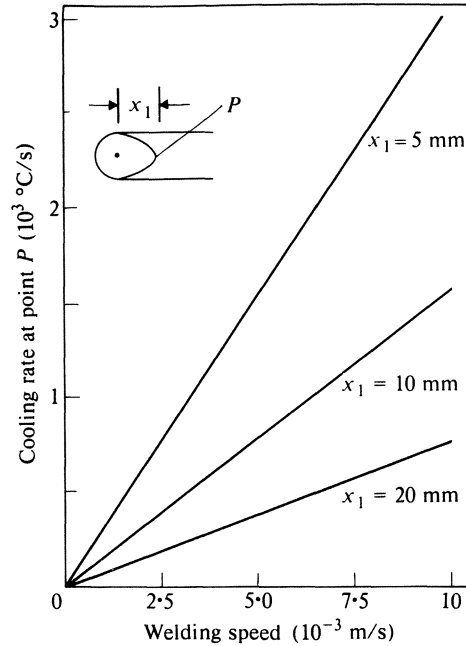


Figure 3.14 Theoretical cooling rate at rear of weld pool for three-dimensional heat flow in carbon steel, assuming a point heat source.

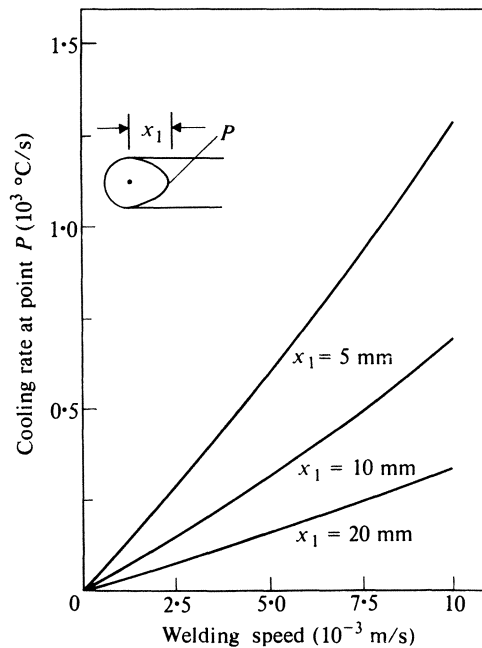


Figure 3.15 Theoretical cooling rate at rear of weld pool for two-dimensional heat flow in carbon steel, assuming a line heat source.

temperatures referred to are those in *excess of the temperature of the metal being welded*. Designating absolute temperatures as θ so that the melting temperature is θ_m and the plate temperature θ_0 we have

$$\left. \begin{aligned} T &= \theta - \theta_0 \\ T_m &= \theta_m - \theta_0 \end{aligned} \right\} \quad (3.43)$$

If the metal is **preheated** prior to welding θ_0 is the **preheat temperature**.

3.5.6 Heat flow in the solid workpiece: experimental

As a means of comparing test results with the theoretical temperature distributions generated by a point heat source, it is convenient to express the various quantities that enter into the equations in non-dimensional terms, so that

$$T_n = \frac{\theta - \theta_0}{\theta_c - \theta_0} \quad (3.44)$$

where θ_c is a chosen reference temperature.

Also

$$\bar{x} = \frac{vx}{2\alpha}; \quad \bar{y} = \frac{vy}{2\alpha}; \quad \bar{z} = \frac{vz}{2\alpha}; \quad \bar{r} = \frac{vr}{2\alpha}$$

and

$$n = \frac{qv}{4\pi\alpha^2\rho C_P(\theta_c - \theta_0)} \quad (3.45)$$

The **operating parameter** n is a non-dimensional heat input rate and governs the dimensions of the weld pool.

In these terms the temperature distribution due to a moving point source on a semi-infinite solid is

$$\frac{T_n}{n} = \frac{1}{\bar{r}} e^{-\bar{r} + \bar{x}} \quad (3.46)$$

and for a line source

$$\frac{T_n}{n} = \frac{1}{\bar{w}} e^{\bar{x}} K_0(\bar{r}) \quad (3.47)$$

where \bar{w} is a non-dimensional thickness $\bar{w} = vw/2\alpha$. By using non-dimensional terms it is possible to plot results for all materials and all welding variables on a single diagram.

Christensen *et al.* (see Further Reading, p. 49) developed the non-dimensional form of the heat flow equation and made a detailed and extensive comparison between the temperature distribution calculated from the point source equation for heat flow in three dimensions (Equation 3.35) and measured values. The test welds were made using SMA, GMA, GTA and SAW processes on steel and aluminium plate, and the results plotted in the non-dimensional form described above.

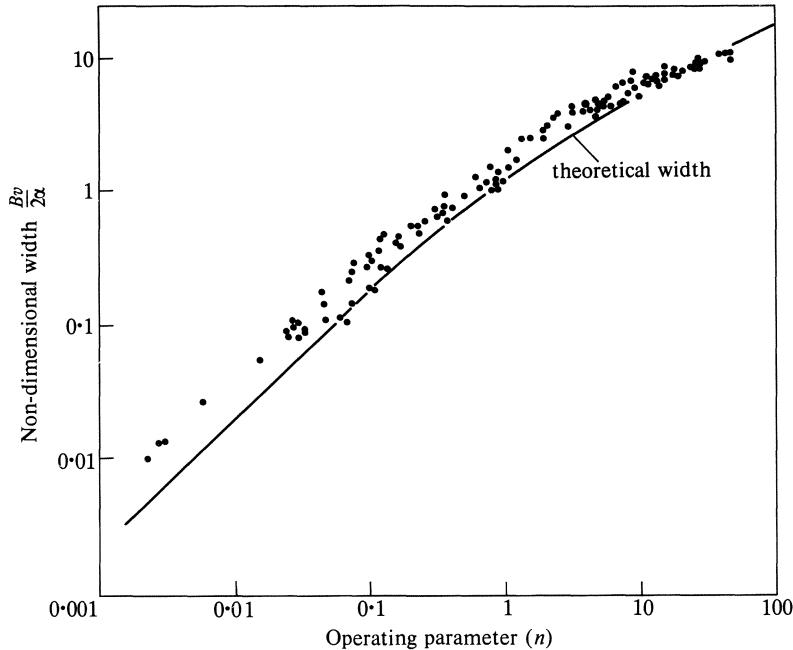


Figure 3.16 Weld bead and recrystallised-zone width.

Generally speaking, there is good qualitative agreement between calculated and measured results. For example, Figure 3.16 shows that even over a range of four orders of magnitude for the operating parameter n , the weld bead non-dimensional width follows the same trend as the theoretical curve. In detail, however, the deviations may be quite substantial: up to twice the theoretical value. The scatter in the case of weld pool depth is over a factor of five, but once again the general trend follows the theoretical curve. Bearing in mind the geometry of the molten pool, as discussed earlier, it is not surprising to find some scatter in the dimensions of the fused zone.

The peak temperature and cooling rate are important variables, particularly in the welding of steel. Figure 3.17 shows relative peak temperatures as a function of distance from the centreline. In almost every case the peak temperatures occur closer to the centreline than calculated: in other words, if the point source formula is used for calculating the peak temperature at any point it is likely to give a high value. Similarly, for cooling rates (Fig. 3.18), theoretical values are generally higher than measured values.

Thus, although the form of the weld thermal cycle can be obtained either by calculation or from the experimental results, there is uncertainty about the location (relative to the weld centreline) in which the particular thermal cycle will occur. Actual measurement of the thermal cycle may also be difficult because of the finite size of the thermocouple, which makes precise location of the measurement point uncertain. Nevertheless, in subjecting samples of

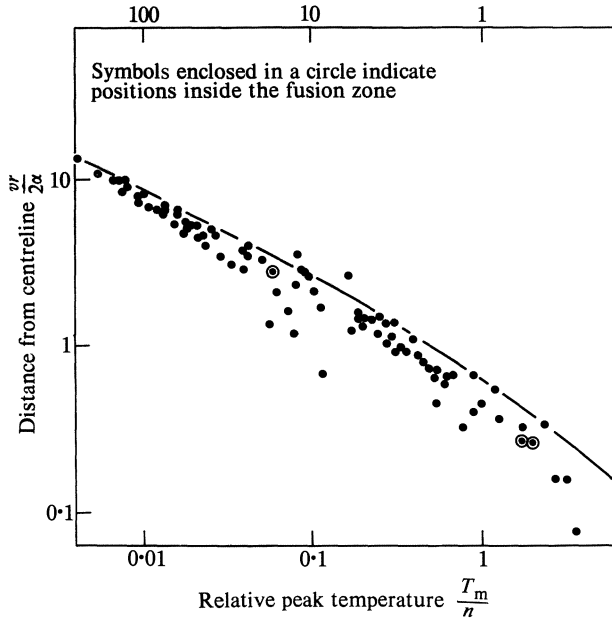


Figure 3.17 Peak temperature as a function of distance from centre line.

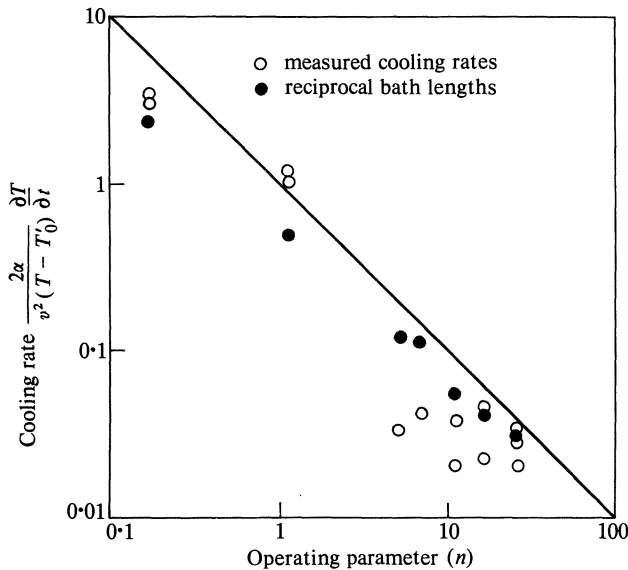


Figure 3.18 Cooling rate at rear of the weld pool (point *P* in Figs 3.14 and 3.15).

metal to simulated weld thermal cycles it is always possible to compare the resulting microstructure with that found in the appropriate portion of the weld heat-affected zone.

In the welding of steel it may be convenient to express the relative cooling

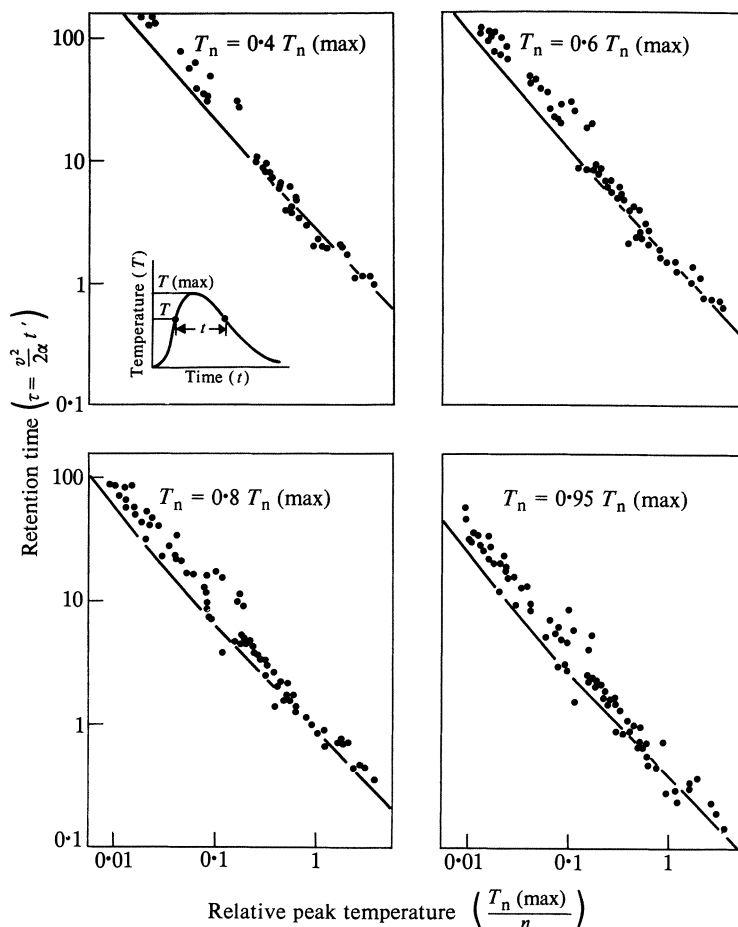


Figure 3.19 Time spent in various ranges below the peak temperature: from $T_n(\max)$ to T_n .

rates of welds in terms of the time that elapses between two fixed temperatures. Figure 3.19 shows the comparison between theory and experiment for cooling times from peak temperature to various fractions of the peak temperature. The measured times are higher than theoretical (i.e. the trend is the same as for cooling rates) particularly at low peak temperature.

The other time that may be of interest (e.g. where precipitation occurs between two temperature levels) is the time spent above a given temperature. Measured and theoretical values for this quantity are shown in Figure 3.20. The material recorded in this section is relevant to three-dimensional heat flow only, and it must be remembered that in two-dimensional flow (applicable to thin plate) temperature distributions are different and cooling rates are in the region of half those calculated for three-dimensional flow. Even for thick plate

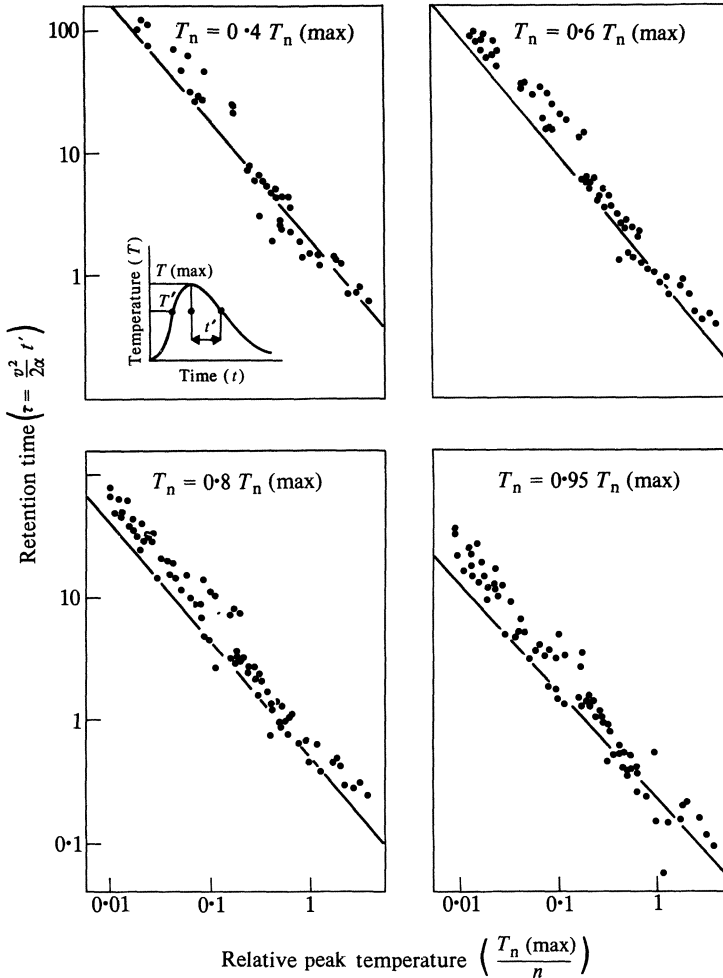


Figure 3.20 Time spent in various ranges below the peak temperature: from T'_n through $T_n(\max)$ to T_n .

deviations from theoretical values are to be expected because of the distortion of weld pool shape by convectional heat flow within the pool, and where accurate figures for cooling rates or other heat flow parameters are required it is necessary to rely on experiment.

FURTHER READING

General

American Welding Society 1976. *Welding handbook*, 7th edn, Section 1. Miami: AWS; London: Macmillan.

Mass flow

- Lancaster, J. F. *Mass flow in fusion welding*. IIW Documents 212-429-78 and 212-409-77.
- Murty, G. S. Instability of conducting fluid cylinder due to axial current. *Archiv för Fysik*, band 18, no. 14, 241–50.
- Murty, G. S. Instability of a conducting fluid cylinder in the presence of an axial current, a longitudinal magnetic field and a coaxial conducting cylinder. *Archiv för Fysik*, band 19, 483.

Heat flow

- Carslaw, H. S. and J. C. Jaeger 1959. *Conduction of heat in solids*. Oxford: Clarendon Press.
- Christensen, N. V. de L. Davies and K. Gjermundsen 1965. Distribution of temperatures in arc welding. *Brit. Welding J.* 12, 54–74.
- Rykalin, N. N. 1961. *Berechnung de Wärmervorgänge beim Schweissen*. Berlin: VEB Verlag Technik.

4 Metallurgical effects of the weld thermal cycle

4.1 METALLURGICAL EFFECTS IN THE WELD METAL

A number of reactions may take place in the liquid weld metal, firstly in the liquid drop at the electrode tip, secondly during transfer from electrode to weld pool, and thirdly in the weld pool itself. These reactions include:

- (a) Solution of gas, causing gas-metal reactions or reaction with elements dissolved in the liquid metal.
- (b) Evolution of gas, causing porosity and/or embrittlement.
- (c) Reaction with slag or flux.

For the most part, gases other than the inert gases have an unfavourable effect on weld metal properties and it is the object of **shielding** methods (discussed in Ch. 2) to minimise any metallurgical damage from this cause. Slag-metal reactions occur mainly during the welding of steel, and will be discussed under that heading.

4.1.1 Gas-metal reactions

Gas-metal interaction may take one of two forms: physical (**endothermic**) reaction, or **exothermic** reaction to form a stable chemical compound. Exothermic reactions may be further divided into three sub-groups: those in which the reaction product is highly soluble in the melt, those in which there is a moderate degree of solubility, and those producing an insoluble compound. The first type of reaction (which occurs mainly with the reactive metals of Groups IV and Va) does not prevent the formation of a weld pool, but generally causes embrittlement of the completed joint (see Section 9.5.1). The second and third types commonly result in the formation of a slag or a surface scale that may physically interfere with welding. In the case of the third type particularly where the compound forms a solid skin on the surface of the molten weld pool, it is necessary either to prevent access of the gas to the melt, or to provide a flux or some other means of dissolving or dispersing the reaction product (as in the case of aluminium: Section 9.1.1).

Endothermic solution does not inhibit fusion, but can result in porosity, either due to supersaturation of the weld pool with a particular gas, or by reaction between two gases. It may also in special cases result in embrittlement

of the heat-affected zone. The mechanism of endothermic solution is of particular importance in welding and will be further discussed below under the following headings:

- (a) Absorption
- (b) Reaction
- (c) Evolution

4.1.1.1 Absorption

The solution of diatomic gases in a liquid metal is described by Sievert's law:

$$S = Kp_g^{1/2} \quad (4.1)$$

where S is solubility, p_g is the partial pressure of the gas and K is a constant. Where the solution is endothermic the solubility increases with temperature. As the temperature of the metal approaches the boiling point, however, its vapour pressure p_m becomes appreciable and for a total pressure of 1 atmosphere, with p_g etc. in atmospheres, the solubility becomes

$$S = K[p_g(1 - p_m)]^{1/2} \quad (4.2)$$

Thus, the solubility reaches a maximum, and then falls away to zero at the boiling point where $p_m = 1$. Figure 4.1 shows hydrogen solubility in a number of metals as a function of temperature and indicates the maximum solubility.

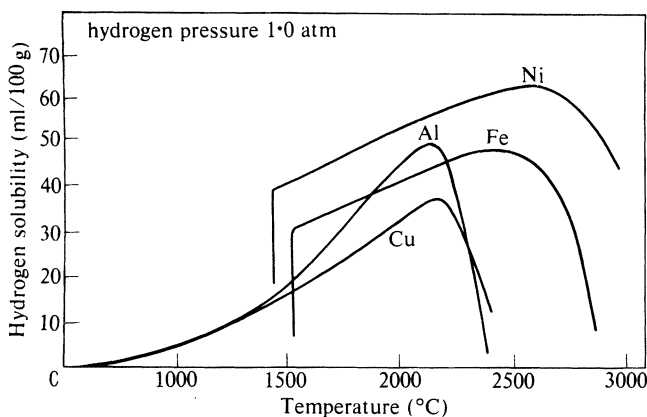


Figure 4.1 Hydrogen solubility-temperature curves. The low-temperature part of the curves is derived from known experimental data, the high-temperature end is obtained by extrapolating these data and then applying a correction for metal vapour (Howden, D. G. and Milner, D. R. 1963. *Brit. Welding J.* 10, 313).

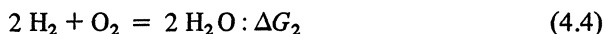
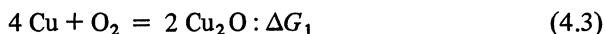
Gas absorption in welding is unlikely to correspond to equilibrium conditions. However, tests carried out with coated electrodes have shown that the amount of hydrogen in solidified weld metal is about equal to the equilibrium solubility

at the melting point, and is proportional to the square root of the partial pressure of hydrogen in the arc atmosphere. In tungsten inert gas welding experiments with arc atmospheres consisting of mixtures of argon and hydrogen have shown that the amount of hydrogen in the **molten weld pool** is also proportional to the square root of hydrogen partial pressure. The concentration of hydrogen in the pool is however substantially greater than the melting point solubility, being close to the maximum solubility for the metals shown in Figure 4.1 although the bulk of the weld pool is at a temperature quite close to the melting point. It is probable that gas is absorbed up to at least the maximum solubility at the arc root, and is distributed throughout the weld pool by metal circulation. It has been determined that nitrogen is dissolved from the arc column in the atomic form. If this is the case with hydrogen, then Sievert's law does not apply and direct solution may give rise to relatively high gas concentrations in the liquid metal.

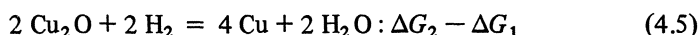
In the case of weld pools that penetrate to the reverse side of the parent material (for example, the root pass in a circumferential pipe weld) the amount of gas that dissolves from the atmosphere on the reverse side is relatively small. When the chromium content of the alloy being welded exceeds about 4% it is desirable in GTA welding to protect the root of the weld from oxidation, which in high-Cr alloys results in a rough, coke-like surface. This is done by providing a **backing gas**, which is usually argon. However, nitrogen and nitrogen/hydrogen mixtures are also used for backing gas in the GTA welding of both ferritic alloy and austenitic chromium–nickel steel. No damaging effects are observed, whereas if the same gases were present in the arc atmosphere they would cause significant embrittlement of the weld metal.

4.1.1.2 Reaction

The probability of reactions between gas and metal and between two gases may be assessed from Figure 4.2 which shows the variation of free energy of formation with temperature for a number of oxides per mole of oxygen. The two lines that represent the free energy of formation of CO by the oxidation of carbon and the free energy of formation of steam form an approximate division between those oxides that may readily be reduced, and those that may not. For example, consider the reactions



where ΔG_1 and ΔG_2 are the free energy changes for the two reactions. Reversing 4.3 and adding to 4.4 gives:



At the melting point of copper (1083 °C)

$$\Delta G_1 = -39 \text{ kcal}$$

$$\Delta G_2 = -81 \text{ kcal}$$

and

$$\Delta G_2 - \Delta G_1 = -42 \text{ kcal}$$

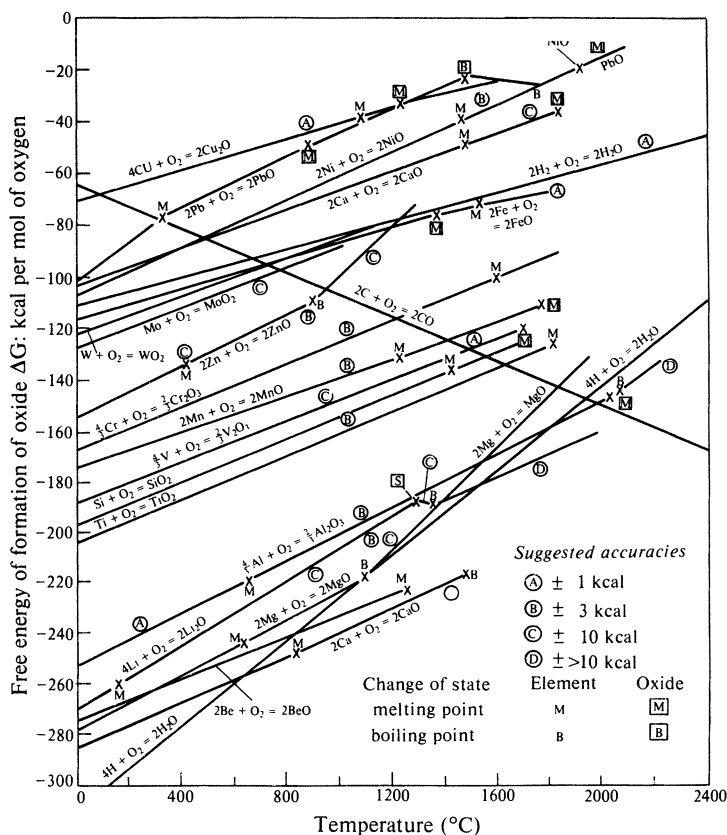


Figure 4.2 Free energy of formation of various oxides, based on the original diagram by Ellingham (Milner, D. R. 1968. *Brit. Welding J.* 5, 98).

Reaction 4.5 therefore goes to the right; thus copper oxide is reduced by hydrogen at 1083°C with the formation of steam. Generally speaking, porosity is likely to occur in the fusion welding of metals whose oxides are reducible by hydrogen or carbon at or just above their melting point. Such metals are those for which the oxide curve lies in the upper part of Figure 4.2, notably iron, nickel and copper. Lead is an exception to this rule, probably because of its low solubility for the reducing elements carbon and hydrogen.

Porosity may be prevented during the fusion welding of the easily reducible metals by adding **deoxidants** to the filler metal. Deoxidants are elements whose oxide curves lie in the lower part of Figure 4.2 (e.g. below the Cr_2O_3 line) at the melting point of the metal to which they are added. The more powerful deoxidants are those lying towards the bottom of the chart (and whose oxides, therefore, have a high free energy of formation). However, deoxidants such as aluminium and titanium may have the disadvantage of forming a solid oxide skin on the surface of the melt, and silicon, manganese, or a combination of

these two elements, are often preferable from this viewpoint. Also metals such as aluminium when added to steel are easily oxidised in the arc, and their effectiveness is thereby reduced.

The correlation between free energy of formation of oxides and the need for deoxidation in fusion welding is not a certain indication that porosity in the metals concerned results from the reduction of oxides to form steam or carbon monoxide. Nitrides follow in general the same trend as oxides; thus, metals whose oxides appear at the top of Figure 4.2 also tend to form unstable nitrides, and, conversely, deoxidants are often **nitride-formers**, that is to say their nitrides are relatively stable. Nitrogen evolution is one of the causes of porosity in steel, nickel and copper. Any of the following types of reaction may give rise to gas evolution and porosity



4.1.1.3 Evolution

Gas which has been dissolved in the high-temperature part of the weld pool and is then transferred to cooler regions will form a supersaturated solution and will normally be evolved. Evolution requires a minimum degree of supersaturation, and the presence of suitable nuclei. Under normal circumstances, nuclei are abundant in the weld pool, and therefore bubbles are likely to appear when the concentration of gas is about equal to the solubility at one atmosphere (this has been confirmed experimentally for hydrogen in aluminium). Now it is known from Milner's experiments with tungsten inert gas welding that the mean hydrogen concentration in the weld pool is approximately equal to the maximum solubility. Therefore, it would be expected that metals having a large difference between their maximum solubility for hydrogen and the solubility at the melting point would be the most susceptible to hydrogen porosity. This would appear to be the case: Figure 4.1 indicates such a large difference in the case of aluminium and copper which are indeed susceptible to porosity when arc welded, whereas at the other extreme steel and nickel are relatively insensitive to hydrogen porosity. Welds in carbon steel made with rutile or cellulosic electrodes may contain up to 30 ml H_2 /100 g weld metal and yet be non-porous, while inert-gas shielded GMA welds in aluminium almost always contain some porosity.

The position in which bubbles nucleate is significant in relation to the incidence of porosity. If nucleation occurs away from the weld pool boundary, there is a possibility that the bubbles will all escape, leaving a rim of degassed metal to solidify without pores. On the other hand, if nucleation persists up to the weld boundary, then bubbles will almost certainly be trapped. This will probably apply, for example, in arc welding aluminium, due to the high degree of supersaturation of the cooler regions of the weld pool. Nucleation at the weld

boundary may also result from the interaction of the liquid weld metal and that region of the parent metal which, at the extreme lateral boundary of the weld pool, is melted and mixed with the weld metal for only a very short period before it solidifies again. Bubbles produced by such weld metal/parent metal reaction may cause porosity localised at the weld boundary.

Gas may also escape from the solidified weld metal by **diffusion**. This process is governed by a relationship of the same form as that for the diffusion of heat, except that the constant α for heat diffusivity is replaced by that for diffusivity of gas, D ; and temperature by the concentration c

$$\nabla^2 c = 1/D \partial c / \partial t \quad (4.9)$$

There are two solutions to this equation that may be relevant to the escape of gas by diffusion. Firstly, consider a slab of thickness $2w$, the centre of which is the plane $y = 0$ (Figure 4.3a). Suppose that the concentration of gas in the slab at time $t = 0$ is uniformly c_0 and the surface concentration is reduced to zero, the concentration c as a function of time is

$$c/c_0 = 4/\pi \sum_{n=0}^{\infty} \frac{(-1)^n}{(2n+1)} \left[e^{-(2n+1)^2 \pi^2 Dt/4w^2} \times \cos \frac{(2n+1)\pi y}{2w} \right] \quad (4.10)$$

Figure 4.3b shows c/c_0 as a function of y/w for different values of Dt/w^2 . The concentration along the centre line begins to fall significantly when Dt/w^2 is about 0.1.

Gas also diffuses out of the weld into the plate. Assume that the form of the weld is that shown in Figure 4.4a, that there is no loss of hydrogen across the metal surface, and that the initial concentration of hydrogen in the weld metal is

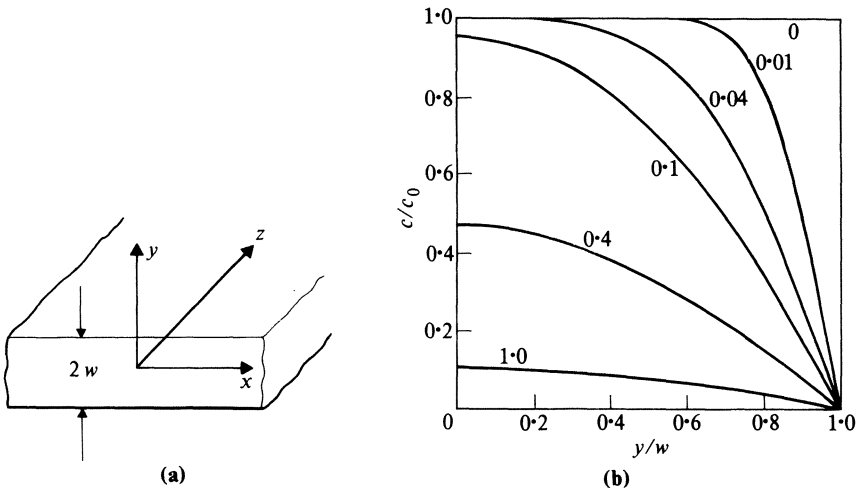


Figure 4.3 Diffusion of gas out of a slab thickness $2w$. Numbers on the curves are values of Dt/w^2 . (4.4b Carslaw & Jaeger – see Further Reading, p. 00.)

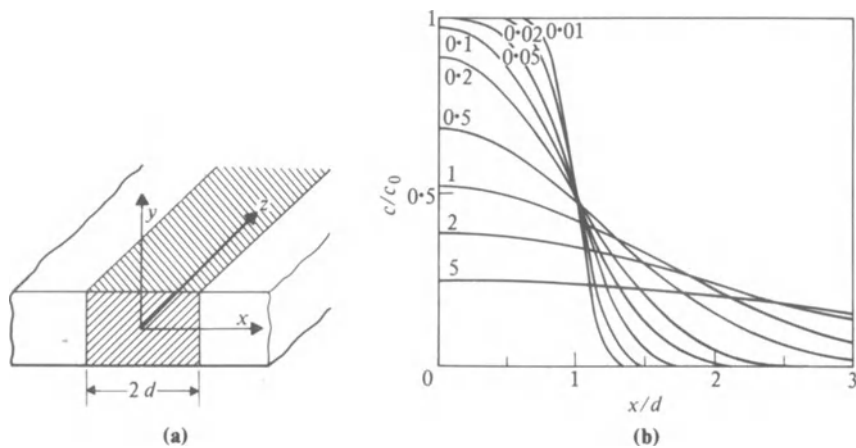


Figure 4.4 Diffusion of gas from a rectangular fusion weld into the plate. Numbers in the curves are values of Dt/d^2 . (4.4b Carslaw & Jaeger – see Further Reading, p. 50.)

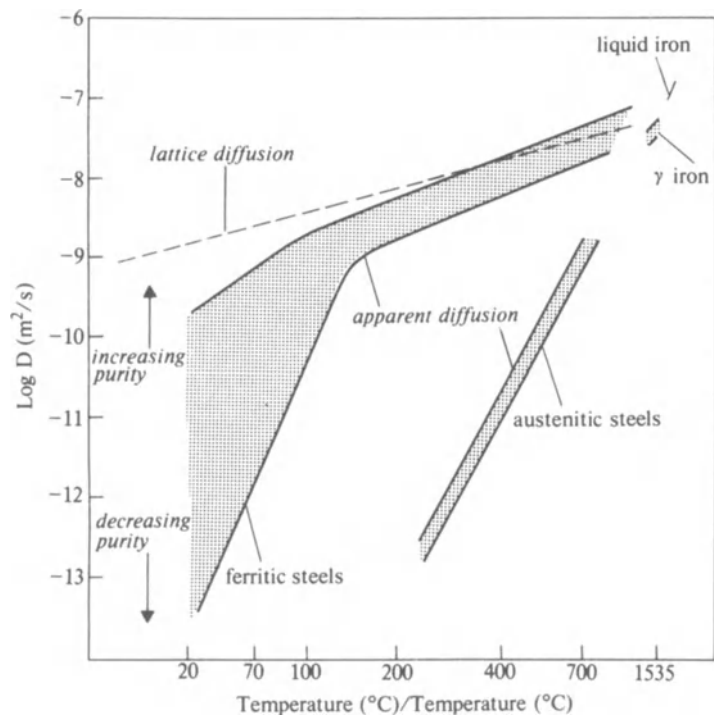


Figure 4.5 Diffusivity of hydrogen in steel as a function of the reciprocal of absolute temperature (Coe, F. R. 1976. *Welding in the World* 14, No. 1/2, 1–7).

c_0 and that in the parent metal is zero. The ratio c/c_0 as a function of distance x from the centreline of the weld is given by

$$c/c_0 = \frac{1}{2} \left[\operatorname{erf} \frac{d-x}{2(Dt)^{1/2}} + \operatorname{erf} \frac{d+x}{2(Dt)^{1/2}} \right] \quad (4.11)$$

where $\operatorname{erf}(z)$ is the error function. c/c_0 is plotted against x/d for various values of Dt/d^2 in Figure 4.4b. In practice, since hydrogen also diffuses out of the surface, Equation 4.10 can only represent the hydrogen distribution during the initial stage of diffusion (up to, say, $Dt/d^2 = 0.1$) and near the mid-plane of the plate. Moreover, the diffusivity of hydrogen in steel varies with temperature in an anomalous manner. Figure 4.5 shows that above about 200°C hydrogen atoms diffuse through the metal lattice in a normal manner. Below 200°C , however, the diffusivity falls sharply, the slope of the curve being greater with more impure steel. This behaviour is attributed to the presence of **traps** (predominantly micro-voids, which may be created by cold working), which absorb hydrogen and impede its flow. Even above the anomalous region the diffusivity falls quite sharply, so that to calculate the hydrogen distribution in and around a fusion weld it is necessary to make stepwise numerical calculations.

4.1.2 Dilution and uniformity of the weld deposit

In most instances, filler metal is added to fusion-welded joints, and the weld deposit therefore consists of a mixture of parent metal and filler metal. When parent metal and filler metal have the same composition this is of no consequence, but where they differ, suitable measures must be taken to ensure that the completed weld has the desired composition.

The degree of dilution depends upon the type of joint, the edge preparation and the process used. **Dilution** (expressed as a percentage) may be defined as

$$D = \frac{\text{weight of parent metal melted}}{\text{total weight of fused metal}} \times 100 \quad (4.12)$$

It is a maximum for single-run welds on thin sections with a square edge preparation, and a minimum in fillet welds or in multi-pass welds with a normal edge preparation (Figure 4.6). Dilution is of particular importance in the case of dissimilar metal joints and in the welding of clad material. It may be minimised in such cases by applying a deposit of the analysis required to the edges of the joint before making the weld proper (**buttering**). In some cases a special alloy is used for this purpose.

Mixing of metal in the weld pool is generally good, and normally the weld bead composition is substantially uniform within the fused zone. If there is a large difference between filler and parent metal composition, some variation may arise, particularly when inert gas tungsten arc welding is used. Such variation is less likely with processes involving metal transfer. On the other hand, alloy steel welds made with coated electrodes occasionally contain partially fused ferro-alloy particles. Some or all of the alloy content of the weld deposit may

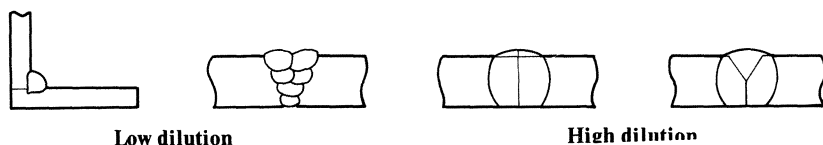


Figure 4.6 Dilution of weld deposit.

be introduced in the form of ferro-alloy or pure metal powder mixed with the coating, and the use of too coarse a grade of powder will result in non-fusion or other forms of segregation.

In most metals and alloys the boundary between the fusion zone and the unmelted part of a fusion welded joint is quite sharp. At the fusion boundary the composition changes from that of the parent metal to that of the more or less uniform weld deposit. For a manual weld with coated electrodes the thickness of this boundary zone lies typically between 50 and 100 μm (between 5×10^{-2} and 10^{-1} mm). In alloys having a long freezing range, partial melting may take place in that portion of the heat-affected zone which is immediately adjacent to the fusion zone, and some of the liquid pockets so formed may become physically continuous with the weld metal. Alloys which behave in this way are usually difficult to fusion weld and (except for cast iron) are rarely met with in practice. Hydrogen may diffuse from the fused zone into the heat-affected zone, but other elements do not so diffuse to any significant extent, either from weld metal to unmelted metal or vice versa, during the welding process. Diffusion may occur during postwelding heat treatment or during service at elevated temperature, however.

4.1.3 Weld pool solidification

The crystals that form during solidification of the weld pool are nucleated by the solid crystals located at the solid/liquid interface. In the welding literature, this type of crystal growth is known as **epitaxial** (the growth modes illustrated in Figure 4.8 are all epitaxial). Each grain forms initially as a continuation of one of the grains that lies along that part of the fusion boundary where the weld width is greatest. As the fusion boundary moves forward grains continue to grow in a columnar fashion. Competition between grains results in some change in relative size, but in general the primary grain size of the weld metal is determined by the grain size of the solid metal at the fusion boundary. The factors that, in turn, govern the grain size of the solid will be considered in Section 4.2.1.

A fusion weld has a primary grain structure, and individual grains have a substructure which results from microsegregation. The type of substructure that appears in weld metal depends on the form of the solidification front. This in turn is influenced by the solute content of the liquid weld metal, and by a solidification parameter equal to the temperature gradient in the direction of solidification G divided by the rate of advance of the solidification front R

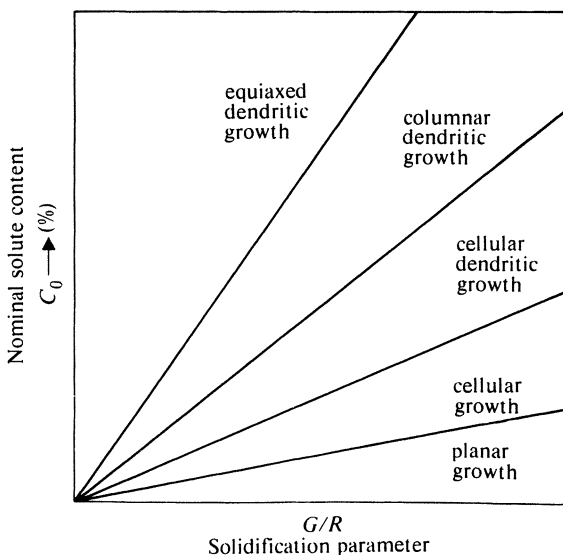


Figure 4.7 Factors controlling the growth mode during the solidification of liquid metals.

(some authors prefer \sqrt{R} but the simpler relationship will be used here). Figure 4.7 shows how, in general, these factors influence the mode of solidification while Figure 4.8 illustrates the form of the various microsegregation patterns. For any given solute content the microstructure tends to become more dendritic as the ratio G/R decreases, while the dendrite spacings tend to increase as the **freezing time** (expressed as $(GR)^{-1/2}$) increases. Eventually at high values of $(GR)^{-1/2}$ the dendrites nucleate at a point and the structures become equiaxed. For the weld pool the solidification velocity is equal to the welding speed v multiplied by the sine of the angle ϕ between the tangent to the weld pool boundary and the welding direction

$$R = v \sin \phi \quad (4.13)$$

The temperature gradient $\partial T/\partial x$ is equal to $\partial T/\partial t / dx/dt = 1/v \partial T/\partial t$ while the theoretical value of $\partial T/\partial t$ may be obtained from Equations 3.40 and 3.41. For three-dimensional heat flow, the gradient at the rear of the weld pool is, numerically

$$G = \frac{1}{v} \frac{\partial T}{\partial t} = \frac{T_m}{x_1} \quad (4.14)$$

where T_m is the melting temperature and x_1 is the distance between the heat source and the rear of the weld pool. At this point $\sin \phi = 1$ and

$$G/R = T_m/vx_1 \quad (4.15)$$

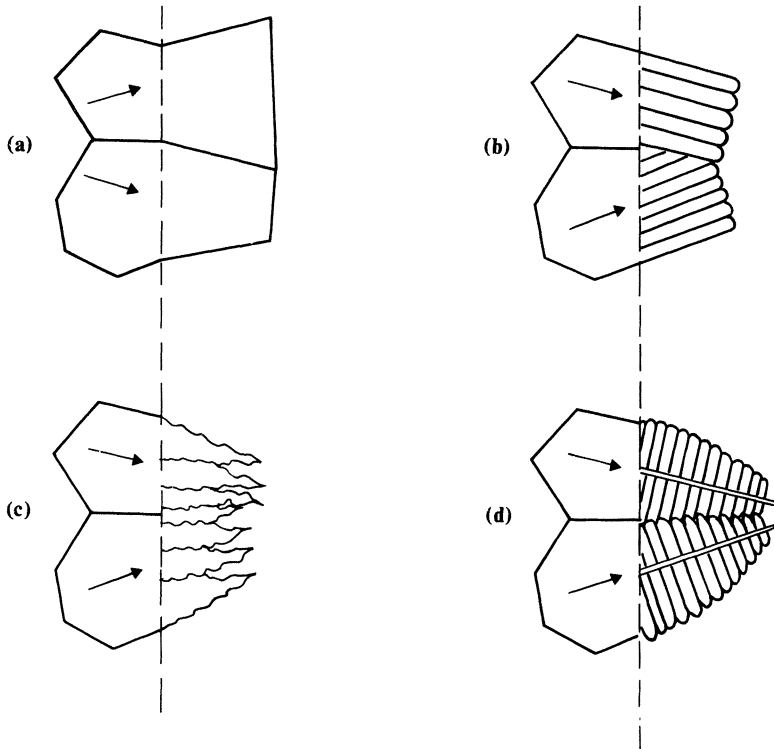


Figure 4.8 Solidification modes: (a) planar, (b) cellular, (c) cellular dendritic, (d) columnar dendritic. The arrows indicate the preferred growth direction ($\langle 100 \rangle$ for steel).

x_1 increases with welding speed and therefore the parameter G/R falls as the welding speed increases. Also, at the boundary of the fused zone $\sin \phi = 0$ and G/R is theoretically infinite.

Thus, the solidification parameter decreases from the fused zone boundary to the central axis of the weld. In practice the tail of the weld may become sharp at high welding speeds and is generally more elongated than theory predicts. Equation 4.15 may not therefore be quantitatively accurate but the indicated trend is correct.

The grain structure of the weld appears to depend mainly on three factors: composition (solute content), the solidification parameter, and the shape of the weld pool. Figure 4.9 shows how the grain structure of a GTA weld in 1.5 mm thick low carbon steel sheet varies with welding speed and heat input rate.

The structures and weld pool shapes are shown in Figure 4.10. At the lowest velocities and high values of the solidification parameter the central part of the weld is occupied by grains running longitudinally, and this is associated with

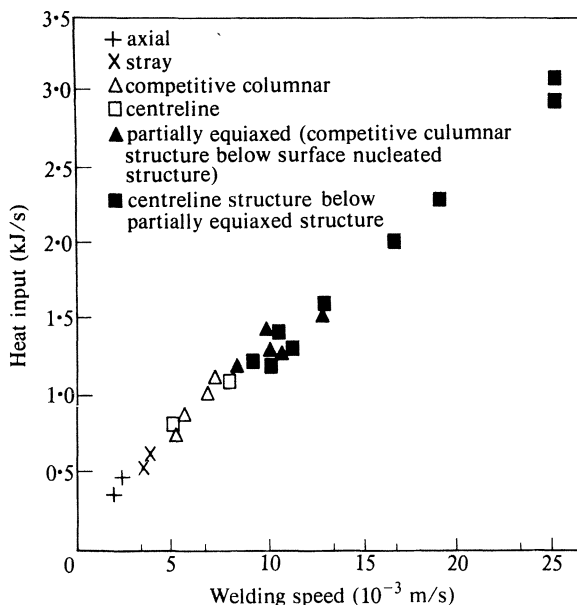


Figure 4.9 Weld macrostructure as a function of welding speed and heat input rate for a steel containing 0.038% C. (From Ganaha, T. and H. W. Kerr 1978. *Metals Technology* 5, 62–9.)

a nearly circular weld pool. With higher speed and a more elongated pool the grains that are established near the fusion boundaries are later blocked by grains growing from the rear of the weld pool, giving a random (stray) grain orientation. At higher speeds still the weld pool becomes kite-shaped and grains form a herringbone pattern. Equiaxed grains are sometimes observed as shown in Figure 4.10(e); these are thought to be nucleated by heterogeneous nuclei and are not necessarily related to the solidification parameter. Planar growth structures have been observed at the fusion boundaries, which is consistent with Figure 4.7 since G/R can have high values in this region. Quite apart from the general effect of solute content, the range of structures obtained may depend on steel composition; i.e. one or more of the structures may not occur in a given steel.

Various techniques for controlling the primary grain size of weld metal have been tested. Ultrasonic vibrations may induce a degree of grain refinement in the case of light metals. Addition of nuclei formers such as titanium may be effective in the case of aluminium fusion welds and electrosag welds. Electromagnetic vibration of the arc and pulsed current in GTA welding has been successful in reducing grain size in stainless steel, nickel alloys, aluminium alloys and tantalum. In general, however, the grain size is determined by that in the heat-affected zone, which in turn is governed by the weld thermal cycle.

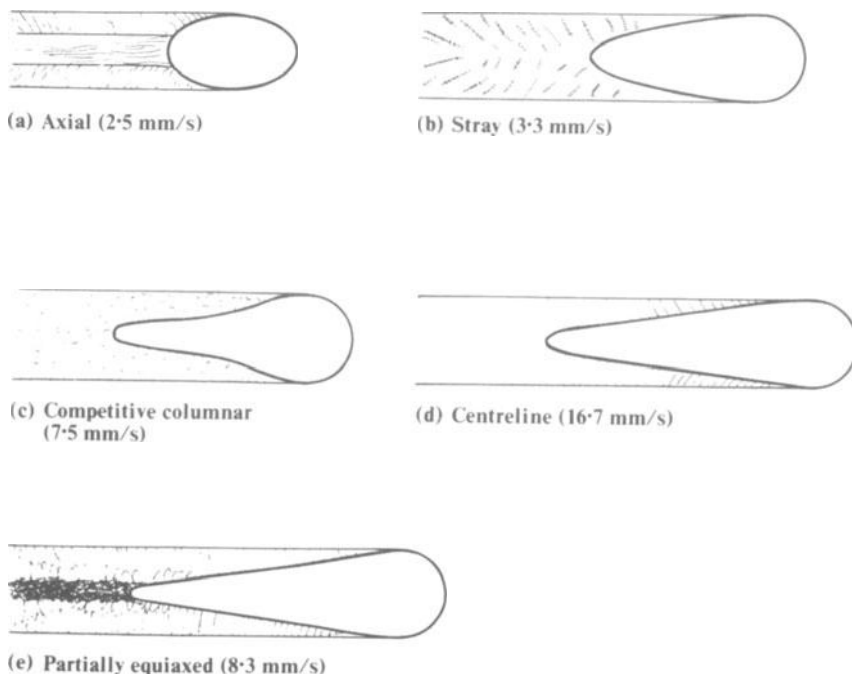


Figure 4.10 Macrostructure observed in flat sections of GTA welds in low carbon steel. (After Ganaha, T. and H. W. Kerr 1978, *Metals Technology* 5, 62–9.)

The size of primary grains has little effect on the properties of face-centred cubic weld metal (although finer **dendrite** spacing may increase the strength) but in the case of ferritic steel the ductile/brittle transition temperature increases with grain size, other things being equal, and the yield strength falls.

4.1.4 Weld cracking

The restrained contraction of a weld during cooling sets up tensile stresses in the joint and may cause one of the most serious of weld defects – cracking. Cracking may occur in the weld deposit, in the heat-affected zone, or in both these regions. It is either of the gross type, which is visible to the naked eye – **macrocracking** – or is visible only under the microscope, in which case it is termed **microcracking** or **microfissuring**. Cracks which form above the solidus temperature are known as **supersolidus** cracks, and those forming below the solidus are **subsolidus** cracks. The terms **hot cracking** and **cold cracking** are also used, the former to signify that the cracks occurred at elevated temperature, while the latter term is often applied to the cracking of low alloy steel welds at room temperature. However, from a metallurgical viewpoint

the distinction between supersolidus and subsolidus cracking is the most significant and the mechanism of crack formation will be discussed under those two headings.

4.1.4.1 Supersolidus cracking

There are two necessary preconditions for the occurrence of cracking during the weld thermal cycle: the metal must lack ductility, and the tensile stress developed as a result of contraction must exceed the corresponding fracture stress. The mechanical properties of the metal in the region of the solidus are therefore important in relation to supersolidus cracking. On cooling a liquid alloy below its liquidus temperature, solid crystals are nucleated and grow until at a certain temperature they join together and form a coherent although not completely solidified mass. At this temperature (the **coherence temperature**) the alloy first acquires mechanical strength. At first it is brittle, but on further cooling to the **nil-ductility temperature** ductility appears and rises sharply as the temperature is still further reduced (Figure 4.11). The interval between the coherence and nil-ductility temperatures is known as the **brittle range**, and in general it is found that alloys which possess a long brittle range are sensitive to weld cracking, while those having a short brittle range are not. Brittleness in the region of the solidus is believed to be due to the presence of continuous intergranular liquid films. The liquid may be a eutectic, as in certain crack-sensitive aluminium alloys, or it may be formed by an impurity such as sulphur in steel. In the case of aluminium alloys the mechanism of cracking is best understood by reference to the equilibrium phase diagram, as discussed in Section 9.1.3. In those cases where cracking is promoted by impurities, a film will only form if

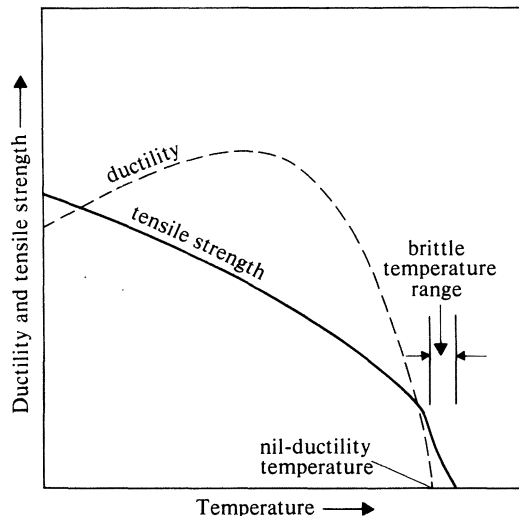


Figure 4.11 Mechanical properties of metals as function of temperature.

the liquid is capable of wetting the grain boundaries: that is to say, if its surface energy relative to that of the grain boundary is low (see Section 6.1.2); thus manganese, which tends to globularise sulphides, helps to inhibit weld cracking due to sulphide films in carbon and low alloy steel.

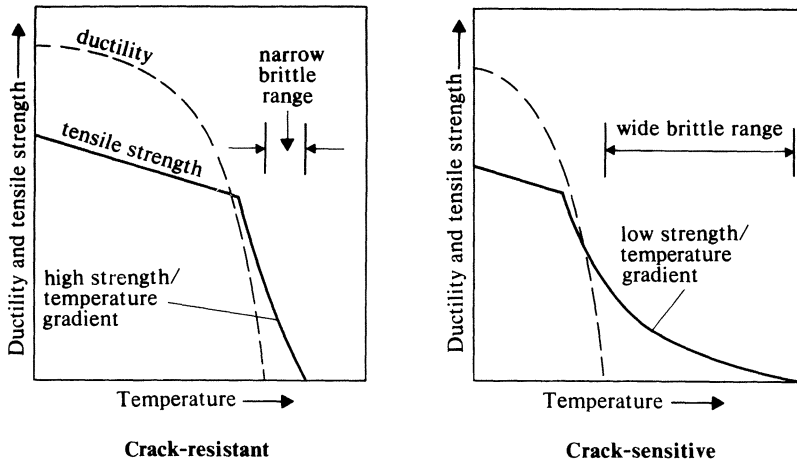


Figure 4.12 Comparison of mechanical properties near the solidus: crack-resistant and crack-sensitive alloys.

It will be evident that the longer the brittle range, the greater the possibility that dangerously high contraction stresses will be set up. In addition, there is in certain alloys a correlation between the tensile strength within the brittle range and the tendency towards weld cracking. In such materials the slope of the strength/temperature curve is low in the case of crack-sensitive material, but relatively high for a crack-resistant type (Figure 4.12). An effect of this type is to be expected since the rate of increase of stress with decreasing temperature due to contraction is $x E \alpha$ where E is Young's modulus, α is the coefficient of expansion, and x is a restraint factor. Clearly, if during the brittle range the rate of increase of tensile strength (or fracture stress) is lower than $x E \alpha$ cracking will occur. It also follows that the higher the value of x (i.e. the higher the degree of restraint), the more likely it is that any given alloy will crack. The degree of restraint is a function of the type of joint, the rigidity of the structure, the amount of gap between the abutting edges, the plate thickness, and the relative thickness of plate and weld metal. Maximum restraint is obtained when two rigidly clamped thick plates are joined by a weld of small cross section, while minimum restraint occurs in a weld of relatively large cross section between two close-butting thin sheets (Figure 4.13). Under conditions of extreme restraint most weld metals will crack, but with light restraint supersolidus cracking is only likely in certain alloys, notably fully austenitic chromium–nickel steel, single (α) phase aluminium bronze, and certain aluminium and magnesium

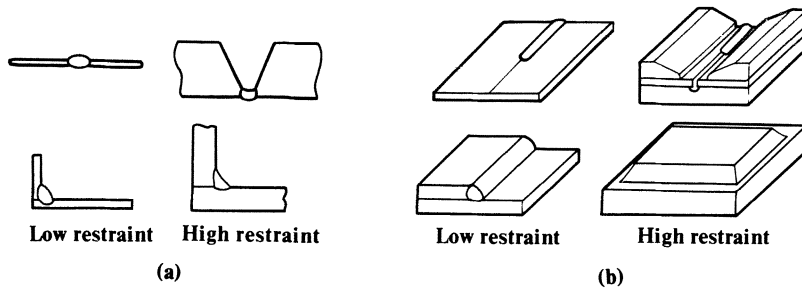


Figure 4.13 (a) Restraint dependent on dimensions of weld and plate; (b) restraint dependent on rigidity of joint or set-up.

alloys. Crack-sensitive materials are usually subject to both micro and macro-cracking, and microcracks are often present when there are no cracks visible to the naked eye.

Tensile stresses capable of generating supersolidus cracking may also arise due to bending. In some joint configurations the weld shrinkage is such as to subject the weld to bending during the solidification period. Supersolidus cracks may also appear at the fusion boundary, running a short distance into the parent metal. Such **hot tears** are most likely to occur under conditions of overall restraint and when there is a relatively acute angle between the weld reinforcement and the parent plate (an acute **wetting angle**).

Weld cracking may also result from inadequate **feeding**. The word 'feeding' is used here in the same sense as in foundry technology: i.e. to describe the geometrical arrangement that permits liquid metal to be drawn into and fill any gaps caused by shrinkage during solidification. Normally, fusion welds are self-feeding, but if the penetration is too deep relative to its width, and particularly if the weld is narrower at the top than at its mid-point, **shrinkage cracks** may form (Figure 4.14). The same type of cracking may occur in electroslog welding if the welding conditions are set up incorrectly, but, in this case, the cracks form a herringbone pattern when seen in a radiograph or longitudinal section. This type of supersolidus cracking may be termed **solidification cracking**. However, cracks may also form due to localised melting of either the parent metal or (in multi-run welds) the weld metal. This may be due to the

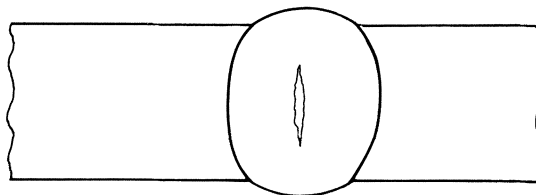


Figure 4.14 Supersolidus cracking due to unfavourable geometry of the fused zone.

fusion of low-melting constituents or phases, or it may be due to segregation of impurity elements to the grain boundaries and melting of the grain boundary regions. Alternatively, the same type of segregation may reduce the cohesion at the grain boundary. Such fusion or near-fusion may result in **liquation cracking**.

4.1.4.2 Subsolidus cracking

The essential requirements for subsolidus cracking are the same as for supersolidus cracking: namely, brittleness combined with tensile stress. A pre-existing crack and/or a stress-raising configuration will further increase the risk of failure. Subsolidus cracking may occur in the weld metal, the heat-affected zone, or in the parent material. Most frequently, parent metal cracks initiate in the weld or heat-affected zone, but there are cases where the tensile stress field set up by welding will result in a crack being initiated by a defect (say an arc strike) remote from the weld itself.

Embrittlement is an important contributory factor to subsolidus cracking, and mechanisms of embrittlement are reviewed briefly in Section 4.2.2. Embrittlement mechanisms are usually time-dependent so that cracking may occur at any time after solidification: sometimes cracks will appear after months of storage or use, or during some postwelding operation such as heat treatment.

The causes of subsolidus cracking are often complex and difficult to elucidate, and in some cases it is difficult to determine with certainty whether the cracking is of the supersolidus or subsolidus type. A number of the more crack-sensitive alloys are subject to both these types of failure, and it is not uncommon for a subsolidus crack to be triggered by a pre-existing crack that formed during welding. In all cases it is necessary to give careful consideration to the probable effect of the weld thermal cycle on the solid material and to assess the possibility of embrittlement.

4.2 METALLURGICAL EFFECTS IN THE PARENT METAL AND SOLIDIFIED WELD METAL

In fusion welding, the heat-affected zone is subject to the full weld thermal cycle and the solidified weld metal is exposed to the cooling part of the cycle. Heating and cooling rates are usually high, and the heated metal is subject to plastic tensile strain during cooling. It is not surprising therefore that the metallurgical effects of the weld thermal cycle are complex and may in some instances result in an unfavourable change in the properties of the material.

4.2.1 Microstructural changes in the heat-affected zone

In general, the heat-affected zone may be divided into two regions: the high temperature region in which major structural changes such as grain growth take place, and the lower temperature region in which secondary effects such as precipitation (which may nevertheless be important) may occur. In the grain

growth region the final grain size for any given alloy will depend mainly on the peak temperature to which it is exposed and the time of heating and cooling (the **residence time**). In the case of steel it is found that for isothermal heating the final mean grain size d_t is given by

$$d_t^n = kt + d_0^n$$

where k is a constant, t is time and d_0 is the initial grain size. If the exponent n and the constant k are determined by isothermal heating, the grain growth in the heat-affected zone may be estimated by a stepwise calculation.

However, it will generally be sufficient to note that the final grain size will increase with increasing peak temperature and increasing residence time. In fact, the maximum peak temperature is the melting point and it is the grain size at the fusion boundary in which we are mainly interested, since this determines the grain size in the weld metal. The only significant variable therefore (assuming the same metallurgy) is residence time. The residence time for three-dimensional heat flow may be obtained from the charts developed by Christensen *et al.*, some of which are reproduced in Chapter 3 (Figs. 3.19 and 3.20). These charts show that residence time is roughly proportional to the parameter q/v (the heat input rate). Thus, welding processes having characteristically high values of q/v , such as electroslog and high-current submerged arc welding would be expected to generate coarse grain in the heat-affected zone and in the weld metal, and this is indeed the case. For carbon and ferritic alloy steel, we are referring here to the austenitic grain size.

If the metal that is subject to the weld thermal cycle has previously been hardened by cold work, then grain growth may be preceded by recrystallisation which, in turn, results in softening. Copper and aluminium are typical of metals that can acquire a useful increase in mechanical properties by cold reduction and fusion welding will usually destroy the effect of cold work in the heat-affected zone. Similarly, alloys that are hardened by precipitation will usually be softened by fusion welding.

There are two ways in which the residence time can be reduced: firstly, by using a process that generates two-dimensional rather than three-dimensional heat flow (residence times for two-dimensional heat flow are about half those for three-dimensional flow), and secondly by decreasing the heat input rate.

Electron-beam and laser welding have these characteristics and it is one of the advantages of such processes that they minimise the metallurgical disturbance in the heat-affected zone.

4.2.2 Precipitation and embrittlement in the heat-affected zone

In addition to grain growth, which may in itself cause embrittlement, there are a number of metallurgical changes that result from the weld thermal cycle and that may alter the properties of the parent metal. Also, the heat-affected zone may be permeated by hydrogen. Hydrogen does not appear to have any significant effect on the properties of austenitic chromium–nickel steel or non-ferrous

metals other than copper. Ferritic steel is embrittled to a greater or lesser degree (see Section 7.4) by hydrogen, and copper, if it is not deoxidised, may be severely embrittled by the reaction of hydrogen with residual oxygen to form steam. The steam precipitates at grain boundaries and generates fissures (Section 9.3.3).

Ferritic alloy steels may be embrittled by the formation of unfavourable transformation products, by carbide precipitation, by grain boundary segregation (temper brittleness) and by strain ageing. Austenitic chromium–nickel steels may embrittle at elevated temperature due to a strain ageing mechanism during postweld heat treatment or in service. These processes will be considered in more detail in sections concerned with the particular alloys in question. Their damaging effects can be mitigated by correct choice of materials and by the use of the proper welding procedure and, in some cases, by control of the weld thermal cycle.

A number of alloys may be embrittled within a specific temperature range, causing **ductility dip** cracking. These include fully austenitic chromium–nickel steels, some nickel–base alloys and some cupronickels. Figure 4.15 shows a plot of ductility against temperature for a number of cupronickels, which indicates that for nickel contents of 18% and higher the ductility falls sharply to a minimum at about 1000 K. Above and below the ductility trough, fracture is by

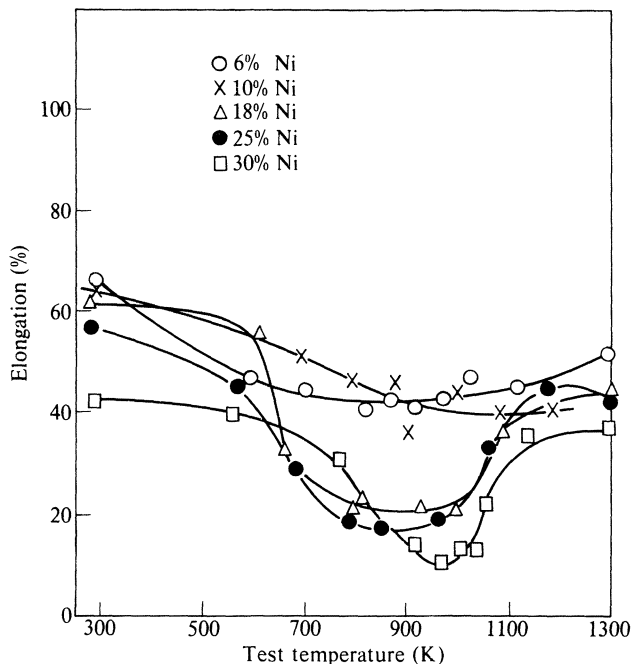


Figure 4.15 Ductility-test results for binary copper–nickel alloys (Chubb, J. P. and J. Billingham, March 1978. *Metals Technology* 5, Part 3, 100–103).

microvoid coalescence; in the trough itself the fractures are intergranular. Such intergranular failure is normally attributed to segregation of impurity atoms (S or P in the case of austenitic Cr–Ni steel) to the grain boundary. In the case of the cupronickel tests illustrated in Figure 4.15, high purity material was used and the segregating element could have been nickel itself.

Ductility dip cracking occurs in multi-pass welding with a susceptible weld deposit composition. Cracks occur in weld metal below the finishing pass due to tensile straining in the susceptible temperature range (possibly during the heating phase of the weld thermal cycle). Such cracks may not be detected by surface crack detection methods, but would show up in destructive testing, particularly side bend tests. Changes in welding procedure, by modifying the thermal cycle, may eliminate the cracking and in some instances the steps used to avoid solidification cracking may be effective: in the case of austenitic Cr–Ni steel, for example, by reducing S and P, increasing manganese, and adding special deoxidants such as calcium or zirconium.

4.2.3. Contraction and residual stress

The **residual stress** due to a fusion weld in plate arises primarily because the strip of material which has been melted contracts on cooling down from melting point to room temperature. If it were unhindered, the longitudinal contraction of the weld would be αT_m where T_m is the difference between the freezing point and room temperature, and α is the mean coefficient of thermal expansion over that temperature range. If the plate cross section is large relative to that of the weld, this contraction is wholly or partly inhibited, so that there is a longitudinal strain of up to αT_m . Assuming only **elastic deformation** the corresponding residual stress would be approximately $E\alpha T_m$ where E is the mean value of Young's modulus over the relevant temperature range. However, except for metals with very low melting points, the value of $E\alpha T_m$ is greater than the elastic limit, so that some **plastic deformation** of the weld takes place during cooling, and the final residual stress in the weld approximates to that of the elastic limit.

Measurement shows that the residual stress in a thin plate after welding consists of a tensile stress in the weld metal itself, falling away parabolically to zero a short distance from the weld boundary, with a balancing compressive stress in the outer part of the plate. Figure 4.16 illustrates typical residual stress field cross sections for a carbon steel plate after making a butt weld down the centre using coated electrodes. In wide plates the residual stress in the weld metal is close to the recorded yield value for weld deposits made with coated electrodes. In a narrow plate the redistribution of stress results in lower values of residual stress in the weld metal but higher values in the plate.

When making a weld between two plates of moderate thickness (for example 10 mm thick) most of the residual stress is built up during the first run. In thick plate, however, there is a contraction stress at right angles to the plate surface, and consequently the stress field may intensify progressively as the joint is built

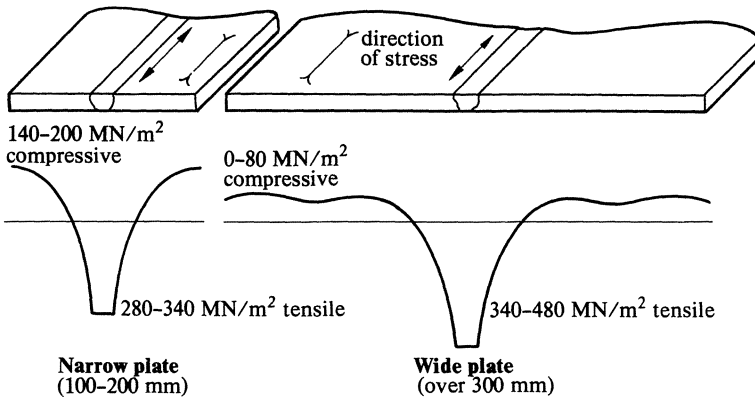


Figure 4.16 Typical residual stress fields in longitudinally welded plate; carbon-steel welded with coated electrodes.

up. Figure 4.17 shows residual stresses along the centreline of a submerged arc weld in 165 mm thick plate of Mn–Mo steel (yield stress nominally 480 MN/m²). The tests were made on a sample, 650 mm long, cut from a larger plate and there may have been some mechanical stress relief, particularly of the longitudinal residual stress. In all three directions – longitudinal, transverse (at right angles to the line of weld and parallel to the plate surface) and short transverse (at right angles to the plate surface) – there is a maximum tensile stress close to each plate surface and a maximum compressive (negative) stress in the centre. Details of the residual stress pattern vary with the weld procedure and may, for example, show a tensile region in one half of the cross section and a compressive region in the other. If it is assumed that the three stresses measured represent principal stresses, the effective residual stress is:

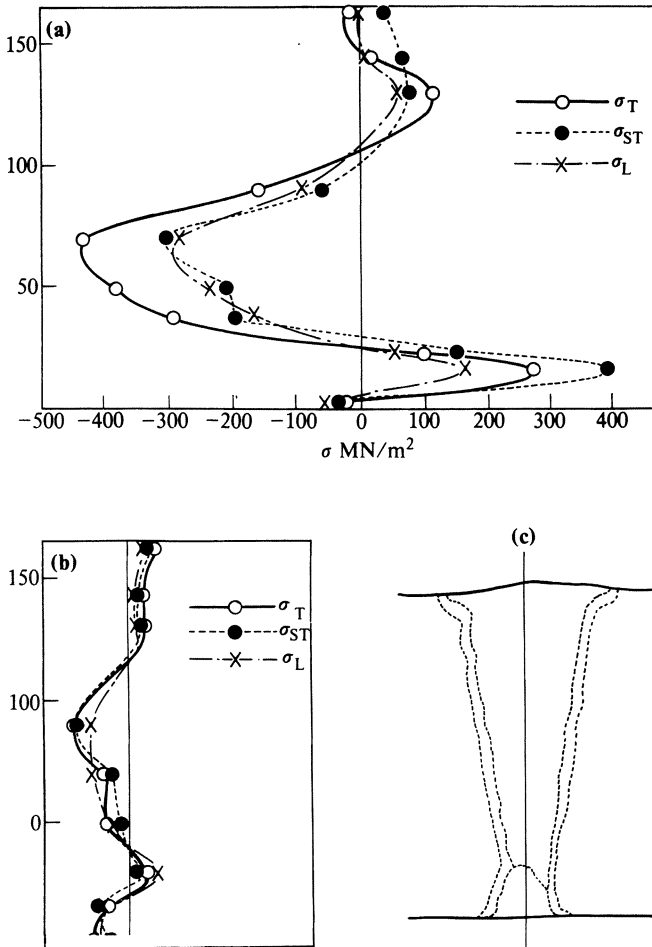
$$\bar{\sigma}_r = 1/\sqrt{2}[(\sigma_T - \sigma_L)^2 + (\sigma_L - \sigma_{ST})^2 + (\sigma_{ST} - \sigma_T)^2]^{1/2} \quad (4.16)$$

The fracture toughness of the weldment K_c (see Chapter 10) is reduced by the presence of a residual stress, and it has been found experimentally that this reduction (ΔK_c) is proportional to the effective residual stress:

$$\Delta K_c = k\bar{\sigma}_r \quad (4.17)$$

For a weld in ductile material ΔK_c is not large enough to affect the behaviour of the joint, but in embrittled material it might well be a significant factor in promoting an unstable fracture.

Residual stress may cause cracking in brittle materials, or in materials that have been embrittled by welding. It may also result in stress corrosion cracking, if the alloy is sensitive to this type of corrosion and is exposed to certain environments. In a ductile metal that is not subject to stress corrosion cracking, such as pure aluminium, the residual stress due to fusion welding has little or no effect on the properties of the joint.



2

Figure 4.17 Distribution of residual stress along the centreline (c) of a submerged arc weld in 165 mm thick Mn–Mo steel: (a) PWHT 1/4 h at 600 °C; (b) PWHT 40 h at 600 °C. σ_T stress transverse to weld; σ_{ST} stress at right angles to plate surface; σ_L longitudinal stress (Sukuzi, M., I. Komura and H. Takahashi 1978. *Int. J. Pres. Ves. & Piping* 6, 87–112).

Residual stress due to welding may be reduced or removed by a **stress relief heat treatment**. Such treatment may have beneficial effects other than the removal of residual stress so that it is usually designated **postweld heat treatment** (PWHT). Guidance as to PWHT cycles and temperatures are contained in, for example, the ASME pressure vessel code. It must be remembered that temperatures and times given in such codes are minima, and that for critical items requiring complete relief of residual stress higher temperatures and/or longer

holding times may be necessary. Residual stresses may also be relieved, or redistributed, by vibration of the structure (**vibratory stress relief**). Although the degree of stress relief achieved in this way is the subject of some disagreement, vibratory stress relief appears to be successful for certain applications such as welded machine beds.

Residual stresses in welds may be measured by observing the change in dimensions after cutting rectangular or circular sections out of a sample. Alternatively, they may be estimated from the heat flow equations using elastic/plastic analysis and, as a rule, numerical methods of calculation.

FURTHER READING

- Davies, G. J. and J. G. Garland 1975. Solidification structures and properties of fusion welds. *International Metallurgical Reviews* **20**, 83–106.
- Pfluger, A. R. and R. E. Lewis 1968. *Weld imperfections*. Reading, Mass.: Addison-Wesley.
- American Welding Society 1977. *Welding handbook*, 7th edn, Section 1. Miami: AWS; London: Macmillan.

5 Solid-phase welding

5.1 FUNDAMENTALS

In order to make a solid-phase weld between two pieces of metal, it is necessary to bring their clean surfaces sufficiently close together for a metallic bond to be formed between them. There are a number of techniques for accomplishing this end, but the essential operation in all cases is to press the two parts together either hot or cold, deforming the surfaces sufficiently to ensure partial or complete contact, and to expose fresh, unfilmed metal. Important factors which enter into the mechanics and metallurgy of this process are surface deformation, the dispersal of surface films, diffusion and recrystallisation. These factors will be discussed separately below.

First, however, it will be necessary to consider very briefly the cohesion of metals and the mechanism of bonding.

5.1.1 The cohesion and strength of metals

The cohesion of a crystalline solid results from the **attractive force** between its constituent atoms. Normally each atom occupies a position in which the net force upon it is zero. When the solid is extended by the action of external loads, however, the atoms move out of their equilibrium positions and a tensile stress is set up within the crystal, which balances the external load. The attractive force between the atoms increases in proportion to their separation up to a certain point, when in brittle solids it reaches a maximum value and starts to decrease. A crystal that is free from defects fails at this point by **cleavage** across the **crystallographic** plane where the interatomic forces are weakest.

In ductile polycrystalline metals the movement of dislocations within the crystal lattices of individual grains results in slip and gross plastic flow. Failure takes place by **plastic instability**: that is to say, a point is reached in extending the solid when the rate of increase of strength due to work hardening is lower than the rate of decrease of cross-sectional area resulting from extension.

Thus the bulk strength of materials is in general lower than the cohesive or bonding forces between the constituent atoms will allow, due essentially to the presence of defects in the crystal lattice. Hence, to make a mechanically sound joint between two metals, it may not be necessary to achieve a bond equal in strength to that between adjacent planes in the metal lattice.

At room temperature the fracture of most ductile metals is transcrystalline, and it is only at elevated temperature, where failure is preceded by creep, that intercrystalline fracture is the rule. It follows that planes where there is a major lattice misfit, such as grain boundaries, are no weaker than the bulk of the metal at temperatures below the creep range. This fact is important in relation to **cold welding** (pressure welding at room temperature), when the weld junction is necessarily a plane of lattice misfit.

So far the discussion has been confined to those instances where a true metallic bond is formed, as in pressure welding, when the metal surfaces approach closer than the normal relaxation distance for the interatomic forces. There are, however, other forces that may significantly affect welding behaviour. These are the **Van der Waals forces** (see Section 6.1.1) that act between molecules regardless of their chemical species. Van der Waals forces are responsible for the **adsorption** of foreign molecules such as gases, water vapour or grease on a metal surface. The magnitude of these forces at close range is not known with certainty, but measurements made between surfaces separated by a few microns show that for flat metal plates the following relation (which has been derived theoretically) holds:

$$\sigma \cong \frac{1}{y^4} \times 10^{-3} \text{ N/m}^2$$

where y is in microns ($1 \mu\text{m} = 10^{-6} \text{ m}$). The van der Waals force at a separation of 10^{-2} mm , for example, is 0.1 MN/m^2 . Note, however, that it falls off very sharply with increasing distance.

In most instances, the attractive force between two surfaces in perfect contact (i.e. separated by no more than normal atomic spacings *over their whole area*) is such that, if a tensile or shear force is applied to the bond, failure will take place in the bulk material rather than at the interface. If two dissimilar materials are bonded in this way, failure will occur in the weaker of the two; if, on the other hand, two similar metals are so joined, the assembly will fail in the same way as a single piece. The central problem in solid phase welding is, therefore, to approach as closely as possible to perfect contact between the surfaces to be joined.

The barriers to obtaining perfect contact are twofold: the presence of non-metallic films, including chemisorbed gases, on the surface, and the physical difficulty of obtaining an exact fit over the whole of the two surfaces to be joined. Films of water, oil or grease are obvious hazards; being fluid they have good contact with the metal surfaces and are strongly bonded thereto, but, since they have no strength, the strength of any joint so contaminated is greatly reduced. Oxide films are commonly brittle, and a joint consisting of the sandwich metal–oxide–metal, even if bonded, will in general be brittle and have low strength. Liquid films are removed by heating or, if welding is to be accomplished cold, by scratch-brushing. Oxide films are also removed by scratch-brushing, by lateral movement of the two surfaces, or by fluxing or melting.

Obtaining good contact by direct pressure between two metal surfaces is

difficult, and joints made in this way have very low strength. For effective mating and bonding **lateral movement is necessary**. When the surfaces are forced together with relatively light normal pressure, the proportion of surface which is brought within bonding range is small. However, the asperities of each surface penetrate the other, and, if the two are moved **laterally relative to each other**, some of these asperities shear, and the clean metal surfaces so produced bond together. Repetition of this process naturally increases the bonded area. Alternatively, if the two surfaces are made to flow **laterally in the same direction (conjoint flow)**, areas of unfilmed metals are formed in close proximity and therefore bonding takes place. **Relative lateral flow** occurs in ultrasonic welding and friction welding, and conjoint flow in butt and flash-butt welding, cold and hot pressure welding, and explosive welding.

5.1.2 Surface deformation

Bulk deformation in pressure welding may be measured as either the percentage increase in interfacial area, which, for round bar, is

$$\frac{d_1^2 - d_0^2}{d_1^2} \cdot 100$$

or, for sheet, the percentage reduction in thickness

$$\frac{t_0 - t_1}{t_0} \cdot 100$$

where d_0 and t_0 are the original diameter or thickness respectively, and d_1 and t_1 are final diameter or thickness. The actual surface deformation may be substantially greater than those so calculated, due to the penetration of each surface by the asperities of the other.

The relationship between deformation of the bulk metal in pressure welding at room temperature and the strength of the joint is illustrated in Figure 5.1. There is a critical or threshold deformation below which no weld is made, and above this critical value the joint strength rises to a value which is close to or equals that of the coldworked material. Increasing the temperature reduces both the critical deformation and that required for optimum joint strength. The effect of temperature is related to the melting point of the metal concerned; at room temperature not far from the melting point strong welds may be made with about 10% deformation. At lower temperature levels the required deformations vary according to the metal between 20% and 95% (Figure 5.2).

In the more sophisticated solid-phase welding processes various means are applied to magnify surface flow relative to the bulk deformation of the material. In ultrasonic welding frictional effects due to lateral vibrations break up surface films. In friction and explosive welding there is macroscopic surface flow, and in the former case lateral movement of the surface occurs independently of bulk deformation.

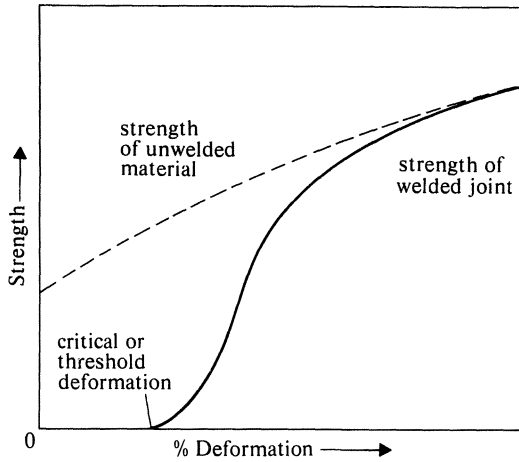


Figure 5.1 Typical relationship between deformation and strength in pressure welds made at room temperature for a face-centred cubic metal such as aluminium.

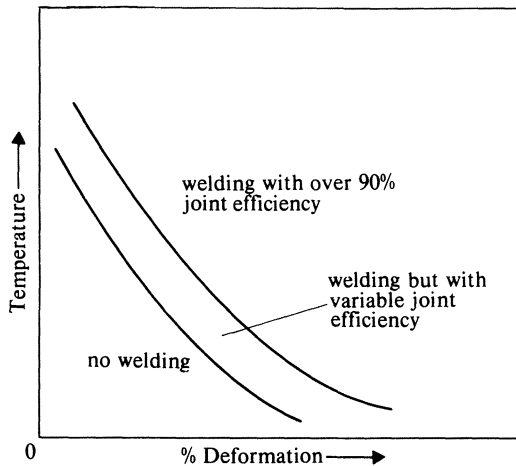


Figure 5.2 Relationship between deformation required for welding and temperature.

5.1.3 Surface films

A metal is normally coated with a film of oxide, sulphide or carbonate, whose thickness lies within the range 10^{-3} to $10^{-1} \mu\text{m}$. It may also have a layer of adsorbed gas, and it may be contaminated by oil, grease or other non-metallic substances.

Oil films inhibit solid-phase welding either partially or completely when the

temperature is such that they can persist. Oxide films hinder, but do not prevent, pressure welding. It is generally considered that during deformation of the surface the oxide film (or the hardened surface layer produced by scratch-brushing) fractures and exposes areas of clean metal, which bond to the opposite surface wherever two clean areas come into contact. The tensile strength of pressure welds is substantially higher than would be obtained by multiplying the normal ultimate tensile strength of the material by the area of clean metal which is theoretically obtained by surface deformation. This effect may be due to local work-hardening combined with the inhibition of slip by the presence of a network of discontinuities at the junction plane.

At elevated temperatures oxide is dispersed partly mechanically and partly by solution in the metal or agglomeration. Excessive amounts of dissolved oxygen cause brittle welds. Oxide inclusions, which may be present in massive form in welds made at elevated temperature, are also damaging to the mechanical properties. Oxide inclusions, dissolved oxygen and voids may be dispersed from the junction zone of carbon steel pressure welds by soaking above 1000 °C for an adequate period, although, if a proper welding technique is used no significant oxide contamination will be present.

5.1.4 Recrystallisation

In welds made at room temperature recrystallisation of a surface zone occurs with low-melting-point metals such as tin and lead, but most engineering metals must be welded at elevated temperature if recrystallisation is to occur during the welding process. Recrystallisation such that grains grow and coalesce across the original interface is not essential to welding, nor does it ensure that the best obtainable properties have been obtained. Steel pressure welds made at temperatures above the upper critical shows continuity of grains across the interface but may still lack ductility due to oxide inclusions or other causes. However, increasing the welding temperature, which favours recrystallisation, also favours the elimination of other defects. Welds made below the recrystallisation temperature are unlikely to have parent metal ductility, whereas above the recrystallisation temperature the ductility of welds improves rapidly.

5.1.5 Diffusion

The relationship of diffusion to the bonding process in solid-phase welding processes other than diffusion bonding has not been studied experimentally and must, therefore, remain a field for speculation. However, it will be evident that surface diffusion could play an important part in modifying the shape and size of voids formed at the interface. Gross macroscopic voids at the interface of pressure welds increase in size and diminish in number if the joint is soaked at elevated temperature, indicating that a process akin to that which causes the increase of density of metal powder compacts during sintering may be at

work. Increasing temperature would favour such a mechanism, and it does in fact improve the ductility of pressure-welded joints.

Diffusion may be important in removing contaminants from the weld zone, particularly oxygen in reactive metals such as titanium. For such material a postwelding solution treatment is required for optimum joint ductility. Diffusion is an essential feature of **diffusion bonding**, which is described in Section 5.2.2.

5.2 PROCESSES

Table 5.1 summarises the characteristics of the major solid-phase welding processes which are described in more detail below.

5.2.1 Pressure welding at elevated temperature

Forge, hammer, butt and oxy-acetylene pressure welding are all techniques designed to make solid-phase welds at elevated metal temperature. In butt welding and oxy-acetylene welding the metal is simply heated to a high temperature (1200–1250 °C in the case of carbon steel) while the joint is subject to axial compression. When the metal in the region of the interface reaches this temperature, it deforms under the axial load and there is a lateral spread which disrupts the surface films and permits welding to take place. Essential controls are the applied pressure and the amount of shortening of the parts being joined. Pressure may be constant or may be increased at the end of the welding cycle.

In resistance butt welding heating is accomplished by passing an electric current across the joint. This process is applied to welding bar and rod, end-to-end welding of strip, and to the manufacture of longitudinally welded tube. The tube is formed from strip by a series of rolls, whence it passes between two copper rollers through which the welding current is applied, then through a pair of forging rolls, which force together the heated edges and make the weld. High frequency resistance welding, the main application of which lies in tube manufacture, is similar in principle, but the high-frequency current heats the joint surface preferentially, so that the heated zone is relatively narrow, and thin material can be more easily handled. Forge welding is also used for tube welding, the formed tube being heated in a furnace before passing through forging rolls.

Flash welding is essentially different in that the two parts are first brought together under light pressure so that contact is localised. On passing a current, metal at the points of contact first melts, and is then violently expelled in the form of globules through the joint gap, producing the phenomenon known as **flashing** (flashing is due to intermittent arcs, the voltage being insufficient to produce a continuous arc). At the end of the flashing period the surfaces have been heated to a high temperature, and they are brought together under an axial pressure. This pressure extrudes the liquid metal and oxide present at the interface, and welds the underlying clean metal surfaces. Because liquid metal is present immediately prior to welding, the flash butt process is sometimes

Table 5.1 Solid-phase welding processes

<i>Process</i>	<i>Heat source</i>	<i>Method</i>	<i>Required Deformations*</i>	<i>Uses</i>
Forge Welding	Forge fire or furnace	Parts to be welded are heated in a forge fire or furnace, withdrawn and then hammered together to make a pressure weld. In tube welding pressure is applied by forging rolls	Variable	Wrought iron, carbon steel manufacture of welded tube
Butt	Electric resistance heating	Surfaces butted together under pressure and heated by passing electric currents until upsetting and welding occurs	About 50%	Production of welded tube. Joining of bar, strip and sections in carbon and alloy steels, copper-base alloys, nickel alloys
Flash	Partly electric arc, partly resistance heating	Surfaces butted together without pressure. Passage of electric current causes flashing and surface melting. Pressure applied to extrude molten metal and slag, upset joint and make weld	Up to 50%	Joining of plate, bar, pipe and sections of carbon and alloy steel, aluminium alloys, copper-base and nickel-base alloys. Joining of rails
Oxy-acetylene pressure welding	Oxy-acetylene ring burners	Surfaces butted together under pressure and heated by oxy-acetylene ring burner until upsetting and welding occurs	Up to about 50%	Joining of bar, pipe and sections in carbon and alloy steels
Diffusion bonding	Furnace	Surfaces to be welded held under light pressure and assembly heated at a sufficiently high temperature to allow inter-diffusion across the interface. Usually carried out in vacuum or inert gas furnace	None	Joining high-melting metals and high-temperature or special alloys

Cold pressure welding	None	Surfaces degreased and scratch-brushed then pressed together to give large deformation or upset. In sheet metal fabrication localised (spot) welds made using suitably shaped indenting tools. In ultrasonic welding joint is vibrated ultrasonically and little deformation is required (5% or less)	50% to 95%	Spot pressure welding of sheet metal components. Longitudinal welds in aluminium cable sheathing. Butt welds in copper wire and rod. Welding of metal foil
Friction welding	Friction between surfaces to be joined	One surface rotated relative to the other while being held in contact under light pressure. Frictional heating occurs and at a suitable point axial pressure is applied and the two components weld together	Up to 50%	Joining bar, tube and other products having circular symmetry. Applicable to carbon and alloy steels, non-ferrous metals and dissimilar metal joints
Explosive welding	None	Surfaces are spaced at a small angle relative to each other or placed in contact and a high explosive charge is detonated so that energy of the explosion is transmitted to the joint	Bulk deformations not essential	Cladding carbon or alloy steel tube sheets with corrosion resistant metal. Tube to tubesheet joints. Thin to thick combinations.

* As defined in Section 5.1.2.

classified as a fusion welding process. However, the bond is (except for accidental inclusion of fused material) formed between solid metal surfaces, and on these grounds it is included here.

In forge welding steel, the two parts to be welded are heated in a forge fire or furnace to between 1200 °C and 1400 °C. The surfaces are fluxed with borax for high carbon steel, or sand for medium carbon steel. Wrought iron and low carbon steel do not require flux, because the melting point of the metal is above that of the oxide. The two parts are then hammered together in order to extrude the molten oxide or slag and make the weld.

The **roll-bonding** of plate material is an important application of pressure welding. In principle, two slabs of the materials to be bonded are placed in contact and welded around the edges or otherwise treated to exclude air. They are then heated and rolled until the required thickness is obtained. Carbon steel is *clad* with (for example) austenitic chromium–nickel steel in this way. A carbon steel weld deposit is laid on the stainless steel slab so that the roll bond is carbon steel to carbon steel, or a nickel interlayer may be used. Alclad sheet is produced in a similar way, but here no interlayer is required. The process is applied to high-strength aluminium alloys that are sensitive to corrosion in atmospheric exposure: a thin pure aluminium or 1% zinc alloy layer is roll bonded to both surfaces. These surface layers are anodic to the underlying alloy and are protective in the same way as galvanising on steel.

The metallurgical effects of solid-phase welding at elevated temperature are milder in character than those of fusion welding. The cooling rates are relatively low, and the embrittling element, hydrogen, is absent, so that it is possible to weld relatively high carbon steel or alloy steel without cracking. The danger of cracking is further minimised by the fact that the whole cross section is joined at once, under compression, so that contraction stresses at high temperature are absent. The observed effects are, indeed, those which would be expected if an unwelded specimen of the metal in question were heated through the welding temperature cycle.

5.2.2 Diffusion bonding

Diffusion bonding is a hybrid between brazing and solid phase welding. Two plane surfaces are joined by placing between them a layer of metal which will diffuse into both parts, whether similar or dissimilar. The preplaced layer may be foil or it may be applied by plating. Alternatively, a diffusion bond may be made between two compatible metals (e.g. W/Ni) without an interlayer. The whole assembly is subjected to longitudinal pressure and heated in a hydrogen or vacuum furnace at elevated temperature. This process has been known since the Bronze Age, but it is now mainly used for high-melting metals such as molybdenum and tungsten, and for high-temperature alloys employed in aerospace structures.

5.2.3 Cold pressure welding

Although cold pressure welding has been used from ancient times, it has only relatively recently found substantial industrial use. Cold welds are made by degreasing the parts, scratch-brushing the surfaces to be joined, then forcing them together under pressure so that a substantial deformation (generally in the range 50–95%) occurs. The resultant weld has, when properly made, good strength, but relatively low ductility. Cold welding is therefore used in joints where ductility is not of great importance.

Scratch-brushing appears to be an essential step in cold pressure welding. Welds made without this preparation have relatively low strength even at high deformations, and welds made at progressively increased time after the scratch-brushing operation are progressively lower in strength. There are two factors which may reduce the strength of such welds: first, the formation of an oxide layer of increasing thickness, and secondly the adsorption of foreign matter (water vapour or gas) from the atmosphere. Scratch-brushing removes the adsorbed film and produces a work-hardened surface layer into which the original oxide skin is folded. This surface layer behaves like a brittle film in that, as the area at the interface increases, it fractures and exposes clean areas which bond to similarly exposed areas on the opposite surface (Figure 5.3). Cold pressure welding is the most widely used solid phase welding process. It is applied to the joining of sheet metal components in a variety of engineering materials by making spot indentations with a suitably shaped tool, for longitudinal welds in aluminium cable sheathing, and for butt welds in copper conductor sections.

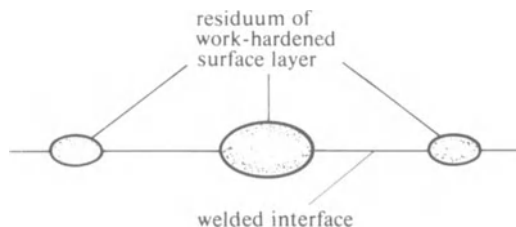


Figure 5.3 Structure of interface of pressure weld.

For thin material where surface indentation is not acceptable, **ultrasonic welding** may be used. Ultrasonic vibrations are induced in a welding tip which applies a small pressure to the overlapping sheets. The vibration breaks down the surface oxide film and allows a solid phase spot weld to be made. Heat may be generated at the interface and this may contribute to the formation of a bond.

5.2.4 Friction welding

In principle friction welding is one of the simplest welding processes (Figure 5.4). One part is rotated relative to the other with the surfaces in contact, so that

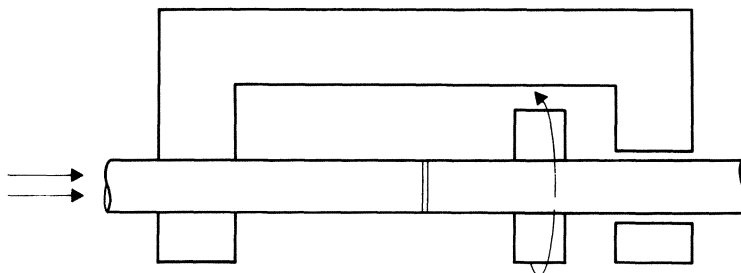


Figure 5.4 Principle of friction welding.

frictional heating of the interface occurs. Initially, the cold parts are subject to dry friction, but as the temperature rises there are local seizures at the interface requiring an increased torque from the machine. Eventually a stage of plastic deformation is reached, when the torque falls and becomes steady. At the end of the plastic phase the rotation is stopped by a brake, and axial pressure is applied to make the weld. The welding machine usually resembles a lathe, but there are numbers of possible geometric arrangements by which friction welds can be made. No melting takes place in friction welding. Any incipient melting reduces the frictional force and heating effect, so that the process is self-regulating. In general, heating and cooling rates are low enough to avoid the metallurgical problems that sometimes result from thermal cycling. Power requirements are moderate compared with flash-butt welding, for example, and the equipment is relatively simple and rugged. An obvious limitation is that the parts to be welded must have rotational symmetry, and the most common application is the joining of bar. The process may be used for a wide range of ferrous or non-ferrous alloys and dissimilar metals, including the most difficult combination, aluminium to carbon steel.

5.2.5 Explosive welding

In principle, an explosive weld is made by placing two surfaces in close proximity and exploding a charge against one of them in such a way that the surfaces close together progressively (Figure 5.5). This may be accomplished by directional detonation of the charge or by spacing the surfaces at an angle to each other. Under correct welding conditions a tongue of plastic material forms where the surfaces come together. This is usually trapped within the finished joint, sometimes with small amounts of fused metal, to form a characteristically waved interface (Figure 5.6).

Explosive welding is of special interest for the bonding of one plate to the surface of another. Normally this is carried out by roll-bonding as discussed in Section 5.2.1. However, as the thickness of the backing plate increases, the interfacial bond becomes less consistent when made using the roll-bonding technique. Therefore, the cladding of thick plate, such as is used for the tubesheet

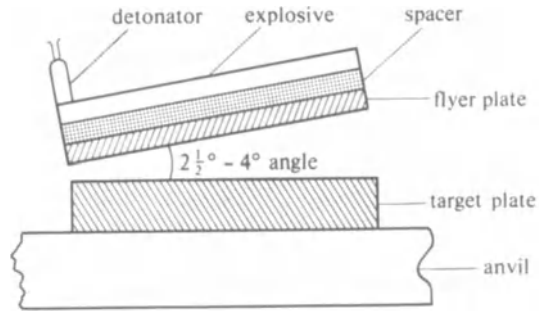


Figure 5.5 Explosive welding.

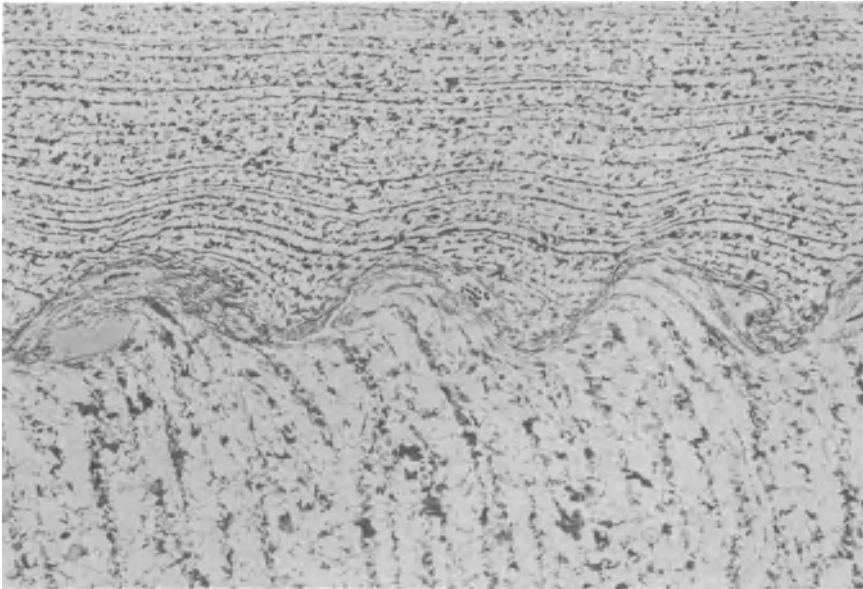


Figure 5.6 Part of the interface of an explosive weld between two C-Mn steel components. Locally fused regions are evident, in some cases containing small pores. (Etched by 2% nital; $\times 50$; reduced by $\frac{1}{4}$ in reproduction. Photo.: Welding Institute.)

of a high pressure heat exchanger, is carried out either by means of a fusion welding process or by explosive welding. Explosive welding also offers the possibility of making clad plate in two metals that cannot be joined satisfactorily by roll-bonding.

In the explosive cladding of ferrous material, it is necessary to take adequate precautions against brittle fracture of the backing plate. Such precautions may include specifying a notch-ductile steel, preheating, and (in the case of machined parts) specifying generous radii.

Explosive techniques may also be used to bond tubes to tubesheets. A detonator is placed centrally in the tube and exploded. If the tubehole is parallel, the tube will actually be expanded without welding, but if the tubehole is flared welding can be achieved. Once again, it is necessary to consider the possibility of distortion or brittle fracture of the tubesheet.

FURTHER READING

- Milner, D. R. and G. W. Rowe 1962. Fundamentals of solid-phase welding. *Metallurgical Reviews* 7, 433–80.
- Tylecote, R. F. 1968. *The solid phase welding of metals*. London: Edward Arnold.
- American Welding Society 1977. *Welding handbook*, 7th edn, Section 3. Miami: AWS; London: Macmillan.

6 Brazing, soldering and adhesive bonding

In **brazing, soldering and adhesive bonding** the objective is the same as in solid-phase welding, namely, to produce a mechanically acceptable bond between two metal surfaces without fusing the bulk material. Whereas in solid-phase welding, however, the joint is made by bonding the two surfaces directly, in the processes now under consideration, a liquid is made to flow into and fill the space between the joint faces and then solidify. The liquid used necessarily has a lower solidification temperature than the metal or metals to be joined. Brazing filler metals comprise mainly copper, nickel, silver and aluminium/zinc alloys, while the most commonly-used solders are lead/tin alloys. Adhesive joints between metals are made using a synthetic resin which solidifies by polymerisation. Although the physical phenomena associated with brazing, soldering and adhesive bonding are essentially the same, the three processes differ in their metallurgical effects, and in the means by which they are applied.

It will be convenient therefore to deal with the common physical aspects first. In so doing, the term **solder** will be applied to both brazing and soldering filler metals.

6.1 PHYSICAL ASPECTS

6.1.1 Bonding

The forces which result in the formation of a bond between a liquid and a solid metal surface are essentially the same as those discussed in Section 5.1.1 in relation to solid-phase welding. Provided that the liquid comes into extensive and intimate contact with the surface, a bond will be formed. The nature of the bond is, however, somewhat more complex in brazed, soldered or adhesive joints than it is in solid-phase welding. In brazing and soldering there is almost invariably some degree of intersolubility between solder and parent metal, and, consequently, there is interdiffusion at the parent metal surface. Even where there is no intersolubility, as for example between lead and steel, a metallic bond will be formed wherever the distance between the two metal surfaces is about equal to the normal lattice spacing. It will be immediately obvious that the probability of achieving the required intimate contact is very much greater when interdiffusion takes place because in such cases the interdiffused layer can spread laterally and may penetrate underneath oxide films.

There is less certainty about the nature of the bond in adhesive bonding. Interdiffusion is impossible in the adhesive joining of metals, and chemical bonding is limited to certain special metal/adhesive combinations. In most cases the attractive forces between the adhesive and the metal surface are physical in character. Two such interactions are known to be significant in quantity: van der Waals forces (already discussed briefly in Section 5.1.1) and **polar** forces. Van der Waals forces, also known as **dispersion** forces, result essentially from the fact that the centres of gravity of the positive and negative charges within the molecule are not stationary and coincident in space, but are in a state of continuous independent movement. Consequently, there is an oscillating, externally directed resultant force. Dispersion forces are relatively weak, having energies of the order of 1/kJ per mole as compared with about 100/kJ per mole for chemical or metallic bonds. Polar forces arise when the adhesive molecule contains a **dipole**: polyvinyl chloride $(\text{CH}_2\text{CHCl})_n$ for example contains the dipole C^+Cl^- . The force between such a molecule and another polar solid is relatively strong, but its interaction with a clean metallic surface would appear to be no greater (and possibly less) than that due to dispersion forces. However, most adhesive bonding of metals is made between oxidised surfaces and polar bonding between adhesive and oxide may be a significant effect.

As an alternative to the notion of polar or dispersion forces providing a bonding force, it has been suggested that an electrical double layer may be formed at the interface. The system is considered to act as an electric condenser, and the work of cohesion (see below) is equivalent to the stored electrical energy of an equivalent condenser. Reasonable values of the bonding energy may be calculated in this way, but experimental evidence is inconclusive.

Another significant contribution to bonding may come from surface roughness. Depending on the nature of the surface, the adhesive will penetrate more or less into pits and hollows, and as a result there will be some degree of physical interlocking with the substrate.

The strength of the bond formed in brazing and soldering is of the same order of magnitude as that within the bulk material, but in adhesive bonding of metals it may be lower. In the former case, discontinuities in the bulk strength of the solder limit the joint strength, but in the latter, a number of factors may affect the result: discontinuities, bond strength, nature of the surface and the bulk strength of the adhesive, for example.

6.1.2 Surface energy and contact angle

The surface energy (or in thermodynamic terms, the **surface free energy**) γ_s of a solid may be defined as the work done in creating new surfaces by cleavage. Conversely, it is possible to define the **work of cohesion** W_{coh} as the free energy change when two surfaces are joined together.

$$W_{\text{coh}} = 2\gamma_s \quad (6.1)$$

Liquids also possess a surface free energy. It was shown by Dupré that the work of adhesion between liquid and solid (i.e. the free energy change when liquid and solid are joined) is

$$W_{adh} = \gamma_S + \gamma_{L/V} - \gamma_{S/L} \quad (6.2)$$

where

$\gamma_{S/L}$ = surface free energy of the solid/liquid interface

and

$\gamma_{L/V}$ = surface free energy of liquid in equilibrium with its vapour.

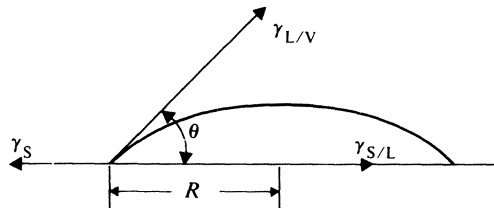


Figure 6.1 Contact between liquid drop and solid surface.

$\gamma_{L/V}$ may be expressed as joules/m² and is numerically equal to the surface tension expressed in newtons/m. Similarly, γ_S and $\gamma_{S/L}$ may be considered as forces, and ignoring the gravitational force for a drop of liquid in contact with a solid surface and having an **angle of contact** equal to θ (Fig. 6.1)

$$\gamma_S = \gamma_{S/L} + \gamma_{L/V} \cos \theta \quad (6.3)$$

The condition for the liquid to completely *wet* a solid surface is that the angle of contact should be zero, in other words that

$$\gamma_S \geq \gamma_{S/L} + \gamma_{L/V} \quad (6.4)$$

Generally speaking, therefore, liquid will wet and run over the surface of a solid if the surface energy of the solid is high relative to the sum of the liquid and solid/liquid interface surface energies. $\gamma_{L/V}$ may be measured in a number of ways, and good values for a number of liquids are available. γ_S is difficult to obtain directly and has only been measured for a few metals. However, γ_S has been calculated from considerations of cleavage strength as the work done in separating two surfaces:

$$\gamma_S = \frac{W_{coh}}{2} = \frac{Ea}{2\pi\gamma_0} \int_0^a \sin\left(\frac{\pi y}{a}\right) dy \quad (6.5)$$

where

a = relaxation distance (effective range) of attractive forces

y = distance at right angles to cleavage plane

γ_0 = lattice constant at right angles to cleavage plane

and the values obtained are of the right order of magnitude (Table 6.1).

Table 6.1 Surface free energy and surface tension of metals and adhesives

<i>Metal or compound</i>	Surface free energy: joules/m ²		
	<i>Liquid:</i> (measured as surface tension close to the melting point)		<i>Solid:</i>
		<i>Calculated*</i>	<i>Measured</i>
Teflon	0.0185		
Graphite		(0001 plane) 0.027	
Polyethylene	0.031		
Polystyrene	0.033		
Polyvinylchloride	0.040		
Nylon	0.046		
Epoxy	0.047		
Water	0.073		
Potassium	0.086		
Sodium	0.190	0.094–0.19	
Sodium chloride		0.077–0.245	0.33
Bismuth	0.376		
Antimony	0.383		
Lead	0.463		
Mercury	0.465		
Cadmium		0.48–0.80	
Magnesium	0.556		
Tin	0.566		0.685
Indium	0.599		
Zinc	0.824		
Aluminium	0.915		
Copper	1.3	0.5–1.46	1.8, 1.1, 1.37
Iron	1.835	1.45–2.83	
Nickel	1.924		
Tungsten		2.68–5.35	

* Averbach, B. L., *et al.*, (eds), *Fracture*, pp. 193–221 (paper by J. J. Gilman, Cleavage, Ductility and Tenacity in Crystals), Wiley and Chapman and Hall, London, 1959.

The figures listed in Table 6.1 give only a very broad guide to the wettability of solids, since not many values of $\gamma_{S/L}$ are available, and there is no simple relationship between γ_S , $\gamma_{L/V}$ and $\gamma_{S/L}$. The free energy of the interface depends upon the mode of interaction between the individual liquid and the individual solid. However, a liquid of high surface energy will not wet one of low surface energy. Thus it is very difficult to solder or braze grey cast iron, since the iron surface is contaminated with graphite having an exceptionally low surface energy. Also, solid metal surfaces generally have high surface energies, and, if uncontaminated, are readily wetted by many organic liquids.

Liquid metals likewise have a high surface energy and as a result are sensitive to contamination by surface-active agents. Consequently, it is exceptional for the values of surface energy quoted in Table 6.1 (which are for pure metals)

to be realised with commercial materials or in a normal industrial environment. For example, the generally accepted figure for the surface energy of liquid steel (which is internally contaminated with carbon, sulphur and phosphorus as well as being oxidised to some degree) is 1.2 J/m^2 as compared with 1.835 J/m^2 for pure iron. Other metals may be similarly affected.

6.1.3 Capillary action

The manner in which a liquid adhesive or solder will fill a capillary is important in two respects; it influences the joint filling capacity (for solders) and the degree to which surface imperfections are filled.

The vertical height H to which a liquid rises between two parallel plates separated by a distance d is given by

$$H = \frac{2\gamma_{\text{L/V}} \cos \theta}{\rho dg} \quad (6.6)$$

where ρ = density of liquid. Also the velocity v of flow at any height h of a liquid into the space between two parallel surfaces of separation d is given by the Poiseuille formula:

$$v = \frac{\gamma_{\text{L/V}} d \cos \theta}{4\eta h} \quad (6.7)$$

where

h = height to which liquid has risen

η = viscosity

It may be deduced that, other things being equal,

- (a) The height to which a liquid rises in a capillary space increases as the separation of the surfaces is reduced.
- (b) The rate of flow into the joint decreases as the separation of the surfaces is reduced.

The behaviour of liquid solder is broadly according to these deductions. However, metallurgical factors, particularly alloying between the solder and the parent metal, have an important and often a dominating effect on soldering and brazing characteristics.

In adhesive joining air may be trapped between the liquid adhesive and pits in the metal surface. The radius r of the gas bubble so formed depends upon the size and shape of the pit and the contact angle θ between liquid and solid, as shown in Figure 6.2a, while the relationship between radius of the bubble interface with the adhesive and the contact angle is shown diagrammatically in Figure 6.2b. The theoretical tensile stress to cause propagation of a crack from such cavities is

$$\sigma = \left[\frac{\pi E_{\text{a}} \gamma_{\text{a}}}{2r(1 - \alpha_{\text{a}}^2)} \right]^{1/2} \quad (6.8)$$

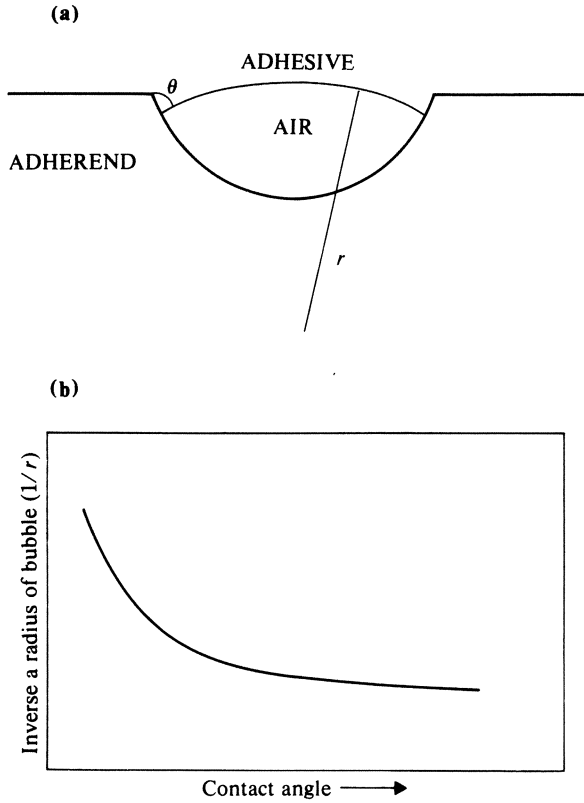


Figure 6.2 (a) Air bubble trapped between adhesive and adherend; (b) relationship between contact angle of bubble and inverse square root of its radius ($1/\sqrt{r}$).

where

- E_a = Young's modulus of adhesive
- γ_a = bonding energy of the joint
- α_a = Poisson's ratio of adhesive

The ordinate of Figure 6.2b is proportional to $1/\sqrt{r}$ and is therefore representative of the theoretical fracture stress as calculated from Equation 6.8. Tensile tests on metal adhesive joints give curves of tensile strength against contact angle that are very similar in character to those of Figure 6.2b, indicating that trapped bubbles may in some instances have a governing effect on joint strength.

Adhesive joints may be expected to fail in a brittle or quasi-brittle manner, and the techniques of fracture mechanics (see Ch. 10) are, in principle, applicable. If U is the strain energy associated with a stressed adhesive joint, then for plane strain

$$\frac{\partial U}{\partial A} = G = \frac{1 - \nu^2}{E} [K_I^2 + K_{II}^2 + K_{III}^2] \quad (6.9)$$

where A is area, G is the energy rate, and K_I , K_{II} and K_{III} are the stress intensity factors associated with the three fracture modes. In lapped joints such as are used in adhesive joining both the opening and the edge sliding modes of failure (represented by K_I and K_{II} respectively) are significant. The condition for failure is:

$$\frac{\partial U}{\partial A} \geq \gamma_a \quad (6.10)$$

where γ_a is the bonding energy of the joint and

$$\gamma_a = \gamma_1 + \gamma_2 + \gamma_3 \text{ etc.} \quad (6.11)$$

where γ_n are the contributions to bonding energy by surface energy, interlocking, plastic work and other factors. Evaluating G or K for an adhesive joint is not straightforward because the geometry does not lend itself to an analytic approach; also, it may be that the stress concentration factor inherent in a lap joint (Section 6.5.1.2) is a dominant factor in determining joint strength.

6.2 SOLDERING AND BRAZING

Brazing and soldering are essentially similar in character; both comprise the introduction of a **filler metal** having lower melting point than the metals to be joined, heating of the assembly, and flow and filling of joint space by the **solder** or **brazing** metal. Thus, in order to obtain a satisfactory brazed or soldered joint, it is necessary for the solder to

- (a) wet the parent metal,
- (b) spread and make contact with the joint opening,
- (c) be drawn into the joint by capillary action.

When the solidus temperature of the filler metal is below about 500°C , the process is termed **soldering**; when the filler metal solidus is higher than 500°C , it is termed **brazing**. This classification is arbitrary, but useful, in that fluxing materials and techniques are different for the two groups of fillers.

6.2.1 Wetting and spreading

In general liquid solders do not wet clean unfilmed solid metals; for example lead–tin solders have a contact angle of between 25° and 70° with a steel surface, depending upon the solder composition. However, tin is capable of alloying with iron, and if a film of tin is in some way deposited on and alloyed with the iron surface, then tin–lead solder will wet it. Alloying is therefore essential to

wetting; lead, for example, which does not alloy with iron, will not wet a steel surface. Alloying also aids spreading since, if the liquid metal dissolves in the solid, it can diffuse beneath small areas of oxide and detach them, and will guide the flow of bulk liquid over the whole surface. In general, a solder will wet a metal surface provided that either (a) it forms an intermetallic compound with the solid; or, (b) the solid metal can take the solder into solution. When a drop of low-melting-point solder is placed on a metal surface and held at an appropriate temperature, it will spread until a state of equilibrium is reached, and there is a definite contact angle between liquid and solid. During the spreading process the solder may diffuse into the surface layer of the solid metal ahead of the main bulk of the liquid, so that the effective surface energy of the solid becomes that of an alloy between the original metal and the solder.

The character and degree of spread depends upon the nature of the two metals, the temperature, the presence or absence of flux, the roughness of the solid surface and its degree of oxidation. In some cases (for example, lead–tin alloys containing less than 30% tin) the equilibrium condition is set up rapidly, with very little spread. With higher-tin alloys, however, the initial spread is followed by a secondary spread which occurs over a substantial period of time. This secondary spread is associated with the formation of a strongly-marked diffusion band. The greatest amount of spread of the lead–tin solders occurs with alloys close to the eutectic composition. In practical soldering such alloys have the best **flow** characteristics.

Oxide layers inhibit wetting and spreading, and it is one of the functions of a flux to remove the bulk of the oxide and expose clean metal. Flux may also modify the surface tensions of the liquid and solid phases, although there is little positive evidence on this point. A more important effect is the deposition of surface films from the flux by electrolytic or chemical action. For example, when a zinc chloride flux is in contact with steel and tin–lead solder, tin goes into solution in the flux (which acts as an electrolyte) and is deposited on the steel – a rapid and effective means of improving the spreading capacity of the solder. Borax, which is used as a brazing flux, is reduced by a number of metals to form low-melting borides, which similarly aid wetting and spreading.

Surface texture has a beneficial effect on spreading if it constitutes a series of interconnecting channels along which solder may be drawn by capillary forces. Lateral diffusion of the solder from such channels then forms a diffusion band, which encourages rapid spreading of the bulk liquid.

Good wetting and spreading is a desirable property in a solder primarily because the mechanics of the process demand that the solder be brought smoothly, rapidly and continuously to the joint opening. It must be emphasised, however, *that wetting is not absolutely essential to the formation of a bond*. For example, although lead does not wet steel, if molten lead is allowed to solidify in contact with a clean oxide-free steel surface, the two metals will be strongly bonded.

6.2.2 Filling the joint

The main factors which govern the effectiveness of joint filling are the contact angle for the solder/parent metal system, **clearance** (i.e. separation of the joint faces), heating rate, uniformity of heating, temperature, and the use of flux.

Maximum joint clearances are quantitatively smaller than would be calculated using Equation 6.6, but the predicted trend is correct; clearances for the light metals aluminium and magnesium (0.125 to 0.625 mm) are substantially greater than for copper alloys (0.05 to 0.40 mm). Where intersolubility of solder and parent metal is a problem, small clearances may result in excessive contamination of the solder, increase of melting point, and premature solidification. Faster heating minimises the effect of intersolubility.

Uneven heating necessarily results in irregular filling. Straight joints are difficult to heat evenly, and, from this aspect, joints with circular symmetry are best, particularly when furnace heating is used. Fluxed joints almost invariably contain flux inclusions. Maximum soundness of brazed joints is obtained by heating in a vacuum without flux.

6.2.3 Solidification range

The most generally useful brazing or soldering alloys are those close to a eutectic composition and which therefore have a narrow melting range. For special purposes, however, a longer melting range may be desirable. For example, in making a wiped joint with plumber's solder it is necessary to manipulate the deposited solder while it is in the pasty condition. In such cases a certain minimum proportion of eutectic must be present in the solidifying mass in order that it should be sufficiently plastic.

Brazing alloys of long melting range may be subject to a defect known as **liquation**. On slow heating the eutectic component of such an alloy melts first and runs out, leaving behind a skeleton structure of the higher-melting component. Liquation may occur, for example, with low-silver copper–zinc–silver–cadmium brazing solders.

Generally speaking, a tendency towards reduced **flowability**, and increased **liquation and brittleness** during solidification makes it necessary to use long-melting-range alloys with care, particularly those remote from the eutectic composition.

6.3 SOLDERING

6.3.1 Joint design

Typical soldered joints are shown in Figure 6.3. Because of the relatively low strength of soldering alloys, it is desirable to design soldered joints so that they interlock mechanically, leaving the solder to act as a sealing and bonding agent.

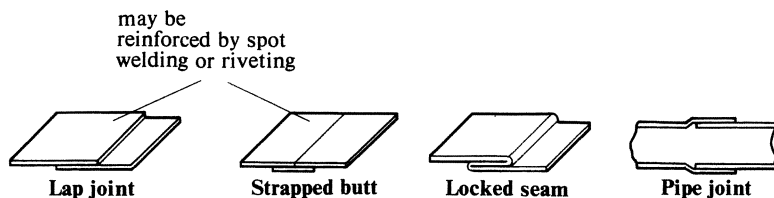


Figure 6.3 Typical soldered joints.

Spot welding is another way of providing added strength; alternatively, the joint may be placed in a position of minimum stress.

6.3.2 Solders

The binary tin-lead alloys are the most commonly used solders. Some lead-tin solders contain antimony, which permits manufacturers to make use of secondary metal derived from bearing metals. Such solders have slightly increased mechanical properties and slightly inferior flowability when compared with the antimony-free equivalent. They cannot be used for zinc or alloys containing zinc, because the joint is embrittled by antimony-zinc compounds. Higher-melting-point solders are occasionally required for elevated temperature applications or for components on which a succession of different soldering operations must be performed (**step soldering**).

6.3.3 Fluxes

Soldering fluxes must dissolve or displace oxide, and, if possible, have a positive effect in promoting rapid wetting and spreading. The least active type of flux is composed of a solution of rosin in petroleum spirit. Rosin consists largely of abietic acid, which becomes active at the soldering temperature but reverts to an inert, non-corrosive form on cooling. It is, therefore, widely used in radio and electronic work, where effective cleaning after soldering would be difficult. Various organic compounds are used as fluxes, either alone or mixed with rosin; examples are the hydrochloride of glutamic acid and hydrazine hydrobromide. Such materials decompose at soldering temperatures, and the residues are easily washed off with water. The soldering of steel requires a zinc chloride flux, which leaves highly corrosive residues and must, therefore, be completely removed by postsoldering cleaning. A solution of zinc chloride in hydrochloric acid, which is used for soldering stainless steel, is even more corrosive.

Generally, the less active the flux, the better must be the wetting and spreading properties of the solder. For example, the more fluid (50Sn50Pb or 60Sn40Pb) solders are normally used with non-corrosive rosin flux.

6.3.4 Soldering methods

Solder may be applied using a soldering iron, by flame heating, resistance heating, induction heating, hot plate heating or oven heating, by dipping or by means of a spray gun. The first three methods are used primarily for manual soldering. The size of heating torch and the composition of the fuel gas is determined by the mass and configuration of the assembly and should be such as to give rapid heating without too much danger of reaching excessive temperatures. Resistance tools employ carbon electrodes and require the solder and flux to be replaced.

In dip soldering a complete assembly is degreased, cleaned and fluxed, and is then dipped in a pot of molten solder, thus simultaneously making numerous joints. Induction heating is applied to quantity production of small parts and is capable of complete mechanisation. In any mechanical soldering operation it is essential that the joint clearance be accurately maintained until the joint has solidified. Ultrasonic transducers may be used for the fluxless soldering of aluminium and other non-ferrous metals. The solder is melted on the surface to be joined, and ultrasonic vibrations are applied by means of a probe to the surface of the solder. The oxide film on the metal surface is thereby broken up and the metal is tinned. This technique cannot be applied directly to the soldering of lapped or crimped joints.

6.3.5 Application to various metals

Soldering temperatures are such that there are no significant metallurgical changes in the parent materials, so that apart from the danger of subsequent corrosion due to residual flux or to galvanic action, soldering does not have damaging side effects.

The oxides that form on stainless steel, aluminium bronze and beryllium copper are resistant to chemical attack and require the use of acid fluxes. Graphitic cast irons are also difficult to wet because of the graphite exposed at the surface, and electrolytic treatment in a salt bath may be necessary. Aluminium and magnesium both present difficulties. Aluminium may be soldered with a tin–zinc or zinc–aluminium solder but the resulting joint has poor corrosion resistance due to galvanic action between solder and aluminium. The same problem arises with magnesium and, in both cases, soldered joints must be protected against moisture.

6.4 BRAZING

6.4.1 Joint design

Typical designs of brazed joints are shown in Figure 6.4. The strength of sound brazed joints is of the same order of magnitude as that of normal engineering materials, so that the additional means of strengthening employed for soldered

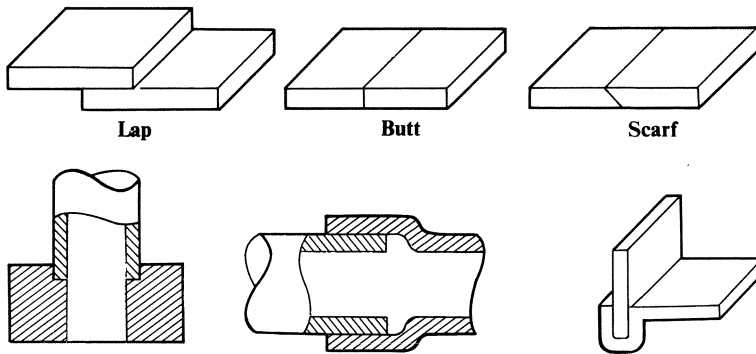


Figure 6.4 Typical brazed joints.

joints are not required. Butt joints in sheet or plate, however, are rarely used, because it is difficult to ensure freedom from defects. Optimum joint clearance is in the range 0.05 to 0.125 mm for most brazing materials; exceptions are copper, which gives strongest joints with an interference fit (maximum 0.075 mm), and light metals, for which gaps up to 0.25 mm are satisfactory.

6.4.2 Brazing solders

The traditional coppersmith's brazing **spelter** is either 50Cu50Zn in the form of granules or 60Cu40Zn rod. Small amounts of tin are sometimes added, but the metallurgical effect, if any, is small. For fine work and alloy steel the quaternary Cu–Zn–Ag–Cd silver solders find increasing use because of their low melting range and good flowability. Pure copper is especially valuable for furnace brazing steel in reducing atmospheres. Phosphorus bearing alloys are intended for copper and copper alloys; they cannot be used on steel or nickel alloys because of the formation of brittle iron or nickel phosphides.

Large numbers of special-purpose brazing alloys have been developed for high temperature applications such as gas turbines. A nickel–chromium–iron–boron alloy, which depends upon the boron addition for its low-melting characteristics, is a commonly used type. Boron diffuses rapidly in stainless and heat-resisting steels, and this promotes wetting and spreading (also in some cases erosion).

6.4.3 Fluxes and protective atmospheres

Borax has been used as a brazing flux for centuries, and remains one of the most useful components of flux to this day. Borax and boric acid are reduced by chemically active metals such as chromium to form low-melting borides. At the same time, they have the power to dissolve non-refractory oxide films at the brazing temperature. Additions of fluorides and fluoroborates to a borax–boric acid mix lowers the melting point to a level where the flux can be used with

silver solders, and increases the activity against refractory films. For aluminium, magnesium, titanium and zirconium the most effective fluxes are mixtures of chlorides and fluorides. Borax flux residues after brazing are often glass-like, and can be removed only by thermal shock (quenching), or abrasive or chemical action. The chloride-fluoride flux residues are water soluble and must be removed to avoid subsequent corrosion.

Brazing is frequently conducted in a furnace with a protective atmosphere, either with or (preferably) without flux (see Table 6.2). The type of atmosphere required may be qualitatively assessed by considering the dissociation of the metal oxide concerned:



for which the equilibrium constant is

$$K = \frac{(a_m)^2 (O_2)}{(a_{mO})^2} = P_{O_2} \quad (6.13)$$

where P_{O_2} is the **dissociation pressure** of the oxide in question, and a_m and a_{mO} are the activities of metal and oxide respectively. Hence

$$\Delta G = -RT \ln P_{O_2} \quad (6.14)$$

The more stable oxides have lower dissociation pressures, and therefore require a lower **oxygen potential** in the protective atmosphere if they are to be effectively reduced. The oxygen potential of the atmosphere results from dissociation of gaseous oxides:



each of which has an equilibrium constant such as

$$K_{\text{H}_2\text{O}} = \frac{[\text{H}_2]^2 [\text{O}_2]}{[\text{H}_2\text{O}]^2} = \frac{P_{\text{H}_2}^2 P_{\text{O}_2}}{P_{\text{H}_2\text{O}}^2} = \exp(-\Delta G_{\text{H}_2\text{O}}/RT)$$

so

$$RT \ln P_{O_2} = -[\Delta G_{\text{H}_2\text{O}} + 2RT \ln (P_{\text{H}_2}/P_{\text{H}_2\text{O}})] \quad (6.17)$$

Thus the oxygen potential of the atmosphere is reduced, other things being equal, by increasing the hydrogen content and reducing the water vapour content. Similarly from Equation 6.15 increasing the CO/CO₂ ratio will reduce the oxygen potential. The dissociation pressure of metal oxides is so small that, if the oxide is in contact with a gas mixture, the value of P_{O_2} will be virtually equal to the oxygen potential of the gas. Therefore, if P_{O_2} for the gas is lower than the dissociation pressure of the oxide, reduction is thermodynamically possible and vice versa. Consequently, the more stable oxides will only be reduced by hydrogen if the partial pressure of water vapour in the mixture is extremely low. In brazing technology the water vapour content of a hydrogen atmosphere is usually measured by the **dewpoint**. The relationship between

Table 6.2 Furnace atmospheres for brazing

<i>Type</i>	<i>Dew point of incoming gas</i>	<i>Approximate composition</i>				<i>Typical use</i>
		<i>range %</i>	<i>H₂</i>	<i>N₂</i>	<i>CO</i>	<i>CO₂</i>
Burnt towns' gas	Ambient	10-12	70-75	8-10	6-8	Copper brazing of low-carbon steel
Burnt towns' gas	Ambient	2-4	80	2-4	12-14	Brazing copper and copper-base alloys
low-hydrogen						Brazing medium and high-carbon steels and alloy steels
Cracked towns' gas	Down to -15 °C	43-50	20-28	25-28		Alloys containing chromium, including stainless steels. Tungsten and platinum contacts
Cracked ammonia	- 50 °C	75	25			Cobalt-base alloys. Carbides
Dry hydrogen	- 60 °C	100				Titanium, zirconium, hafnium
Inert gas			Argon			All non-volatile metals
Vacuum			Vacuum			

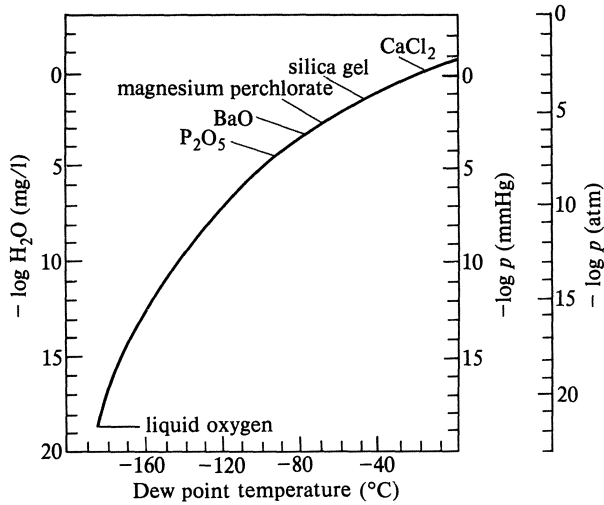


Figure 6.5 Relationship between the various scales of measurement of the saturated vapour pressure of ice and the dew point (*Brit. Welding J.* 1958, 5, 99).

dewpoint and the equilibrium vapour pressure of water or ice is shown in Figure 6.5.

Burnt towns' gas provides a cheap reducing atmosphere for the flux-free copper brazing of steel and for brazing copper alloys. Cracked towns' gas, which is obtained by passing hydrocarbon gas over a heated catalyst, is a suitable atmosphere for low alloy steel, but more refractory materials require progressively lower dewpoints, as obtained from dissociated (cracked) ammonia, nitrogen/hydrogen mixtures or dry hydrogen. Increasing use is now made of purified argon or vacuum furnaces for brazing high temperature alloys and metals such as titanium and zirconium. Flux-free brazing is possible in pressures substantially higher than the dissociation pressure of the oxide concerned; for example, stainless steel is wetted by copper at a pressure of 10^{-4} mm Hg, whereas the dissociation pressure of chromic oxide at the brazing temperature is about 10^{-23} mm Hg. It seems probable that at low pressure the oxide film is reduced in thickness or disrupted, so that it may be penetrated by the brazing alloy.

6.4.4 Brazing methods

Brazing may be achieved by means of a torch, by resistance or induction heating, by dipping or in a muffle-type furnace. Torch brazing is the common manual technique, an oxy-coal gas or oxy-acetylene torch being used. Induction heating is useful for repetition work suitable for brazing in the open air, the induction heating coil being designed and shaped for each specific application. Dip-brazing is applied to aluminium; sheet coated with a $7\frac{1}{2}\%$ silicon brazing alloy is formed

to the required shape, and then dipped into a flux bath at the correct temperature. In manual brazing the filler alloy is added in the form of rod, which may be dipped in flux before application. Alternatively, it may be in the form of granules (50/50 copper/zinc spelter), or it is preplaced around or in the joint in the form of wire or metal foil.

6.4.5 Bronze welding

The term **bronze welding** is used for the gas welding of iron or steel using a brazing filler metal. In brazing, the joint is raised to brazing temperature, and the filler (if not already in position) is added so that it flows into the whole of the joint at once. In bronze welding, on the other hand, a small area is heated with an oxy-acetylene torch, a globule of filler (common brazing metal) is deposited on the joint with flux, and the torch is then withdrawn slightly in order to allow this globule to solidify. A second adjacent area is then heated, and filler metal added, so that it unites with the first. The procedure is then continued along the joint.

In bronze welding the joint strength may be achieved by means of an external fillet, and filling the joint space by capillary action is not an essential feature of the process. The risk of intergranular penetration of the parent metal by brazing metal is lower in bronze welding than when the joint is brazed in the normal manner. Bronze welding may be applied to many metals but is most frequently used for steel and cast iron. Butt welds and fillet welds can be made and the process has the advantage that it is performed at a relatively low temperature. Bronze welding is mainly used for maintenance and repair, but is also applied to production work.

6.4.6 Application to various metals

Copper which is furnace or torch brazed must be oxygen-free or deoxidised, since tough pitch copper is embrittled by hydrogen. Steel, copper alloys, nickel and nickel alloys are particularly susceptible to intergranular penetration and cracking by brazing material if residual or applied stresses are present during the brazing operation, or if the brazing temperature is too high, so they should be stress-relieved before brazing and supported so as to minimise stress. If stress relief is impracticable, a low-melting silver brazing alloy is used. Austenitic stainless steels that may be exposed to a corrosive environment after brazing must be of the extra-low-carbon, titanium-stabilised or niobium-stabilised type, since during brazing the metal is held in the carbide-precipitation range. As in welding, nickel and nickel alloys must be free from surface contaminants – sulphur, lead, bismuth and other low-melting metals – otherwise cracking may occur.

In certain applications the operating temperature is so high that available brazing alloys would melt. Such joints are made with a normal brazing metal (copper, for example), and then held at an appropriate temperature until the

brazing alloy has completely diffused into the parent metal, a process known as **diffusion bonding** (Section 5.2.2).

Graphite on the surface of grey, malleable and nodular cast iron may prevent effective wetting and the cleaning techniques recommended for preparation before soldering must be used.

The strength of a defect-free brazed joint in carbon steel increases as the joint clearance is reduced, and may be substantially higher than the strength of the brazing metal in bulk form. However, when the gap is reduced below a certain level, the joint will contain defects and therefore there is an optimum range of joint clearance for maximum soundness and strength. Typical figures are 0.075 to 0.4 mm for brazing copper with spelter (60/40 brass), and zero to 0.075 mm for the copper brazing of steel.

The effect of the brazing heat on the mechanical properties of hardened and tempered steels or precipitation-hardened alloys must be carefully considered. In the case of certain tool steels the tempering temperature is close to the brazing temperature for silver solder, so that it is possible to combine the tempering and brazing operations. Likewise in the case of precipitation-hardening materials, it may be possible to combine brazing with solution treatment. Careful selection of the brazing material and heating cycle is necessary if it is required to combine the brazing operation with heat treatment.

6.5 ADHESIVE BONDING

The joining of metals by adhesives is used mainly in the manufacture of automobiles and aircraft. Joint designs are very similar to those used in brazing, but the character of the joint differs substantially. The uncertainties which attend the correct flow and filling of the joint space by a liquid metal do not affect adhesive bonding; adhesives may be applied in liquid form at room temperature, and the surfaces subsequently joined by the application of heat and pressure. The ease and certainty of making the joints must, however, be contrasted with the relatively low strength of both the bond and the filler material. In brazed and soldered joints the bond is essentially similar in character to that within the bulk of the metal, but in adhesive jointing the bond results either from polar forces between the adhesive and a relatively brittle oxide film, or Van der Waals forces between the adhesive and the unfilmed metal. The elastic properties of brazing metal and solders are not greatly different from those of the metals being joined, but those of the organic materials used for adhesives (in particular their coefficients of thermal expansion and moduli of elasticity) may differ by one or two orders of magnitude from the equivalent metal properties. The mechanical properties of adhesive joints are therefore of some concern, and the factors which affect them will be considered below.

6.5.1 Mechanical strength

The mechanical strength of an adhesive-bonded joint depends upon the joint configuration, its dimensions, the nature of the adhesive and its thickness. Generally speaking the strength of a lap joint increases with the amount of overlap (although the strength *per unit area of joint* decreases), and decreases with increasing thickness of adhesive. Factors which may influence this behaviour are contact angle between adhesive and metal, residual stress, and stress concentration in the adhesive.

6.5.1.1 Contact angle

One of the possible mechanisms by which contact angle can affect joint strength has already been discussed, namely by determining the radius of air bubbles formed at the metal/adhesive interface. The smaller the angle of contact, the smaller the radius of the interface between the air and the adhesive and the higher the bond strength.

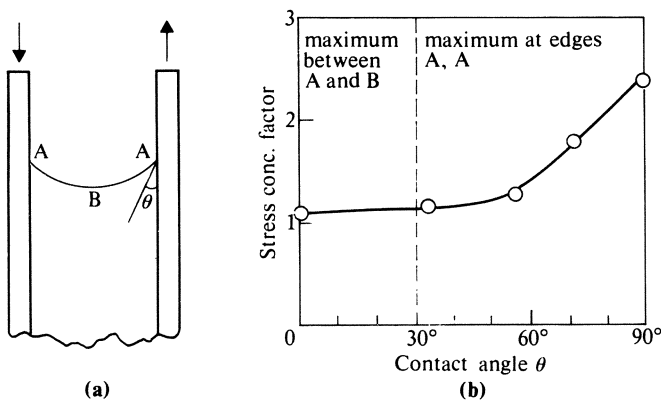


Figure 6.6 Stress concentration in adhesive between two rigid plates as a function of contact angle (Eley, D. D. 1961. *Adhesion*. Oxford: Oxford University Press).

In addition, it has been demonstrated that if a meniscus forms at the free surface of the adhesive (Fig. 6.6a), then the point where the maximum stress concentration arises depends upon the contact angle (Fig. 6.6b). With low contact angles the stress concentration factor is small, and the maximum stress is at the free surface of the adhesive away from the interface, so that fracture will tend to occur (other things being equal) through the body of the adhesive. With higher contact angle the stress concentration factor increases, and the maximum shifts to the edge of the interface, tending to promote fracture along the interface. The latter condition is likely to give lower mechanical strength. In practice adhesive is usually extruded outside the overlap area when pressure is applied to make the joint, so that the equilibrium meniscus is not necessarily formed.

Table 6.3 Shear strength of 12.5 mm redux bonded lap joints at room temperature

<i>Material</i>	<i>Thickness (mm)</i>	<i>Mean failing stress (MN/m²)</i>
Bright mild steel	1.6	34
Stainless steel (similar to AISI Type 301)	1.2	39
Magnesium alloy (HK31A–H24)	1.6	22
Commercially pure titanium (I.C.I. Titanium 130)	1.3	28
Aluminium alloy (2024–T3 Alclad: Duralumin)	1.6	34

Mechanical properties of redux (20 °C)

<i>Cured 30 minutes at 150 °C</i>	<i>MN/m²</i>
Young's modulus	3.3×10^3
Shear modulus	1.2×10^3
Ultimate tensile strength	70
Ultimate shear strength	60

6.5.1.2 Residual stress and stress concentration factors

All adhesives shrink as they set. This may be due to cooling from the molten state, to loss of solvent, or to polymerisation and the formation of cross-linkages during curing. The adhesive in a completed joint is therefore in a state of residual tensile stress, which may reduce the joint strength. The greater the thickness of the adhesive, the greater the shrinkage and residual stress, so that the joint strength should theoretically diminish with increasing thickness of adhesive. This is in accordance with experience. Even when the adhesive thickness is small, however (which is generally the case for metal joints), the shear strength of a lap joint in tension is usually between 30% and 60% of the shear strength of the bulk adhesive, and varies according to the alloy being joined (Table 6.3). The reason for this reduction of strength is that there is a stress concentration at each end of the overlap, due to the shape of the adhesive surface (Section 6.5.1.1), to the difference between the elastic moduli of metal and adhesive, to bending of the joint under load (Fig. 6.7) or to a combination of these factors.

The effect of different elastic moduli was analysed by Volkerson for a lap joint between two rigid plates with an overlap of $2c$ and adhesive thickness d (Fig. 6.7). The **stress concentration factor**, n , equal to the maximum shear stress divided by the average shear stress, is approximately

$$n = \left[\frac{2c^2 G_a}{etd} \right]^{1/2} \quad (6.18)$$

where

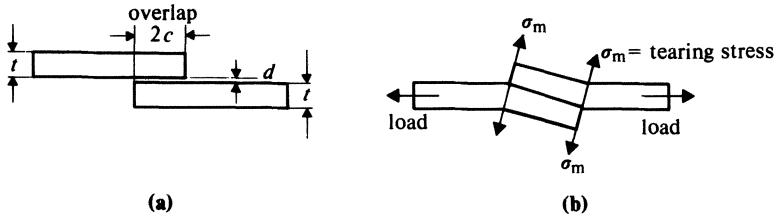


Figure 6.7 (a) Dimensions of adhesive bonded lap joint; (b) bending of adhesive bonded lap joint in tension and location of maximum tearing stress.

E = Young's modulus of metal

t = thickness of plates (assumed equal)

G_a = shear modulus of adhesive

Equation 6.18 gives acceptable results for $n > 1.5$, which is generally the case for metal joints. Typical figures for aluminium might be $c = 6$ mm; $G_a = 1.2 \times 10^3$ MN/m²; $E = 7 \times 10^4$ MN/m²; $t = 1.2$ mm $d = 0.25$ mm; using these figures Equation 6.18 gives a stress concentration factor of about 3.

The failure stress σ'_B of the joint, according to Equation 6.18 is

$$\sigma'_B = \frac{\sigma'_S}{n} = \frac{\sigma'_S}{c} \frac{Etd}{2G_a}^{1/2} \quad (6.19)$$

where σ'_S is the shear strength of the adhesive. Equation 6.19 indicates that the shear stress at failure should be inversely proportional to the overlap. In fact, the failure shear stress does decrease as the overlap increases; in a typical case it is inversely proportional to \sqrt{c} . Thus, Equation 6.19 is indicative of a trend, but is not precise. Other theoretical formulae for joint strength have been developed, but in no case is the agreement with experimental results particularly good. It must in any event be remembered that joint configurations used in practice may behave differently under load than small test specimens, so that the experimental results themselves must be interpreted with caution, except where they are validated by full-scale tests.

6.5.2 Bonding methods

The types of joint that may be used in the adhesive bonding of metals are illustrated in Figure 6.8. In making bonded joints there are essentially three steps – preparing the surface, applying the adhesive, and curing the joint – and these are described below.

6.5.2.1 Preparing the surface

There are two essential steps in preparing a metal surface for adhesive bonding: degreasing and roughening the surface by chemical etching or mechanical abrasion. Aluminium alloys are first degreased in a vapour bath and then dipped

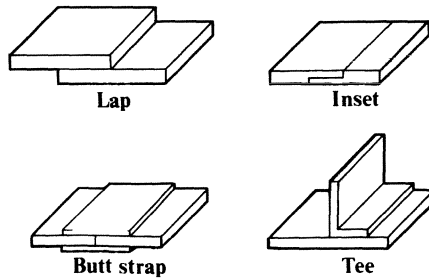


Figure 6.8 Typical joint design for adhesive bonding

in a chromic–sulphuric acid bath or anodised in chromic acid. Alternatively, the metal may be roughened with an abrasive. Steels are first shot-blasted to remove rust and mill-scale, and then degreased. Chemical etching may be necessary for high chromium materials.

6.5.2.2 *Types of adhesive and the mode of application*

Generally speaking, the essential component of a metal adhesive is a **thermo-setting resin**, although adhesives used in practice may be complex mixtures. **Ethoxyline (epoxy)** and **isocyanate resins** both form excellent bonds with suitably prepared metal surfaces. One of the most successful adhesive techniques is **redux bonding**. In one adaptation of this technique metal is first given a coat of **phenol formaldehyde** (taken up in a suitable solvent). **Polyvinyl formaldehyde** powder is then scattered on the prepared surfaces, and subsequently they are brought together under pressure and cured. The polyvinyl resin is the main adhesive but the precoating of phenol formaldehyde is necessary to bond it to the metal. Other successful metal adhesives consist of combinations of phenol formaldehyde resin with **nylon**, **neoprene**, or **polyvinyl butyrate**.

Adhesives may be applied in the form of liquid, the active ingredients being dissolved in a solvent which evaporates after application. They are also applied as sheet or powder, generally on a precoated surface. Liquids are brushed or sprayed on the metal surface, or applied by means of a roller.

6.5.2.3 *Curing the joint*

When there is a solvent present in the adhesive, it is necessary to allow sufficient time for it to evaporate before placing the surfaces together. The parts are then clamped with a moderate pressure, typically in the range 0.1 to 1.0 MN/m^2 in a suitable press. Complex parts are placed in a plastic bag which is then evacuated, allowing atmospheric pressure to apply the clamping force. Surplus adhesive is removed when possible and the assembly is heated through the curing cycle, preferably in an oven although electric heating pads are sometimes used for large items. A typical curing period is 30 minutes at 145°C , but shorter times combined with higher temperatures may be applicable. Curing times are reduced (with some loss of bond strength) if an **accelerator** is added to the adhesive.

6.5.2.4 Testing

In aircraft applications particularly, routine testing is carried out in order to control joint quality, and various other tests are employed in checking batches of adhesive, or in development work. The most commonly used destructive test is the shear test, in which a lap joint 25 mm wide with a 12.5 mm overlap is loaded in tension along a line parallel to the plane of the joint. More rarely a butt joint is tested in tension by loading in a direction at right angles to the joint line (also known as the **glue line**). Impact tests in which the joint is broken in shear using a pendulum-type impact machine may be useful in comparing different adhesives.

Attempts have been made to develop non-destructive tests of adhesive joints, but without much success. Ultrasonic testing can detect gross discontinuities in a lap joint, but interpretation of the results is difficult. Therefore routine quality control must rely primarily on destructive tests of samples made at the same time as the production assemblies.

6.5.3 Applications

Adhesive bonding of metals is employed mainly in aircraft and automobile construction. The redux process was developed primarily as an alternative to riveting for aircraft structures during the decade before 1944, and since that date has been used as one of the joining processes in a number of military and commercial aircraft. Typical applications are the fastening of stiffeners to the aircraft skin and in assembling **honeycomb** structures, which consist of a honeycomb core bonded between two sheet metal skins. In automobiles, adhesive bonding is mainly of interest for attaching brake linings to shoes, and for stiffeners and fabricated box sections.

FURTHER READING

General

Milner, D. R. 1958. A survey of the scientific principles related to wetting and spreading. *Brit. Welding J.* 5, 90–105.
American Welding Society 1976. *Welding handbook*, 7th edn, Section 2. Miami: AWS; London: Macmillan.

Soldering

Thwaites, C. J. 1977. *Soft-soldering handbook*. London: International Tin Research Institute Publication no. 533.

Brazing

Brooker, H. R. and E. V. Beatson 1953. *Industrial brazing*. London: Associated Iliffe Press.

Adhesive bonding

Eley, D. D. 1961. *Adhesion*. Oxford: Oxford University Press.

Houwink, R. and G. Salmon 1965. *Adhesion and adhesives*, 2nd edn. Amsterdam: Elsevier.

Semerdjiev, S. 1970. *Metal to metal adhesive bonding*. London: Business Books.

Anderson, G. P., S. J. Bennett and K. L. de Vries 1977. *Analysis and testing of adhesive bonds*. New York and London: Academic Press.

7 Carbon and ferritic-alloy steels

7.1 SCOPE

It is the intention to discuss in this chapter those steels that have a body-centred cubic form at or above normal atmospheric temperature. Included are carbon steels with carbon contents up to 1.0%, carbon–manganese steels with manganese content up to 1.6%, and steels containing other alloying elements up to the martensitic type of 12% Cr steel and maraging nickel steel. Higher-alloy ferritic and ferritic/austenitic steels are also included, although they may not suffer an α to γ transformation. Other than this last group, the common feature about these alloys is that they may all, to a greater or lesser degree, be hardened as a result of passing through the weld thermal cycle and may therefore suffer a change in properties in the region of a fusion-welded joint. General metallurgical questions will be considered first, and a later section will deal with the individual alloys and alloy groups that are used in welded fabrication. Cast iron is included in the material groups since, from a welding viewpoint, it suffers the same type of transformation in the HAZ of fusion welds as steel, albeit in an extreme form.

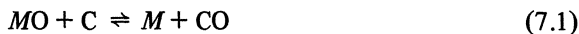
7.2 METALLURGY OF THE LIQUID WELD METAL

7.2.1 Gas–metal reactions

Oxygen, nitrogen, steam, carbon dioxide and carbon monoxide may all react with ferrous weld metals, and it is one of the objectives of the design of welding processes to control such reactions and mitigate any damaging effect they may have. Hydrogen reacts with certain metals but not normally with iron, and its effect is mainly through physical solution. Hydrogen may, however, react with the more easily reducible oxides to form steam. Other reactive permanent gases are only rarely present in welding atmospheres and will not be considered here. The inert gases helium and argon are used to shield the molten weld metal and prevent unfavourable gas–metal reactions. They do not react with iron nor are they dissolved to any significant extent.

The free energies of formation of metal oxides, CO and CO₂ are plotted as a function of temperature in Figure 4.2. These are of course equilibrium values, and in welding the time-scale may be such that equilibrium is not achieved. Moreover, segregation may result in the concentration of reactants being different

from the anticipated mean values. Nevertheless, Figure 4.2 gives a correct general indication of the direction that chemical reactions are likely to take. In particular, it is clear that the reaction



(where M is any metal) is more likely to go to the right at high temperatures and vice versa.

7.2.1.1 Reactions in the transferring drop

In the case of an arc welding process with a consumable electrode the reactions in the drop at the electrode tip will be governed by three factors: the oxidising effect of the arc atmosphere, the concentration and the nature of deoxidants in the drop itself, and the temperature of the liquid metal. If no deoxidants are present (e.g. in the case of coated electrodes with an oxide/silicate coating, BS Class O, or GMA welding with a rimming steel wire) carbon and oxygen are simultaneously present in the drop and the reaction (7.1) goes to the right. One or more bubbles form in the drop and eventually the drop bursts, generating a fine-spray type of transfer. In the case of normal commercial coated electrodes of the cellulosic, rutile or basic types, and in submerged arc and GMA welding with deoxidised wire there is sufficient silicon and manganese present to inhibit CO formation and bubbles form only occasionally.

In GMA and other processes where carbon dioxide forms a substantial proportion of the shielding gas, there may be some carbon pick-up in the drop:



The second reaction is catalysed at the metal surface. However, it may go in either direction and in carbon-dioxide-shielded GMA welding the carbon content of the deposit tends to adjust to about 0.12% regardless (within normal limits) of the carbon content of the wire.

Most alloying elements in the drop are oxidised to some degree in arc welding with a consumable electrode, and coated electrodes are formulated to compensate for this effect. Aluminium and titanium are severely oxidised, and it is not in general practicable to employ these elements in SMA welding. Where filler wire is added separately, as in GTA and plasma welding, little oxidation takes place and elements such as titanium can be transferred to the weld pool.

7.2.1.2 Reactions in the weld pool

The weld pool is cooler and has a smaller surface-to-volume area than the transferring drop. Because of the lower temperature, there is a tendency for gas to evolve. The following reactions are possible:





Such reactions may result in porosity in the completed weld.

Knowledge of the detailed cause of porosity in carbon steel welds made by the various processes is rather limited. The porosity that is normally present in welds made with non-deoxidised iron oxide coated rods is generally assumed, with good reason, to result from the rejection of carbon monoxide. Porosity in argon-shielded metal arc welds made with non-deoxidised or poorly deoxidised wire is at least partly due to carbon monoxide evolution, and may be eliminated from the bulk of the weld deposit provided that the silicon content exceeds $6.25(\text{C})^2$ where (C) is the percentage carbon content. However, the degree and type of deoxidant required depends upon the welding process, shielding gas and the type of steel being welded. With flux-shielded processes silicon and manganese are used for carbon, low alloy and chromium–nickel alloy weld deposits, but for special alloys calcium, titanium, zirconium or aluminium may be added to the electrode coating. Addition of an optimum amount of such elements may have a beneficial effect on mechanical properties. In the case of GMA welding titanium, zirconium and aluminium are present in **triple-deoxidised** wire. Such wires are used to obtain welds free from porosity in rimming or semi-killed steel or in the presence of surface contamination. Silicon and manganese are, however, sufficiently strong deoxidants for most GMA applications, particularly when argon–oxygen mixtures are used for shielding rather than carbon dioxide.

Welds that are deposited by carbon-dioxide-shielded welding may be porous if the arc length is excessive or if too high a proportion of nitrogen (over about 1%) is present in the shielding gas. In the latter case it has been established that porosity is caused by nitrogen evolution. Nitrogen is also thought to be the cause of porosity in the root run of a pipe weld made using basic-coated electrodes.

Porous welds may also be the result of gross contamination of the parent metal or the welding consumables. Greasy, rusty or wet plate, damp electrode coatings or submerged arc flux, or contamination of gas lines for GMA welding by moisture or air may generate porosity, particularly at restarts.

7.2.2 Slag–metal reactions

The nature of slag–metal reactions is largely determined by the composition of the flux or electrode coating. However, the mechanics (or physics) of the interaction may be important and will be discussed first.

7.2.2.1 *The mechanics of slag–metal interaction*

The form of electrode tip in SMA welding is illustrated in Figure 7.1. The coating forms a cone within which a liquid drop forms. Interaction between slag and metal takes place initially at the junction between cone and liquid. If alloying elements are added through the coating, they dissolve at this point

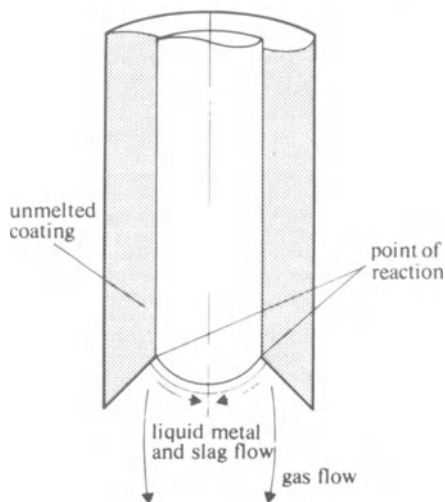


Figure 7.1 Slag–metal reaction in SMA welding.

and are mixed well enough for the drop, when it detaches, to be almost homogeneous. This indicates rapid circulation in the drop, due to electromagnetic effects and/or drag from the gas evolved by the coating. At the same time, the liquid metal is heated to a high temperature. In all probability the more important chemical interactions, particularly the absorption of oxygen, occur at this point. In practice the drop profile is by no means as regular as shown in Figure 7.1: it is in a state of constant movement, as is the arc root. This does not, however, affect the basic geometry of the arrangement.

In the case of flux-cored wire the situation is very different, in that the metal sheath normally melts before the flux either melts or detaches. Little interaction can take place at the electrode and the flux–metal reactions must occur in the weld pool. When flux-cored wires are used without a gas shield the liquid metal absorbs substantial amounts of oxygen and nitrogen and this effect can only be partly compensated by reaction with deoxidants in the weld pool.

In submerged arc welding the arc operates in a cavity of liquid slag and the liquid metal drops frequently transfer through the slag cavity or occasionally around the cavity wall. Once again, because of the high temperature and the large surface-to-volume ratio of the drop, it is likely that significant slag–metal reactions take place at this point. The deep penetration characteristic of submerged arc welding may also be relevant to slag–metal reactions. Suppose that it is desired to add an element M through the flux (or through the wire, for that matter), the final concentration of M in the weld pool will depend on the degree of dilution. Thus, special additions may, in submerged arc welding, need to be restricted to applications where the degree of dilution is known.

7.2.2.2 The chemistry of slag-metal interaction

The nature of the chemical reactions between slag and liquid weld metal has been studied largely in connection with the SAW process, but in general terms the conclusions that have been reached, particularly in relation to flux basicity, apply also to SMA welding.

The **basicity** index of a flux is usually determined as the sum of the basic components divided by the sum of acid and amphoteric components, one formula being that due to Tuliani, Boniszewski and Eaton:

$$B = \frac{\text{CaO} + \text{MgO} + \text{BaO} + \text{SrO} + \text{K}_2\text{O} + \text{Li}_2\text{O} + \text{CaF}_2 + \frac{1}{2}(\text{MnO} + \text{FeO})}{\text{SiO}_2 + \frac{1}{2}(\text{Al}_2\text{O}_3 + \text{TiO}_2 + \text{ZrO}_2)} \quad (7.8)$$

where CaO etc. represent the mole percentage of the constituent. When B is less than 1 the flux is classified as acid, 1 to 1.5 is neutral, 1.5 to 2.5 is semi-basic, and greater than 2.5, basic. Some authors consider that CaF_2 should not be included in calculations of the basicity index since it is a salt. Eliminating CaF_2 reduces the absolute value of the index, but the correlations with Mn and Si partition and oxygen content of the weld deposit are qualitatively similar to those obtained using the Tuliani equation. Basic fluxes generate basic slags, but with modified chemistry depending on the wire composition and welding parameters.

Figure 7.2a shows diagrammatically the effect of slag basicity on the partition of Mn and Si between metal and slag. The silicon content of weld metal falls sharply as the basicity index increases. The manganese content increases generally but not in a very regular manner, possibly because the MnO reaction is sluggish and does not proceed to completion.

The sulphur content of the weld metal is reduced by increasing the basicity of the slag. Phosphorus is not so affected; indeed there may be a tendency to increased phosphorus because of the composition of minerals used to manufacture basic fluxes. The oxygen content of weld metal deposited under basic fluxes is also lower than with acid fluxes. This is not related to basicity as such, but to the fact that the basic oxides are less easily dissociated than acid oxides such as silicon dioxide, and therefore generate a lower oxygen partial pressure at the metal surface.

Corresponding to the reduced oxygen content is a reduced inclusion content of the weld metal. Oxygen has a low solubility in steel so that most is present in compound form, for example as silicates. These form globular inclusions some of which are of macroscopic size. There is in addition a large number of spherical inclusions that are resolved by electron microscopy but not by the optical microscope. Such inclusions are generally detrimental to notch-ductility. Figure 7.2b shows weld metal oxygen content as a function of basicity.

The term **neutral** is also used for a flux which does not contain any significant amount of metallic deoxidant or other metallic component as opposed to an **active** flux where such deoxidants are present and where the amount of manganese and silicon in the weld metal may be affected by welding variables such as heat input rate, voltage and electrode stick-out. Cases have been known

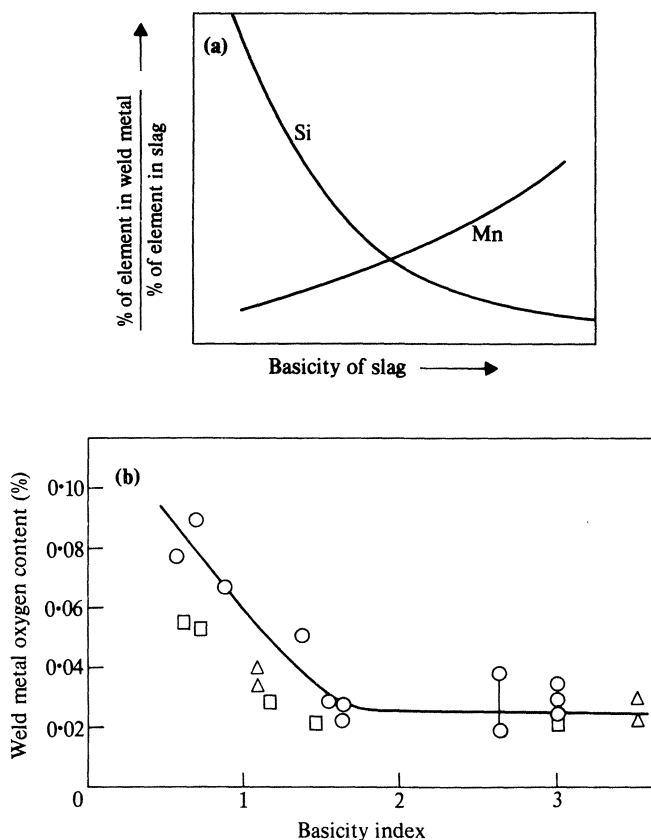


Figure 7.2 (a) Effect of slag basicity on partition of Mn and Si; (b) weld metal oxygen content as a function of flux basicity, as calculated using the Tuliani equation (Eager, T. W. 1978, *Welding J.* 57, 77).

where deviations from the prescribed welding conditions led to excessive silicon and manganese contents, resulting in high weld hardness and ultimate failure due to stress corrosion cracking. Similarly, where alloying elements are added via submerged arc flux, variations in the welding parameters may result in failure to obtain the required weld composition. Consequently, some authorities specify 'non-active' or 'neutral' fluxes. In SMA welding, on the other hand, the weld metal composition is not affected in this way, and it is normal practice to add alloying elements via the electrode coating in the case of low alloy steels.

Submerged arc fluxes may be **fused**, **sintered**, or **agglomerated (bonded)**. Fused fluxes are melted, cast and ground to the required size. Sintered fluxes are partially fused, while agglomerated fluxes are mixed and then baked at a temperature below that required for sintering. Fluxes may also consist of a blend of fused and bonded types, or of minerals mixed with metallic deoxidisers.

All these methods of manufacture may be used to produce a satisfactory flux. One of the more important requirements for a flux is that it should not be hygroscopic, and that for any given moisture content it should produce the lowest possible hydrogen content in the weld metal. Basic fluxes are more sensitive in this respect than semi-basic or acid fluxes, and it is thought that the **chevron cracking** (Section 7.5.4) that has been found in weld metal produced with a basic flux may be due in part to excessive hydrogen content. Basic fluxes are used because the low silicon, oxygen and sulphur contents give better notch-ductility in the weld metal. On the other hand, slag removal from the deeper weld preparations may be difficult with a fully basic flux, and for some applications it may be preferable to use a semi-basic type. Fluxes that absorb moisture need special handling and storage, and may require drying before use.

7.2.3 Solidification and solidification cracking

The primary structure of carbon and low alloy steel weld metal is similar to that of other metals: it is epitaxial with elongated columnar grains extending from the fusion boundary to the weld surface. The substructure is cellular at low solidification rates and dendritic at higher rates. The phase structure at solidification depends mainly on the carbon and nickel contents. Figure 7.3 shows the upper left-hand corner of the iron–carbon phase diagram. When the carbon content is below 0.10% the metal solidifies as delta ferrite. At higher carbon contents the primary crystals are δ but just below 1500 °C, a peritectic reaction takes place

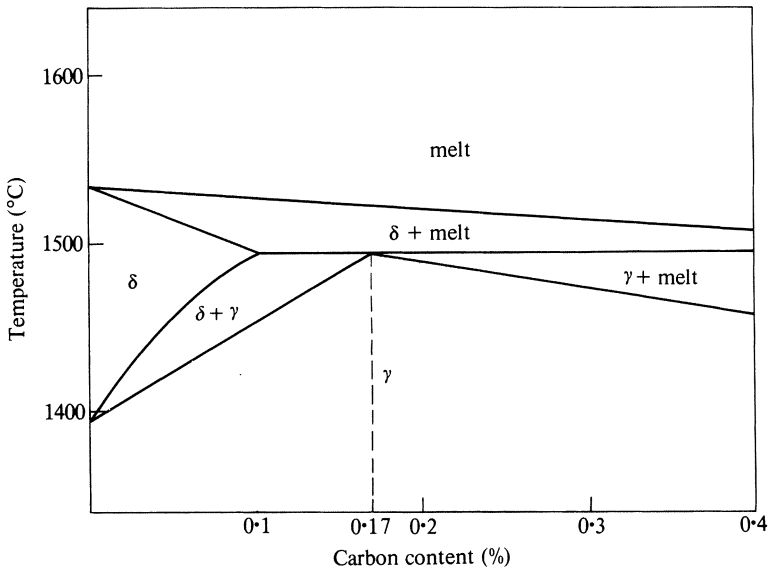


Figure 7.3 Section of iron–carbon equilibrium diagram showing the peritectic reaction.

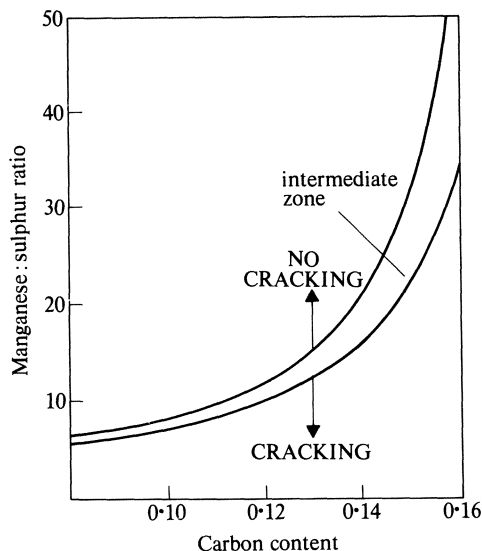


Figure 7.4 Effect of manganese:sulphur ratio and of carbon content on susceptibility of carbon steel weld metal to hot cracking.

and the remainder of the weld solidifies as austenite. The solubility of sulphur in ferrite is relatively high but in austenite it is relatively low. Consequently, there is a possibility with $C > 0.1$ that sulphur will be rejected to the grain boundaries of primary austenite grains, promoting intergranular weakness and solidification cracking. Manganese tends to inhibit the effect of sulphur, but the higher the carbon content the higher the manganese:sulphur ratio required to avoid cracking, as shown in Figure 7.4. Sulphur may also segregate to interdendritic regions and promote interdendritic cracks.

Other elements that behave in a similar manner to sulphur are phosphorus and boron, both of which have a low solubility in the freshly solidified metal. Nickel behaves in a similar way to carbon in that a peritectic reaction occurs during solidification at about 1500°C and above about 3% Ni. At higher nickel contents the risk of hot cracking increases progressively and it is not normally possible to make fusion welds with more than about 4% Ni in the deposit. Other common alloying elements, such as chromium and molybdenum, have a relatively small effect on the solidification cracking of steel.

The risk of solidification cracking is minimised by:

- Maintaining a low carbon content in the weld deposit.
- Keeping sulphur and phosphorus contents as low as possible.
- Ensuring that the manganese content is high enough to allow for possible dilution (and ingress of sulphur) from the plate material.

It is normal practice to use low-carbon rimming steel as the core wire for carbon and low-alloy steel electrodes and a typical carbon steel all weld metal deposit contains 0.05 to 0.10 C. In low-alloy (e.g. Cr–Mo) steel carbon contents are usually about 0.1% but may be reduced below 0.06% by using low-carbon ferro-alloys in the coating, or by using a low-carbon alloy core wire.

7.3 TRANSFORMATION AND MICROSTRUCTURE OF STEEL

Regardless of the primary phase structure, carbon and low-alloy steels transform to austenite at a temperature not far from the solidification point, and finally to ferrite. The equilibrium structure of iron–carbon alloys is shown in Figure 7.5. At temperatures where the steel falls within the region designated ‘ γ Phase’ the steel is austenitic. On *slow* cooling transformation starts when the temperature falls to the point on the low boundary of this region corresponding to the carbon content of the steel – the **upper critical temperature**. Ferrite containing a small amount of carbon in solid solution is precipitated leaving austenite grains

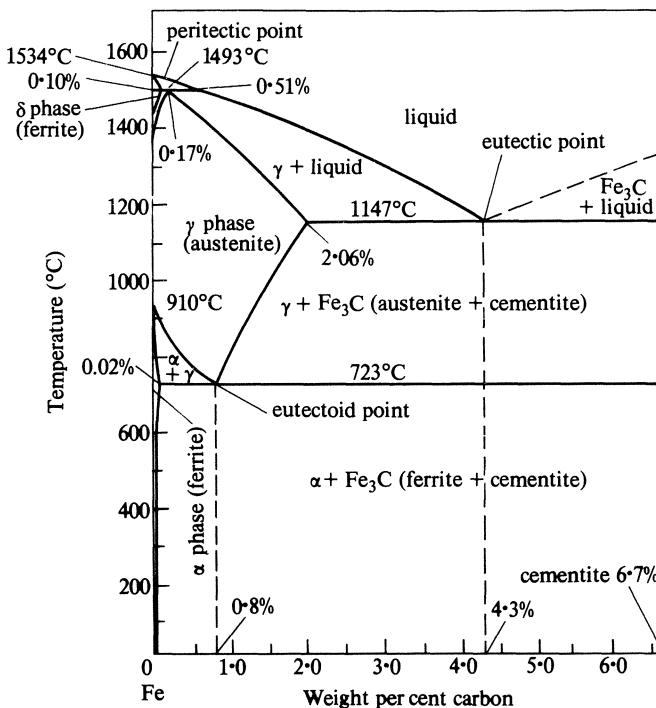


Figure 7.5 The metastable system Fe–Fe₃C. (From Hansen, M. and K. Anderko 1958. *Constitution of binary alloys*, 353. New York: McGraw-Hill. Used by permission.)

that become smaller and are progressively enriched in carbon as the temperature falls. At 723°C (the **lower critical temperature**) the residual austenite, which now contains about 0.8% carbon, transforms into **pearlite** — a laminated eutectoid mixture of ferrite and cementite (Fe_3C). The structure so obtained by slow cooling consists of intermingled grains of ferrite and pearlite. Cementite decomposes to iron-plus-graphite if held at elevated temperature for long periods: this is why the term 'metastable' is used in the caption of Figure 7.5.

Rapid cooling depresses the temperature at which the gamma to alpha change takes place. As the **transformation temperature** falls, the distance over which carbon atoms can diffuse is reduced, and there is a tendency to form structures involving progressively shorter movements of atoms. Whereas on slow cooling carbon can segregate into separate individual grains of austenite, with more rapid cooling carbides precipitate around or within the ferrite, which now appears in the form of needles or plates rather than equiaxed grains, a structure known as bainite (Figure 7.6). At even more rapid rates of cooling the transformation is depressed to a temperature (M_s), where **martensite** is formed. This **transformation product** is produced by a shear movement of the austenite lattice, the carbon being retained in solid solution in a distorted body-centred cubic lattice. Generally speaking, the transformation product is harder and more brittle the lower the transformation temperature and (particularly in the case of martensite) the higher the carbon content.

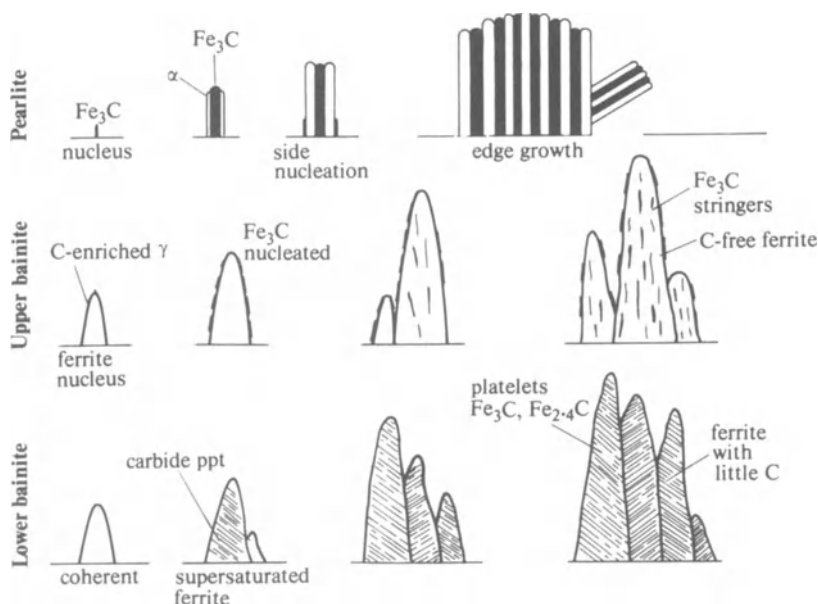


Figure 7.6 Diagrammatic representation of the formation of pearlite, upper bainite and lower bainite. (From Rollason, E. C. *Metallurgy for engineers*. London: Edward Arnold.)

The cooling rate in fusion welding increases as the heat input rate q/v decreases, and as the welding speed increases. It is higher for multi-pass welding in thick plate than for single-pass welding in thin plate, other things being equal. It is reduced by increasing the preheat temperature. The weld metal and heat-affected zone structures form under conditions of continuous cooling, and a **continuous cooling transformation (CCT)** diagram such as that illustrated in Figure 7.12 may indicate the type of structure to be expected. However, there are certain special features to be observed in the microstructure of welds, as discussed below.

7.3.1 Transformation and microstructure of weld metal

In low carbon steel the first phase to form on cooling below the transformation temperature is alpha ferrite (**pro-eutectoid ferrite**). This usually occurs as a network or in parallel laths (Figure 7.7). Between the ferrite laths the residual austenite transforms according to cooling rate and alloy content. In the case of carbon steel the structure is normally **acicular ferrite**, as illustrated in Figure 7.8. Between the ferrite grains higher-carbon transformation products such as fine pearlite, bainite and martensite may occur and there may be some retained austenite (Figure 7.9). With increasing alloy content the acicular ferrite is replaced by bainite or martensite and the pro-eutectoid ferrite may no longer be present.

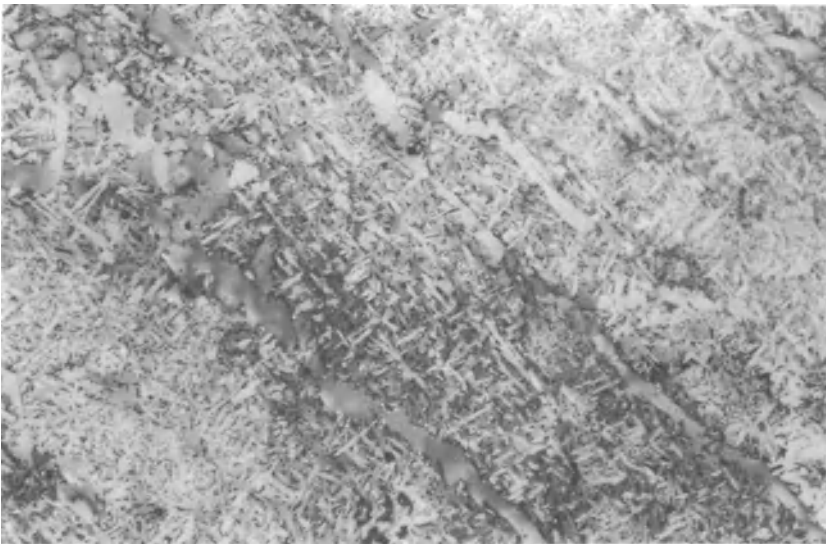


Figure 7.7 Proeutectoid ferrite in carbon steel weld metal ($\times 320$; reduced by $\frac{1}{2}$ in reproduction). (From Almquist, G., S. Polgary, C. H. Rosendahl and G. Valland 1972. Some basic factors controlling the properties of weld metal. In *Welding research relating to power plant*, 204–31. London: CEGB.)

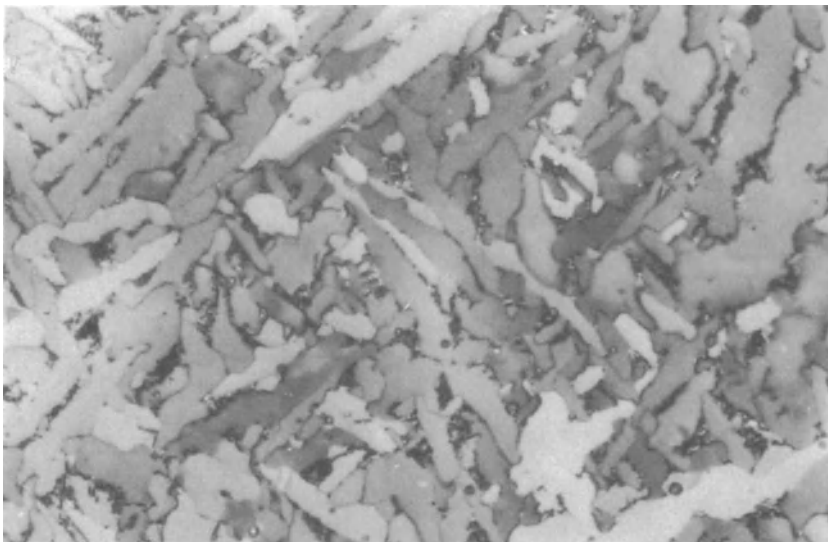


Figure 7.8 Part of Figure 7.7 at high magnification showing acicular ferrite with some carbides at grain boundaries ($\times 1600$; reduced by $\frac{1}{3}$ in reproduction). (From Almquist, Polgary, Rosendahl & Valland 1972.)

In the case of a multi-pass weld deposit each succeeding pass forms a heat-affected zone in the weld metal immediately below. As a result the microstructure is complex. However, the general effect of subsequent passes is to refine the grain and improve the properties of the underlying metal.

Weld metal may also contain slag inclusions, ranging in size from several millimetres down to the fine spherical particles that are visible only under the electron microscope. The number of fine slag inclusions increases with the oxygen content of the metal.

There is evidence that in carbon and steel an increased oxygen content, and hence a larger concentration of microinclusions (such as may be produced by using a longer arc) promotes the formation of upper transformation products and thereby generates a coarser microstructure with a correspondingly lower notch-ductility. Carbon steel welds are also characterised by a high dislocation density, probably because of the plastic strain that occurs during cooling.

7.3.2 Transformation and microstructure in the heat-affected zone

Whereas in the weld metal we are concerned mainly with solidification and cooling, in the heat-affected zone the complete thermal cycle is effective in determining microstructure. On heating the steel through the temperature range between the upper critical temperature and somewhere about 1200°C , the austenite grains form and grow relatively slowly, but above a specific point

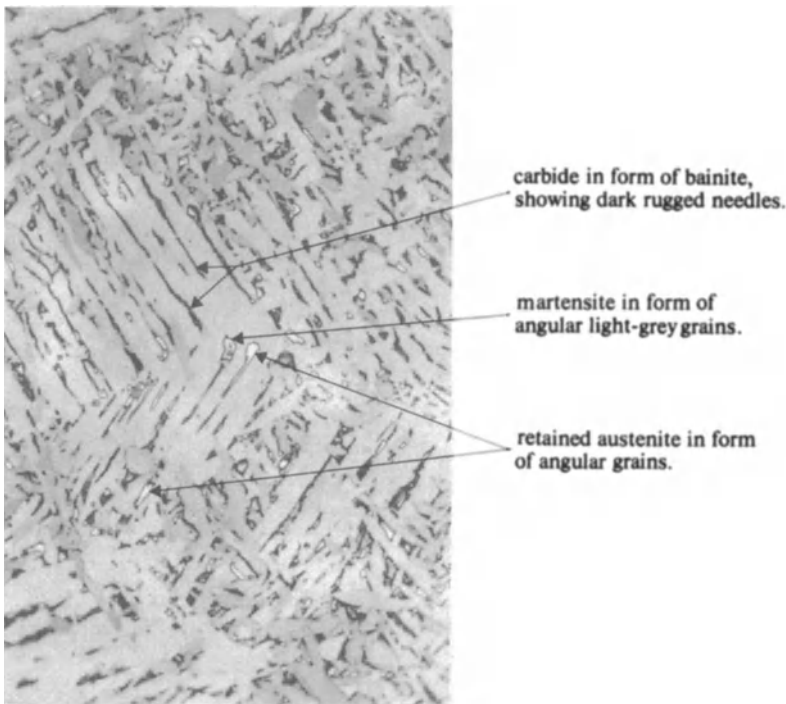


Figure 7.9 Transformation products in carbon-steel weld metal ($\times 1000$; reduced by $\frac{1}{3}$ in reproduction). (From Almquist, Polgary, Rosendahl & Valland 1972.)

(the **grain coarsening temperature**) the rate of growth increases sharply. Below the grain coarsening temperature, grain boundary movement is impeded by the presence of certain particles such as aluminium nitride. However, these particles go into solution at a specific temperature level and, above this level, grain growth is unimpeded. Aluminium is added to steel in order to produce fine grain, and it does so by impeding the growth of austenite grains during the various thermal cycles to which the steel is subjected during processing. The effectiveness of grain refining additives such as aluminium, niobium or vanadium is greater the higher the solution temperature of the nitride or carbo-nitride particles that are formed. In this respect, niobium is less effective than aluminium.

From a metallurgical viewpoint the heat-affected zone of a fusion weld in steel may be divided into three zones: supercritical, intercritical and subcritical. The supercritical region may in turn be divided into two parts: the **grain growth** region and the **grain refined** region. Grain growth occurs where the peak temperature of the weld thermal cycle exceeds the grain coarsening temperature. Below this temperature the thermal cycle will usually produce a grain size that is smaller than that of the parent metal.

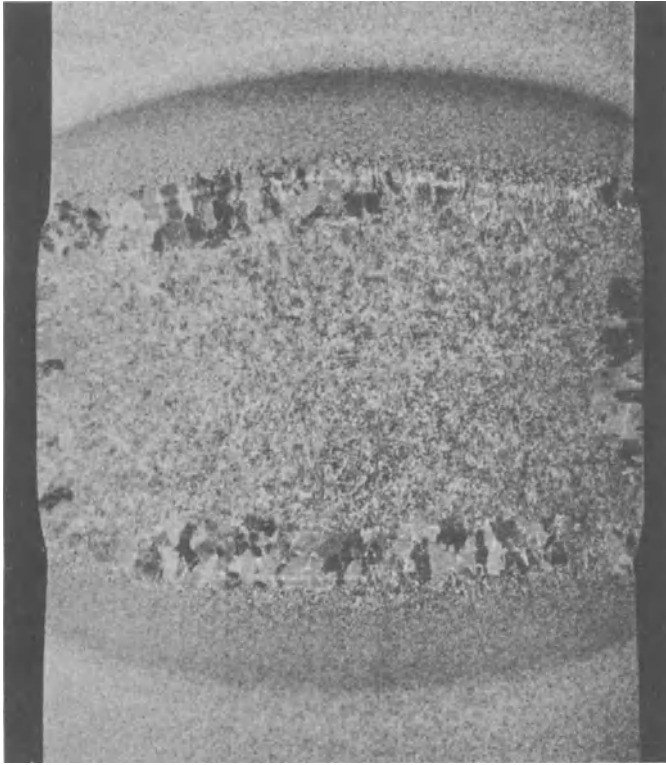


Figure 7.10 Macrosection of electroslog weld in 3-inch-thick carbon steel. The heat-affected zone is 8–12 mm wide. Note the coarse grain at the outer edges of the fused zone, and at the inner edge of the heat-affected zone (full size). The HAZ of a manual SMA, GMA or GTA weld is typically 2–3 mm wide. (Photo: Welding Institute).

The microstructure of the grain growth region is dominated by two features: the austenite grain size and the transformation structure within the grain. The grain size is in turn governed by two factors: the nature of the weld thermal cycle and the grain coarsening temperature of the steel. For any given steel, the greater the heat input rate the longer the time spent above the grain coarsening temperature, and the coarser the grain. Thus, electroslog welding generates a large grain size near the fusion boundary (Figure 7.10). Also, for any given weld thermal cycle, the higher the grain coarsening temperature the shorter the time for grain growth. Aluminium-treated carbon steels contain aluminium nitride particles which inhibit the growth of austenite grains up to a temperature of about 1250°C. Above this temperature the aluminium nitride particles go into solution and grain growth is rapid, such that the grain size at the fusion boundary is not much different to that of steels that do not contain aluminium.

The type of microstructure in the coarse-grained region depends on the carbon and alloy content of the steel, on the grain size and on the cooling rate. In low carbon steel pro-eutectoid ferrite separates first at the prior austenite grain boundaries, and inside the grain a ferrite-pearlite and/or a ferrite-bainite structure develops. The pearlitic constituent may consist of parallel arrays of small globular cementite particles. With increasing cooling rates and/or increasing carbon and alloy content, the pro-eutectoid ferrite disappears and the austenite grains transform completely to acicular structures: upper bainite, lower bainite or martensite, or a mixture of these components. The coarser the prior austenite grain size, the coarser the microstructure — for example, the wider the spacing between martensite laths, or the larger the bands or blocks of pro-eutectoid ferrite. Also, a coarse austenitic grain size may promote the formation of harder microstructures than would result from the transformation of a finer-grained material, e.g. upper bainite may form instead of a ferritic/pearlitic structure.

Partial melting (liquation) may occur near the fusion boundary in the case of certain alloys. Niobium may form patches of eutectic, and in the case of high (0.4%) carbon high tensile steel there may be grain boundary liquation, associated with sulphur and phosphorus, leading to liquation cracking. The latter type of cracking is controlled by maintaining very low levels of sulphur and phosphorus: increasing the manganese : sulphur ratio does not appear to have much effect.

With increasing distance from the weld centreline, both peak temperature and cooling rate decrease. Consequently, the grain-refined region may have a range of microstructure, being similar to that of normalised steel on the outside.

In the intercritical region, which is relatively narrow, partial transformation may take place. For example, in a carbon steel having a ferrite/pearlite structure prior to welding, the pearlite islands, which are of eutectoid carbon content, transform to austenite on heating and to martensite or bainite on cooling. In the 'as-welded' condition this region may therefore consist of hard grains embedded in a relatively soft, untransformed ferritic matrix (Figure 7.11).

The subcritical region does not normally undergo any observable microstructural change except that a small region of spheroidisation may occur — this is generally difficult to detect. However, if there is a pre-existing crack the steel around the crack tip may suffer strain ageing. This situation can arise, for example, if during one run of weld hydrogen cracks form in the heat-affected zone. A subsequent run may plastically deform the original HAZ and, at the same time, heat the crack tip in the temperature range ($\sim 200^{\circ}\text{C}$) where strain ageing is relatively rapid. In the absence of a crack there may also be a moderate degree of strain ageing embrittlement. This type of ageing is associated with the presence of free nitrogen in the steel, and may be mitigated by adding nitride-formers such as aluminium.

With multi-run welding fresh heat-affected zones are formed in previously deposited weld metal and previously formed HAZs. Transformed regions are re-transformed: coarse grains may be refined and vice versa. It may, nevertheless, be useful to attempt to assess the probable microstructure using a CCT diagram.

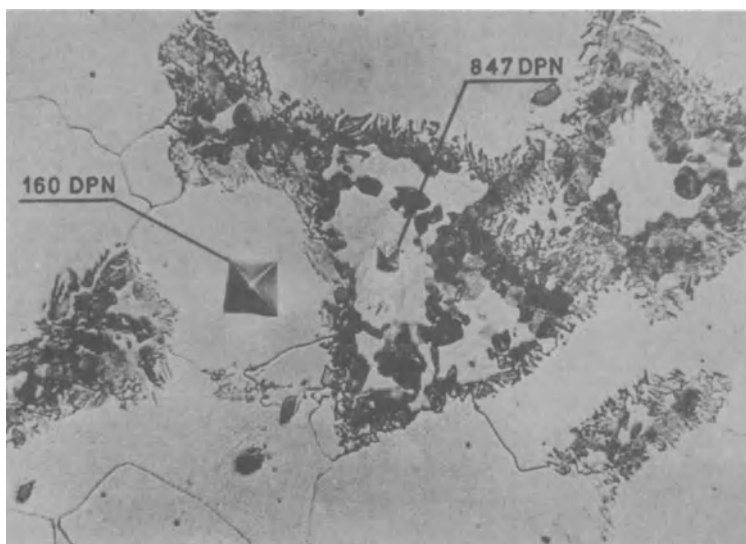


Figure 7.11 Region of partial transformation in the heat-affected zone of a carbon steel weld. Solution of carbide and transformation to austenite has occurred preferentially in the centre of the pearlite grains. On cooling martensite has formed in the transformed areas, as evidenced by the microhardness-test results ($\times 820$; reduced by $\frac{1}{3}$ in reproduction).

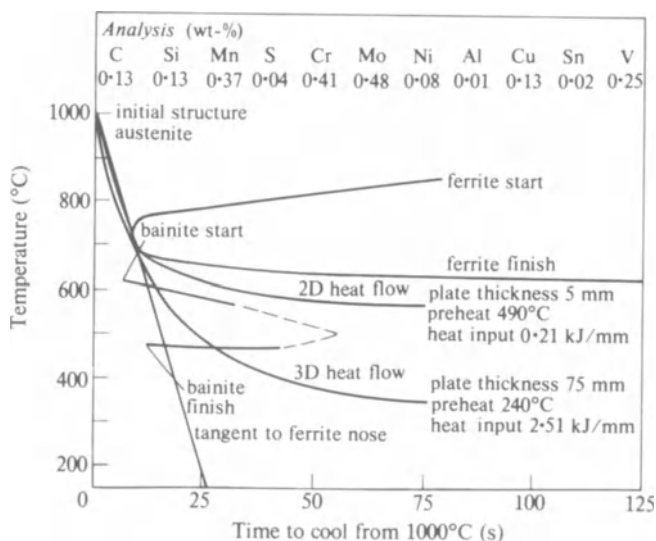


Figure 7.12 Continuous cooling transformation diagram; fine-grained simulated $\frac{1}{2}$ Cr $\frac{1}{2}$ Mo $\frac{1}{4}$ V HAZ (Alberry, P. J. and W. K. C. Jones 1977, *Metals Technology* 4, 360).

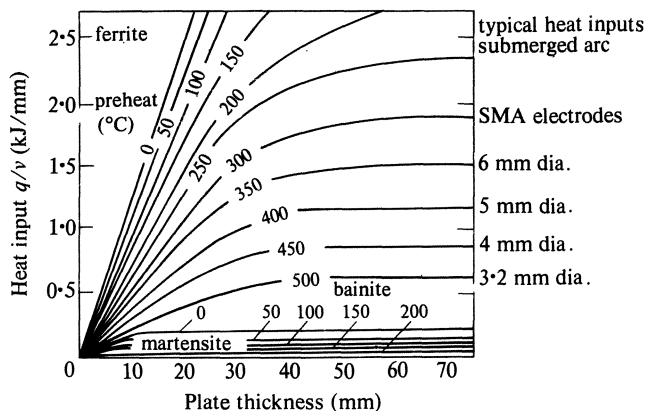


Figure 7.13 Welding-microstructure diagram for fine-grained simulated 0.5 Cr-Mo-V HAZs (Alberry, P. J. and W. K. C. Jones 1977. *Metals Technology* 4, 360).

Structure may be sensitive to austenite grain size and to the variation in cooling rate that is typical of the weld thermal cycle. Ideally, the CCT diagram should be made using simulated weld thermal cycles. Figure 7.12 is such a CCT diagram for $\frac{1}{2}$ Cr $\frac{1}{2}$ Mo $\frac{1}{4}$ V steel. Using measured retention times (Figure 3.19) or calculated cooling rates, and making due allowance for section thickness as indicated in Section 3.5.2 it is possible to generate a diagram (Figure 7.13) that shows microstructure as a function of heat input rate, preheat and section thickness for the grain-refined region and the HAZ. For example, consider 20 mm 0.5 Cr-Mo-V plate welded with 6 mm diameter electrodes. The ordinates for these two variables intersect on the line marked '200', which means that under such conditions a preheat of 200 °C is required to produce a minimum of 5% ferrite in the microstructure of the fine-grained region. A higher preheat will increase the amount of ferrite, and vice versa.

7.4 THE MECHANICAL PROPERTIES OF THE WELDED JOINT

It will be evident from the discussion of microstructure that there must be variations in properties from point to point across the welded joint. The properties of the joint as a whole may also be affected by the form of the weld profile and the way in which the weld is disposed relative to the principal applied stress. To take the simple case of a butt weld in plate, the angle between the reinforcement and the plate surface is a measure of the stress concentration at the fusion boundary. The greater this stress concentration, the lower the fatigue strength (Figure 7.14). Likewise, the probability of cracking due to other embrittlement mechanisms such as hydrogen embrittlement is increased as the reinforcement wetting angle is reduced.

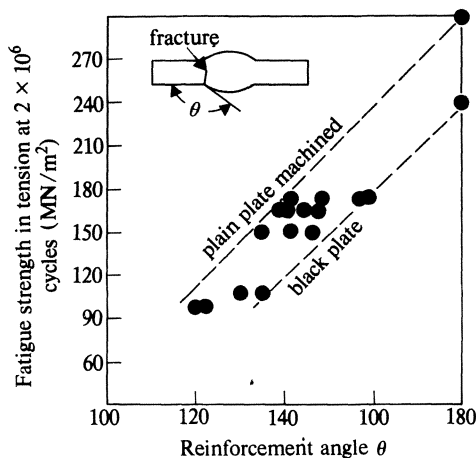


Figure 7.14 Effect of joint profile on the fatigue strength of transverse butt welds in carbon steel (Newman, R. P. 1960. *Brit. Welding J.* 7, 172).

7.4.1 The mechanical properties of weld metals

For any given composition (and particularly for carbon and carbon-manganese steels) one of the important factors governing mechanical properties is the ferrite grain size. The term grain size is used here in a general sense and refers to a characteristic dimension for the structure in question: for example, in carbon steel weld metal as shown in Figure 7.8 the width of the acicular ferrite grains may be a good measure of grain size, but the properties of the weld metal may also be influenced by the size and morphology of the pro-eutectoid ferrite. In the case of bainitic or martensitic structures the width of the needles provides a measure of grain size. However, it must be recognised that a precise correlation between grain size alone and mechanical properties is not possible since these may be influenced by the morphology and distribution of carbides, the presence of grain boundary precipitates, and other features.

With these reservations, it may be said that in general the yield strength of weld metal increases and the impact transition temperature falls as the ferrite grain size is reduced. The ferrite grain size is largely determined by the size of the prior austenite grains and this, as pointed out earlier, is a function of the weld thermal cycle. Thus, high heat input rate processes such as electroslag and submerged arc generate a relatively coarse-grained weld metal, while that produced by SMA, GMA and GTA welding is relatively fine. Weld metal usually contains a relatively high density of dislocations, which also contributes to increased yield strength in the case of carbon and carbon-manganese steels. The final result is that weld metal normally has higher tensile and yield strength than the equivalent plate material, even when the carbon and/or alloy content is lower. These higher properties are maintained after subcritical heat treatments.

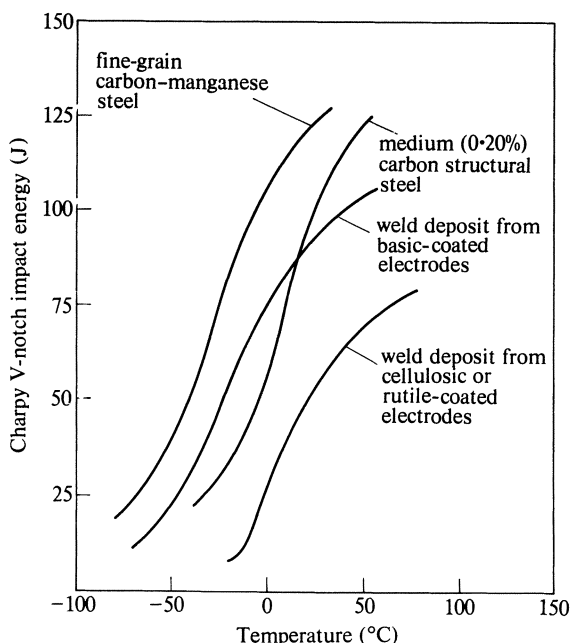


Figure 7.15 Typical impact energy–temperature relationships (transition curves) for carbon-steel plate and weld metal.

In the case of carbon steel there is no grain growth and little softening at such temperatures, probably because of the carbide network surrounding the ferrite grains (Figure 7.8). Indeed there is more concern about the danger of excessive yield strength in the weld metal which may generate high residual stresses and render the joint susceptible to stress corrosion cracking (Ch. 10). The hardness of weld metal correlates with ultimate strength in the same way as for wrought steel and hardness testing is used as a method of controlling weld metal strength.

The notch-ductility of weld metal, as measured, for example, by impact testing, depends mainly, for any given composition, on microstructure, grain size and inclusion content. Notch-ductility is reduced, other things being equal, by the presence of pro-eutectoid ferrite in the structure, and particularly when it is coarse and block-like in form. Ideally, the weld metal should consist entirely of fine acicular ferrite. The notch-ductility is also reduced as the amount of martensite in the structure increases. The grain size of weld metal deposited by the SAW process is such that the impact properties are adequate for the common run of applications, but where more stringent requirements prevail (such as impact testing at -30°C) it is necessary to use basic or semi-basic fluxes to reduce oxygen and sulphur (and thereby inclusion) contents. Electroslag welds are too coarse-grained to pass impact testing at room temperature, and for high-duty applications such as pressure vessels are usually normalised. With the low heat input rate processes, on the other hand, it is possible to match

wrought metal, except at the lowest testing temperatures. Figure 7.15 illustrates typical properties for carbon and carbon–manganese steels. The difference between basic-coated and rutile or cellulosic electrodes illustrated here is due to differences in inclusion content and manganese content.

The elevated temperature properties of weld metal have been studied to a rather limited extent. Generally speaking, the short-time elevated temperature properties of SMA weld metal are similar to those of wrought material of the same composition, although there is considerable scatter in the results obtained. Creep-rupture properties are equal to or lower than those of wrought steel of the same composition.

The effect of increasing carbon and alloy content of weld metal is, in general, to increase strength and hardness. Carbon in particular has a strong effect on these properties. However, for the best combination of fracture toughness and cracking resistance, it is desirable to keep the carbon content within the range 0.05–0.12%. For alloy steel in particular, maintaining about 0.06% C in the deposit helps to avoid excessive hardness values.

Postweld heat treatment in the subcritical range has the effect of reducing the hardness and strength of alloy steel weld deposits, and (in thicknesses over about 30 mm) increasing the ductility and the fracture toughness of the joint as a whole. Impact strength may, however, be reduced, in part because of the reduction in yield strength.

7.4.2 The mechanical properties of the heat-affected zone

In describing the mechanical properties of weld metal it has been assumed that these are uniform across the fused zone: as would be more or less the case for a single-pass weld. In practice, most welds are multi-pass, and the weld metal, as well as the unmelted parent metal, contains one or more heat-affected zones. In this section we are concerned with the properties of the heat-affected region as compared with those of the unaffected weld metal or parent plate. The yield and ultimate strength of the HAZ in steel are almost always higher than those of the parent material and the properties of main interest are fracture toughness and hardness.

7.4.2.1 The hardness of the HAZ

The hardness of the HAZ is a measure of the tensile strength of the steel and, for any given alloy type, gives an indication of the degree of embrittlement. For carbon–manganese and some low alloy high tensile steels a hardness of over 350 BHN in the HAZ would be considered as excessive, and indicating a susceptibility to cracking. On the other hand, the HAZ of nickel alloy steels may be adequately tough with a hardness of 400 BHN.

Hardness depends on the hardenability of the steel, on the cooling rate and, to a lesser degree, on the prior austenite grain size. The hardenability of a steel may be generally correlated with the carbon equivalent (CE). In a carbon equivalent formula the hardening effect of each alloying element is compared

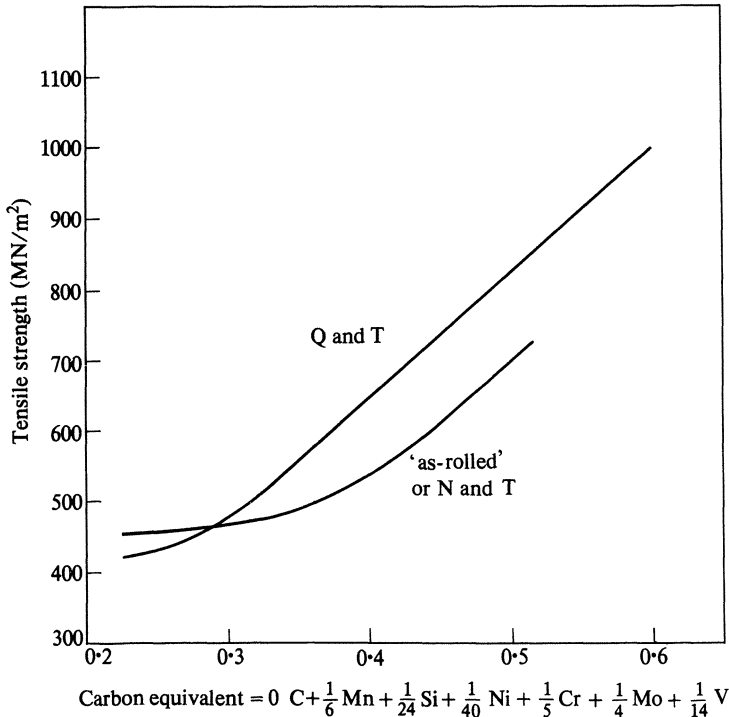


Figure 7.16 Tensile strength of steel as a function of carbon equivalent. (After Sekiguchi – see Further Reading, p. 177.)

with that of carbon, and the relevant alloy content is divided by a factor that gives the carbon equivalent of that element. Figure 7.16 shows the correlation between CE and ultimate strength for normalised and tempered and quenched tempered steel, and Figure 7.17 gives the corresponding hardness in the weld HAZ. The curves show median values and there is a fairly wide scatter band. Carbon equivalent formulae are applicable to a relatively narrow range of alloy types. The correlation shown in Figure 7.16 is good for steels of a low alloy content, but would not apply to, for example, a 9% Cr 1% Mo steel. Even for steel of a given composition a number of different carbon equivalent formulae are used.

Hardenability, and therefore CE, is a factor in determining the susceptibility of a steel to hydrogen embrittlement and cracking during welding, and a formula commonly used in this connection is:

$$\text{CE} = \frac{\text{Mn}}{6} + \frac{\text{Cr} + \text{Mo} + \text{V}}{5} + \frac{\text{Ni} + \text{Cu}}{15}$$

This formula takes no account of silicon, which has about the same relative effect as manganese in hardening both weld metal and HAZ. Nevertheless, Si does not appear to influence the susceptibility to hydrogen cracking. One means

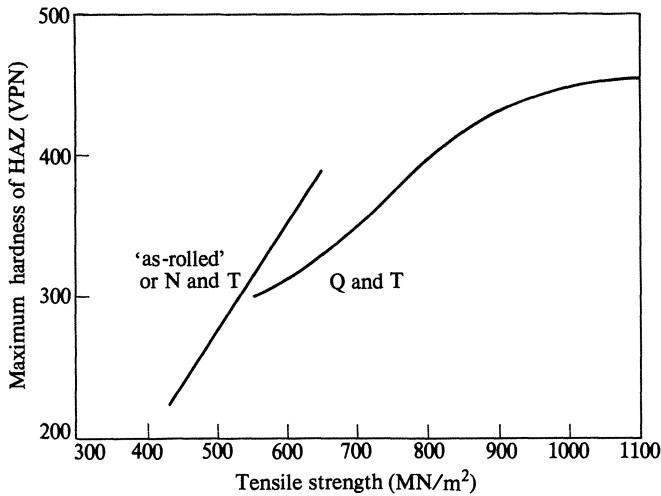


Figure 7.17 Maximum Vickers hardness in the HAZ of fusion weld as a function of tensile strength. (After Sekiguchi – see Further Reading, p. 177.)

of controlling material composition so as to minimise the risk of hydrogen cracking is to specify a maximum carbon equivalent, typically in the region of $CE = 0.45$. However, other factors need to be taken into account and these are considered in Section 7.5.3.7.

It may be required to control carbon steel weld metal and/or HAZ hardness in order to reduce the risk of stress corrosion cracking in service (see Ch. 10). Also, in the case of alloy steel, a **hardness traverse** may be taken across transverse sections of procedure test specimens in order to demonstrate that no excessive hardening or softening of the joint has occurred.

7.4.2.2 The fracture toughness of the HAZ

In some cases all the regions of the HAZ – coarse grain, grain refined, inter-critical and subcritical – are embrittled to some degree as compared to the parent material. However, if the fracture toughness of the parent material is relatively low, the HAZ may have better properties, particularly in the grain-refined region. The factors affecting HAZ toughness are the nature of the weld thermal cycle, grain coarsening temperature, transformation characteristics, alloy content and non-metallic content. As would be expected, low heat input rate processes which give relatively high cooling rates generate a finer-grained HAZ and less embrittlement in low carbon steel. In more hardenable steels (including carbon-manganese steels) this effect may be offset by the formation of bainitic or martensitic microstructures. The higher the carbon content, the more brittle the transformed structure and high-carbon twinned martensite is the most brittle of the structures found in the weld HAZ or steel. For any given martensite content, the toughness is improved by a reduction of the width of

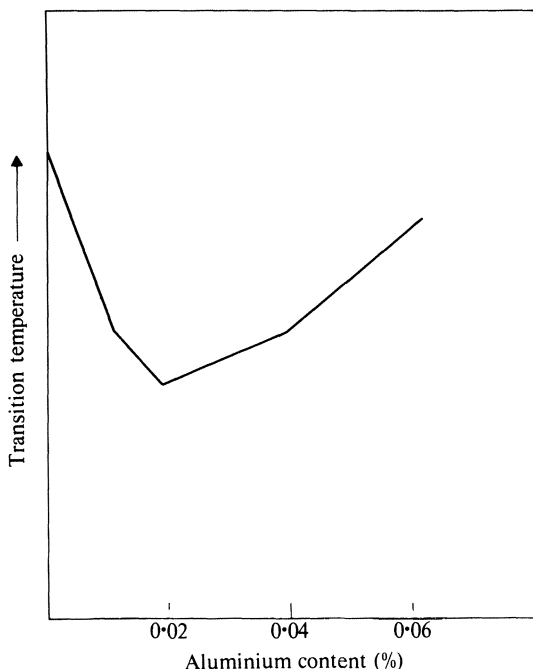


Figure 7.18 Typical relationship between aluminium content and Charpy V-notch transition temperature for a quenched and tempered low-alloy steel.

martensite colonies. However, **auto-tempered martensite** (low carbon martensite that forms at a high enough temperature for tempering to occur during further cooling) is a relatively tough product and has better properties in general than bainite. Thus, in a low carbon low alloy steel, high cooling rates may, due to the formation of martensite rather than bainite, generate a more notch-ductile HAZ than low cooling rates.

The addition of aluminium or niobium to produce grain-refinement of carbon-manganese steel may or may not be beneficial to HAZ toughness. There is in most instances an optimum content of micro-alloying elements such as Al, Nb or V. For example, in the case of aluminium additions to carbon-manganese steels the optimum content is about 0.01%. Higher additions produce an equally fine-grained steel but the fracture toughness deteriorates until at about 0.06% Al it may be little better than for an Al-free steel (Figure 7.18). As pointed out, even with an optimum Al addition the coarse-grained region may suffer just as much grain growth as for an Al-free steel. Nevertheless, the average grain size is likely to be lower, and the overall fracture toughness correspondingly higher. Niobium has the effect of suppressing the formation of pro-eutectoid ferrite and promoting the bainite transformation, as a result of which the coarse-grained region of the HAZ has lower toughness than that of a plain carbon-manganese steel welded at the

same heat input rate. The formation of niobium eutectics near the weld boundary may further embrittle this region.

Nickel additions improve the toughness of the HAZ and of the steel in general. The lowering of the ductile–brittle transition temperature is greater with increasing nickel content, such that with a 9% Ni addition the HAZ has acceptable impact properties down to liquid nitrogen temperatures in the ‘as-welded’ condition. Other alloying elements such as chromium and molybdenum affect the toughness of the HAZ primarily by modifying the transformation characteristics. Carbon increases hardenability and also decreases the toughness of any transformation products that are formed, particularly martensite.

The relative degree of embrittlement of the various HAZ regions depends on the hardenability of the steel. Carbon or carbon–manganese steel with a carbon equivalent of around 0.3 will usually form a pearlite/bainite structure in the supercritical region and this may be tougher than a strain-age embrittled subcritical region (strain-age embrittlement is discussed in Section 7.3.2). On the other hand, where martensite forms in the supercritical region, as may happen with a CE of 0.45 and above, the subcritical region is tougher than the supercritical.

The toughness of the HAZ may be tested using either Charpy V-notch impact specimens or by the crack opening displacement test. In both cases it is necessary to locate the notch in the correct part of the HAZ. Even so, a plastic zone forms below the notch during testing and this may include other regions of the HAZ or even the parent plate. Such tests therefore indicate how the HAZ as a whole is likely to behave when notched in a particular region. Alternatively, the steel in question may be given a simulated weld thermal cycle so that tests can be performed on a homogeneous microstructure. Both types of test have their place in the study of this complex problem.

The effect of PWHT on the fracture toughness of the HAZ of a Mn–Mo steel has been investigated using the techniques of linear elastic fracture mechanics. Tests were made on the full section thickness of 165 mm and also on 25 mm × 25 mm and 10 mm × 10 mm specimens, in which any residual stress would be partially or completely removed. Two heat treatments were used, one of 1/4 hour at 600 °C, giving minimal stress relief, and one of 40 hours at 600 °C, after which residual stresses were low. Tests were conducted at –196 °C so that failures were in the elastic condition and the tests were valid to ASTM E-24 (see Section 10.3.2). The results are shown in Table 7.1.

Table 7.1 Fracture toughness ($\text{MN}/\text{m}^{3/2}$) of weld HAZ in ASTM A533 (Mn–Mo) steel at –196 °C (from Suzuki, M., I. Komura and H. Takahashi. 1978. *Int. J. Pres. Ves. and Piping* 6, 87–112)

	1/4 h PWHT	40 h PWHT
Full Section	32.7	40.2
25 mm × 25 mm	57.8	44.2
10 mm × 10 mm	75.4	50.3

It will be evident that stress relief due to PWHT has improved the fracture toughness of the complete joint. In the case of the 10 mm × 10 mm specimens, however, which are both free from residual stress the PWHT has *reduced* the fracture toughness. A similar effect is often found in impact tests of welded steel before and after PWHT.

7.5 STRESS INTENSIFICATION, EMBRITTLEMENT, AND CRACKING OF FUSION WELDS BELOW THE SOLIDUS

The embrittlement (or toughening) of the weld metal and the HAZ due to transformations occurring during the weld thermal cycle has been described above. In exceptional cases, the degree of embrittlement so caused may be sufficient to result in cracking either during the welding operation or in service. Normally, however, some additional factor is required, either to augment the applied or residual stress, or to increase the degree of embrittlement, before any cracking will occur.

7.5.1 Stress concentration

The effect of weld profile on the stress concentration at the fusion line has been discussed generally in Section 7.4. Figure 7.19 shows the **stress concentration factor (SCF)** for the fatigue of carbon steel butt welds as a function of reinforcement angle. This curve is derived from Figure 7.14 and gives some indication of the stress concentration under static loading conditions. For the toe of a fillet weld the SCF is usually assumed to be about 3, while for the root of a partial penetration butt weld or the root of a fillet weld the SCF may be as high as 7 or 8.

The strain concentration may be further augmented if, due to weld distortion, the joint is subject to bending. For example, consider a butt weld that is welded from both sides. If one side is welded out completely, followed by back-gouging and complete welding of the second side, shrinkage of the second side weld will cause bending around the weld centreline. If the angle of bend is θ radians and the bending takes place over a length equal to nw where n is a number and w the plate thickness, it may be shown that the average strain on the weld surface is θ/n and the strain at the fusion boundary is $\theta/n \times \text{SCF}$. More complex strain fields due to distortion are, of course, quite possible.

7.5.2 Embrittlement of fusion welds

Strain-age embrittlement may occur during the welding operation, as already discussed, but there are a number of mechanisms that may result in postwelding embrittlement. The most important of these are hydrogen embrittlement, secondary hardening and temper embrittlement. Cracking may result from poor

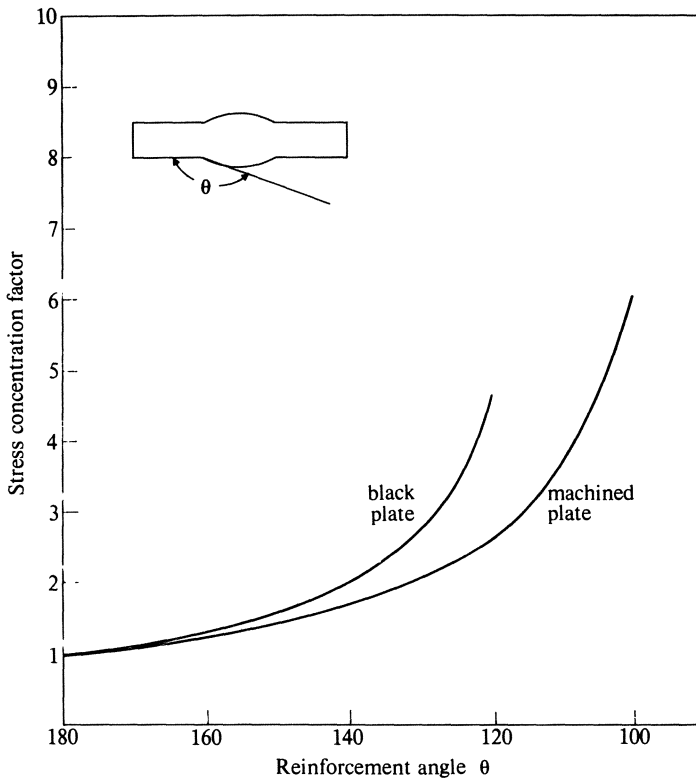


Figure 7.19 Stress concentration factor (SCF) for fatigue of butt welds as a function of reinforcement angle.

transverse ductility in the plate material, and propagation of cracks in service may be due to a number of mechanisms, including stress-corrosion and strain-age cracking. The mechanisms that may generate subsolidus cracks during or shortly after welding are discussed below while those which result in cracking during service will be considered in Chapter 10.

7.5.3 The hydrogen embrittlement and cracking of welds in steel

Steel may suffer two types of embrittlement due to the presence of hydrogen. The first type occurs at elevated temperature and affects carbon and low alloy steel. It results from chemical reaction between hydrogen and carbides, and causes permanent damage, either decarburisation or cracking or both. The second type occurs at temperatures between -100°C and 200°C . This embrittlement is due to physical interactions between hydrogen and the crystal lattice, and is reversible in that after removal of the gas the ductility of the steel reverts to normal.

7.5.3.1 Hydrogen attack

The elevated temperature effect, known as **hydrogen attack**, has been observed mainly in petroleum and chemical plant where hydrogen forms part of the process fluid. Initially the metal is decarburised but at a later stage intergranular fissures appear and the metal is weakened as well as being embrittled. Dissolved hydrogen reacts with carbides to form methane (CH_4) which precipitates at the grain boundaries. There is an incubation period before any damage can be detected in normal mechanical tests. This incubation period may be very long (sometimes of the order of years) at low temperature, but it decreases sharply with increasing temperature. Increasing the chromium and molybdenum content of the steel raises the temperatures above which hydrogen corrosion occurs, and austenitic chromium–nickel steels of the 18 Cr 10 Ni type are immune from attack. Decarburisation and fissuring that resembles hydrogen attack has been observed in laboratory tests of high tensile steel welded with cellulosic electrodes. Small areas around defects such as pores and inclusions were decarburised and cracked. It would appear, however, that the properties of the joint were not significantly affected, probably because of the small dimensions of the corroded areas. Of much greater importance in welding is the temporary form of hydrogen embrittlement, since this may cause **hydrogen-induced cold cracking**.

7.5.3.2 Hydrogen embrittlement

Embrittlement due to hydrogen may be assessed in a normal tensile test by comparing the reduction of area of a hydrogen-charged specimen δ_{H} with that of a hydrogen-free specimen δ_0 . The degree of embrittlement E may then be expressed as

$$E = \frac{\delta_0 - \delta_{\text{H}}}{\delta_0} \quad (7.9)$$

Alternatively, a V-notch may be machined around the circumference of a cylindrical specimen. If such a testpiece is charged with hydrogen and then subjected to a sufficiently high constant tensile load, it will fail after a lapse of time. The type of result obtained is illustrated in Figure 7.20. The reduction of strength, and the step in the strength/time curve both increase with increasing hydrogen content.

A test that produces more useful quantitative results (although requiring an exacting experimental technique) uses a standard ASTM fracture toughness specimen loaded in an atmosphere of high-purity (oxygen-free) hydrogen. The stress intensity required to maintain crack growth is measured as a function of hydrogen pressure and this in turn may be related to the hydrogen content of the steel. Figure 7.21 shows the result of such a test on a quenched and tempered alloy steel with a K_{IC} value in air of $66 \text{ MN/m}^{3/2}$.

7.5.3.3 The solution of hydrogen

Hydrogen dissolves in steel in two ways: as an interstitial constituent, and in **traps**. The interstitial solubility of hydrogen in alpha iron is governed by Sievert's law:

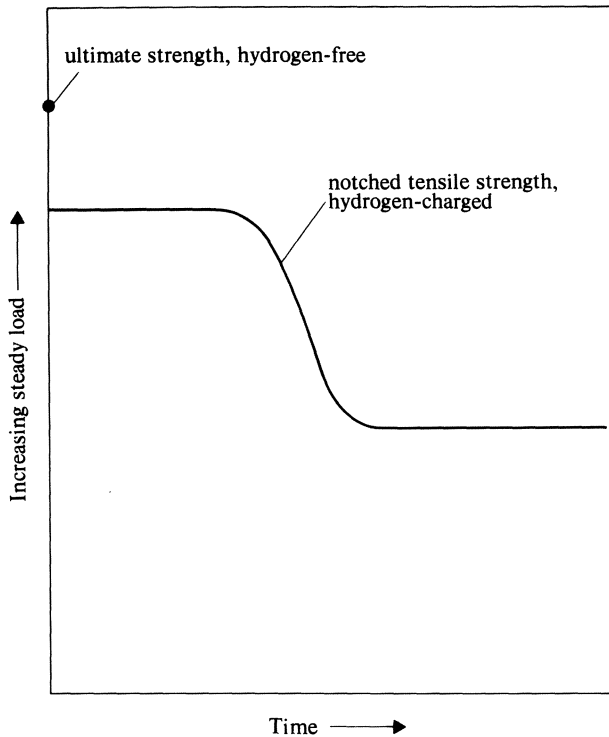


Figure 7.20 Notched tensile strength of steel when charged with hydrogen.

$$C_H = 6.2 \times 10^{-4} p^{1/2} \text{ ppm by mass} \quad (7.10)$$

(p in atmospheres). The solubility increases exponentially with temperature with a heat of solution of approximately 27 kJ/mol. These figures are for a pure iron in the annealed condition. In steel hydrogen may be adsorbed or trapped at interfaces, in particular grain boundaries, carbides and non-metallic inclusions, and at dislocations or microvoids. The local concentration of hydrogen in traps is much higher than in the lattice; for example, it has been suggested that $[H]$ at grain boundaries is 10^4 times the interstitial value. In fusion welding the overall hydrogen concentration immediately after welding is in the range 1–100 ppm: i.e. four to six orders of magnitude greater than the equilibrium value at room temperature in contact with 1 atmosphere hydrogen. However, this hydrogen appears likewise to exist partially as an interstitial (supersaturated) solution and partly in traps, since a proportion of the hydrogen (**diffusible** hydrogen) diffuses out of the weld at room temperature while the remainder can only be removed by vacuum fusion techniques, to give a measure of the **total** hydrogen content. Diffusible hydrogen is measured by plunging a weld sample into mercury and collecting the evolved gas in a burette. Traditionally, diffusible hydrogen contents have been expressed as ml per 100 g or ppm of **deposited**

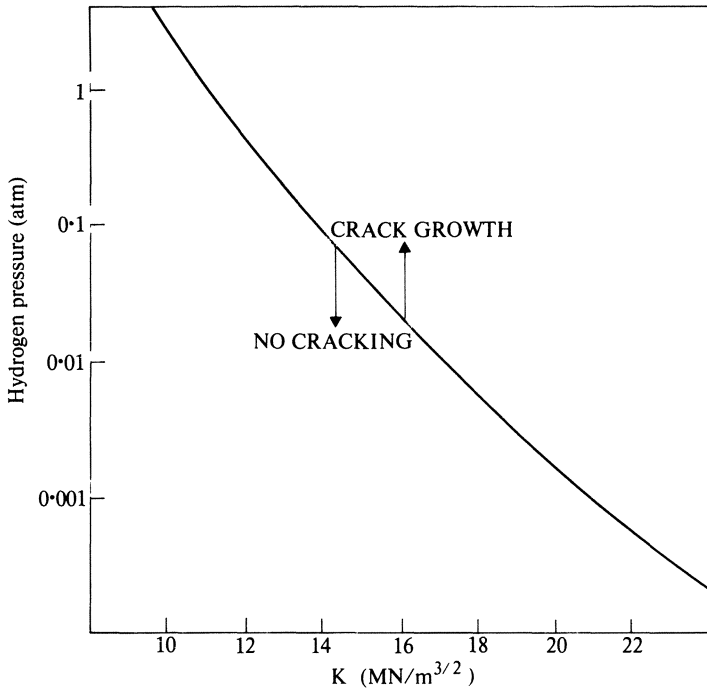


Figure 7.21 Conditions for crack growth in AISI 4340 steel hardened to a yield strength of 1700 MN/m^2 and exposed to oxygen-free hydrogen at various pressures. (After Oriani, R. A. and P. H. Josephic 1974. *Acta Metallurgica* 22, 1065–74.)

metal. This method may cause difficulties in comparing SMA with SAW tests because the amount of dilution is higher with SAW. To overcome this problem results may be expressed as ppm or g/ton of fused metal (1 ppm = 1 g/ton = 1.12 ml/100 g).

There is evidence that the incidence of hydrogen cracks in steel ingots is greater when the sulphur level is reduced to low levels such as 0.01% and below. It has been suggested that reducing sulphur contents in this way may reduce the number or size of traps, and thereby increase the embrittling effect of any given level of hydrogen. However, decreasing the sulphur content to very low levels also increases the hardenability of the steel, which may in turn be the cause of increased cracking.

7.5.3.4 Cracking due to dissolved hydrogen

Hydrogen embrittlement only manifests itself during processes that lead to fracture of the metal; it does not, for example, increase the hardness of the steel as measured by an indentation test. There has been much speculation regarding the mechanism of the embrittlement. An early hypothesis suggested that hydrogen gas accumulated in voids within the metal and built up sufficient

pressure to cause fracture. Although **hydrogen blistering** does undoubtedly occur as a result of hydrogen penetration due to corrosion, this mechanism is not now considered to be responsible for hydrogen embrittlement. It has also been suggested that the surface energy of steel may be reduced by hydrogen adsorption. There is, however, more general support for the **decohesion** theory. Where there is a pre-existing crack or discontinuity and a tensile stress is applied, hydrogen is considered to diffuse preferentially to the region of greatest strain (i.e. to just below the crack tip). The presence of relatively large concentrations of hydrogen reduces the cohesive energy of the lattice to the extent that fracture occurs at or near the crack tip. This view is consistent with the nature of hydrogen cracking, which is relatively slow and quite often discontinuous; the crack velocity being dependent on the diffusion rate of hydrogen. Hydrogen is evolved from the crack, due it is thought to relaxation of strain by cracking resulting in the hydrogen being supersaturated at the crack surface. Cracking is intergranular with respect to the prior austenite grains when the stress intensity factor is low, and transgranular when it is high. The intergranular mode may be associated with the high intergranular concentration of hydrogen but may also be promoted by intergranular weakness (caused, for example, by temper embrittlement). Thus, in welding, the region most susceptible to hydrogen cracking is that which is hardened to the highest degree, although coarse grain is a contributory factor. The most susceptible microstructure is high-carbon twinned martensite.

7.5.3.5 *Hydrogen-induced cold cracking in welds*

The physical appearance of hydrogen cracks in welds is illustrated in Figures 7.22 and 7.23. In Figure 7.22 the crack has initiated at the small region of lack of fusion at the root of the fillet and has travelled through the HAZ, mainly in the coarse-grained region. In fillet welds subject to longitudinal restraint, hydrogen cracks tend to be transverse to the weld axis, running through the weld itself. The same applies to hydrogen cracks in a root pass made in thick steel by the SMA process. In both these cases the restraint is such as to produce the maximum strain in the longitudinal direction. The location of cracks will also depend on the relative hardenability and the carbon contents of the weld metal and parent metal. If the compositions are the same and the longitudinal restraint not too severe, centreline cracks may appear in the weld metal, since the maximum cooling rate is along the weld axis. Many high tensile steels, however, are welded using a filler metal of low carbon and alloy content and in such cases HAZ cracking is more likely. Transverse cracks tend to be straight, but longitudinal and HAZ cracks are jagged. The cracking may be intergranular, transgranular or both intergranular and transgranular relative to the prior austenite grains.

Hydrogen cracking in fusion welding occurs as a result of the simultaneous presence of four predisposing factors: hydrogen in the weld metal, tensile stress and strain, a crack-sensitive microstructure, and temperature between 200 °C and – 100 °C. These factors will be discussed separately below.

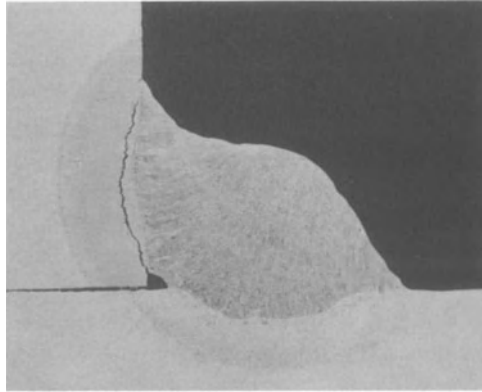


Figure 7.22 Cracking in the heat-affected zone of a fillet weld in high tensile steel. (Photo: Welding Institute)

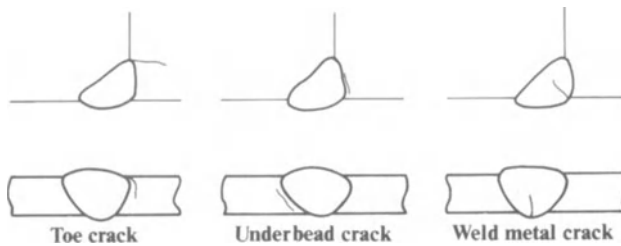


Figure 7.23 Typical forms of cold cracking.

Hydrogen is derived from hydrogenous chemical compounds that are dissociated in the arc column. These compounds are for the most part either hydrocarbons or water. In both cases they may be introduced into the arc by contamination of gas lines, electrodes or the workpiece. However, the most important source of hydrogen is electrode coatings or fluxes. Electrode coatings consist of minerals, organic matter, ferro-alloys and iron powder bonded with, for example, bentonite (a clay) and sodium silicate. The electrodes are baked after coating, and the higher the baking temperature the lower the final moisture content of the coat. Rutile and cellulosic electrodes contain organic matter and cannot be baked at more than about 200°C , whereas basic coatings, being all mineral, may be baked at $400\text{--}450^{\circ}\text{C}$. The relationship between moisture content of the coating and hydrogen content of the weld deposit for a typical basic-coated rod is shown in Figure 7.24. In the case of rutile and cellulosic electrodes hydrogen is generated by both residual water and cellulose, to give a hydrogen content in the standard test that is typically 20–30 ppm.

Submerged arc fluxes may be fused, sintered or agglomerated. The first two contain no water, but agglomerated fluxes are made in a similar way to

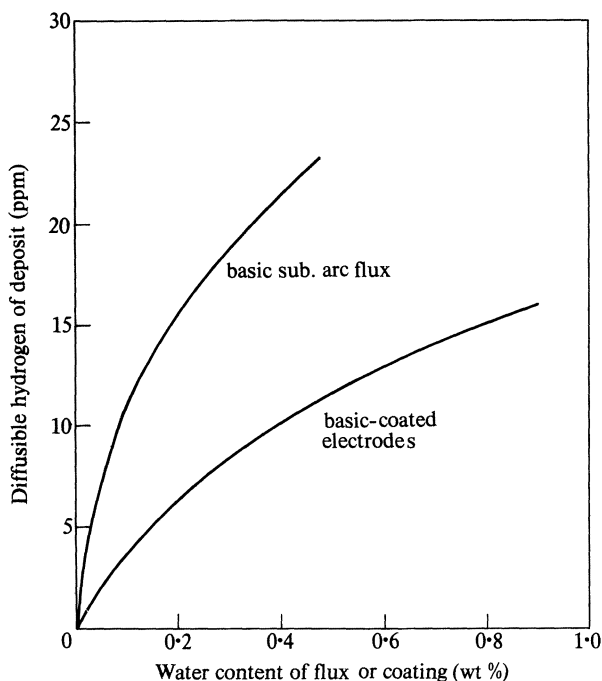


Figure 7.24 Hydrogen content of deposit as a function of water content of flux. (After Evans, G. M. and H. Baach 1976, Metals Technology Conference, Paper 4-2, Sydney.)

electrode coatings and may have a residual moisture content. Basic submerged arc fluxes may be of this type and Figure 7.24 shows the residual water/hydrogen in weld metal relationship. Note that for the same water content, basic submerged arc flux generates about twice as much hydrogen in the deposit as basic electrode coatings. Flux dried at 800 °C can, however, produce hydrogen contents below 10 ppm.

Basic coated electrodes and basic fluxes may pick up moisture if exposed to the atmosphere. The susceptibility to water absorption depends on baking temperature and on the type of binder that is used, as illustrated in Figures 7.25 and 7.26. In setting up shop procedures for the use of basic rods and fluxes it is good practice to determine the maximum exposure time of the consumables by making a series of exposure tests and determining the hydrogen content of weld deposits produced using the exposed electrodes or flux. The IIW recommended terminology for such hydrogen contents is:

- (a) Very low = 0–5 ml/100 g deposit
- (b) Low = 5–10 ml/100 g deposit
- (c) Medium = 10–15 ml/100 g deposit
- (d) High = over 15 ml/100 g deposit

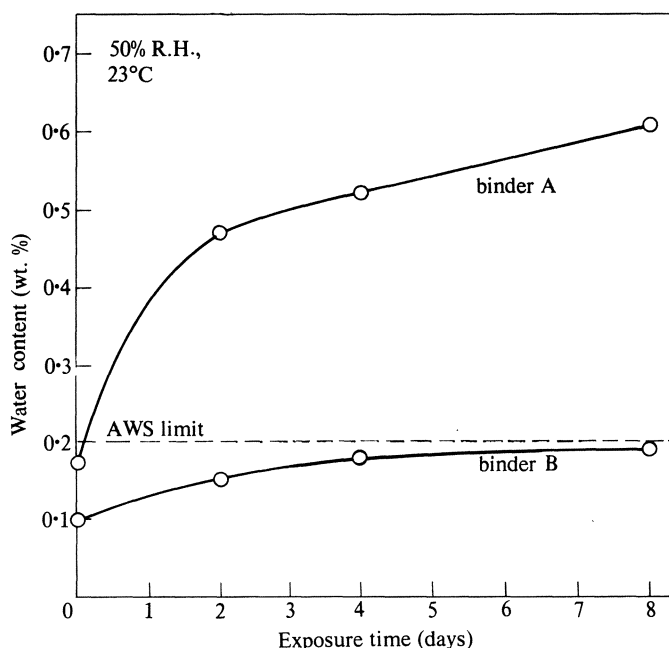


Figure 7.25 Effect of binder on the amount of water absorbed by basic-coated electrodes after exposure. (After Evans, G. M. and H. Baach 1976, Metals Technology Conference, Paper 4-2, Sydney.)

Where hydrogen cracking is a risk the hydrogen content is maintained in the low or very low range. In US practice the moisture content of the coating of basic low hydrogen electrodes is controlled, the upper limit according to AWS standards being as shown in Table 7.2.

Table 7.2 AWS requirements for moisture content of hydrogen-controlled electrode coatings*

Specified minimum ultimate strength of weld deposit		Maximum moisture content, % by mass
lbf/in ²	MN/m ²	
70 000	482.6	0.6
80 000	551.6	0.4
90 000	620.5	0.4
100 000	689.5	0.2
110 000	758.4	0.2
120 000	827.4	0.2

* Applicable to electrodes supplied in sealed containers.

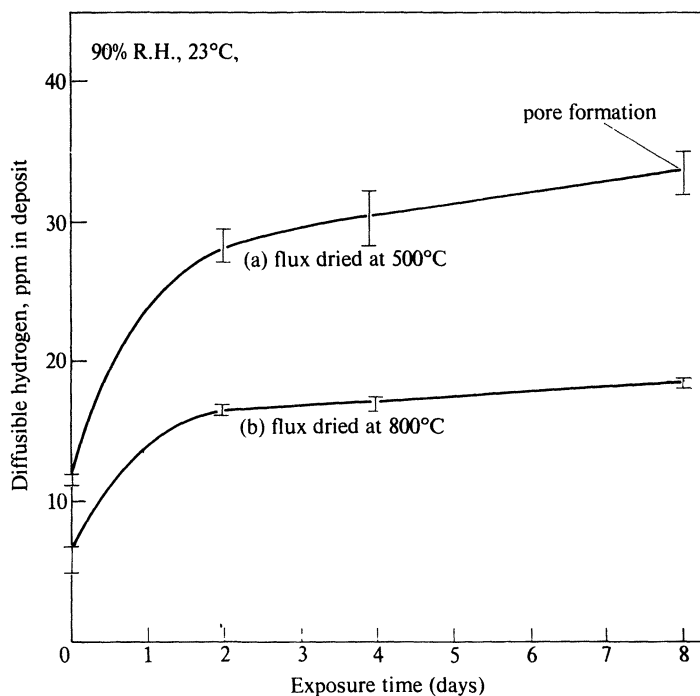


Figure 7.26 Effect of exposing a basic submerged arc flux (a and b previously baked at 500 °C and 800 °C, respectively) on the subsequent weld-metal hydrogen content. (After Evans, G. M. and H. Baach 1976. Metals Technology Conference, Paper 4-2, Sydney.)

Note that the diffusible hydrogen contents quoted in this section were all measured using standard techniques which require quenching the specimen immediately after welding. In actual welded joints, where the weld metal is allowed to cool in still air and the hydrogen has the opportunity to diffuse out between passes, the hydrogen content may be much lower. Figure 7.27 shows a comparison between pipeline welds made with cellulosic and basic-coated electrodes. When air cooled, the cellulosic weld metal gives a hydrogen content of less than 4 ml/100 g, as compared with 20–30 ml/100 g for the same electrodes as tested by a standard method. Clearly, the hydrogen content of welds may depend upon details of the welding procedure as well as on the type of electrode coating, particularly in the case of SMA welding.

The stress that acts as a driving force for hydrogen cracking is in most instances the welding residual stress, although in exceptional cases transients such as thermal stress may play a part. The level of residual stress depends on the yield strength of the weld metal and the degree of restraint. In conditions of complete restraint the residual stress is equal to σ_y , but in most instances the structure relaxes elastically to some degree so that the residual stress is lower

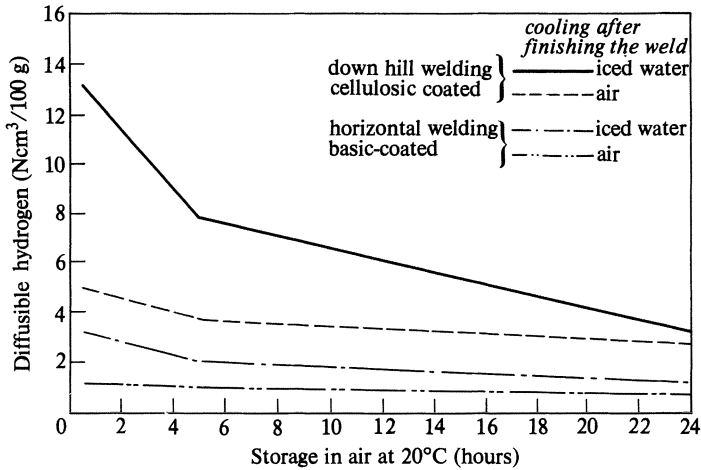


Figure 7.27 The content of diffusible hydrogen in a 10 mm V-joint, depending on cooling rate and time of storage. Cellulosic and basic-coated electrodes; steel: AP15L X 60 (Rabensteiner, G. 1976. *Development of electrodes*. Metals Technology Conference, Paper 16-5, Sydney.)

than yield. Residual stress may act longitudinally with respect to the axis of the weld, transversely, and at right angles to the plate surface (in the through-thickness direction). Through-thickness stresses may be high below welded-on attachments or in butt welds between thick components, but normally the longitudinal and transverse stresses dominate.

Apart from the stress field at the root of any crack that may be present, stress concentrations may form internally around non-metallic inclusions. The degree of stress concentration depends on the shape of the inclusions, and it has been found in practice that cerium-treated steel, which contains rounded inclusions, is less susceptible to hydrogen cracking than steel without such treatment and containing elongated inclusions (this factor may also be significant in lamellar tearing: see Section 7.5.5). Inclusions may also generate 'fish-eyes'. These are bright circular areas surrounding an inclusion and found on the rupture face of a tensile test that failed in the weld metal. The bright area is a region of brittle failure that occurred due to hydrogen accumulation around the inclusion during the test. The fact that 'fish-eyes' are not found on impact fracture surfaces indicates the need for hydrogen diffusion. Lattice strain is generated by the martensite transformation in the weld metal and HAZ, and the amount of strain so produced increases with the carbon content. This internal strain, although difficult to quantify, makes an important contribution to the driving force for hydrogen cracking.

There is evidence to show that while stresses at or below the yield point can initiate microcracks in a hydrogen-charged weld HAZ, plastic deformation is necessary for the crack to propagate. The plastic deformation may be localised (e.g. at the tip of a notch), or it may initially be uniform. Once a crack has

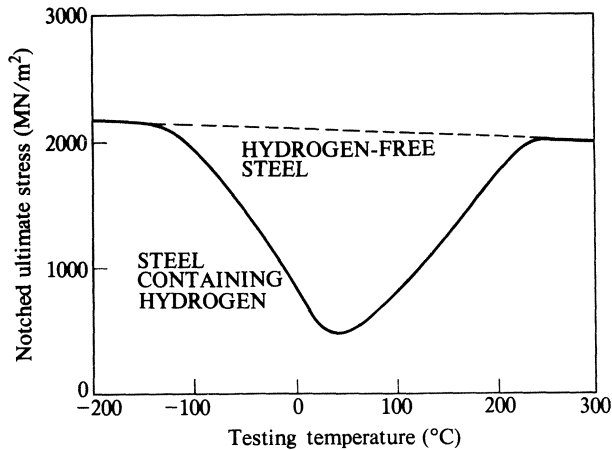


Figure 7.28 Notched tensile strength of quenched and tempered low alloy steel containing hydrogen in the quenched condition, as a function of testing temperature.

started to propagate, a plastic zone forms around the crack tip and the system is self-maintaining. The formation of the plastic zone is promoted by the presence of hydrogen. Increased strain normally decreases the incubation time for crack initiation and increases the rate of growth, but in some instances may inhibit growth by blunting the crack tip.

The most crack-susceptible microstructures are usually formed in the coarse-grained region of the HAZ although sometimes the degree of embrittlement may be greater in the fine-grained region. As stated earlier, the most crack-sensitive microstructure is high carbon martensite. Structures that have a hardness below 300 VPN have a low susceptibility to cracking: above 350 VPN the risk is significant. Other types of embrittlement as discussed earlier, may also promote cracking.

The effect of temperature on the notched tensile strength of a quenched and tempered steel is shown in Figure 7.28. Note that the most severe embrittlement occurs at about room temperature. This is generally true, but tests indicate that the probability of cracking increases if the steel is cooled to a subzero temperature after welding instead of cooling to room temperature. On the other hand, holding at an elevated temperature after welding reduces the probability of cracking, as indicated by Figure 7.29. In the case illustrated one effect of the cooling arrest may be to increase the mobility of hydrogen and reduce its concentration at points of high strain. Equally, if not more important, is the fact that holding just below the M_s temperature (the temperature for start of the martensite transformation) tempers the martensite initially formed, reduces the lattice strain and allows the formation of more ductile transformation products.

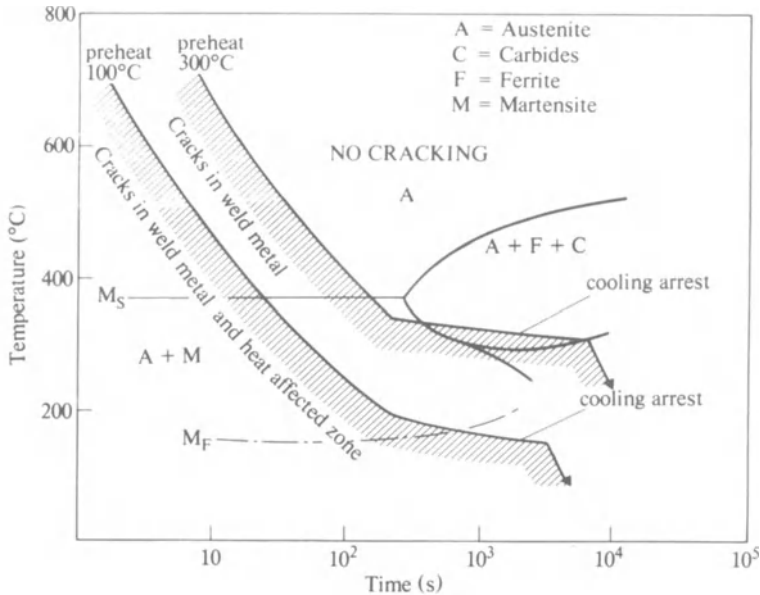


Figure 7.29 Relationship between transformation characteristics, weld cooling cycle and cracking of 2.75 Cr–Ni–Mo–V steel welded with 2.75 Cr–Mo electrodes (Granjon, H. P. 1962. *Welding J.* **41**, 7–s; courtesy American Welding Society).

The combined effects of stress, hydrogen content and embrittlement may be expressed by comparing the stress intensity in the weld or HAZ with the fracture toughness of the ‘as-welded’ material. If the residual stress is σ_r and there are cracks or cracklike defects of depth a_0 present in the joint, the stress intensity factor (see Section 10.3.2) is:

$$K = k_1 \sigma_r a_0^{1/2} \quad (7.11)$$

where k_1 is a factor $1 < k_1 < \pi^{1/2}$. Also we can put $\sigma_r = k_2 \sigma_y$ where k_2 is a restraint factor and σ_y is the yield strength of the weld metal. If the fracture toughness of the most severely embrittled area of the joint is K_{IC} the critical crack length is

$$a_{0c} = \left[\frac{K_{IC}}{k_1 k_2 \sigma_y} \right]^2 \quad (7.12)$$

Taking $K_{IC} \approx 10 \text{ MN/m}^{3/2}$ (as indicated by Figure 7.20 for a high tensile quenched and tempered alloy steel) and $k_1 k_2 \sigma_y \approx 1000 \text{ MN/m}^2$ Equation 7.12 gives $a_0 \approx 0.1 \text{ mm}$. Equation 7.12 indicates that the basic factors governing the probability of hydrogen cracking are the length of pre-existing cracks, fracture toughness of the weld and HAZ, restraint and yield strength of the weld metal. Pre-existing cracks of the order 0.1 mm in length are likely to be present in alloy

or high tensile steel welds due to grain boundary liquation, liquation of sulphide inclusions, hydrogen attack, fracture of martensite plates or other causes.

For small values of a_0 the initial rate of crack growth may be very low, and in practice hydrogen cracks in welds may take days or even months to develop. More often they appear immediately or a short time after welding. Because of the incubation time required for crack development hydrogen cracking is also known as **delayed cracking**. Note, however, that apparently delayed cracking can take place in other metals such as aluminium alloys, where the hydrogen mechanism is not applicable. The appearance of such cracks may be due to stress relaxation opening up cracks that were in fact present immediately after welding.

Hydrogen cracking probably accounts for **flakes** (cracks) in heavy forgings and steel ingots. On a fine scale, the lower reduction of area obtained in hydrogen-charged tensile test specimens is probably due to premature void nucleation in the necked region.

7.5.3.6 Testing for hydrogen-induced cold cracking

Laboratory tests for hydrogen cracking in welds were developed for a number of reasons: for example, to determine the variables that govern the cracking phenomenon, to compare the susceptibility of different steels, or to develop procedures for preventing cracks.

Cold cracking tests fall into two categories: self-restraint tests such as the Lehigh slit groove test and the Welding Institute Controlled Thermal Severity (CTS) test, and tests in which a known external load is applied to a specimen.

The Lehigh test simulates conditions in a butt weld. A plate 12" \times 8" (305 mm \times 203 mm) of the thickness to be tested is prepared with a central slot in the form of a double U-preparation. Slits are made laterally along the long edges of the test pieces, the depth of the slit determining the restraint (Figure 7.30). A weld run is made in the root of the joint, and the depth of slit required to prevent cracking is determined. Alternatively, the percentage length of crack is recorded.

In the Controlled Thermal Severity (CTS) test a square plate of the required material is fillet welded to the base plate along two opposite sides. The remaining two sides are then welded up, the second weld being laid down immediately after the first. The assembly is allowed to stand for a period of time, after which the welds are sectioned and examined for cracks. The severity of the test may be varied by altering the thickness of the plates, the hydrogen level in the test welds and the composition of the weld metal (Figure 7.31). The cooling rate is designated by means of a **Thermal Severity Number (TSN)**. TSN 1 is the thermal severity corresponding to heat flow along a single steel plate 6 mm thick. TSN 2 is obtained in a butt weld between 6 mm plates, while in a 6 mm tee joint, where there are three heat flow paths, the thermal severity number is 3. The TSN number is also increased in proportion to the plate thickness, so that the second test weld in a CTS testpiece (which also has three heat flow paths) in 12.5 mm plate would have TSN 6.

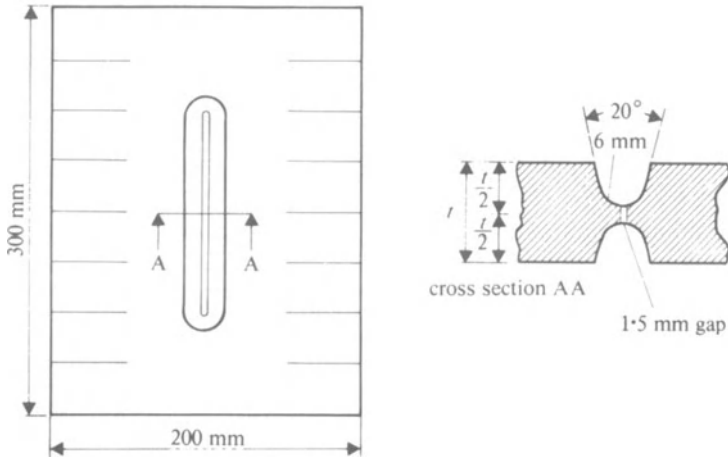


Figure 7.30 Lehigh cracking test.

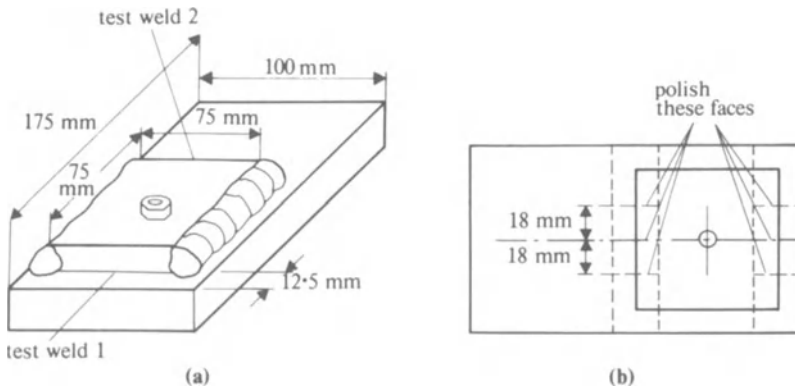


Figure 7.31 CTS cracking test.

After CTS test had been in use for some time, it was found that setting a gap (typically 1.5 mm) at the root of the test weld gave more severe cracking conditions: this variant is known as the **modified CTS test**.

In more recently developed tests it is customary to apply a known load or strain to the test specimen. The **Implant** test uses a cylindrical specimen of the steel to be tested. This specimen is notched and then inserted in a hole in a plate made from similar or compatible material. A weld run is then made over the specimen (or row of specimens), which are located so that the notch lies in the HAZ. After welding and before the weld is cold a load is applied to each specimen and the time to failure is determined. The plot of stress against time to failure gives an assessment of the relative susceptibility of different steels. Alternatively, the critical cooling time between 800 °C and 500 °C below

which cracking occurs may be recorded, and used to predict required welding procedures.

The **Rigid Restraint Cracking (RRC)** test employs a heavy frame in which two test plates are clamped. These plates are welded together by a partial penetration weld in a single run. The restraint is measured by strain gauges mounted on the frame, and cracking is detected by a fall in the registered strain. Restraint may be varied by changing the restraining length, the plate thickness or the heat input rate. Essential variables are cooling time 800°C to 500°C, hydrogen content, restraint intensity and type of steel. This test gives a better correlation between carbon equivalent and cracking than does the Implant test (Figure 7.32).

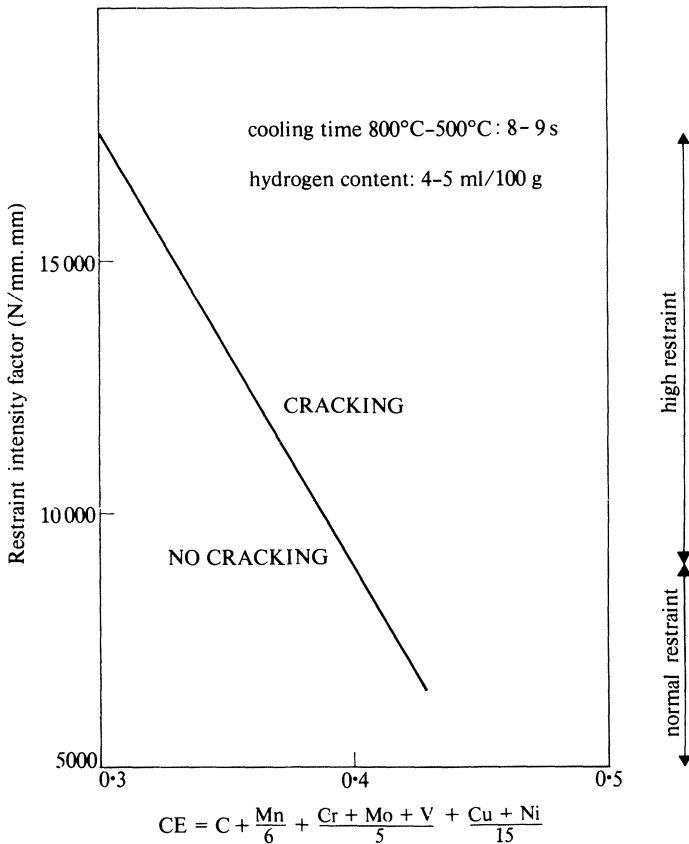


Figure 7.32 Relationship between carbon equivalent, restraint intensity factor and cold cracking in the RRC test. (After Fikkers, A. T. and T. Muller 1976. Metals Technology Conference. Sydney.)

A test developed at Rensselaer Polytechnic Institute (RPI) employs small specimens (51 mm × 13 mm) which are stacked together so that a weld bead can be laid along one edge. These are then held in a fixture which imposes a

uniform stress or a uniform plastic strain, and the development of cracks is observed through a microscope on a previously polished surface. For stresses below the yield point the curve of strength against time to initiate microfissures has the same form as that for notched tensile specimens shown in Figure 7.20. Such curves permit different steels to be compared. In the RPI test cracks do not propagate unless the specimen is notched or plastically deformed.

Tests such as those described above are mainly of use for determining the effect of variables such as steel composition on the hydrogen crack susceptibility, although the CTS test has been employed to develop recommendations for welding procedures. The RRC test may also be of value in establishing procedures for structures in which the restraint factor is known. Normal practice, however, is to rely on empirically developed procedures that are conservative enough to make some allowance for human error.

7.5.3.7 Measures to avoid hydrogen-induced cold cracking

The risk of hydrogen-induced cold cracking is minimised by reducing the hydrogen content of the weld deposit, by developing a non-sensitive microstructure, by avoiding excessive restraint and, where necessary, maintaining the temperature above the cold cracking range. These objectives may be accomplished by:

- (a) Material selection,
- (b) Design to avoid restraint,
- (c) Selection of welding process,
- (d) Control of welding procedures: in particular preheat, heat input rate, and postweld heat treatment.

Material selection is generally a compromise between the need to obtain maximum design strength at minimum cost on the one hand, and weldability on the other.

In general, weldability is improved by reducing the carbon content and carbon equivalent, by minimising alloy content and by aiming for low yield strength and high ductility. Fine-grain steel is usually less sensitive to cracking than a coarse-grained steel of equivalent yield strength. As carbon and alloy contents increase so it becomes necessary to restrict the content of sulphur and phosphorus and to control residuals that might promote temper embrittlement. Likewise, more stringent precautions need to be taken in welding. In the case of high-strength alloy steel for land-based operations the carbon content should be maintained at the lowest practicable level, preferably below 0.18%.

Low sulphur content is generally desirable in that it improves ductility and reduces the risk of solidification cracking. However, when the sulphur content is very low (say below 0.015%) the susceptibility to hydrogen cracking increases. This is considered to be due to the increased hardenability of such steels. The effect is not very marked and has been encountered in practice in a limited

number of cases only. In developing welding procedures, however, a slightly increased carbon equivalent should be assumed for low sulphur steel.

Much can be done at the design stage to avoid details that have too much self-restraint. In structural work it may be possible to calculate restraint factors and establish an upper limit. In many instances, however, calculations of restraint are not practicable, and empirical rules must be used. For example, in pressure piping it is customary to place welds not closer than 50 mm. In the case of alloy steel pressure vessels, nozzles and attachments should be sited so that the distance between the toes of adjacent welds is, preferably, more than three times the plate thickness. Rigid box-like structures should be avoided in crack-sensitive materials. Figure 7.32 shows the relationship between restraint, carbon equivalent and cold cracking for carbon, carbon–manganese and micro-alloyed steels, as determined by the RRC test. This relationship applies only to the specific welding conditions quoted and is not general. A general formula for welding high tensile quenched and tempered (QT) low alloy steel without preheat is given in terms of a parameter P_w :*

$$P_w = CE + \frac{H}{60} + \frac{K}{40\,000} \quad (7.13)$$

where CE is the Ito–Bessyo carbon equivalent

$$CE = C + \frac{Si}{30} + \frac{Mn + Cu + Cr}{20} + \frac{Ni}{60} + \frac{Mo}{15} + \frac{V}{10} + 5B \quad (7.14)$$

H is hydrogen content in ml/100 g and K the restraint intensity factor in N/mm^2

$$K = \frac{\text{Youngs modulus} \times \text{plate thickness}}{\text{restraining length}} \quad (7.15)$$

For a double side V preparation it is required that $P_w < 0.3$ to avoid cracking. For micro-alloyed and carbon–manganese steels this formula is conservative and the limit value for P_w is nearer 0.35.

The freedom of choice of welding processes is necessarily limited. The application must be practicable and economic. Further constraints may be applied by the job specification: for example, a requirement for impact testing may make it necessary to use SMA instead of SAW, or it may necessitate the use of a basic flux with SAW, which in turn increases the risk of hydrogen contamination of the weld. In general, automatic processes (electroslag, submerged arc) or semiautomatic GMA welding are a lower risk than SMA because their higher heat-input rates reduce the cooling rate. In welding high tensile or alloy steel it is normal practice to use basic-coated electrodes, but for plain carbon steel cellulosic or rutile-coated electrodes are often a better selection.

Very often the material, design and process selection are determined by others and the only freedom of action lies in the control of welding procedures.

* See IIW Docs IX-631-69 and IX-846-73

Here the essential steps include control of hydrogen content of consumables, heat input rate to the workpiece, preheat and postwelding heat treatment. The hydrogen content of basic-coated electrode coatings and basic submerged arc flux is controlled by storage under dry conditions, usually in a heated or air-conditioned store, or by baking before use. Procedures are set up to ensure that rods or flux are not exposed to atmosphere beyond a certain length of time, surplus material being returned to store for re-baking. Periodic checks may be made of moisture content and/or diffusible hydrogen in welds. Basic-coated electrodes are frequently kept in a heated canister after issue from the stores and until they are used.

Preheat is effective in reducing cooling rate, and thereby modifying the transformation products, and in reducing weld and HAZ hardness. It may also take the metal out of the region of maximum sensitivity to hydrogen embrittlement (see Figure 7.28) and may allow hydrogen to diffuse out of the weld. Preheat is in most instances applied locally to the weld and it is important that a sufficient width of plate (say three times thickness minimum) is uniform in temperature. In joining sections of dissimilar section thickness it may be necessary to apply more preheat to the thicker part. Heating may be by flame or by electric elements: both are satisfactory but electric heating lends itself more readily to automatic control. Control is by temperature-indicating crayons, optical pyrometer, or thermocouples. Although local heating is the norm, it may be desirable in the case of severely restrained parts to heat the whole component. In such cases it would be good practice to maintain the preheat until the component is given its postweld heat treatment. In most cases, however, it is undesirable or impracticable to maintain preheat, and instead the weld is cooled slowly to room temperature, or the preheat is maintained for a period of say 30 minutes after completion and before cooling. Postweld heat treatment finally reduces the hydrogen content to a low level so that further cold cracking is improbable.

7.5.4 Chevron cracking

The use of basic submerged arc fluxes has been attended from time to time by a type of cracking known as *staircase*, 45° or *chevron cracking*. Figure 7.33 shows a longitudinal section from a weld so affected. Sometimes the cracks are relatively straight, but in many cases they have a zig-zag shape, whence the term 'staircase'. The cracks were at first ascribed to hydrogen, since the early basic fluxes were baked at 500°C . As will be seen from Figure 7.26, such a flux may generate a high weld-metal hydrogen content if it has been exposed to the atmosphere for a relatively short time. Increasing the preheat temperature overcame this problem. At the same time, the baking temperature of the flux was increased to 800°C . Cracks have nevertheless been found in welds made with the improved flux.

The circumstantial evidence favours hydrogen embrittlement as a cause of chevron cracking. However, the morphology of the cracking is not characteristic

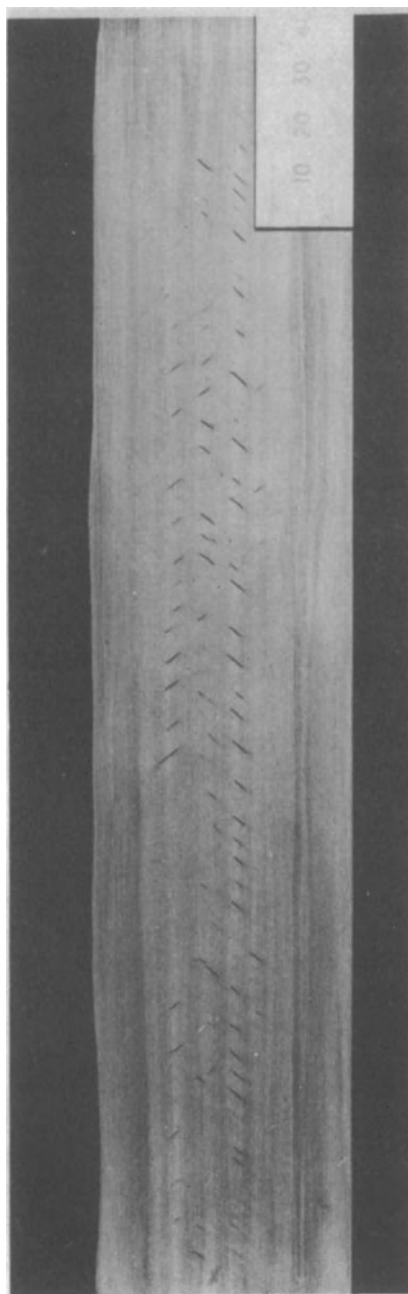


Figure 7.33 Longitudinal section of submerged arc weld showing chevron cracks. (Photo.: Cranfield Institute of Technology.)



Figure 7.34 Chevron crack located in the recrystallised region of weld metal. (Photo.: Cranfield Institute of Technology.)

of a normal hydrogen crack. Figure 7.34 shows a typical staircase in which there are a series of open, intergranular cracks joined by fine transgranular cracks. The open cracks are staggered so as to form a line at 45° to the weld axis, hence the typical form. The intergranular surfaces (which are intergranular relative to prior austenite grains) show thermal facets, indicating that they have been exposed to high temperature.

It has been shown that under laboratory conditions chevron cracks form in a progressive manner. No cracks appear until the later weld passes have been made; at this stage microfissures form in the lower runs, and as the weld is completed these extend to form a staircase crack. Two hypotheses have been advanced to explain the experimental evidence. The first suggests that the weld metal is subject to **ductility dip cracking**. Steel weld metal may lose ductility as it cools from 1200°C to 1000°C , after which it recovers and is normal at about 800°C . This loss of ductility is thought to be due to segregation of impurity atoms (such as sulphur and phosphorus) to grain boundaries, and may be promoted by some constituent of the flux. Thus, intergranular ductility dip cracks form at elevated temperature, and at low temperature these cracks join by a hydrogen cracking mechanism.

The second hypothesis suggests that the cracking is all due to hydrogen, but that once again it occurs in two stages. In the first stage intergranular microcracks form in earlier passes, and later these join by transgranular hydrogen cracking.

Although this defect has been found mainly in submerged arc welds, it is also known to occur in SMA welds made with basic-coated electrodes. Only a small number of such cases have been recorded.

7.5.5 Lamellar tearing

Lamellar tearing is a form of cracking that occurs in the base metal of a weldment due to the combination of high localised stress and low ductility of the plate in the through-thickness direction. It is associated with restrained corner or tee joints, particularly in thick plate, where the fusion boundary of the weld is more or less parallel to the plate surface. The cracks appear close to or a few millimetres away from the weld boundary, and usually consist of planar areas parallel to the surface joined by shear failures at right angles to the surface. Figure 7.35 illustrates a typical case.

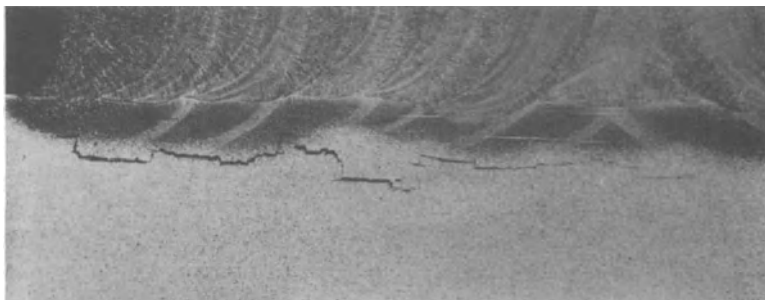


Figure 7.35 Lamellar tear under T-butt weld in C–Mn steel. Note the step-like morphology of the crack illustrating its tendency to run in planes parallel to the plate surface ($\times 5$). (Photo.: Welding Institute.)

The susceptibility to lamellar tearing depends upon the type of joint and the inherent restraint, on sulphur and oxygen contents, on the type and morphology of inclusions (which affect the **through-thickness ductility**) and on the hydrogen content of the weld.

Lamellar tearing has affected weld fabrication in the machine tool industry, where tee and corner joints in heavy plate are required for frames and bed plates. It is also a hazard in the fabrication of offshore oil platforms, and in welded-on attachments to boilers and thick-walled pressure vessels.

Lamellar tears initiate by separation or void formation at the interface between inclusions and metal, or by shattering of the inclusion itself. The voids so formed link together in a planar manner by necking, microvoid coalescence, or cleavage. Subsequently these planar discontinuities, when they exist at different levels, are joined by vertical shear walls. It would be expected that susceptibility to lamellar tearing would correlate with the number of inclusions as counted using a Quantimet apparatus, but this does not appear to be the case except in very broad terms. It is possible that submicroscopic inclusions play a part in generating this type of crack.

Silicate and sulphide inclusions both play a part in initiating lamellar tearing. Testing does not always show a clear correlation between sulphur and silicon content on the one hand and tearing susceptibility on the other, but reduction

of sulphur content is generally regarded as one of the methods of control. Cerium or rare earth metal (REM) treatment is another means of control, but it is not much used in practice. Hydrogen has a significant effect on lamellar tearing. In high-strength steels that form martensite in the HAZ, hydrogen-induced cold cracks will generally form preferentially, but in plain carbon steels of low hardenability, hydrogen increases the susceptibility to lamellar tearing quite markedly. There is little or no correlation between heat input rate and the incidence of lamellar tearing, but in the presence of hydrogen a low heat input rate might tip the balance towards hydrogen cracking.

Lamellar tearing may, in principle, be avoided by ensuring that the design does not impose through-thickness contraction strains on steel with poor through-thickness ductility. Some possible design modifications are illustrated in Figure 7.36. Such changes will usually entail an increase in cost and therefore need to be justified by experience. It is also possible to grind or machine away the volume of metal where tearing is anticipated, and replace the cut-away portion with weld metal, a process known as **buttering**. In severe cases the assembly is then stress-relieved before welding on the attachment. The risk of tearing may be further reduced by specifying a material of high through-thickness ductility, which is usually achieved by limiting the sulphur content to a low value, say less than 0.007%. Preheating may also reduce the risk of lamellar tearing in some cases.

The most widely used test for susceptibility to lamellar tearing is the through-thickness ductility test. Plates are welded at right angles to and on opposite sides of the plate to be tested, or round bar may be friction welded thereto. Specimens are then cut out of this assembly and machined to a round test bar so that the original plate forms the central part of the gauge length. If the plate is thick enough the whole testpiece may be machined from it.

The ductility in a tensile test made on such a specimen is taken as a measure of susceptibility; material having a through-thickness ductility less than, say, 25% is regarded as susceptible. Other tests employ restrained or externally loaded welded specimens. Attenuation of an ultrasonic beam was at first considered to be a possible means of testing for lamellar tearing susceptibility, but this proved not to be the case.

Lamellar cracks (i.e. cracks parallel to the plate surface) have also been observed adjacent to butt welds in thick sections of carbon–manganese steel welded by the SAW process. These cracks are located near the centre of the plate section in or close to the HAZ. They appear to be associated with banding (alternate bands of relatively low and relatively high carbon content formed during rolling of the steel plate). There is no evidence that such cracking is associated with inclusions but this possibility cannot be excluded.

7.5.6 Reheat cracking

Reheat or stress relaxation cracking may occur in the HAZ of welds in alloy steel during postweld heat treatment or during service at elevated temperature.

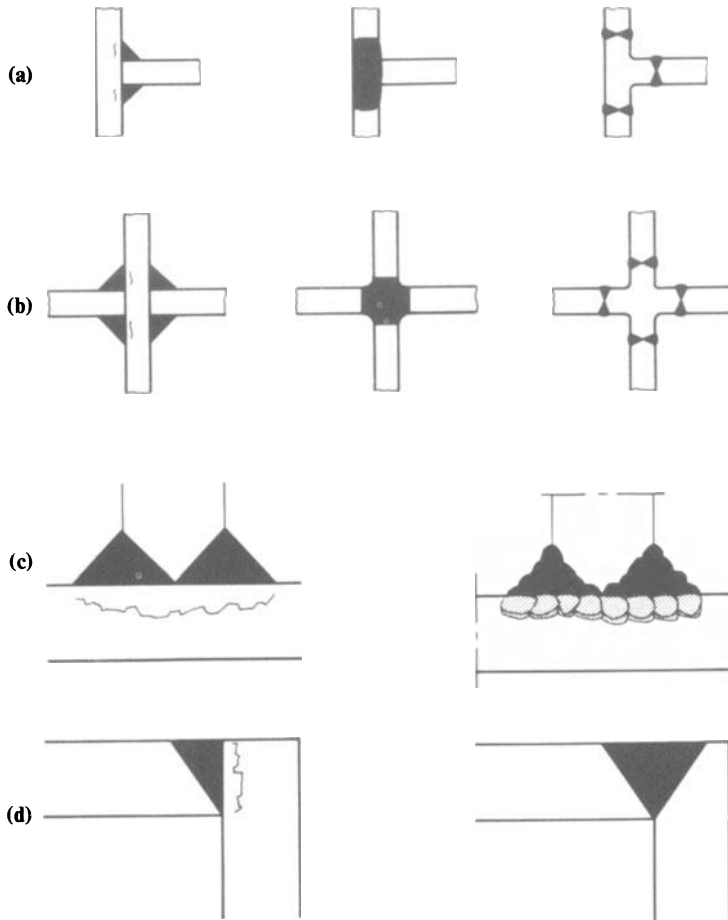


Figure 7.36 Redesign to avoid lamellar tearing: (a) and (b) replace fillets with solid weld metal or forged sections; (c) buttering; (d) modify preparation of corner joints. (In part after Dorn and Lai Choe Kming 1978. *Schweißen und Schneiden* 30, 84–6.)

Cracking is due to the combined effects of embrittlement and strain. At elevated temperature, precipitation occurs within the HAZ grains but not at the grain boundaries, where there is a denuded zone. Consequently, the interior of the grain is relatively hard and the boundary region relatively soft and when the residual welding strain relaxes, the deformation is concentrated at the weld boundaries. If the degree of strain exceeds the ductility of the grain boundary regions, cracking will take place. Cracks are intergranular and follow the prior austenite boundaries (Figure 7.37). They may initiate at the toe of welds or may be sub-surface.

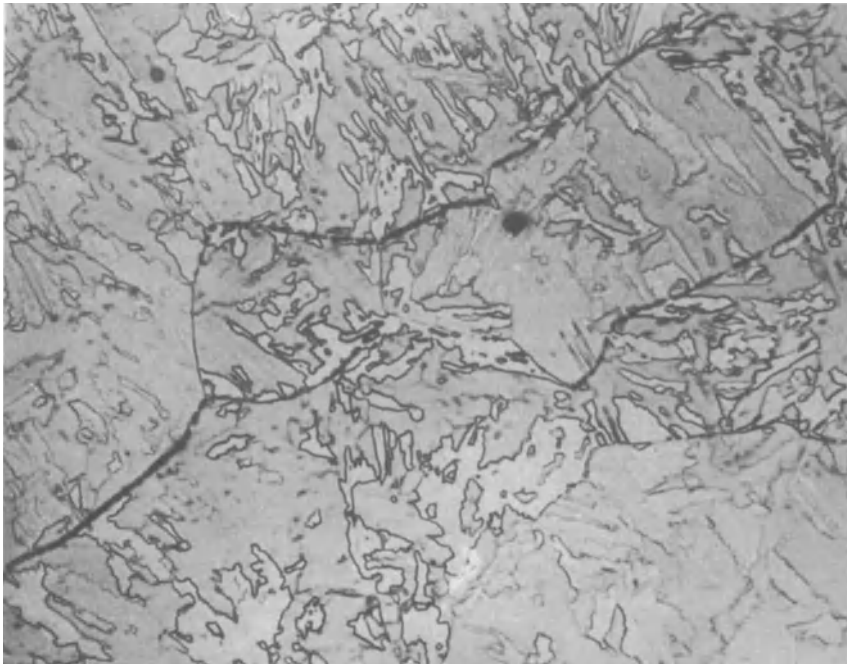


Figure 7.37 Typical reheat crack in Cr–Mo–V coarse-grain HAZ (Glover *et al.* 1977. *Metals Technology* 4, 329).

The factors that contribute to reheat cracking are:

- (a) A susceptible alloy composition.
- (b) A susceptible HAZ microstructure.
- (c) A high level of residual strain combined with some degree of triaxiality.
- (d) Temperature in the strain relaxation (creep) range.

Most alloy steels suffer some degree of embrittlement in the coarse-grained region of the HAZ when heated at 600 °C. Elements that promote such embrittlement are Cr, Cu, Mo, B, V, Nb and Ti. Molybdenum–vanadium and molybdenum–boron steels are particularly susceptible, particularly if the vanadium is over 0.1%. The relative effect of the various elements has been expressed quantitatively in formulae, due to Nakamura and Ito:

$$P = \text{Cr} + 3.3\text{Mo} + 8.1\text{V} - 2 \quad (\text{Nakamura})$$

$$P = \text{Cr} + \text{Cu} + 2\text{Mo} + 10\text{V} + 7\text{Nb} + 5\text{Ti} - 2 \quad (\text{Ito})$$

When the value of the parameter P is equal to or greater than zero, the steel may be susceptible to reheat cracking. Compositions that have suffered reheat cracking in practice are Mo or Cr–Mo steels with more than 0.18% V, all of

which have parameter values greater than zero and a $\frac{1}{2}$ Mo–B steel, which proved to be particularly subject to this type of defect. Another susceptible material is the $\frac{1}{2}$ Cr $\frac{1}{2}$ Mo $\frac{1}{4}$ V steel used by the steam power industry in the UK. Cu and Sb are detrimental in this steel, while titanium deoxidation is superior to aluminium deoxidation.

There are indications that a structure having a poor ductility (such as upper bainite) will be more susceptible to elevated temperature embrittlement. Likewise coarse-grained material is more likely to crack than fine-grained. It follows that the use of low heat-input processes (GMA or SMA) will be better than SAW. The elevated temperature strength may also be important. If the coarse-grained region of the HAZ is stronger than the parent metal at the PWHT temperature, then relaxation takes place outside the HAZ and the risk of cracking is reduced. The degree of restraint and the yield strength of the weld metal are important factors, as with hydrogen cracking. However, reheat cracking generally affects only thick sections (over about 50 mm) suggesting that a higher level of residual stress is required to cause failure. This would indeed be expected since the cracks form above 400 °C where the residual stress has already been reduced. High-pressure steam drums with closely spaced nozzles have failed due to reheat cracking in the nozzle and plate material. Cracking of the same type may occur below stainless steel weld-deposit cladding if the backing steel is susceptible and is given a PWHT after cladding. The stress here is due to the differential expansion between austenitic and ferritic steel. The cracks generally occur in PWHT during the heating cycle before reaching soaking temperature, probably in the 450–550 °C range. The heating and cooling rates do not appear to have any significant effect on the result.

Reheat cracks may also form or extend in service if the welded component is operating at elevated temperature and if joints are exposed to tensile stress, due either to inadequate PWHT or to service loads.

Reheat cracking tests may be divided into three types: self-restraint tests, high-temperature tensile tests, and strain relaxation tests. One technique is to make up butt welds with about two-thirds of the weld completed. The samples are cut into strips, and the strips welded to an austenitic stainless steel bar. This assembly is then heated and held for 2 hours at the PWHT temperature. The greatest length of sample in which no cracks are observed is a measure of susceptibility.

Hot tensile tests are made after first subjecting the specimen to a simulated weld thermal cycle. Subsequently a tensile test is made at 600 °C and both strength and reduction of area are measured. A combination of strength below that of the base metal and reduction of area below 20% indicates susceptibility to reheat cracking. This test is probably the most generally useful since it is simple and gives quantitative results.

Reheat cracking is avoided and/or detected by:

- (a) *Material selection.* For heavy sections limit alloy content as indicated by the Japanese formulae and limit vanadium to 0.10% max.

- (b) *Designing to minimise restraint.* Where restraint is unavoidable consider making a PWHT after the vessel is part-welded.
- (c) *Using a higher preheat temperature.* Dressing the toes of fillet and nozzle attachment welds. Using a lower-strength weld metal.
- (d) *Carrying out ultrasonic and magnetic particle testing after PWHT.*

7.6 WELDING PROBLEMS WITH IRON AND STEEL PRODUCTS

In this section cast irons and the various types of steel used in welded construction will be described, together with the type of welding problem with which they may be associated. Some materials – cast iron and rail steel for example – were inherited from the period before the advent of fusion welding, but to an increasing extent steel development aims at an optimum combination of mechanical properties and weldability. In general this aim is achieved most economically by means of low carbon fine-grained steel, since the fine grain size improves yield strength, notch-ductility and weldability at one and the same time. Low carbon is beneficial to weldability and notch-ductility, but there are a number of types of high-tensile steel where a relatively high carbon content is unavoidable, and where welding procedures must be adjusted accordingly.

Weldable steels may be divided into two main groups: those used primarily for their mechanical properties and those used for resistance to corrosion. Both these main groups may be further divided into two sub-groups: materials for low or ambient temperature and those for use at elevated temperature (creep-resistant or heat-resistant steels). In practice most of the steels used for resistance to corrosion and oxidation at elevated temperature fall into the high-alloy group and will be dealt with in Chapter 8. First, however, some of the available means of welding cast iron will be described.

7.6.1 Cast iron

The grades of cast iron that are welded include **grey iron** and **spheroidal graphite (SG) cast iron**. Grey iron is the most common and least costly of all cast materials; it is a $2\frac{1}{2}$ – $3\frac{1}{2}$ % carbon iron in which much of the carbon is present as graphite flakes. The distribution of graphite in grey iron causes it to be brittle, and consequently the standard set for welds in this material is not very high. SG iron, on the other hand, is cast with magnesium, nickel or rare earth additions, and as a result the graphite is in the form of spheroids, with a ferritic or pearlitic matrix. Unlike ordinary grey cast iron it has some ductility in the ‘as-cast’ state, up to about 4% elongation in a tensile test, and after annealing this is increased to 15–25%.

The weldability of SG iron is somewhat better than that of grey iron, because the sulphur and phosphorus contents are generally at a lower level, so that the risk of hot tearing in the weld metal is reduced. The metallurgical changes which

take place in the heat-affected zone of fusion welds in these two materials are, however, basically the same. In the region that is heated above the eutectoid temperature the ferrite is transformed to austenite. Above about 800°C graphite starts to go into solution and simultaneously cementite is precipitated, first at the grain boundaries, and at higher temperatures, when more graphite is dissolved, within the austenite grains. At still higher temperatures some melting occurs. On cooling, the cementite network remains but the austenite transforms—high carbon regions to martensite and low carbon regions to pearlite. Thus the heat-affected zone of fusion welds in cast iron has a complex structure comprising remelted regions, undissolved graphite, martensite, fine pearlite, coarse pearlite and some ferrite. Needless to say this structure is very hard and brittle and, if such a weld is tested in tension or bending, it fails through the weld boundary zone (Figure 7.38).

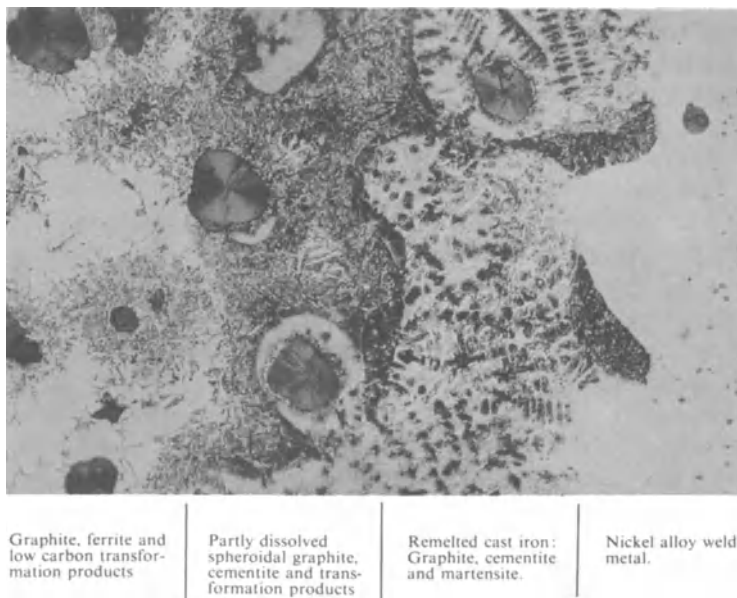


Figure 7.38 The heat-affected zone of a fusion weld on spheroidal graphite cast iron ($\times 300$; reduced by $\frac{1}{3}$ in reproduction). (Photo.: International Nickel Co. (Mond) Ltd.)

There are various ways of mitigating these effects. Preheat (combined with the use of low-hydrogen electrode coatings) may be used to minimise the danger of hard-zone cracking, although it is not always practicable, particularly in repair welding. An optimum preheat temperature is 300°C . The hardness of the heat-affected zone may be reduced by postwelding heat treatment at 650°C . It may be still further reduced by means of a full anneal. The effect of annealing, however, is to decompose the cementite; the graphite forms in a fine chain-like

pattern, which impairs the ductility of SG iron and weakens grey iron (high preheat temperatures over 450°C have a similar effect). Therefore 650°C is the optimum postwelding heat treatment temperature. Where preheat is not used, it is desirable to reduce the heat input rate to the lowest practicable level by making short runs and allowing the metal to cool between each run. This minimises the width of the HAZ and reduces the extent to which graphite is dissolved and reprecipitated as carbide. Correctly applied, this technique is capable of producing sound load-bearing joints.

Various filler alloys have been used for cast iron. For the repair of castings by gas welding a cast-iron filler rod may be applied – in the case of SG iron a cerium-bearing SG iron rod. Castings so treated are preheated to between 400 – 475°C and cooled slowly under insulation. Cast iron is not suitable as a filler material for arc welding, however, and for this purpose coated electrodes depositing a 55% nickel 45% iron alloy are the most successful. These electrodes have the advantages of relatively low melting point and low yield strength, which minimise the hardening effect and degree of restraint respectively. They are also relatively tolerant of sulphur, and the metal transfer is of the large droplet type, which reduces the amount of dilution of the weld deposit. A suitable technique for joining SG iron with the nickel–iron type of electrode is to preheat at 300°C , ‘**butter**’ the edges (i.e. apply a surface deposit on the edges of the joint to be welded) with 55% Ni 45% Fe and then heat treat at 650°C . Where distortion must be avoided, the preheat and postheat of the **buttering run** are omitted. Subsequently the joint may be completed using 55% Ni 45% Fe electrodes without preheat or postheat. It is characteristic of cast iron that even when welded in the manner described above, the joint strength and ductility vary erratically. Coated electrodes with a nickel or monel core wire are also used for welding cast iron.

The metal inert gas process with 55% Ni 45% Fe filler, operated in the spray transfer range is not successful because the weld cracks due to excessive penetration and dilution, with consequent sulphur and phosphorus contamination of the deposited metal. Ferritic coated electrodes (e.g. low-hydrogen carbon-steel rods) are, when applied in the normal way, unsatisfactory due to cracking either in the weld or at the weld boundary. However, fractured grey iron castings may be repaired by a method known as **studding**. Holes are drilled and tapped into the casting on either side of the fracture, and studs are screwed into these holes. Carbon-steel weld metal is then deposited over the area which includes the fracture and the studs, thereby making a mechanically strong joint (Figure 7.39). The weld deposit commonly cracks away from the casting, so that such a joint is not leak-tight.

7.6.2 Steels used primarily for their mechanical properties

Steels for ambient temperature operation will be considered first, and the more specialised alloys employed at subzero temperature later.

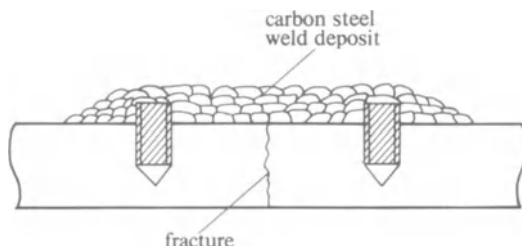


Figure 7.39 Repair of cast iron by studding.

7.6.2.1 Carbon and carbon–manganese steels

These fall into four main groups: carbon and carbon–manganese steels, micro-alloyed steels, high tensile normalised and tempered (NT) steels and high tensile quenched and tempered (QT) steels.

Carbon steels for welded construction generally have a carbon content of 0.35% or less, manganese up to 1.5% and silicon up to 0.35%. **Rimming steels** are those to which no deoxidants (commonly silicon and manganese) have been added, and in plate form consist of outer layers of almost pure iron, with a central core containing augmented amounts of carbon, sulphur and phosphorus. The weldability of such steel is inferior to that of other carbon-steel grades. **Semi-killed** or **balanced steel** has deoxidants added to it, but the amounts are such as to allow some carbon monoxide to form during solidification which, by compensating for solidification shrinkage, prevents the formation of a shrinkage pipe in the ingot. In **killed steel**, sufficient deoxidant is added to inhibit the carbon monoxide reaction completely. Semi-killed and killed steels are generally considered to be weldable without reservation.

Air-blown acid or basic **Bessemer steel** is less satisfactory than **open-hearth**, **electric furnace** or **oxygen convertor steel** as a material for welding because of its relatively high nitrogen content. Rimming or semi-killed Bessemer steel has a high ductile-to-brittle transition temperature, and in the welded condition this temperature is increased still further; it may also be subject to strain-age embrittlement. These disadvantages may be overcome to some degree by modification of the steelmaking process; by deoxidation with aluminium, or blowing with steam–air mixtures for example.

Most carbon steels used in welded construction have a relatively low carbon equivalent and are not crack-sensitive. However, when the section thickness is greater than 25 mm it may be necessary to consider preheat to say 100 °C, particularly if the restraint is high and/or the carbon content is near the upper limit.

Increasing the manganese content of the steel increases yield and ultimate strength and generally improves notch-ductility. The maximum addition to plain carbon–manganese steels is 1.6%, since above this limit islands of martensite may form in the ‘as-rolled’ steel. Carbon–manganese steel may be killed or semi-killed. To obtain fine grain for good notch-ductility, aluminium may be added,

and the steel is said to be **aluminium treated**. As with other grain-refining elements there is an optimum addition (0.01 to 0.02% for Al) above which the grain-refining effect remains the same but the notch-ductility deteriorates. Fine grain is also achieved by **controlled rolling** in the steel mill. The carbon equivalent is widely used as a means of controlling weldability in carbon–manganese steels. Standard specifications for weldable structural steels may contain CE limits. In addition the carbon equivalent may be used in conjunction with standard charts, some of which take account of section thickness and type of welding electrode, to establish preheat temperatures (see, for example BS5135). More often, preheat temperatures are established by simple, conservative rules: e.g. it might be specified that a preheat of 100 °C be applied to all thicknesses greater than 25 mm when the nominal tensile strength is 500 MN/m² or greater.

For reasons that have been discussed earlier weld metal deposited by coated electrodes will normally overmatch a parent metal of the same composition, but with high heat-input rate processes such as submerged arc and electroslag it may be necessary to introduce small amounts of alloying elements to improve strength and notch-ductility. This is not required for electroslag welds if they are given a normalising PWHT.

Rail steel and the high-tensile grades of concrete reinforcing bar may have relatively high carbon contents, typically in the range 0.5% to 0.8%. Rails are usually joined by flash butt welding and because this is a solid-phase welding process the tensile stress associated with welding is low, and the risk of cracking correspondingly small. It is, however, possible to join rails and reinforcing bar by fusion welding, applying a preheat of 100–250 °C and using basic-coated electrodes. Guidance as to procedures for fusion welding reinforcing bar is given in AWS Standard D12-1. Rails are also joined by thermit welding. The technique is essentially the same as that used for copper (see Section 9.3.6), except that the exothermic powder is a mixture of iron oxide and aluminium. Thermit welding is used for joints that cannot readily be made using the flash-butt process; for example, at points and bends.

7.6.2.2 Microalloyed steels

The term **microalloying** refers to the addition of small amounts of aluminium, vanadium, titanium or niobium to a carbon–manganese steel in order to enhance mechanical properties. Such steels, also known as **high-strength low-alloy (HSLA)** steels, may also contain 0.5% Mo and/or small amounts of nickel or chromium. HSLA steels were developed to provide high-tensile, notch-tough materials for structural applications such as offshore oil platforms, storage tanks and spheres, and line pipe.

A precursor of this family of steels was the German St 50, an aluminium-treated carbon–manganese steel with a tensile strength of about 500 MN/m². This steel was developed following the brittle failure of welded bridges, and the aluminium addition had the effect of reducing the susceptibility to strain-age embrittlement and at the same time improving fracture toughness. In the

UK niobium was used for increasing yield strength and fracture toughness in preference to aluminium because niobium can be added to semi-killed steels whereas aluminium can not.

Niobium has also been used for line pipe steel to API 5 LX, but the higher-strength line pipe steels may contain Mo and V. Line pipe may be subject to fast ductile shear failure, which may propagate for long distances before arrest. To minimise this hazard it is necessary to raise the upper shelf (post-transition) Charpy value to the highest practicable level, and this is done by grain refinement, limitation of carbon content and limitation of sulphur content.

In the case of line pipe there are two welding problems: the longitudinal weld that forms the pipe, normally made by submerged arc welding, and the circumferential welds joining lengths of pipe, normally made by stove-pipe welding. Stove-piping is a downward welding procedure using cellulosic electrodes, and it has the advantage of being much faster than alternative manual techniques for pipe wall thickness up to about 10 mm. For both types of weld it is normal practice to specify minimum Charpy impact values as close as possible to that specified for the plate material.

In formulating a flux/wire combination for submerged arc welding it is necessary to bear in mind that the weld metal transferred from the electrode is diluted by about twice the amount of parent metal, and the composition may be modified accordingly. To obtain good impact results it is necessary to aim at a microstructure consisting of acicular ferrite with the minimum amount of coarse pro-eutectoid ferrite (see Section 7.3.1). Even small amounts of martensite are detrimental if, as is normally the case, welds are not postweld heat treated. Therefore the amount of coring (microsegregation) must be kept to a minimum, and this is done by keeping the carbon content down. Alloy additions promote the formation of acicular ferrite but also increase the risk of martensite formation. Further, microalloying constituents in multi-run deposits may cause embrittlement by precipitation in reheated zones or during PWHT. Figure 7.40 shows a CCT diagram for carbon steel weld metal, and illustrates the restricted conditions under which an ideal microstructure forms. The dotted curves on the right are for a more highly alloyed region such as may result from microsegregation during solidification. In practice a boron-treated wire has given good results for single-pass welds but in multi-pass welds the microalloy content must be controlled to low levels. Semi-basic or basic fluxes are necessary in combination with such wires in order to control oxygen content and thereby improve impact properties. The higher the strength of the base metal the greater the care necessary in control of procedure and consumables.

Achieving impact strength requirements is not so much a problem with the manual circumferential welds because of the lower heat-input rate and correspondingly finer structure. Nor is hydrogen-induced cold cracking a serious problem, even though the welds are made with cellulosic electrodes. The reason for this is the relatively short time between passes in stove-pipe welding such that the interpass temperature is relatively high even under cold ambient conditions. Also, the actual hydrogen content may, as seen earlier, be much

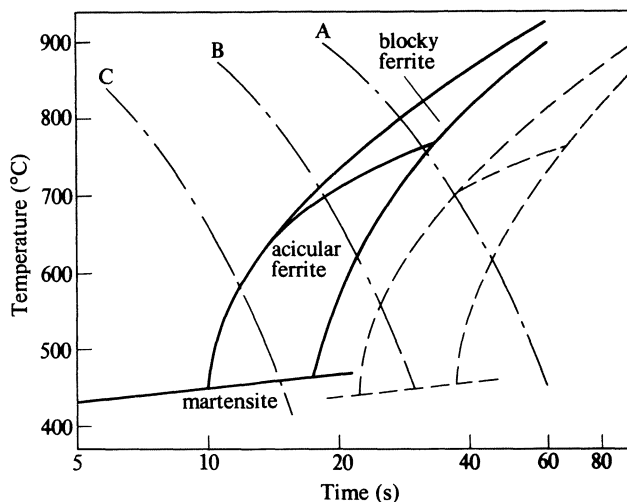


Figure 7.40 CCT diagram for carbon steel weld metal. Cooling rates indicated are: curve A = 10°C/s , B = 20°C/s , C = 45°C/s . (R. David Thomas Jr. 1977. Metal Progress III, 30–36).

lower than might be assumed from the results of diffusible hydrogen tests. In the Alaska pipeline, which was welded under severe arctic conditions, only 28 cracks were found in 1200 km of pipeline, and these were thought to be due to excessive bending during handling rather than to welding.

Table 7.3 shows the API standard grades of steel for high-strength line pipe. In addition, two special types have been developed for the higher-strength grades, namely **acicular ferrite** and **pearlite-reduced steels**. The composition of acicular ferrite steel is formulated so that ‘as-rolled’ plate has a microstructure rather similar to that of carbon steel weld metal. It consists of acicular ferrite grains with islands of martensite and scattered carbides. The pro-eutectoid ferrite found in weld metal is absent, but there may be some polygonal ferrite. This

Table 7.3 High-strength line pipe steel

Spec No	Grade	Ladle analyses (%)						Yield stress min (N/mm^2)	Ultimate stress min (N/mm^2)	Elongation min (%)
		C max	Si	Mn	V min	Nb min	Ti min			
API Std	× 42	0.28	—	< 1.25	—	—	—	290	410	25
	× 46	0.28	—	< 1.25	—	—	—	315	430	23
	× 52	0.28	—	< 1.25	—	—	—	360	450	22
	× 56	0.26	—	< 1.35	0.02	0.005	0.03	385	490	22
SLX	× 60	0.26	—	< 1.35	0.02	0.005	0.03	415	520	22
	× 65	0.26	—	< 1.40	0.02	0.005	—	450	550	20
	× 70	0.23	—	< 1.60	—	—	—	480	560	20

type of structure may be obtained from a steel with 0.06% C max, 1.5–2.2% manganese, 0.1–0.4% Mo and 0.04–0.10% Nb. Acicular ferrite steel (AFS) of this general type to API 5 LX 70 can achieve impact properties of more than 200 J/cm² at –30 °C.

Pearlite-reduced steel (PRS), as the name implies, is a low carbon ferrite–pearlite steel with a lower proportion of pearlite in the microstructure than with the normal API grades. Some typical proprietary compositions are shown in Table 7.4. Like AF steel, PRS has a good combination of impact and tensile properties, suitable for large-diameter longitudinally welded pipes used in arctic conditions.

Table 7.4 Typical compositions of pearlite-reduced X 70 line pipe steel

Grade	No.	Chem. composition (%)					
		C	Si	Mn	Al	V	Nb
API	1	0.15	0.13	1.35	0.05	0.05	0.03
5LX	2	0.10	0.18	1.17	0.06	0.04	0.03
70	3	0.09	0.27	1.71	0.067	0.08	0.049

Submerged arc weld metal for high-strength line pipe steel may contain manganese, molybdenum, nickel, niobium and sometimes small amounts of titanium. A combination of 0.01–0.02% Ti and a basic flux in submerged arc welding can give an impact transition temperature in the weld metal as low as –60 °C. The HAZ, however, is normally lower in impact strength than the parent metal. Cellulosic-coated rods for the circumferential seams are manganese–nickel or Mn–Mo–Ni, the lower heat-input rate permitting a lower alloy content. With automatic GMA welding (**orbital welding**) the cooling rates are high enough to allow the use of carbon-steel filler metal.

Microalloyed steels are also used for pressure vessel and structural applications, but only exceptionally for pressure piping other than line pipe. For most applications aluminium-, niobium- or vanadium-treated carbon–manganese steels are adequate, and the welding requirements are less exacting than for line pipe. It is normal practice to use carbon or carbon–molybdenum weld metal, and in SMA welding basic-coated electrodes are used for the higher tensile grades. In the case of offshore oil rigs exposed to severe conditions, however, as in the North Sea, it is necessary to apply much the same precautions as have been detailed for line pipe in arctic exposure.

7.6.2.3 Low-alloy normalised and tempered (NT) steels

Table 7.5 shows the composition and mechanical properties of some high tensile NT steels used for welded applications. Steels of this type are used for boilers and pressure vessels where the design conditions make the use of alloy steel economic. Welding filler material is usually of the Mn–Mo type for SMA welding, but additional alloy content may be required for SAW. For heavy-wall

Table 7.5 Low-alloy high-tensile NT steels for welded fabrication

<i>Type of steel</i>	<i>Designation</i>	<i>Heat treatment</i>	<i>C max</i>	<i>Chemical composition (%)*</i>						<i>Specified minimum properties MN/m²</i>		
				<i>Mn</i>	<i>Mo</i>	<i>Cr</i>	<i>Ni</i>	<i>Cu</i>	<i>Nb</i>	<i>V</i>	<i>Yield stress</i>	<i>Ultimate stress</i>
											20 C	350 C 20 C
Manganese–molybdenum	ASTM A302 Gr. B (USA)	As-rolled or N or N & T	0.25	1.15/ 1.50	0.45/ 0.60						345	290 552
Nickel–molybdenum–vanadium	Ammo 65 (France)	N & T	0.15	1.55 max	0.45/ 0.55	(0.25 max)	0.60/ 1.0	(0.25 max)		0.10 max	462	353 621
Nickel–molybdenum	BHW 38 Germany	N & T	0.18	1.0/ 1.65	0.2/ 0.6		0.5/ 1.2				421	363 586
Chromium–molybdenum–vanadium	BS 1501-271	N & T	0.17	1.5 max	0.28 max	0.70 max	(0.30 max)	(0.20 max)		0.10 max	414	354 553
Chromium–nickel–molybdenum–vanadium	Asera 60N (Italy)	N & T	0.20	1.5	0.25	0.60	0.60			0.20 max	462	345 586
Copper–nickel–molybdenum–niobium	WB 36 (Germany)	N & T	0.17	0.8/ 1.2	0.25/ 0.40		1.0/ 1.3	0.5/ 0.8	0.02		431	353 607

* Figures in brackets are residuals.

Table 7.6 Low-alloy high strength QT steels for welded fabrication

<i>Type of steel</i>	<i>Designation</i>	<i>C</i> <i>max</i>	<i>Chemical composition (%)</i>					<i>Specified minimum properties MN/m²</i>		
			<i>Mn</i>	<i>Mo</i>	<i>Cr</i>	<i>Ni</i>	<i>Yield stress</i> 20 C	350 C	<i>Ultimate stress</i> 20 C	
Manganese–molybdenum–	ASTM A533 C1·1 (USA)	0·25	1·15/ 1·5	0·45/ 0·60		Up to 1·0	345	290	552	
2½ Chromium 1 molybdenum	ASTM A542 C1·1 (USA)	0·15	0·3/ 0·6	0·9/ 1·1	2·0/ 2·5		586		724	
2½ Chromium–molybdenum	24 CrMo 10 (Germany) 2·5 FDO (France)	0·28	0·5/ 0·8	0·1/ 0·3	2·3/ 2·6	0·8 max	441	352	634	
Low-alloy	WES 135 HT 60 QT (Japan)			Various			618		687	
	WES 135 HT 80 QT (Japan)			Various			687		785	

boiler and pressure vessel fabrication, basic or semi-basic submerged arc flux is usually necessary in order to meet impact test requirements, the limiting factor normally being the weld metal rather than the HAZ. Reheat cracking is a significant risk with some of the NT steels, as would be predicted from the formulae quoted earlier (Section 7.5.6). This defect is best avoided by a combination of material selection and design to minimise restraint.

7.6.2.4 Low-alloy quenched and tempered (QT) steels

QT steels have the advantage of fine grain with correspondingly good impact properties, but have the disadvantage of high yield strength, which increases the risk of various modes of cracking (as seen earlier in relation to hydrogen cracking, see Section 7.5.3.5). Table 7.6 shows QT steels that have been used for solid-wall pressure vessels. QT steel has been used for storage spheres in Japan and the welds in some vessels have cracked in service. The QT 2½ Cr 1 Mo steel showed a similar tendency when first used, but subsequently the steel was tempered to a lower yield strength and the problem appears to have been overcome. In both cases relatively thick plate has been used: up to 250 mm in the case of QT 2½ Cr steel.

QT steel is used in thinner sections for multilayer pressure vessels, for highly stressed applications such as welded compressor wheels, and for aerospace parts such as rocket cases. The low-alloy steels used for multilayer vessels and compressors do not present any special welding difficulties. Rocket cases may, however, be fabricated from low-alloy QT sheet metal with a carbon content in the region of 0.4%. The risk of hydrogen cracking is minimised by using GTA welding, and sulphur and phosphorus are kept to the lowest practicable level to avoid liquation cracking in the HAZ.

Maraging steels are low-carbon Ni–Co–Mo steels with small additions of Ti and Al. They have been developed to combine high proof stress with good fracture toughness. High tensile and proof-stress values are obtained by a martensite transformation followed by age hardening at a temperature of about 500 °C. The steel is solution-annealed at 820 °C and air cooled, which is normally sufficient to obtain 100% martensite, and is then age hardened. The combination of low carbon content with 10% Ni promotes good fracture toughness; in addition, the steel is vacuum melted and Si, Mn, B, Pb and non-metals are kept at a low level. Table 7.7 shows the composition and mechanical properties of three grades of maraging steels compared with typical values for AISI 4340, which is a competitive high-carbon high-strength steel. The main application for such materials in the welded condition is in aerospace components, but they are also used for dies, gears, automotive parts and ordnance. Welding is by GTAW and GMAW with matching filler material. The SMAW and SAW processes are unsuitable due to cracking and poor toughness in the weld metals. With inert gas shielding (normally argon) there is no HAZ cracking problem and the steel may be welded without preheat. After welding the mechanical strength of the weld is equal to the parent metal in the solution-annealed condition, but postweld ageing at 480 °C for 3 hours gives properties that match those of the fully heat-treated alloy.

Table 7.7 Ultra high-strength maraging and QT steels for welded fabrication

Designation	Nominal composition (%)						Typical properties				
	C	Ni	Co	Mo	Ti	Al	0.2% Proof (MN/m ²)	UTS (MN/m ²)	Elong. (%)	RA (%)	K _{IC} (MN/m ^{3/2})
18 Ni 1400†	0.03	18.0	8.5	3.0	0.2	0.1	1400	1435	12	55	100
18 Ni 1700†	0.03	18.0	8.0	5.0	0.4	0.1	1700	1735	10	45	90
18 Ni 1900†	0.03	18.0	9.0	5.0	0.6	0.1	1900	1935	8	40	65
AISI 4340	0.40	1.75	Cr 0.8	0.25			1700	1850	5	22	60

[†] Double vacuum melted.

7.6.3 Steels for subzero temperature use

The selection of steel for low temperature use is influenced by section thickness as well as by temperature, and guidance on the temperature/thickness relationship may be found in BS 5500 and the ASME pressure vessel code. In general, however, it is possible to employ impact tested carbon steel down to -50°C , $3\frac{1}{2}\%$ Ni steel down to -100°C , 5% Ni steel down to -120°C , and 9% Ni steel, austenitic Cr–Ni steel and non-ferrous metals down to the lowest operating temperatures. Below a particular temperature (-20°F in US practice, but somewhat higher in most other countries) the notch-ductility of ferritic steel is controlled by impact testing. Welds are likewise tested in the weld metal and often in the HAZ. In the case of carbon steel and $3\frac{1}{2}\%$ Ni steel it is possible when using matching electrodes to obtain impact values in the weld and HAZ that are acceptable to (for example) the ASME code. With SAW, however, there may be difficulties in obtaining good results with carbon steel, even using a multi-run technique with basic flux, at the lower end of the temperature range. Under these circumstances it is necessary to use an alloy filler, usually 1% Ni or $2\frac{1}{2}\%$ Ni.

When the nickel content exceeds a nominal $3\frac{1}{2}\%$ it is no longer practicable to use matching filler material because of the high susceptibility to solidification cracking. Normal practice is to employ a nickel-base coated electrode or wire, with which there is no difficulty in obtaining the required impact results. The nickel-base fillers originally used for 5% Ni and 9% Ni steel were substantially lower in strength than the parent metal, but subsequently higher-strength fillers have been developed. PWHT is not required for 9% Ni except (to the ASME code) in sections thicker than 50 mm, nor for $3\frac{1}{2}\%$ Ni below 19 mm. The value of PWHT for nickel alloy steels is uncertain, but when it is carried out the soaking temperature for $3\frac{1}{2}\%$ Ni should be below 620°C , the lower transformation temperature being reduced by the Ni content.

7.6.4 Low-alloy corrosion- and heat-resisting steels

Carbon–molybdenum and chromium–molybdenum steels are used for their enhanced strength at elevated temperature, for resistance to hydrogen attack (see Section 7.5.3.1) and for resistance to corrosion by sulphur-bearing hydrocarbons. The two steels most frequently used for elevated temperature strength are $\frac{1}{2}\%$ Cr $\frac{1}{2}\%$ Mo $\frac{1}{4}\%$ V and $2\frac{1}{4}\%$ Cr 1 Mo. Both steels are used for main steam lines in major power stations, and the $2\frac{1}{4}\%$ Cr steel is also employed for hydrocracker reactors, where it is required to withstand hydrogen attack. The $\frac{1}{2}\%$ Cr $\frac{1}{2}\%$ Mo $\frac{1}{4}\%$ V steel presents major welding problems because it is particularly susceptible to reheat cracking. This alloy is welded with a $2\frac{1}{4}\%$ Cr 1 Mo filler, and the cracking is almost entirely in the coarse-grained HAZ. Cracks appear after PWHT or after a period of service at elevated temperature. The susceptibility to cracking is reduced by controlling residual elements such as copper, arsenic, antimony and tungsten to a low level, and by using a low heat-input rate process to limit

the grain growth in the HAZ. How far these precautions are adequate to prevent reheating cracking in $\frac{1}{2}$ Cr $\frac{1}{2}$ Mo $\frac{1}{4}$ V steel welds is not certain.

$2\frac{1}{4}$ Cr 1 Mo steel is welded using matching electrodes and, as would be expected from the composition, has a low susceptibility to reheating cracking. Provided that the correct preheat temperature is maintained this steel does not present any outstanding welding problems. The same applies to the $1\frac{1}{4}$ Cr $\frac{1}{2}$ Mo, 5 Cr $\frac{1}{2}$ Mo and 9 Cr 1 Mo steels that are used for corrosion resistance in the petroleum and petrochemical industries (Table 7.8). These steels are welded with matching electrodes, and are normally given a postweld heat treatment, with a possible exemption for thin-walled pipe. Pressure vessels are fabricated from alloy plate up to 5 Cr, but the higher alloys are usually in the form of pipe. There is also a 12 Cr 1 Mo steel with similar weldability that is used to a limited extent for steam lines and superheaters.

Table 7.8 Heat-resistant and corrosion-resistant chromium–molybdenum steels

Designation	Nominal composition (%)					Mechanical properties				
	C	Cr	Mo	V	Other	0.2%				
						Proof	UTS	Elong.	Preheat	PWHT
	max					MN/m ²	MN/m ²	(%)	(°C)	(°C)
$\frac{1}{2}$ Mo	0.30	—	0.5	—	—	200	380	22	80	595–720
$\frac{1}{2}$ Cr $\frac{1}{2}$ Mo $\frac{1}{4}$ V	—	0.5	0.5	0.25	—	—	—	—	—	—
$1\frac{1}{4}$ Cr $\frac{1}{2}$ Mo	0.15	0.25	0.5	—	—	200	400	22	150	700–725
$2\frac{1}{4}$ Cr 1 Mo	0.15	2.25	1.0	—	—	200	400	22	175	700–750
5 Cr $\frac{1}{2}$ Mo	0.15	5.0	0.5	—	—	200	400	22	175	700–750
9 Cr 1 Mo	0.15	9.0	1.0	—	—	200	400	22	175	700–750

7.6.5 Ferritic and austenitic/ferritic chromium stainless steels

In this section we are concerned with steels containing over 11% Cr and with a primarily ferritic matrix. Such steels are resistant to chloride stress corrosion cracking so that, combined with the advantage of lower cost, they may be preferred to austenitic chromium–nickel steels for certain applications.

There are four main categories of ferritic Cr steels: the 12 Cr, the 18 Cr, the 27 Cr and the ferritic/austenitic types such as 26 Cr 4 Ni. All these basic types may be modified by additions of Mo, Ti and Nb. Against their advantages must be set three major disadvantages: poor weldability, brittleness and susceptibility to temper embrittlement.

These problems may in part be related to the Fe–Cr phase diagram. This is shown for an 0.05% C alloy in Figure 7.41. The higher Cr alloys solidify entirely as δ ferrite and below 20% Cr transform to $\gamma + \delta$ on cooling below 1150–1400°C. At lower temperatures the austenite is either retained or transforms to martensite. The martensite appears at grain boundaries and may cause intergranular brittleness.

If the steel is held in the δ ferrite region for a significant length of time (as during the weld thermal cycle), rapid grain growth takes place. The grain boundary

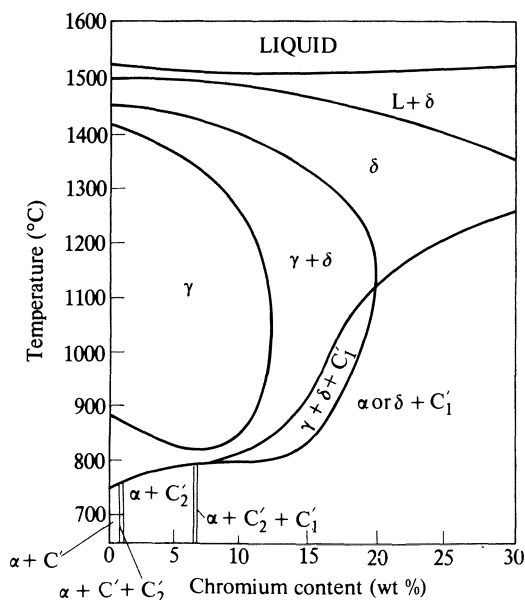


Figure 7.41 Chromium–nickel phase diagram for a carbon content of 0.05%.

area is reduced and the grain boundaries are correspondingly enriched by impurities. This further aggravates grain boundary embrittlement. In addition, carbides or carbo-nitrides may precipitate at the grain boundaries causing the steel to be susceptible to intergranular (IG) corrosion. Sensitisation of ferritic stainless steel to IG attack is caused by heating to the austenising temperature (above 925 °C) and rapid cooling. The susceptibility is removed by slow cooling or by annealing at 775–800 °C.

To minimise the IG corrosion problem niobium or titanium may be added to the steel, so that, ‘as-rolled’, the interstitial carbon is very low. The effect of so reducing carbon in solution is to reduce the extent of the γ field (the **gamma loop**) shown in Figure 7.41 to lower levels of Cr. Consequently, on heating through the weld thermal cycle, even a 12 Cr steel may be ferritic as it passes the nose of the gamma loop. Initially grain growth is inhibited by the presence of carbo-nitride particles but at a higher temperature these go into solution and grain growth (and possibly some austenite formation) may occur. On cooling the carbides reprecipitate as a fine dispersion and may harden and embrittle the HAZ, or they may precipitate in an intergranular form and render the steel susceptible to IG corrosion. Adding stabilising elements does not necessarily prevent IG corrosion in ferritic stainless steel, and limitation of carbon and nitrogen to very low levels is necessary for immunity.

In spite of these complex and somewhat intractable problems, commercial 12 Cr alloys may be welded in the form of sheet material and good properties obtained. Two such alloys are shown in Table 7.9. Welding is by GTA or GMA

Table 7.9 Chemical composition of ferritic and ferritic/austenitic stainless steels

Designation	Type	C	Cr	Ni	Nominal composition (%) [*]				
					Mo	Al	Ti	Nb	N
AISI 405	Ferritic 12 Cr	0.08	11.5/ 14.5	0.6	—	0.1/ 0.3	—	—	—
AISI 409	Ferritic 12 Cr	0.08	10.5/ 11.75	0.5	—	—	6 × C 0.75 max	—	—
AISI 410	Martensitic 12 Cr	0.15	11.5/ 13.5	0.75	—	—	—	—	—
NSS 21–2 409 D	Ferritic 12 Cr	0.06	11.5	—	—	0.5	—	—	0.02
AISI 430	Stabilised 12 Cr Ferritic 17 Cr	0.01 0.12	11.4 16.0/ 18.0	— 0.75	—	—	0.22 —	—	0.02 —
1803 T	Stabilised 17 Cr	0.015	17.5	—	—	—	0.5	—	0.02
19 : 2 Nb	Stabilised 17 Cr	0.018	19.0	—	2.0	—	—	0.5	0.03
18 : 2 Ti	Stabilised 17 Cr	0.018	18.0	—	2.0	—	0.3	—	0.03
AISI 446	Ferritic 27 Cr	0.20	23.0/ 27.0	0.6	—	—	—	—	0.25
ASTM A669	Ferritic/Austenitic	0.03	18.0/ 19.0	4.25/ 5.25	2.5/ 3.0	—	—	—	—

^{*} C and Ni are max. except where indicated.

using a Type 309 (23 Cr 12 Ni) or 310 (25 Cr 20 Ni) filler, and with a heat input rate preferably in the range 0.8–1.2 kJ/mm. Welded 12 Cr steel is used in automobile exhaust systems, for mildly corrosive food industry applications such as sugar, and for seaborne containers. AISI Types 405 and 410 steels, which have no stabilising elements added, are used extensively in the petroleum industry for lining towers, drums and heat exchangers handling sulphur-bearing hydrocarbons at elevated temperature. The material used is carbon or low-alloy steel plate roll-clad with 12 Cr, but since the cladding is not required to take any load, local weakening or embrittlement is not a problem. The filler metal on the clad side is AISI Type 309 or 310. The welding of solid-wall 12 Cr steel for pressure parts is not normal practice in hydrocarbon processing. Note that Type 410 steel has sufficient carbon to be martensitic in the HAZ: for this reason a low-carbon variety, Type 410S, is sometimes preferred. It is possible to weld Type 410 steel with a matching electrode, but this is not a common procedure.

18% Cr steels are used where higher corrosion resistance is required, and the standard AISI Type 430 and some commercial alloys are listed in Table 7.9. Type 430 is not often welded, being more susceptible to embrittlement due to grain growth and the presence of interstitial elements than the 12 Cr type. This embrittlement is minimised by electron beam refining or other sophisticated steel-making techniques, and/or by the addition of stabilisers (Ti and Nb) and molybdenum. Addition of molybdenum also increases the corrosion resistance to a level similar to that of the austenitic chromium–nickel steels. Thus, 18 Cr 2 Mo steel has potential advantages for sheet metal fabrication and particularly where chloride SSC is a known hazard. The metallurgical problems are similar to those for 12 Cr types; in particular Ti must be limited to avoid precipitation hardening in the HAZ, while excessive niobium may cause liquation cracking, also in the HAZ. The high chromium ferritic steels as specified by AISI (e.g. Type 446, Table 7.9) are not suitable for welding except for lightly loaded welds or emergency repairs. These steels are mainly used for heat-resisting duties, where their intrinsic brittleness is accepted. Welds are made by SMA using a low heat-input rate technique as for cast iron with no preheat and a Type 309 or 310 filler.

A 26 Cr 1 Mo steel (E-brite) made by EB remelting and having very low C and N has been developed for special corrosion-resistant duties. This steel can be welded but the corrosion resistance of the joint is not equal to that of the parent metal.

The ferritic/austenitic stainless steels are normally designed to resist chloride stress corrosion cracking and consist of islands of austenite in a ferritic matrix. These steels, one of which is listed in Table 7.9, have the advantages of the 12 Cr and 18 Cr ferritic (resistance to chloride SSC) together with some of their disadvantages (susceptibility to temper brittleness). They do not, however, suffer excessive grain growth in the HAZ and consequently their weldability is much better. The Mo-bearing types may have a corrosion resistance equal to that of Type 316 SS. Welding is possible using GTA, GMA and SMA processes with austenitic Cr–Ni filler. There are a number of proprietary steels similar to A669, for example, UHB 44L and Sandvik 3 Re 60.

The ferritic and ferritic/austenitic steels are not very widely used in welded fabrication. In part this is due to the metallurgical disadvantages and in part it is due to the fact that individual alloys are rarely available in all product forms. They are most suitable for thin sections, and find their largest output in the form of sheet (for example, for automobile trim and exhausts) and as tube for heat exchangers. In stressed applications the operating temperature is limited to a maximum of 400°C because of temper embrittlement. The 27 Cr and ferritic/austenitic steels may be further embrittled by sigma phase formation at operating temperatures above 600°C. When such steels are used for heat-resisting applications the parts must be designed to accommodate the expected embrittlement.

FURTHER READING

- Linnert, G. E. 1965. *Welding metallurgy*, vol. 1. Miami: American Welding Society.
- Linnert, G. E. 1967. *Welding metallurgy*, vol. 2. Miami: American Welding Society.
- American Welding Society 1972. *Welding handbook*, 6th edn. Section 4: *Metals and their weldability*. Miami: AWS; London: Macmillan.
- Dolby, R. E. (ed.) 1975. *The toughness of heat-affected zones*. Cambridge: The Welding Institute.
- Sekiguchi, H. 1976. *Fundamental research on the welding heat-affected zone of steel*. Tokyo: Nikkau Kogyo Shimibun.

8 Austenitic and high-alloy steels

8.1 Scope

Austenitic steels considered in this chapter are the **austenitic chromium nickel corrosion-resistant steels** of the 18 Cr 10–12 Ni (commonly known as 18/8) type and the **creep-resistant** and **scaling-resistant steels** containing up to a nominal 25% Cr. Hardenable high-alloy steels are arbitrarily classified as those containing more than 20% of alloying elements but which are capable of being hardened by heat treatment. The corrosion and oxidation resistance of these steels results from the formation of a self-healing surface film of chromium oxide. They may be welded by any of the major processes, but chief consideration will be given to the phenomena associated with fusion welding, particularly SMA, GTA and GMA welding.

8.2 Metallurgy of the weld metal and heat-affected zone

The austenitic chromium–nickel steels have relatively good weldability. The lack of a martensite transformation combined with the toughness that is characteristic of metals with a face-centred cubic lattice means that there is no susceptibility to hydrogen-induced cold cracking. At the same time, the susceptibility to porosity is low. Therefore, it is not difficult to achieve sound welds using correctly formulated electrodes or filler wire. The metallurgical problems that do arise with the welding of austenitic steels are usually associated with conditions of known hazard, such as producing a fully austenitic weld deposit or exposure to severely corrosive environment. Nevertheless, it is important to understand the metallurgical changes that take place during the fusion welding of these materials so as to be able to specify the correct combination of alloy and welding procedure for specific applications, particularly for corrosion-resistant duties.

8.2.1 Alloy constitution

Sections of the ternary chromium nickel–iron constitution diagram are reproduced in Figure 8.1. At 18 Cr, alloys containing less than about 5 Ni solidify as ferrite and above about 11 Ni they solidify as austenite. Irrespective of the solidus phase, the solidification range is small.

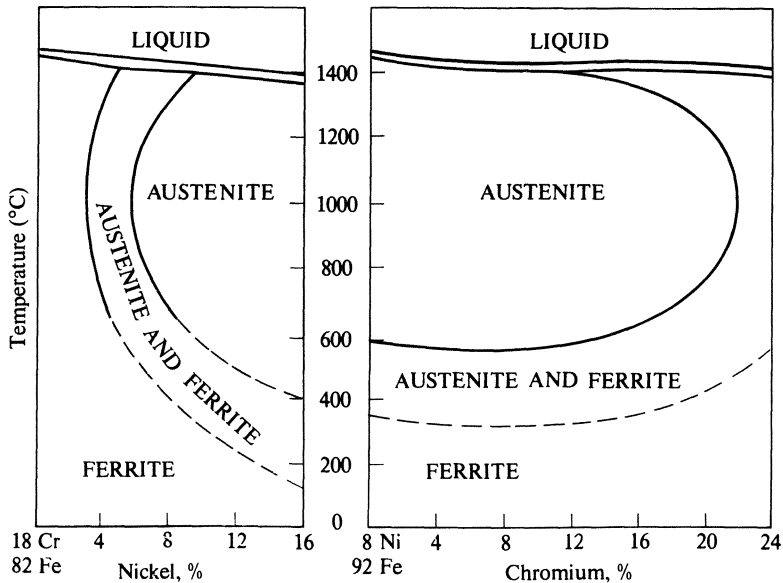


Figure 8.1 Sections of ternary Cr–Ni–Fe constitution diagram (Bain, E. C. and R. H. Aborn; courtesy American Society for Metals).

On cooling an 18Cr 10Ni steel from the solidus, part or all of the ferrite transforms to austenite. The low temperature transformation does not necessarily occur on cooling to room temperature, so that the structure of 18Cr 10Ni steel consists typically of metastable (retained) austenite, sometimes with a little delta ferrite. Increasing the nickel content has the effect of reducing the transformation temperature of the austenite, while the presence of chromium makes the transformation sluggish. Thus the stability of the austenite is increased by raising the nickel content. With low nickel (about 4% for example) it is possible to obtain a martensite transformation by cooling to subzero temperature, and such compositions are used for hardenable high-alloy steel in machine and aircraft construction. When the nickel content is about 6%, the $\gamma \rightarrow \alpha$ transformation may only be achieved by cold-working the steel, and in annealed 18Cr 10Ni the austenite remains untransformed down to the lowest attainable temperature.

The actual structure obtained in austenitic chromium–nickel steel weld metal varies with composition and cooling rate. For manual welding with coated electrodes the differences in cooling rate may for this purpose be ignored, so that constitution depends primarily on composition. The various alloying elements used may be classified as either **austenite formers** or **ferrite formers** and, depending upon their balance, so will the structure be more or less austenitic. Chromium, molybdenum, silicon, niobium and aluminium are the common ferrite-forming elements, while nickel, carbon, nitrogen and manganese favour the formation of austenite. The combined effects of ferrite and austenite formers

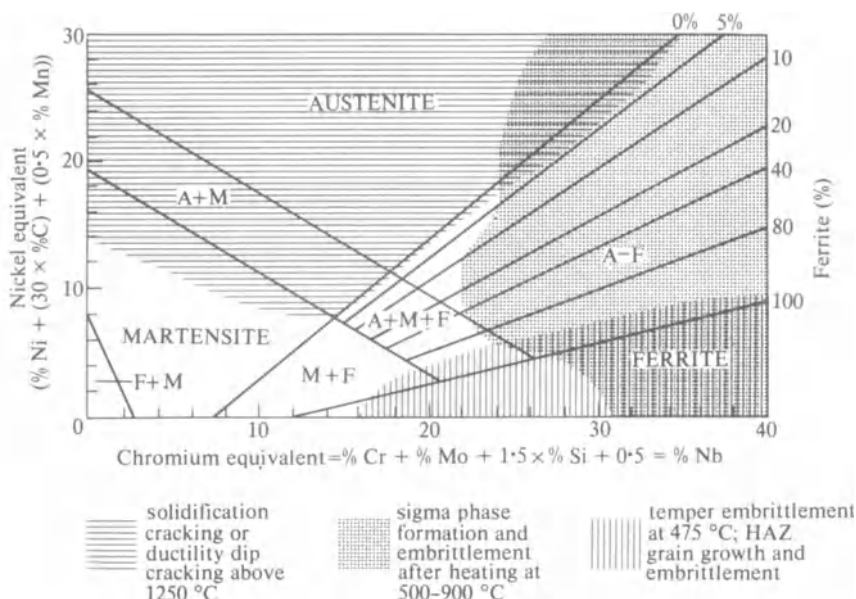


Figure 8.2 Constitution or Schaeffler diagram for Fe–Cr–Ni weld metal showing approximate regions in which typical defects may develop (courtesy Prof. R. L. Apps).

on the constitution of weld metal are summarised in Figure 8.2 which is due to Schaeffler. This diagram has been widely used as a simple means of predicting weld metal constitution. Although the Schaeffler diagram applies specifically to weld metal, the constitution of wrought material follows a similar trend. However, wrought alloys tend to contain less ferrite for any given composition. Actual ferrite content (the control of which is important for the prevention of hot cracking) may be measured by means of a magnetic balance or by a direct reading magnetic gauge.

In austenitic chromium–nickel steels that contain a proportion of ferrite the transformation from ferrite to the brittle sigma phase may occur if the material is held at temperatures between 600 °C and 850 °C for a period of time. The degree of embrittlement is not very serious in the case of 18Cr 10Ni types containing less than 10% ferrite, but higher-ferrite 18Cr 10Ni types and steels containing greater amounts of chromium, for example, 25Cr 20Ni, may suffer a substantial loss of ductility when heated in the sigma-forming temperature range.

8.2.2 Carbide precipitation

Figure 8.3 shows the time–temperature relationship for intergranular precipitation of carbides in austenitic chromium–nickel steels and weld metal as a function of carbon content. Precipitation occurs between 425 °C and 800 °C.

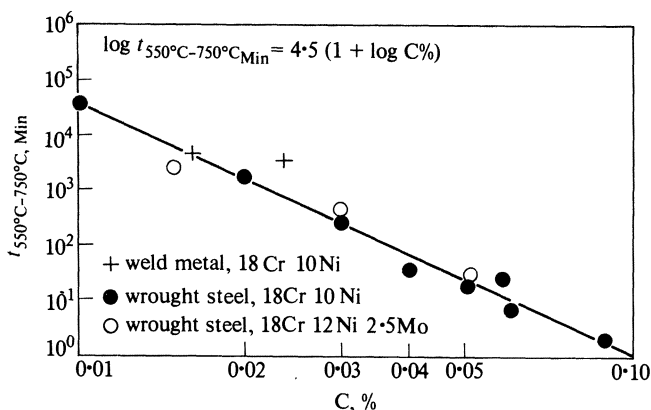


Figure 8.3 Sensitisation time for austenitic chromium–nickel steels as a function of carbon content. t is the time to cool from 750°C to 550°C . (Polgáry, S. 1976. *Metal construction* 8, 445).

Under welding conditions it is most rapid at about 650°C and occurs preferentially at grain boundaries, within the ferrite phase (if present) or along slip planes in cold-worked material. The carbide so formed is normally chromium carbide Cr_{23}C_6 , and it may be redissolved by heating at between 1000°C and 1100°C for a short period. Quenching in water or, for thin sections, rapid cooling in air, will retain carbides in solution (**solution treatment**), provided that the carbon content does not exceed about 0.12%. Note that in ferritic chromium steels this heat treatment cycle results in carbide precipitation; this is because of the lower solubility of carbon in the ferritic alloy.

In fusion welding or brazing 18Cr 10–12Ni austenitic steel there is a region of the heat-affected zone which is heated within the **carbide precipitation temperature range** and in which **intergranular carbide precipitation** will occur. Such precipitation is damaging to the corrosion resistance (see Section 8.3.1) and various means are used to circumvent it. The most common method is to add to the steel either niobium or titanium, both of which have a greater affinity for carbon than chromium, and form carbides which do not go into solution at the normal hot working and annealing temperature of the steel. Thus the percentage of carbon in solution in a niobium- or titanium-bearing steel is normally extremely low and, when it is reheated within the precipitation temperature range, chromium carbide is not precipitated. **Niobium** and **titanium-stabilised** 18/8 steels are resistant to intergranular corrosion in the heat-affected zone of welds except in special circumstances, which will be discussed later.

An alternative method of avoiding carbide precipitation is to reduce the carbon content of the steel to a low level, ideally below 0.03%. Such **extra low carbon (ELC)** steel is not subject to carbide precipitation during welding and is used to an increasing extent.

Electrodes and filler rod for welding stabilised austenitic steels must also be stabilised, since in multi-run welds the weld metal is heated within the precipitation

range by subsequent runs. In coated electrode welding and in other processes where there is metal transfer through the arc, titanium cannot be used as a stabilising element, since too high a proportion is lost by oxidation. Niobium, on the other hand, transfers satisfactorily and is employed to stabilise coated electrodes and wire for metal inert gas and submerged arc welding. The oxidation losses in oxy-acetylene and tungsten inert gas welding are small, and for these processes titanium-stabilised filler wire may be applied. For extra-low-carbon steel either an extra-low carbon or a stabilised electrode is used.

It is possible to remove the damaging effect of intergranular precipitation by heat treatment of the welded joint. Two alternative treatments have been used; either **carbide solution** treatment, which requires heating at between 1000°C and 1100°C for a short period followed by rapid cooling, or a **stabilising anneal**, which consists of heating at $870\text{--}900^{\circ}\text{C}$ for 2 hours. The stabilising heat treatment may complete precipitation, remove microstresses and/or diffuse chromium into depleted regions. There are conflicting reports as to the effectiveness of a stabilising anneal. In either case it is necessary to heat the entire component, since local heat treatment develops a zone of carbide precipitation just outside the heated band. Generally it is more practicable and economic to use stabilised or extra-low-carbon steel rather than apply postwelding heat treatment to an unstabilised steel.

Stabilisation with niobium and titanium is not completely effective under severely corrosive conditions. If a stabilised steel is heated to very high temperature (1100°C and over for Ti-bearing, and 1300°C and over for Nb-bearing steel), some of the titanium or niobium carbide goes into solution. If it is subsequently cooled slowly or held within the carbide precipitation range, a steel so treated will suffer intergranular precipitation of chromium carbide. Now the parent metal close to a fusion weld boundary is heated through the temperature range in which titanium or niobium carbides are dissolved, while subsequent weld runs may heat all or part of the same region in the carbide precipitation range. Hence, there may be a moderate intergranular chromium carbide precipitation close to the weld boundary even in stabilised steels, and this can be damaging if the joint is exposed to attack by (for example) a hot mineral acid. The degree of precipitation, and hence the risk of corrosion, is diminished by reducing the carbon content of the steel.

8.2.3 Solidification cracking in the weld deposit

The factors influencing solidification cracking of welds in austenitic chromium–nickel steels are substantially the same as for other steels, namely, structure and impurity content. Weld metal that solidifies as ferrite is inherently much less susceptible to cracking than that which solidifies as austenite. Mixed structures which contain more than 3% ferrite at room temperature (the corresponding ferrite content on solidification is probably somewhat greater) have in practice adequate resistance to hot cracking, but fully austenitic weld metal is very crack sensitive. 18Cr 10Ni type weld deposits are formulated to contain some

ferrite, but the heat-resisting 25 Cr 20 Ni and 15 Cr 35 Ni weld metals are fully austenitic. Cracking may take the form of **intergranular microfissuring**, which may be detected in microsections or by its effect in reducing ductility and tensile strength. Alternatively, it may appear as **gross intergranular fissures**, which may be found by **penetrant dye inspection** if they extend to the surface.

The combined effects of sulphur and manganese are similar to those on carbon and low-alloy steels; the ratio of manganese to sulphur must exceed a certain value (about 35 in the case of fully austenitic steel) to avoid cracking. However, **free-machining austenitic steels** containing substantial amounts (0.25% to 0.50%) of sulphur may be welded satisfactorily without cracking, the sulphides being present in the form of globules rather than films. Normally sulphur in electrode core wire is restricted to 0.02% maximum, preferably 0.01% bearing in mind that dilution from the parent metal and contamination from the coating may increase the final sulphur content of the deposit.

Phosphorus has a similar effect to sulphur and actively promotes cracking when more than about 0.025% is present in fully austenitic weld metal. The phosphorus content of welding material must be severely restricted if fissuring of fully austenitic welds is to be avoided.

Silicon and carbon affect cracking, but are mainly significant in relation to heat-resisting compositions, which normally contain substantial amounts of both elements. Increasing silicon content promotes cracking, whereas increasing carbon content reduces crack sensitivity. The combined effect of these two elements on a 15 Cr 35 Ni weld deposit with low sulphur and phosphorus contents is illustrated in Figure 8.4. For this and other fully austenitic weld deposits the carbon content should exceed $0.22\sqrt{\text{Si}}$ to keep cracking to acceptable levels. This requirement cannot be met by low carbon deposits, which therefore contain 4–6% Mn and 0.1–0.15% N to improve cracking resistance. High carbon weld metal has low ductility because of the presence of substantial amounts of primary carbide in the structure, while low carbon metal has low ductility because of microfissuring. Hence, there is a carbon:silicon ratio for optimum ductility. Fissuring due to silicon may be a serious problem in welding heat-resistant castings, where silicon is added to promote castability or, in the case of the wrought 15 Cr 35 Ni 2 Si alloy, where the silicon is added to improve scaling resistance. In both cases low silicon welding materials are used and the welding technique adjusted to minimise dilution of weld metal by the parent metal.

Although the addition of carbon is beneficial in reducing the risk of hot cracking in 25 Cr 20 Ni welds, it reduces ductility when added to the parent metal, and may cause further embrittlement in service at elevated temperature due to carbide precipitation.

Niobium is a common addition to 18 Cr 8 Ni type weld metal, generally in amounts of 1% or less. It forms a low-melting intergranular constituent, which is readily visible in microsections. This constituent promotes cracking in fully austenitic structures, but does not appear to be damaging when ferrite is present, as in the normal type of 18 Cr 10 Ni niobium-bearing weld deposit. Zirconium,

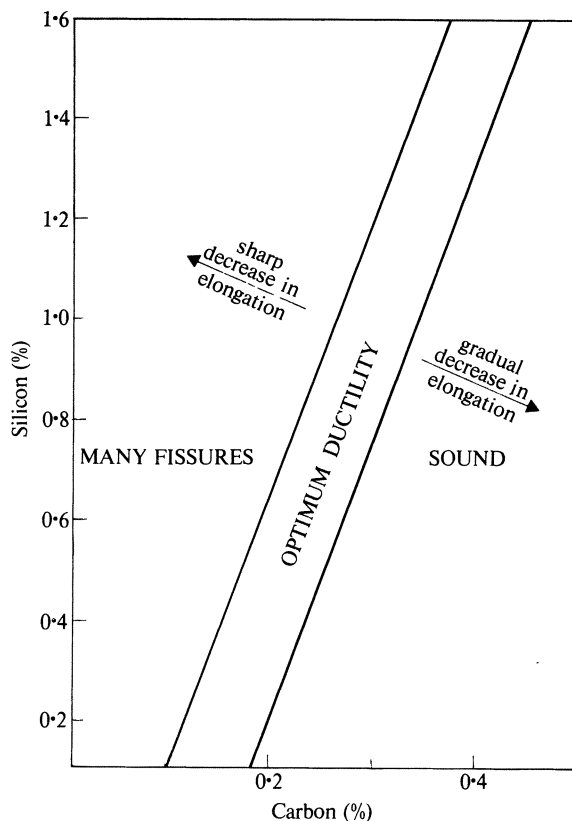


Figure 8.4 Effect of carbon and silicon on microfissuring and ductility of 15 Cr 35 Ni type weld metal. (Rozet, D., H. C. Campbell and R. D. Thomas 1948. *Welding J.* 27, p. 484. Courtesy American Welding Society.)

which is not so frequently added to austenitic steel, has a similar effect. Copper also increases the tendency to solidification cracking. Molybdenum, on the other hand, tends to make the weld deposit more crack-resistant, and the 18 Cr 12 Ni 3 Mo type weld metal is sometimes used for welding difficult materials because of this property.

Ductility dip cracking may occur in fully austenitic weld deposits of the 25 Cr 20 Ni type. Cracking is intergranular and is found in the earlier passes of a multi-pass deposit. The cracks result from the combined effects of tensile residual stress and heating (by subsequent passes) in a low-ductility temperature range. The low ductility in turn is caused by segregation of non-metallics, particularly sulphur and phosphorus at the grain boundaries. Once ductility dip cracking has occurred it will usually propagate through successive passes of weld metal but not necessarily through the capping pass, so that cracks may be subsurface.

8.2.4 Hot cracking in the heat-affected zone during welding

Cracks sometimes appear in the parent metal close to the weld boundary immediately after welding. This type of defect is very much less common than weld metal cracking, and is most troublesome under conditions of severe restraint, or when welding relatively thick sections (over about 18 mm) of certain grades of stainless steel, particularly the fully austenitic 18 Cr 13 Ni 1 Nb type. Cracking is intergranular and frequently starts at the plate surface immediately adjacent to the weld boundary and propagates inwards, either at right angles to the surface or following the weld boundary profile (Fig. 8.5).

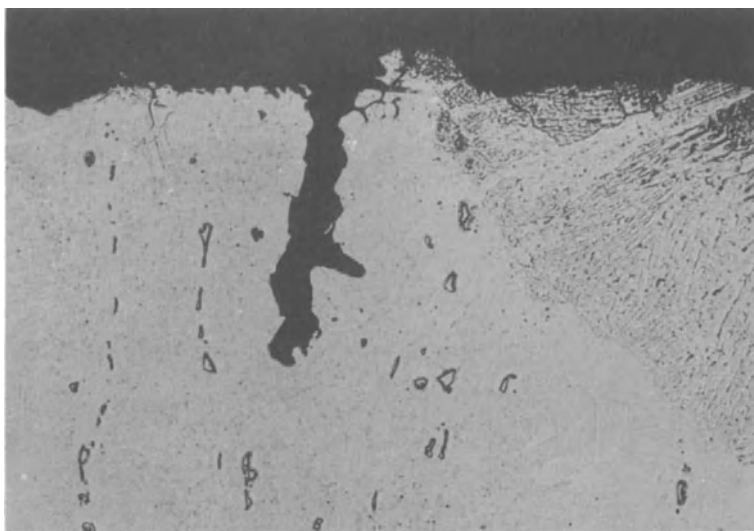


Figure 8.5 Hot cracking in the heat-affected zone of an austenitic chromium-nickel steel weld. This type of crack occurs during welding ($\times 200$). (Photo: Welding Institute.)

Various tests have been used to evaluate the susceptibility of a material to heat-affected zone cracking, notably tests which simulate the welding thermal cycle, and which measure the temperature, either during heating or cooling of the specimen, at which the ductility falls to zero (the **nil-ductility** test). There is a general correlation between the temperature range below the solidus over which ductility is zero or small and the cracking tendency; the greater the nil-ductility range, the greater the tendency to cracking adjacent to the weld. Indications from this type of test are that niobium, zirconium and boron are damaging addition elements.

The mechanism of this type of cracking is not well understood. Cracking starts in high temperature regions, where there is micrographic evidence of the liquation of low-melting constituents, but may propagate through regions of substantially lower temperature, where there is no liquation. Nor can direct

evidence of low-melting constituents be found along the crack boundaries. However, the correlation between nil-ductility range and cracking tendency does suggest that a grain-boundary segregation or liquation mechanism is involved.

8.2.5 Reheat cracking

As well as being susceptible to heat-affected zone cracking during fusion welding, the 18 Cr 13 Ni 1 Nb type steel may also crack adjacent to the weld during post-welding heat treatment or during service at elevated temperature. Generally speaking, such behaviour has been shown by welds in thick material (over 20 mm) and when the service or stress-relieving temperature has exceeded 500 °C. The presence of notches produced by undercutting or other defects close to the weld boundary increases the risk of cracking. Cracks are intergranular and run through the HAZ close to the weld boundary (Fig. 8.6).

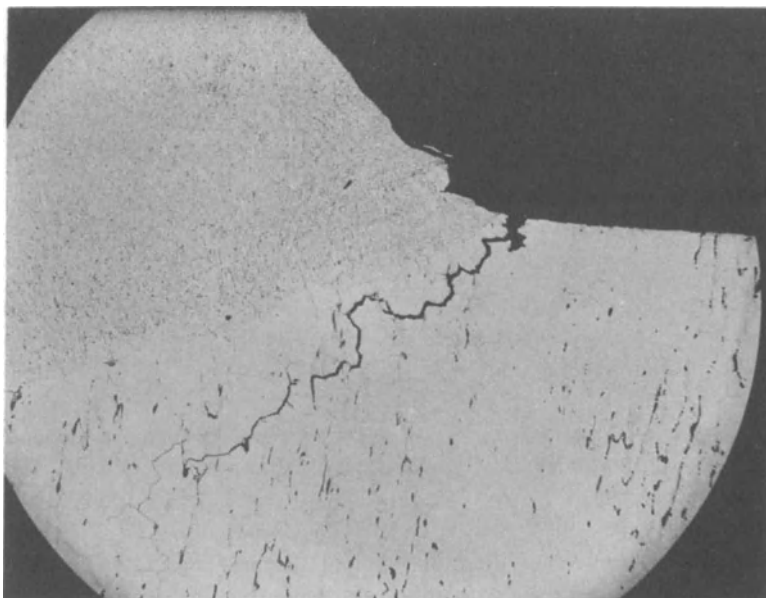


Figure 8.6 Reheat cracking of a niobium-stabilised austenitic stainless steel ($\times 50$; reduced by $\frac{1}{3}$ in reproduction). (Photo.: Welding Institute.)

The mechanism of reheat cracking in austenitic Cr–Ni is similar to that already described for ferritic alloy steel (Section 7.5.6).

Fine carbides precipitate within the grains (**intragranular** precipitation) causing the grain to be harder and more resistant to creep relaxation than the grain boundaries. Thus any relaxation of strain due to welding or to externally applied loads is concentrated in the grain boundary regions and, if the strain so generated exceeds the rupture ductility, cracks may be initiated. Figure 8.6 shows a case where reheat cracking has been initiated by a small hot tear located

at the toe of the weld, and one way of reducing the cracking risk is to grind the toes of all welds prior to heat treatment or service. However, a more effective solution (as with ferritic alloy steels) is to select a non-sensitive alloy.

Of the commonly available 18 Cr 8 Ni type parent materials, the most crack sensitive is the niobium-stabilised grade, followed by titanium-stabilised and unstabilised types. The molybdenum-bearing 18 Cr 10 Ni $2\frac{1}{2}$ Mo grade has little, if any, tendency to crack in the heat-affected zone. The intragranular precipitate does not form in the straight molybdenum-bearing alloy. However, if niobium is present in a molybdenum-bearing steel intragranular precipitation and reheat cracking is possible, the risk increasing with the amount of niobium. Therefore, when molybdenum-bearing steels are used for duties where reheat cracking is possible, the niobium and titanium contents of the alloy should be controlled.

8.3 Corrosion

The corrosion problems specifically associated with welded joints in austenitic chromium–nickel steel are discussed below.

8.3.1 Intergranular corrosion

If an unstabilised 18 Cr 10 Ni type steel containing about 0.1% carbon or more is brazed or welded, and is then exposed to certain corrosive solutions, intergranular (IG) corrosion will occur in the zone of carbide precipitation, which runs parallel to the weld (Fig. 8.7). The severity of this type of attack, which is known as **weld decay**, increases with the carbon content and with the corrosivity of the environment. Steels containing 0.08% carbon and less may suffer weld decay attack in thick sections, but not when the thickness is 3 mm or less. Steels containing 0.03% carbon and less and those stabilised by the addition of titanium or niobium are immune from weld decay in all thicknesses. The time–temperature relationships for sensitisation of various grades of austenitic Cr–Ni steel are shown in Figure 8.8.

The susceptibility of a steel to intergranular corrosion after welding is commonly tested by heating a sample at 650 °C for half an hour, and then immersing it in a standard test solution such as one of those listed in Table 8.1 for the specified period. The most commonly used tests are the copper sulphate/sulphuric acid and the boiling 65% nitric acid tests. For detailed procedures the relevant ASTM or British Standard should be consulted. Tests may also be made in solutions representing the process fluid to which the welds will be exposed.

The addition of titanium in amounts exceeding four times the carbon content, or niobium in amounts exceeding ten times the carbon content, inhibits carbide precipitation in the normal weld decay zone but does permit some intergranular precipitation close to the fusion zone (see Section 8.2.2). Subsequent exposure to hot strong mineral acids may result in corrosion along a narrow zone adjacent to the weld boundary (Fig. 8.9). Such corrosion is known as **knife-line**

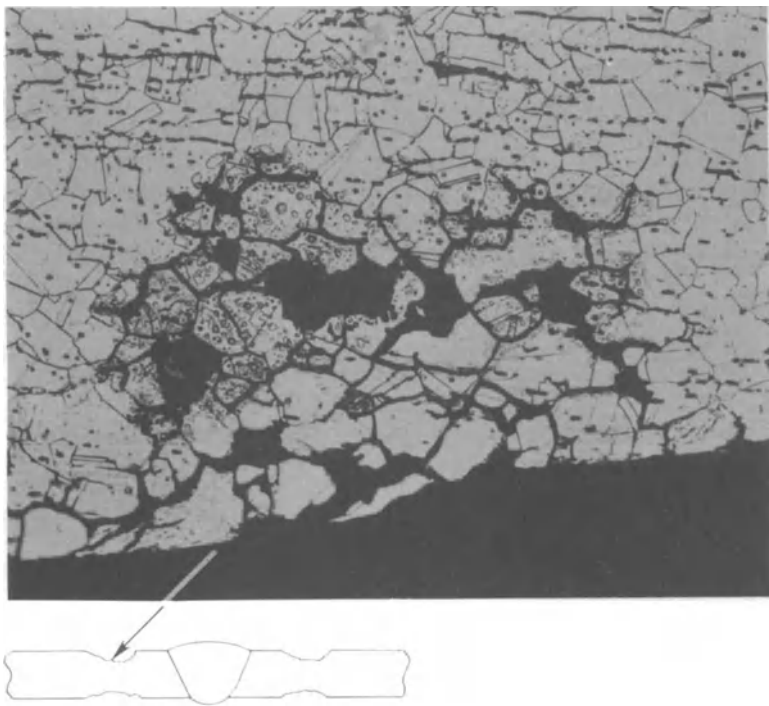


Figure 8.7 Intergranular corrosion in the heat-affected zone of a weld in unstabilised austenitic chromium–nickel steel. (Photo.: Samuel Fox & Co. Ltd.)

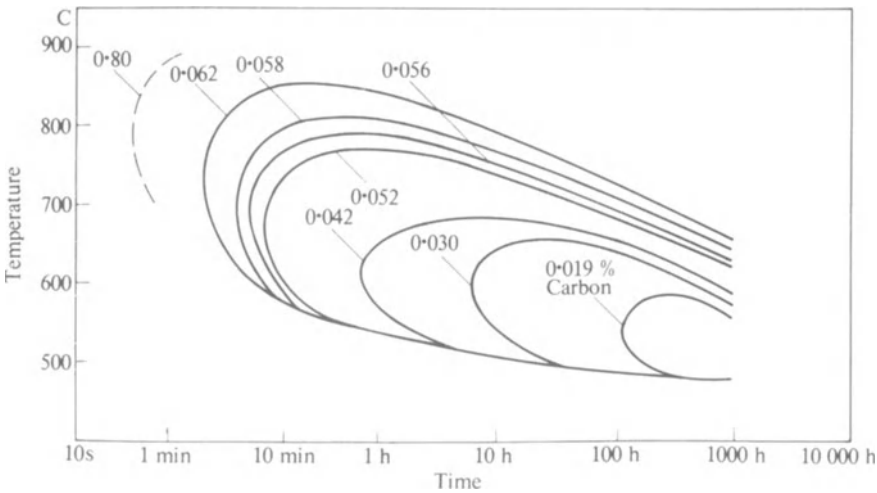
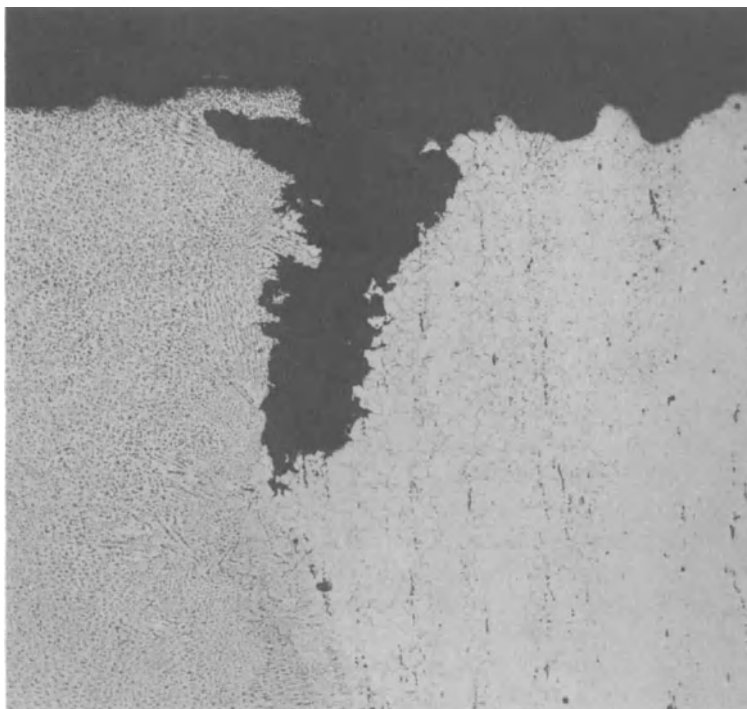


Figure 8.8 Effect of carbon on carbide precipitation. The time required for formation of harmful amounts of chromium carbide in stainless steels with various carbon contents (AISI SS607-477-20M-HP *The role of stainless steel in petroleum refining*).

Table 8.1 Standard intergranular corrosion tests for stainless steels

<i>ASTM standard</i>	<i>Test media</i>	<i>Common test names</i>
A 393-63	boiling 5·7% CuSO ₄ + 15·7% H ₂ SO ₄	Strauss, Hatfield, Krupp
A 262-70, Practice A	10% oxalic acid, electrolytic at ambient temperature	Streicher
A 262-70, Practice B	boiling 50% H ₂ SO ₄ + Fe ₂ (SO ₄) ₃	Streicher
A 262-70, Practice C	boiling 65% HNO ₃	Huey
A 262-70, Practice D	10% HNO ₃ + 3% HF at 70 C	Warren
A 262-70, Practice E	same as A 393 but with specimen in contact with copper metal	Accelerated Strauss

**Figure 8.9** Intergranular corrosion close to fusion zone of a weld in austenitic stainless steel: knife-line attack ($\times 50$). (Photo.: Welding Institute.)

attack. For any given carbon content niobium-stabilised steel is more resistant to knife-line attack than the titanium-stabilised type because of the higher solution temperature of niobium carbide. The risk of this type of corrosion may be greatly minimised by limiting the carbon content of the titanium-stabilised steel to a maximum of 0·06%. Steels containing less than 0·03% C are not subject to knife-line attack.

The molybdenum-bearing grade with 0.08% carbon maximum suffers weld decay only under severe conditions, for example, when immersed in hot acetic acid containing chlorides. For such environments the extra-low-carbon variety is used, or niobium or titanium is added in amounts sufficient to stabilise the carbon.

There are several theories concerning the mechanism of intergranular attack. The most widely held view is that the precipitation of chromium carbide at the grain boundary depletes the adjacent region of chromium, and this region then becomes anodic to the bulk of the metal and is preferentially attacked in corrosive media. Alternatively, it has been suggested that the precipitate is coherent, and that the coherency strains which are set up make the grain boundary region anodic and sensitive to preferential attack. Yet another theory is that the carbides are more noble than the surrounding matrix and cause galvanic corrosion of the intergranular regions. There is indeed some evidence that carbides are more noble than the base alloy, but in general it is not possible to find evidence that indicates positively which theory is most likely to be correct.

There are many non-corrosive or mildly corrosive conditions under which stabilisation of austenitic stainless steel is not necessary – for example, in subzero temperature and decorative applications – and where for cost reasons unstabilised material is preferred. Such steels may have carbon contents up to 0.15%, but in practice are best limited to 0.08% maximum. Electrode and filler rod should in any event produce a weld deposit containing not more than 0.08% carbon.

8.3.2 Stress corrosion cracking

When austenitic chromium–nickel steels are stressed in a corrosive environment containing chlorides, **stress-corrosion cracking (SCC)** may occur. Such cracking is typically transgranular and branched (Fig. 8.10). Penetration may occur in a few seconds when sheet metal is exposed to hot concentrated chlorides, but at lower temperatures and lower chloride concentrations penetration may take many hours. Increased nickel content slightly improves the resistance of a steel to this type of attack, while at the opposite extreme ferritic or substantially ferritic chromium steels are not susceptible to stress corrosion. (While ferritic chromium steels do not suffer stress corrosion cracking by chlorides, they may be so affected by wet hydrogen sulphide.) The **threshold stress** below which this attack will take place is not well defined and must be assumed to be low; the residual stress developed by welding even thin sheet is sufficient to cause cracking if the corrosive environment is severe. Chloride SCC is usually caused either by accidental contamination of process streams by a chloride-containing aqueous solution, or by contamination of the metal surface by chlorides during manufacture or transport, followed by exposure to elevated temperature. The most severe condition is that in which the chloride-containing water is allowed to concentrate in contact with the metal surface. The design of stainless steel equipment must be such as to avoid pockets or crevices where concentration

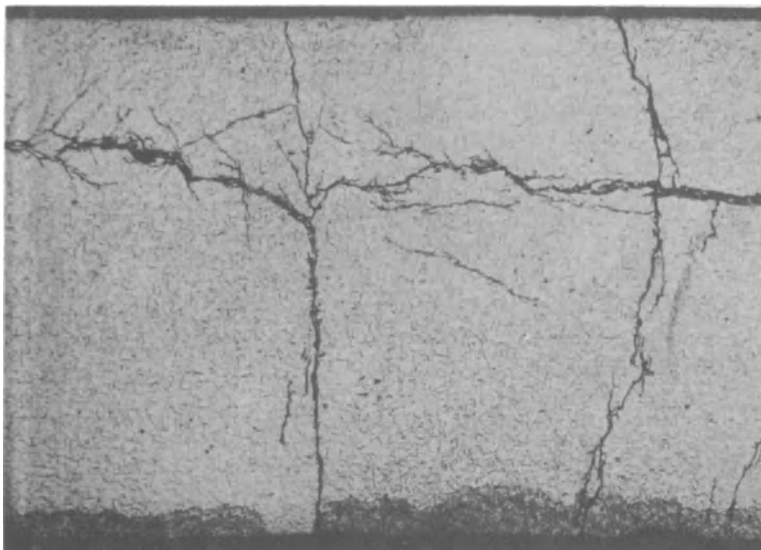


Figure 8.10 Stress corrosion cracking in an austenitic stainless steel close to the weld ($\times 100$; reduced by $\frac{1}{3}$ in reproduction). (Photo.: Welding Institute.)

can take place, and in manufacture, transport and storage, precautions must be taken against accidental contamination, for example, by sea water.

Intergranular penetration and cracking of austenitic Cr–Ni steels may result from contamination of the surface by low-melting alloys followed by exposure at elevated temperature. Zinc from galvanised steel may cause such cracking in welds between stainless and galvanised steel. Spelter (60 Cu 40 Zn) will penetrate austenitic Cr–Ni steel at elevated temperature so that brazing is carried out with low-melting silver brazing alloys. Generally speaking, it is advisable to avoid any contamination of austenitic stainless steel (e.g. by paint) if it is to be exposed to temperatures above, say, 400°C .

Stress relief of welds at $900\text{--}1000^{\circ}\text{C}$ is sometimes employed as a means of avoiding SCC in piping. Where this is done a stabilised or ELC steel must be used, the joint must be adequately supported to avoid hot cracking, and (in the case of local PWHT) temperature gradients must be low enough to prevent the formation of residual stress at the edge of the heated zone. Lower PWHT temperatures are sometimes used but in so doing the danger of sigma phase formation and/or carbide precipitation at temperatures below 750°C must be considered.

8.3.3 Preferential corrosion of welds

Under conditions of active corrosion a weld deposit will usually corrode more rapidly than an austenitic stainless wrought steel of the same composition. **Preferential attack** of this type may be prevented by improving the corrosion

resistance of the welding filler rod or electrode. For example, in the case of molybdenum-bearing stainless steel the corrosion resistance to environments other than strong nitric acid increases with increasing molybdenum content, so that preferential corrosion of welds in this steel may be avoided by welding with an electrode having higher molybdenum content than the parent metal.

Preferential attack on the ferrite present in austenitic Cr–Ni steel welds may occur in strong mineral acids and in strongly reducing media such as ammonium carbamate. Carbamate is an intermediate product in the manufacture of urea, and it is common practice to specify a maximum ferrite content of 2% for welds in the 316L material used for such plant. To obtain crack-free deposits in low-ferrite 316L alloy requires special electrode formulation and very low sulphur and phosphorus contents.

8.4 CORROSION-RESISTANT STEELS: ALLOYS AND WELDING PROCEDURES

The more common grades of corrosion-resistant austenitic Cr–Ni steels are listed in Table 8.2. The AISI designations used here are internationally accepted, and the group of steels shown are known as the **300 Series**.

Table 8.2 Corrosion-resistant austenitic Cr–Ni steels

<i>AISI No.</i>	<i>Composition %</i>						
	<i>C max.</i>	<i>Cr</i>	<i>Ni</i>	<i>Mo</i>	<i>Ti</i>	<i>Nb</i>	<i>Electrode type*</i>
304	0.08	18/20	8/11	—	—	—	E308
304L	0.035	18/20	8/13	—	—	—	E308L
304H	0.04/0.10	18/20	8/11	—	—	—	E308
316	0.08	16/18	11/14	2/3	—	—	E316 or E16-8-2†
316L	0.035	16/18	10/15	2/3	—	—	E316L
316H	0.04/0.10	16/38	11/14	2/3	—	—	E316
321	0.08	17/20	9/13	—	5 × C 0.07	—	E347
347	0.08	17/20	9/13	—	—	10 × C 0.10	E347
309	0.15	22/24	12/15	—	—	—	E309
310	0.15	24/26	19/22	—	—	—	E310

* To AWS A5.4-69.

† For high-temperature creep-resisting applications.

Type 304 is normally specified in US practice for mildly corrosive conditions such as weak organic or inorganic acids, and it is welded with a matching filler, E308. Some carbide precipitation occurs in the HAZ but intergranular corrosion will not take place except in the case of thick plate (where the HAZ is reheated by successive weld runs) and/or strong corrodents. It is not easy to determine the breakpoint between IG corrosion and no IG corrosion, however, and in

European practice it is more common to specify stabilised steel, usually type 321, for all corrosive duties except those requiring more highly alloyed steel. Type 347 steel may be required for the containment of strong mineral acids where type 321 might be subject to knife-line attack. An alternative solution to such problems is to use 304L welded with 304L filler. Joints so made are not subject to any form of intergranular corrosion, and the absence of niobium decreases the risk of liquation cracking. A potential disadvantage of ELC steels is that carbon may be picked up during steel fabrication: for example, if tube is annealed without thorough removal of drawing compounds it may be internally carburised. Check-analysis of weldments may be desirable for critical applications. A second disadvantage is that ELC grades have low tensile strength, particularly at elevated temperature. Where a positive assurance of elevated temperature properties is required (generally for temperatures over 400 °C) the H grade, which has a specified minimum carbon content, may be used.

The addition of molybdenum improves the corrosion resistance of austenitic Cr–Ni steel to almost all media except strong nitric acid. It also diminishes the risk of reheat cracking and, for any given ferrite content, makes weld metal more resistant to solidification cracking. The normal 316 grade (usually produced with about 0.06% C) is resistant to IG corrosion, except in the more aggressive solutions such as the boiling mixtures of acetic acid and salt that are encountered in the food industry. In such cases, the ELC grade is employed. It is possible to stabilise 316 steel using titanium or niobium but the corrosion resistance may be reduced by the presence of titanium or niobium compounds. One of the more critical applications for type 316L steel is in the carbamate circuit of urea plants, as noted earlier. The parent metal is normally resistant to carbamate, but if shielded from oxygen by deposits of foreign matter the steel may corrode rapidly. Weld metal is less resistant and ferrite is preferentially attacked, so that the ferrite content is limited to say 2%. At this level 316L weld metal is resistant to solidification cracking. 316L may also be marginally more resistant to chloride SSC than 304 because of a higher resistance to chloride pitting corrosion.

Type 316H steel may be specified for heavy sections (say over 25 mm) as a precaution against reheat cracking. Type 316 was used successfully for the main steam lines in supercritical power boilers, the welds being made with 16 Cr 8 Ni 2 Mo coated electrodes.

Austenitic Cr–Ni steels may be welded by all welding processes except some specialised types such as thermit welding. Preheat and PWHT are not normally required. Indeed, preheat may promote solidification cracking, and for the same reason it is advisable to keep the interpass temperature below 200 °C. SMA electrodes are usually basic-coated but lime–titania coatings are also used, and give a more uniform weld profile.

8.5 WELD OVERLAY CLADDING AND DISSIMILAR METAL JOINTS

Weld overlays are used to provide a corrosion-resistant cladding to a carbon or ferritic-alloy steel in those cases where the section thickness is too great for

roll-bonding to be reliable, and where the geometry is not favourable to explosive bonding. Overlays may be applied manually by SMAW or automatically by SAW, using single, multiple or strip electrodes. A major problem with SAW is that of dilution, and for this reason most cladding is done in two passes. For an 18 Cr 10 Ni type deposit the first layer is made with type 309 (23 Cr 12 Ni) alloy and the second layer with the required alloy composition. The welding parameters are carefully controlled to avoid excessive or non-uniform penetration and dilution, and to minimise the risk of solidification cracking by control of composition and of the wetting angle of the deposit. Dilution may also be controlled by welding on to a strip of the alloy material placed in contact with the backing material, and if this is properly controlled it may be possible to clad in a single run.

Type 309 or 310 welding consumables may also be used for joints between austenitic and ferritic steels. A thin layer of martensite forms at the fusion boundary on the ferritic steel side, but this does not have any significant effect on the joint properties. However, if the joint is postweld heat-treated, carbon may migrate from the ferritic side into the weld metal, causing embrittlement. In such cases joints should be made using nickel-base alloys, which are resistant to carbon migration (see Section 9.4.4). Dissimilar metal joints are normally made using coated electrodes, so that dilution (particularly of austenitic filler metal by ferritic steel) is minimised. However, in welding stainless-clad carbon steel from the carbon steel side some dilution is inevitable. One solution to this problem is to make the root pass using type 309 or 310 filler, and complete the joint using a nickel-base electrode. Alternatively, it may be filled using a basic-coated low Cr–Mo alloy electrode, having determined by procedure testing that the weld metal is sufficiently ductile.

8.6 HEAT-RESISTING STEELS: ALLOYS AND WELDING PROCEDURES

Table 8.3 lists a selection of alloys used for creep and oxidation resistance at temperatures up to 1000 °C. In addition, type 316 steel (Table 8.2) has been used for creep-resistant duties in the 400–600 °C temperature range. At higher temperatures type 316 may, under stagnant conditions, be subject to rapid oxidation (**catastrophic oxidation**), and the 25 Cr and 20 Ni steel is more

Table 8.3 Heat-resistant austenitic Cr–Ni alloys

Designation	Chemical composition %							Remarks
	C	Cr	Ni	Al	Ti	Nb	Other	
HK40	0.35/0.45	23/27	19/22	—	—	—	—	Centrifugally cast
HU50	0.40/0.60	17/21	37/41	—	—	—	—	Centrifugally cast
Incoloy 800H	0.05/0.10	21	32.5	0.4	0.4	—	—	Extruded
Incoloy 802	0.4	21	32.5	0.6	0.8	—	—	Extruded
24 24 1½	0.3	24	24	—	—	1.5	—	Centrifugally cast
50/50 Nb	0.05	48.5	50	—	—	1.5	—	Centrifugally cast

generally useful. Type 310 steel has relatively low strength and is mainly employed for tubing or for sheet-metal liners inside piping or vessels that are internally insulated. For high temperature applications (800–1000 °C) and especially where there is a significant operating stress, the higher carbon grades such as HK40 are employed. These steels are welded with matching electrodes by SMA, GMA or automatic GTA welding. HK40 weld deposits made with basic-coated electrodes have about half the rupture strength of the parent metal and welds made by this process may suffer creep cracking in service. GMA and GTA deposits are much closer to the parent metal in creep strength, and SMA deposits may be improved by using high-purity material in combination with a lime–titania coating.

Centrifugally cast HK40 is widely used for tubes in steam/methane reformer furnaces and ethylene pyrolysis furnaces, for which it is the most economic material. Incoloy 800 is used in similar furnaces where greater ductility is required: matching electrodes cannot be used because of their susceptibility to solidification cracking, and nickel-base alloys are employed. Some of these alloys have a rupture strength equal to that of the parent material. Incoloy 802 is an extruded high-carbon Incoloy 800, and has a better resistance to carburisation (which is a problem in ethylene furnaces) than HK40. The 802 alloy and the 24 Cr 24 Ni $1\frac{1}{2}$ Nb alloy are more costly than HK40 and their use is correspondingly limited. The 24 Cr 24 Ni $1\frac{1}{2}$ Nb alloy has improved rupture ductility, and welds with matching electrodes have a rupture strength equal to that of the parent metal. The 50 Cr 50 Ni $1\frac{1}{2}$ Nb alloy is used for resistance to fuel-ash corrosion (elevated temperature attack by deposits containing sodium and vanadium). It is welded by the GTA and SMA processes using matching electrodes. The higher-carbon heat-resistant alloys do not have much ductility at room temperature and in making procedure tests the bend test is omitted.

8.7 HARDENABLE HIGH-ALLOY STEELS

The hardenable stainless steels, which are used for rocket parts and for corrosion-resistant pumps and other machinery, may be divided into three groups:

- (a) single-treatment martensitic age-hardening (17–4 PH);
- (b) double-treatment austenitic/martensitic age-hardening (17–7 PH and FV 520);
- (c) austenitic age-hardening.

The metallurgy of steels in group (a) is similar to that of 18% Ni maraging steels (see Section 7.6.2.4), and in particular the properties of welded joints may be largely restored by ageing after welding. The 17–4 PH type, which contains 17 Cr 4 Ni 4 Cu and 0.3 Nb, may however suffer cracking along the weld boundary during hardening when the restraint is severe, and under such conditions it is best to weld in the over-aged condition and fully heat treat

after welding. 17–4 PH castings are hot-short (i.e. brittle at elevated temperature), and crack in the heat-affected zone if the copper content is too high; a maximum of 3% copper is necessary for welding.

The second group of steels are substantially austenitic after solution treatment at 1050 °C and cooling to room temperature. A small amount of delta ferrite is normally present and sometimes some martensite, but the ductility is high so that normal forming and pressing operations are possible. Subsequent heating *conditions* the austenitic matrix, so that on cooling and holding at ambient or subzero temperature it transforms to martensite. There are two generally used transformation treatments: the first is to heat at 750 °C for 90 minutes, air cool to 20 °C and hold for 30 minutes; the second requires similar heating at 750 °C or alternatively short-time heating at 950 °C, followed by cooling to –75 °C and holding for 8 hours to complete the martensite transformation. Ageing occurs in the temperature range 500–570 °C. Of this group, the 17–7 PH type of steel (17 Cr, 7 Ni, 1.2 Al) is usually welded in sheet form using the d.c. tungsten inert gas process. It is not subject to cracking either in the weld or heat-affected zone. Various combinations of welding with heat treatment are possible, but, in order to obtain 95–100% joint efficiency, it is necessary to weld with the parent material in the solution-treated condition, and subsequently carry out one of the two transformation and ageing treatments.

Type 17–10 P is a fully austenitic chromium–nickel steel containing phosphorus, and hardens to a moderate degree due to carbide and phosphide precipitation when heated at 700 °C. This alloy is used where a combination of non-magnetic properties and hardenability is required. High-phosphorus austenitic steel is extremely hot-short, so that fusion welding with a matching filler alloy is impossible. Crack-free weld metal may be obtained by using coated electrodes giving a 29 Cr 9 Ni deposit. Such deposits are partially ferritic and are not hardenable, and the full mechanical properties are not obtainable in welded joints. Moreover, hot cracking may occur in the heat-affected zone, so that fusion welding of this alloy is difficult. Flash butt welding on the other hand gives satisfactory joints.

None of the hardenable high-alloy steels discussed in this section requires any preheat before welding.

FURTHER READING

American Welding Society 1972. *Welding handbook*, 6th edn. Section 4: *Metals and their weldability*. Miami: AWS; London: Macmillan.

9 Non-ferrous metals

9.1 ALUMINIUM AND ITS ALLOYS

9.1.1 Processes and materials

Aluminium and aluminium alloys may be joined by arc-fusion welding, resistance welding, solid-phase welding, brazing and adhesive bonding. Low-melting aluminium–zinc solders have also been used to a limited extent. Fusion welding was first accomplished by the oxy-acetylene process but is now carried out by means of GTA and GMA welding and sometimes using coated electrodes. The power source for GTA welding is usually an a.c. transformer with high frequency re-ignition. When the electrode is positive a non-thermionic cathode (see Section 3.5.2.1) forms on the aluminium surface; the cathode spot wanders over the weld pool surrounding plate surface and removes most of the oxide. With d.c. electrode-positive most of the arc heat is absorbed by the tungsten electrode, and at normal welding currents this melts and is difficult to manage. With a.c. welding, a compromise is possible; during the electrode-positive half-cycle the oxide film is removed while during the electrode-negative half-cycle the workpiece is heated. However, d.c. electrode-positive may be used for special purposes. Welds may also be made with d.c. electrode-negative using helium as the shielding gas, but this too is for special applications. In general GTA welding is applicable to lighter sections than GMA welding.

The GMA process is operated with d.c. electrode-positive, and the cathode has the same effect of cleaning up the surface as with GTAW. At medium current levels the weld pool is roughly semicircular in cross section, but as the current increases, a finger-shaped projection develops in the centre of the fusion bead (as illustrated in Table 2.2 against gas-shielded arc welding, high current). This finger-shaped penetration is undesirable in that it is intolerant to misalignment between the electrode and the centreline of the joint, and is thus more subject to lack of fusion along the centreline. This problem may be avoided by using helium or a helium–argon mixture as the shielding gas. With helium shielding the pool cross section remains semicircular at high currents.

Fusion welding is used mainly for pure aluminium, the **non-heat-treatable** Al–Mn and Al–Mg alloys, and the Al–Mg–Si and Al–Zn–Mg **heat treatable** alloys. The higher-strength aluminium alloys of the Al–Cu–Mg and duralumin types, which are specified mainly for aircraft structures, are difficult to fusion weld effectively. Such alloys are normally joined by riveting, although a few

fabricators employ spot welding as a joining method, and fusion welding is applied to space vehicle applications in certain cases.

Resistance spot welding is employed for joining sheet aluminium, for example in the automobile industry. Aluminium is, however, an intrinsically difficult material to spot weld. The presence of a refractory oxide film on the metal surface may cause uncontrolled variations in the surface resistance, and standardised cleaning methods are required. The electrical and thermal conductivities are high, so that high current welding transformers are required. The volume changes on solidification and cooling require careful and rapid control of electrode loading. Low-inertia heads are also needed for projection welding because of the low elevated-temperature strength of the metal. Metal pick-up results in a relatively short electrode life. However, in spite of these disadvantages (as compared, say, with mild steel) spot welding has been used for a number of years as a means of joining sheet metal. Any of the aluminium alloys may be so joined, including the heat-treatable Al–Cu alloys that are very difficult to arc fusion weld.

Cold pressure welding is used in joining aluminium for certain special applications, notably cable sheathing. Most of the more recently developed methods such as ultrasonic welding, friction welding, explosive welding and electron beam welding may be applied to aluminium and its alloys. Flash butt welding is used for special applications.

For certain applications of complex form (for example, automotive radiators and core-type plate heat exchangers) brazing is used for joining aluminium. Aluminium–silicon alloys may be employed as the brazing filler alloy and in some cases it is convenient to use sheet aluminium clad with the brazing alloy, the whole assembly being dipped in a bath of molten flux to make numerous joints simultaneously. Fluxes are normally corrosive and special procedures may be necessary for their removal. Potassium fluoroaluminate based fluxes are, however, relatively non-corrosive.

9.1.2 Porosity

Porosity in aluminium fusion welds is due almost entirely to rejection of hydrogen. The sensitivity of aluminium to hydrogen porosity is associated with two factors: first, the high ratio between the volume of hydrogen which can be absorbed in the weld and the solubility of this gas in the region of the melting point; and secondly, the presence of hydrogen in the arc gases. Gas reactions other than hydrogen rejection do not occur in the weld pool because of the high affinity of aluminium for oxygen and nitrogen; thus aluminium is self-deoxidising.

Fusion-welding processes develop porosity in aluminium to a varying degree; it is most severe with SMA welding and least with GTA welding. The joint design and welding position also affect the degree of porosity. In general the more difficult the welding position, the greater the risk of gas entrapment; overhead or horizontal vertical joints are particularly subject to this defect. Porosity appears most frequently or severely at the start of a weld run.

There are many potential sources of hydrogen in aluminium welding. The first is the oxide film, which is to some degree hydrated, and on which an adsorbed film of moisture is invariably present when the metal is exposed to the atmosphere. In GTA welding evaporation of the oxide also evaporates any adsorbed or combined moisture which may be present, thus providing a mild source of contamination of the arc column. The effect of surface is more serious in GMA welding, where a fine wire with high surface-to-volume ratio is fed continuously into the arc; for instance, lubricant residues on cold drawn wire are a source of hydrogen. Cleanliness of the wire is therefore of first importance in the GMA process. Coated electrodes contain moisture in the coating, and under some conditions corrosion of the core wire underneath the coating may occur. The degree of contamination and, correspondingly, the weld porosity may be minimised by using electrodes as soon as possible after manufacture, by storing in a dry place, and by drying before welding. Regardless of the welding process, the material to be welded must be clean and dry. So also must be the welding equipment; condensation in gas leads, torch or welding gun of inert gas processes may cause severe porosity. Porosity in the form of large discontinuous cavities or long continuous holes may occur due to the use of excessive currents in GMA welding with projected transfer. This defect (**tunnelling**) is due to excessive current causing turbulence in the weld pool. It may be overcome by limiting the current per pass, by using a gravitational transfer technique or by improving the inert gas shielding.

The main effect of porosity is to reduce the strength of the weld metal, and in designing welded aluminium structures or pressure vessels a joint efficiency factor corresponding to the anticipated weld quality must be used. In the case of fully radiographed shop fabricated work it is practicable to set up a radiographic standard for porosity corresponding to a joint efficiency of 95%.

Radiographically sound welds can be made in aluminium alloys by means of the inert-gas shielded processes, provided that adequate attention is paid to cleanliness of plate and welding materials, and that the work is done in a fabrication shop. In *site welds* some degree of porosity is to be expected because the necessary precautions are difficult to implement fully. Sound positional welds may, however, be made in piping where a backing bar is used.

9.1.3 Cracking

Aluminium alloys may be subject to solidification or liquation cracking, and may suffer embrittlement and cracking at temperatures below the solidus. The higher-strength alloys may also fail by stress corrosion cracking.

The solidification cracking of aluminium and its alloys is associated in the main with intentionally added alloying elements rather than, as in the case of steel, with the presence of low-melting impurities.

The cracking of aluminium welds has been shown to follow the same pattern in its relation to alloy constitution as the cracking of castings and crack sensitivity relationships for castings may be taken as being applicable also to weld metal.

The relationship between composition and the hot cracking of restrained castings in binary aluminium–silicon alloys is shown in Figure 9.1 and the corresponding section of the aluminium–silicon phase diagram in Figure 9.2. The degree of cracking rises to a maximum at about 0.5% silicon and then decreases rapidly as the alloy content is increased.

The cracking curve follows the same trend as the solidification temperature range under equilibrium conditions, but is displaced to the left. Under continuous cooling conditions the constitution diagram is also displaced to the left,

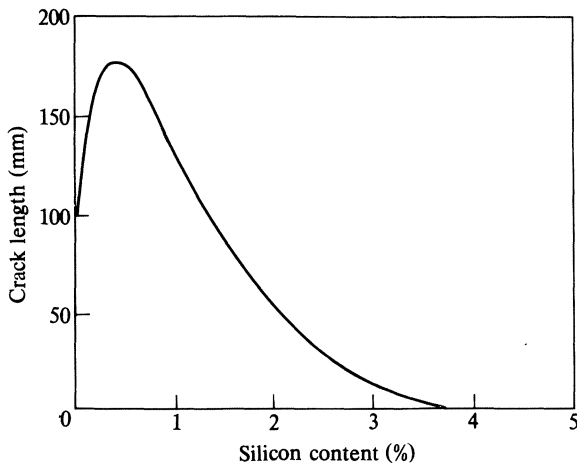


Figure 9.1 Length of cracking in restrained castings of binary aluminium–silicon alloys as a function of silicon content.

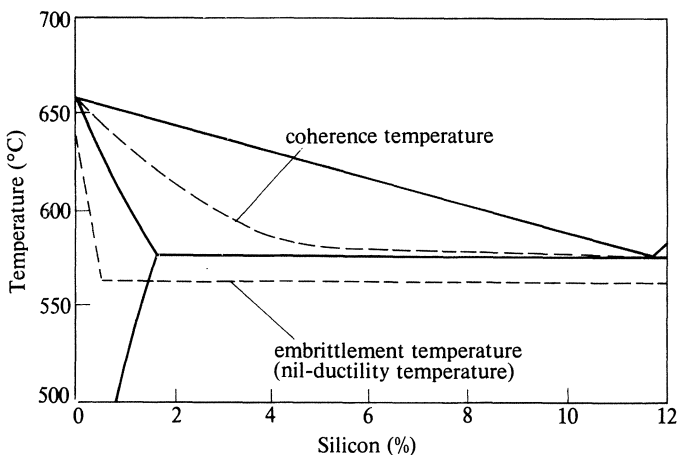


Figure 9.2 Equilibrium diagram for aluminium–silicon alloys (solid lines) showing also coherence and nil-ductility temperatures on cooling (dotted lines). Lower dotted line represents supposed solidus under cooling conditions.

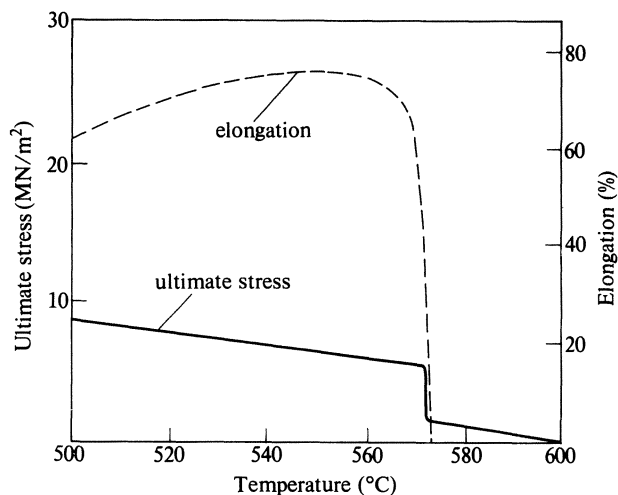


Figure 9.3 Mechanical properties of aluminium–1% silicon alloy on heating to temperatures close to the solidus. (From Pumphrey, W. I. and P. H. Jennings 1948–9. *J. Inst. Metals* 75, 203–33.)

as shown by the dotted line in Figure 9.2, and the alloy content for maximum cracking is close to that for maximum freezing range in the modified diagram. Mechanical tests of cast aluminium–silicon alloys in the region of the melting point yield the type of result shown in Figures 9.3 and 9.4. On cooling from the liquidus, the crack-sensitive 1% silicon alloy acquires mechanical strength before it has any ductility, and there is a considerable temperature range over which it is very brittle. The 12% silicon alloy, on the other hand, is not crack sensitive, and correspondingly has a very narrow brittle temperature range, as would indeed be expected from an alloy close to the eutectic composition. Pure aluminium also has a low crack susceptibility and narrow brittle range, but is much more sensitive to contamination than is the eutectic composition (see Figure 9.1). The mechanism of this type of hot cracking in welds has already been discussed generally in Section 4.1.4.1. In a long-freezing-range alloy which is cooling from the liquidus, the growing crystals are at first completely separated by liquid and the alloy has no strength. As the temperature level falls the volume of solid increases relative to that of the liquid, and at some point (the coherence temperature) the growing crystals meet and cohere. However, a limited volume of liquid still remains and persists down to the eutectic temperature, causing the metal to be brittle. At the same time, the solid portion contracts, and is therefore subject to a tensile stress which may be high enough (depending on the degree of restraint) to cause failure of the weak, brittle matrix. The risk of cracking is greatest when a critically small volume of liquid metal is present below the coherence temperature. If the volume of eutectic present is relatively large, incipient cracks are healed by liquid that flows in from the weld pool.

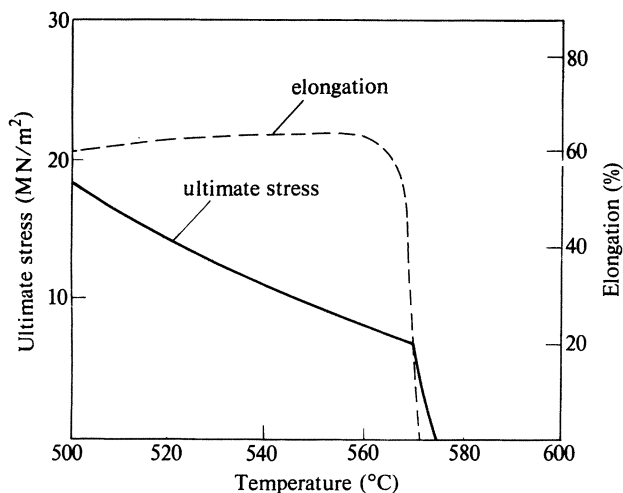


Figure 9.4 Mechanical properties of aluminium–12% silicon alloy on heating to temperatures close to the solidus. (From Pumphrey, W. I. and P. H. Jennings 1948–9. *J. Inst. Metals* 75, 203–33.)

Such healed cracks may sometimes be seen in macrosections of aluminium welds.

Solidification cracking is most severe with weld metal of the 3/4 Mg 1 Si (Mg_2Si) type of composition and the fusion welding of this alloy with matching filler metal is only practicable under conditions of very low restraint. The higher-strength heat-treatable alloys are also prone to solidification cracking with the exception of Al–Zn–Mg types, which are only slightly susceptible. Crack-sensitive alloys are usually welded with a filler metal, such as 5 Mg, 5 Si or 12 Si, that brings the weld metal composition out of the cracking range. In so doing, allowance must be made for dilution of the weld metal by parent metal (see Section 4.1.2).

Liquation cracking in the heat-affected zone may occur when welding high-strength aluminium alloys of the Duralumin or aluminium–magnesium–zinc types. This type of cracking is caused by the presence of low-melting constituents in the structure and is associated with relatively low heat-input rates. It may be overcome by using a low-melting-point filler alloy or by increasing the welding speed. Cracking has also been observed well below the solidus (at about 200 °C) in high-strength aluminium alloys. This effect is also due to the formation of intergranular films at or near the solidus. These intergranular constituents cause embrittlement, which manifests itself as low-temperature cracking.

9.1.4 Mechanical properties

Sound welds in annealed pure aluminium or any of the annealed non-heat-treatable alloys made with filler rod or electrodes of matching composition have a strength almost equal to that of the parent metal. When work-hardened plate is

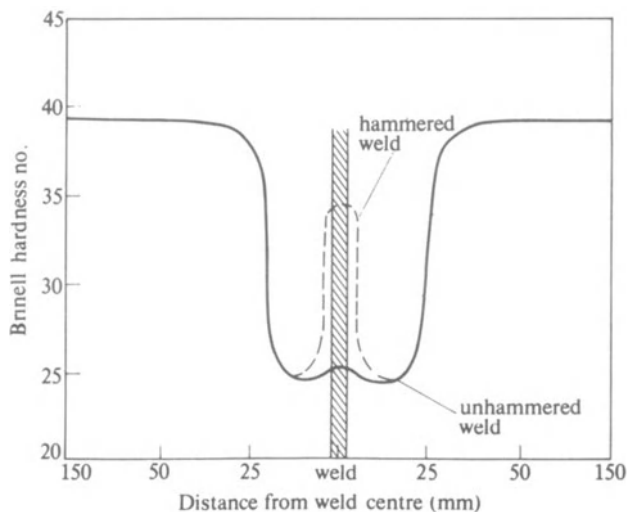


Figure 9.5 Hardness of welded joint in work-hardened aluminium plate. (After West, E. G. 1951. *The welding of non-ferrous metals*. London: Chapman & Hall.)

welded, however, the heat-affected zone is fully or partially annealed, and the strength correspondingly reduced. Softening of the heat-affected zone also occurs as a result of welding an age-hardening alloy. The loss of strength is reduced by increasing the welding speed, partly because of the shorter time within the over-ageing temperature range, and partly because the softened zone is narrower. Softening of work-hardened material is irreversible, although the strength of the weld metal itself may be augmented by rolling or hammering (Figure 9.5). The strength of heat-treatable alloy welds made with matching electrodes may, however, be completely (or almost completely) recovered by solution treatment and ageing of the whole component (Figure 9.6). This procedure is not often practicable, first, because of the crack sensitivity of the heat-treatable compositions, and secondly, because of the distortion resulting from heat treatment. Many attempts have been made to develop fusion-welding filler alloys and procedures capable of giving strong crack-free joints in the high-strength aircraft alloys such as Duralumin, but with only moderate success. It has not been possible to find a filler alloy which combines good crack resistance with high mechanical properties, and for general engineering applications fusion welding is restricted to the medium strength heat-treatable alloys. Welded high-strength aluminium alloys have, however, been used for space vehicle applications.

Various devices are used to overcome weld softening in medium-strength heat-treatable alloys. The first is to make allowance for this effect in the design stress used. The ASME code, for example, permits a design stress of 10 500 psi for unwelded Al-Mg-Si alloy and 6000 psi for the same alloy in the welded condition. It is sometimes possible in structural applications to place the weld

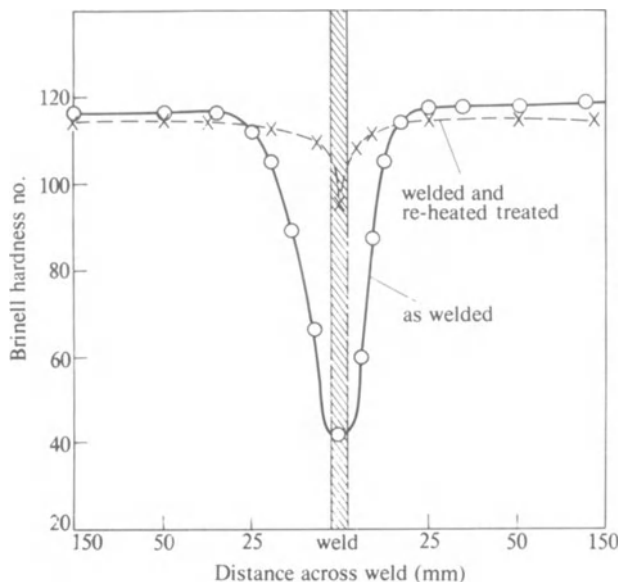


Figure 9.6 Hardness of welded joint in heat-treatable aluminium alloy. (After West, E. G. 1951. *The welding of non-ferrous metals*. London: Chapman & Hall.)

in a region of low stress. In pipework, special pipes with thickened ends may be used for welding, the extra thickness being sufficient to compensate for softening.

The Al–Zn–Mg alloys are exceptional in that although the HAZ is softened by the weld thermal cycle, the softening is due to solution of precipitates rather than to over-ageing. Consequently, it is possible to recover the HAZ properties in part either by natural or artificial ageing, a process known as **reversion**.

The high-strength heat-treatable aluminium alloys are in general susceptible to stress corrosion cracking in relatively mild environments such as weak chloride solutions or even in normal atmospheric exposure. Unwelded material is protected by cladding with Al–1 Zn, which is anodic to the base material. Most SCC failures in Al–Zn–Mg weldments have been found in locations remote from welds. The Al–5 Mg alloy may be susceptible to SCC due to precipitation of the β phase at slightly elevated temperatures. Al–Mg–Si heat-treatable alloys and the non-heat-treatable alloys other than the higher Al–Mg type do not suffer SCC.

9.1.5 Alloys and welding procedures

Commercially available aluminium alloys fall into three groups:

- pure aluminium and non-heat-treatable alloys,
- medium strength heat-treatable alloys,
- high strength heat-treatable alloys.

Of the first group, pure aluminium is used for its corrosion-resistant properties where strength is unimportant, and the aluminium–manganese and aluminium–magnesium alloys for corrosion-resistant and low-temperature applications where moderate tensile strength is necessary. These materials are normally welded using the GTA or GMA processes, with filler materials of matching composition. In the medium strength group, the Mg_2Si (e.g. 3/4 Mg 1 Si) alloys combine good corrosion resistance with moderate cost and medium tensile strength, and in welded fabrication find their main use for piping. Welding is carried out with an inert-gas-shielded process using a 5% Si or 5% Mg filler. The medium strength heat-treatable Al–Zn–Mg alloys may be employed in applications where light weight must be combined with strength and structural integrity in the welded joint. These alloys have been used for military bridging and for cylindrical storage tanks. Welding is by the GTA or GMA processes with an Al 5 Mg or matching filler metal. Natural ageing for 3 months fully restores the 0.2% proof strength and the ultimate strength of the welded joint is 90–95% of that of the unwelded material.

The high-strength alloys are used in aircraft construction where high **strength-to-weight ratio** is of paramount importance. These alloys have poor corrosion resistance (in general they must be protected by means of an anodic coating of pure aluminium or aluminium–zinc alloy) and, as indicated previously, they are not amenable to fusion welding. Spot welding is not so damaging to the mechanical properties of the joint as a whole, since it is a lap joint and has double the plate thickness. Spot welding is therefore used for joining Duralumin-type alloys in certain aircraft applications. Adhesive bonding is likewise employed for this type of alloy.

9.2 MAGNESIUM AND ITS ALLOYS

9.2.1 Alloys and welding procedures

Magnesium finds its widest application in the aircraft industry, where its excellent strength : weight ratio can be used to full advantage. The pure metal has too low a strength for engineering use. The alloys may be divided into three main groups: the **aluminium–zinc**, **zinc–zirconium** and **thorium-bearing** types respectively. The Mg–Al–Zn alloys were the earliest in development and have the disadvantage of being susceptible to SCC; nevertheless, the 3 Al 1 Zn 0.4 Mn alloy remains one of the most generally applicable and readily welded type. The Mg–Zn–Zr alloys with 2% zinc or less also have good weldability, as do the thorium alloys, which are designed specifically for good strength at elevated temperatures.

There are a number of casting alloys which may be joined into structures by welding, or which may be repaired by welding. The principles outlined below apply to these alloys also.

9.2.2 Oxide film removal

Like aluminium, magnesium forms a refractory oxide which persists on the surface of the molten metal and tends to interfere with welding. However, magnesium oxide recrystallises at high temperature and becomes flaky, so that the surface film breaks up more easily than that which forms on aluminium.

The mechanism of oxide removal by means of a flux in oxy-gas welding is probably similar to that in aluminium welding. Fluxes are typically mixtures of chlorides and fluorides of the alkali metals (e.g. 53% KCl, 29% CaCl₂, 12% NaCl and 6% NaF), and are highly corrosive to the base metal. For this and other reasons gas welding is little used for magnesium and its alloys, the most important fusion-welding process being GTA welding with alternating current. Oxide removal is achieved during GTA welding by arc action during the half-cycle when the workpiece is negative. Mechanical cleaning of the weld edges is essential for fusion welding. For spot welding, chemical pickling is necessary, combined with mechanical cleaning (with steel wool) immediately before welding.

9.2.3 Cracking

Zinc and calcium additions both increase the susceptibility of magnesium alloys to solidification cracking during welding. Zinc is a constituent of a substantial proportion of the alloys; in amounts of up to 2% it is not deleterious, but alloys containing larger quantities, particularly those with 4–6% Zn, have poor weldability. Aluminium, manganese and zirconium have little effect on this characteristic, but thorium and rare-earth elements are beneficial and tend to inhibit solidification cracking. Generally speaking, the most crack-sensitive magnesium alloys are the higher-strength high-alloy type, which suffer from cracking both in the weld and at the weld boundary.

9.2.4 Mechanical properties

Weld deposits of magnesium alloys solidify with fine grain and have a tensile strength which frequently is higher than that of the equivalent wrought material. Thus welded joints tested in tension commonly fail in the heat-affected zone. Alloys which have been hardened by cold-work, and age-hardened material, soften in the heat-affected zone. Generally, however, the joint efficiency of fusion welds in magnesium alloys is good, and it is possible to use a relatively low-melting filler metal (e.g. the 6½ Al 1 Zn type) for a wide range of alloys and achieve 80–100% joint efficiency ‘as-welded’.

9.2.5 Corrosion resistance and fire risk

Magnesium alloys are commonly protected against atmospheric corrosion by means of a chromate dip. The green chromate layer must, of course, be removed from the vicinity of the joint before welding.

Aluminium-containing magnesium alloys are susceptible to stress-corrosion cracking in the heat-affected zone of the welds, and must be stress-relieved (generally at about 250 °C) after welding to prevent this type of attack. The zirconium and thorium-bearing alloys are not susceptible to stress-corrosion and do not require stress relief after welding.

There is a risk of fire if magnesium is allowed to accumulate in finely divided form, and proper attention must be paid to cleanliness in all operations involving cutting, machining and grinding. Except in the joining of foil there is no direct risk of fire due to either fusion or resistance welding of magnesium.

9.3 COPPER AND ITS ALLOYS

9.3.1 Processes and materials

Gas welding was the first fusion process to be applied successfully to commercially pure copper, joints of acceptable strength being possible in the **phosphorus deoxidised metal**. More recently, inert-gas welding, using argon, helium or nitrogen as a shielding gas, has greatly broadened the applicability of fusion welding to copper alloys. Coated electrode welding of pure copper, brass and cupronickel has not been successful in practice and, although satisfactory **tin bronze** and **aluminium bronze** electrodes are available, these are mainly used for weld overlays and dissimilar metal joints.

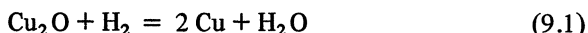
9.3.2 Heat input

The **high heat conductivity of pure copper** makes spot and seam welding impracticable, although resistance butt welding using high capacity machines is possible and is practised for joining wire bar. The alloys have much lower conductivities, however, and normal resistance welding methods are possible.

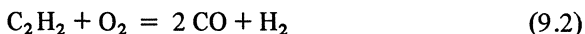
Heat conductivity may give rise to difficulties such as cold shuts and lack of side wall fusion in welding pure copper, particularly when the section thickness is 25 mm or more. In order to increase the heat input per ampere, nitrogen is sometimes used as a shielding gas both for GTA and GMA welding. With nitrogen shielding and tungsten-arc welding, 5 mm copper may be joined in one pass without preheat, as compared with 3 mm thickness under argon shielding. With pure nitrogen shielding, the transfer characteristics of metal inert-gas welds are poor, but with argon–30% nitrogen mixtures the good penetration of nitrogen shielding is combined with the good transfer characteristics of argon. Penetration per pass may be still further improved by using two GMA welding guns mounted side by side along the weld seam. In this way high heat inputs may be obtained without the porosity which appears when the welding current is excessive. If the heat input obtained by such methods is still inadequate, it is necessary to preheat. Preheat temperatures of up to 600 °C have been used for welding thick copper. Such preheats necessitate insulation of the article to be welded and protective clothing for the welder.

9.3.3 Porosity

Unlike aluminium, copper has a relatively low affinity for oxygen and does not react with nitrogen at all. At elevated temperature (above about 500 °C) copper oxide is reduced by hydrogen to form steam:



This reaction (known as the **steam reaction**) can take place in both liquid and solid metal. In the weld pool it may result in porosity, while in the parent metal close to the weld steam is precipitated at the grain boundaries, causing fissures to develop and the metal to be embrittled. In oxy-acetylene welding, hydrogen is formed during the first stage of combustion



and therefore the steam reaction may take place and cause cracking in the weld-heat-affected zone, unless the copper is deoxidised by the addition of between 0.02 and 0.10 phosphorus. Phosphorus is a particularly useful element for this purpose because it is relatively cheap, does not give rise to problems in copper production, and does not form an oxide skin on the weld pool. It is completely effective in preventing gassing and embrittlement adjacent to the weld. However, the weld metal itself is rarely free from porosity, and as a result the tensile strength of 'as-welded' oxy-acetylene welds in **phosphorus-deoxidised** copper is substantially lower than that of the parent metal. Gas welds in copper are frequently **hammered** or **rolled** to remove distortion, and this treatment improves their tensile strength.

Inert-gas-shielded welding does not cause gassing of the parent metal, whether or not it contains phosphorus. The weld metal itself, however, is grossly porous unless it is deoxidised. Phosphorus is not adequate for this purpose and a combination of either silicon and manganese or titanium and aluminium is added to filler wires and electrodes. Even using such powerful deoxidants porosity may still occur in manual GTA welding particularly at restarts. Phosphorus-deoxidised plate is normally specified for GTA or GMA welding. Shielding gases are argon, helium or nitrogen, the latter being used when higher rates of heat input are necessary. There is little difference between argon and nitrogen shielding as regards the incidence of porosity, but helium-shielded welding appears to be somewhat less sensitive to this defect. Helium may not be available at an acceptable price outside the USA however. Porosity (tunnelling), which is associated with turbulence in the weld pool, may occur in GMA welds if the current is too high – over about 350 A for nitrogen shielding and 450 A for argon shielding.

Copper alloys containing deoxidising elements – aluminium bronze, tin bronze and silicon copper – are not subject to porosity, and may be welded without special additions to the filler metal. **Copper-nickel** alloys, however, suffer the same type of porosity as copper itself and require deoxidised filler rod. **Brasses** (both 70/30 and 60/40 types) are difficult to weld because of

volatilisation of zinc, and this effect, apart from interfering with visibility during welding, may also be associated with weld deposit porosity. In oxy-acetylene welding such porosity may be minimised by using an oxidising flame and by adding a filler rod deoxidised with silicon, manganese or phosphorus. A copper with about 1½% zinc, known as **cap copper** may, however, be welded by means of the GTA process without deoxidised filler wire, and the resultant welds are sound.

The fact that deoxidation plays so important a part in minimising porosity, and that alloys containing deoxidant are not subject to this defect, suggests that oxygen may be an important factor, and that the steam reaction is either a direct or contributory cause of pore formation. On the other hand, analysis of gas in the pores shows that it consists largely of hydrogen. Moreover, steam formation requires the simultaneous presence of hydrogen and oxygen in the weld pool, and the sources of these two elements in the inert-gas-shielded welding of copper has not been established. The mechanism which gives rise to porosity in copper and copper alloys remains, therefore, to be determined.

9.3.4 Cracking

Copper and copper alloys are rendered brittle and sensitive to hot cracking if excessive amounts of low-melting impurities, notably bismuth and lead, are present. A useful test for such embrittlement is a hot bend test conducted at 600°C, the bending jig being heated if necessary. Alternatively, the ductility in a tensile test at 450°C may be used as a measure of crack sensitivity. However, the only copper alloy notably sensitive to this defect is **aluminium-bronze**, the characteristics of which are discussed below (Section 9.3.6).

9.3.5 Mechanical properties

The mechanical properties of *unhammered* oxy-acetylene welds in copper are lower than those of the parent plate due to the presence of porosity. Inert-gas-shielded welds may also have lower strength than the parent plate in thick sections, but the reduction is less than for oxy-acetylene welds.

The strength of work-hardened or age-hardened copper alloys is reduced in the heat-affected zone. However, the age-hardenable copper alloys, particularly **beryllium-copper** and **chromium-copper**, are rarely welded. In the case of hard temper (work-hardened) copper, it must be assumed that the strength of a fusion butt weld is equal to that of the annealed material.

9.3.6 Alloys and welding procedures

There are two coppers which are mainly used for electrical transmission lines, **tough pitch** and **oxygen-free high conductivity copper**. Arc welds in these materials are not very satisfactory; usually they contain defects and at best have undesirably high electrical resistance due to the use of deoxidised filler

material. Cold pressure welding is applicable to rod and is used to make joints in electrical conductors. The process that is generally used for joining copper in electrical conductors is thermit welding, using a mixture of aluminium and copper oxide for the exothermic reaction. The mixture is held in a graphite crucible, with a steel disc covering the exit hole. It is ignited and in a very short time a pool of molten copper is formed which melts the retaining disc and flows out into a mould surrounding the joint. The liquid copper has sufficient superheat to melt the joint faces and produce a sound weld. A collar of metal is left around the joint for strength and to ensure good electrical conductivity.

Phosphorus-deoxidised copper is the standard material for welded sheet and plate applications in copper. The **copper 1½% zinc alloy (cap copper)** has been employed for domestic hot water tanks which are welded by the GTA process without filler wire. This material gives sound ductile joints when so welded. **Silicon bronze** may also be welded by the inert gas processes without special additions, and gives sound ductile joints of mechanical strength equal to the parent metal. Resistance welding (and of course soldering) finds substantial application in sheet metal products made from brass.

Aluminium bronze is one of the more difficult materials to fabricate and weld due to its susceptibility to hot cracking. The type most frequently specified is the single-phase Cu 7 Al 2½ Fe alloy. Except for single-pass welds in thin material, the use of a matching filler material for welding this type of aluminium bronze is impracticable. Even if fissuring of the weld can be avoided, multi-pass joints may suffer embrittlement due to heat treatment of the weld deposit by subsequent runs. A duplex filler material containing about 10% aluminium is, however, virtually free from any tendency to crack. A composition which has been successfully used for GTA and GMA welding is nominally 10% aluminium, 2½% iron and 5½% nickel.

Although weld metal cracking may be overcome by the proper choice of filler alloy, 93 Cu 7 Al plate material may sometimes crack during hot forming or welding. In welding, these cracks may extend for some distance away from the weld boundary. Intergranular cracking has also been observed close to the weld boundary. Such cracking is due to a deficiency of the plate material, the nature of which has not yet been explained.

Cracking of the weld metal appears to be associated with phase constitution in a manner analogous to that which occurs in fully austenitic steel; the single-phase alloy is subject to cracking, while two-phase alloys are not. A further similarity is that both materials have a narrow freezing range, so that cracking due to a wide freezing range inherent in the constitution of the alloy (as for example in aluminium alloys) is not possible. If cracking occurs at high temperature, it is probably due to the formation of liquid intergranular films of low-melting constituents. Alternatively, cracking may take place at lower temperatures due to the formation of brittle intergranular constituents.

Cupronickel is used mainly in sheet form for fabricated work, and the most suitable welding process is GTA welding. Cracking is not a serious problem, and porosity is minimised by using a filler rod containing deoxidant. Cupronickel

alloys vary in nickel content, typical compositions containing 5%, 10%, 20% or 30% nickel. If a matching filler is not available, the deoxidised 70/30 composition may be used. A suitable deoxidant is titanium.

Silicon bronzes present few welding difficulties; they have relatively low thermal conductivity (54.4 W/mK) and are not subject to cracking or porosity in fusion welding. Silicon bronze may be welded using all the major welding processes. Generally, the speed of welding is high, and preheating rarely necessary, while the energy requirements for resistance welding are much lower than for other copper alloys – a reflection of their higher electrical resistance compared with copper.

9.4 NICKEL AND ITS ALLOYS

Nickel has physical properties similar to those of iron, but differs metallurgically in that it does not undergo a $\gamma \rightarrow \alpha$ transition, the face-centred cubic lattice structure being maintained down to room temperature. Metallurgical problems associated with the welding of Ni and its alloys include weld porosity, embrittlement by sulphur and other contaminants, and loss of corrosion resistance due to the formation of intergranular precipitates.

9.4.1 Cracking

Hot-shortness of nickel and nickel alloys may be caused by contamination with sulphur, lead, phosphorus and a number of low-melting elements such as bismuth. These contaminants form intergranular films which cause severe embrittlement at elevated temperature. Hot cracking of weld metal may result from such contamination, but more frequently it occurs in the heat-affected zone of the weld, and is caused by intergranular penetration of contaminants from the weld metal surface (Figure 9.7). Sulphur is a common constituent of cutting oils used in machining and therefore is frequently present on metal surfaces. Grease, oil, paint, marking crayons, temperature indicating sticks, or dirt may contain one of the harmful ingredients. Damaging elements may also be present on the surface of nickel which has been in service and which requires weld repair.

Prior to any welding or brazing process where heat is applied, the metal surface must be cleaned. New material is scratch-brushed using a stainless steel wire brush for a distance of at least 25 mm on either side of the joint, and then degreased with carbon tetrachloride, trichlorethylene, or other solvent. Metal which has been in service needs more drastic treatment. It is ground, shot blasted or pickled in the region adjacent to the weld, and then degreased, as before. During fabrication suitable steps must be taken to minimise the danger of contamination, in particular by establishing clean working conditions and by annealing either in electric furnaces or in furnaces fired with sulphur-free fuel. Cracking may occur in the weld or heat-affected zone of nickel and high nickel

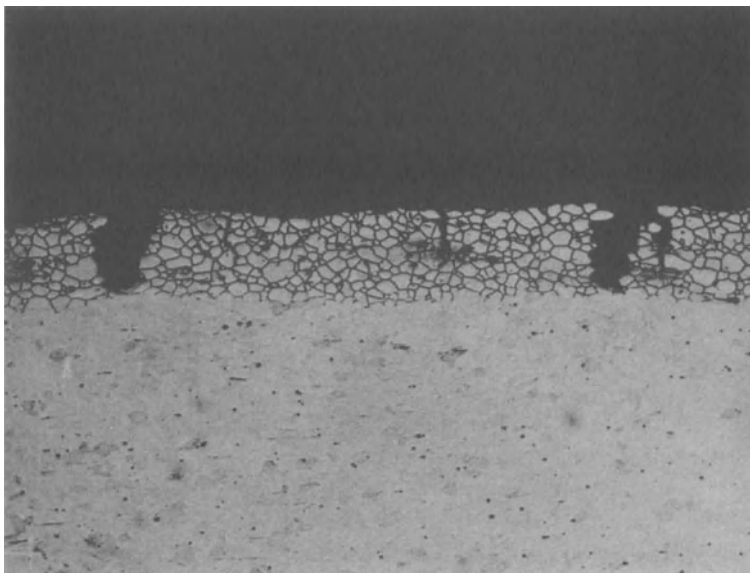


Figure 9.7 Hot cracking of nickel due to sulphur contamination of the surface ($\times 100$). (Photo.: International Nickel Co. (Mond) Ltd.)

alloys that have been work-hardened or age-hardened. Material should therefore be in the annealed or solution-treated condition before welding.

Welds made in the silicon-bearing 18 Cr 38 Ni alloy are likely to suffer from hot-cracking if a matching filler metal is used. This alloy should be welded with a low silicon 80 Ni 20 Cr type filler, avoiding dilution.

9.4.2 Porosity

Pure nickel, the Ni–30 Cu alloy Monel, and (to a lesser degree) the nickel–chromium–iron alloys are subject to porosity if the weld metal does not contain nitride-forming and deoxidising elements. Filler rods and electrodes for the arc welding of these alloys are designed to give a weld deposit containing aluminium, titanium, or niobium, or a combination thereof.

The cause of porosity has not been established with certainty. Porosity can be caused by the evolution of carbon monoxide, or nitrogen, or by these reactions occurring in combination. In either event, such porosity may be minimised by the addition of elements such as aluminium and titanium, which form stable compounds with nitrogen and oxygen, and by avoiding atmospheric contamination, if necessary preventing the access of air to the underside of the weld.

Rather unexpectedly porosity in GTA nickel welds may be eliminated in single-pass welds by the use of argon with up to 20% hydrogen as a shielding gas. The hydrogen may act as a scavenging gas, nitrogen diffusing into the bubbles of

hydrogen which form in the weld pool. Alternatively, it has been suggested that hydrogen prevents the formation of nickel oxide on the surface of the weld, and thus reduces the risk of carbon monoxide formation. Excessive amounts of hydrogen may however result in hydrogen porosity, so that its use is not without risk.

9.4.3 Mechanical properties

The mechanical properties of properly made welds in annealed nickel and nickel alloys, other than the age-hardening types, are equal to those of the parent metal. Age-hardening alloys are normally welded in the solution-treated condition and age-hardened after welding. With an optimum combination of parent and filler metal compositions, joints of strength close to that of the fully heat-treated parent metal are obtained. Age-hardening treatments for nickel alloys are in the temperature range 580–700°C. A number of filler alloys for the non-ageing materials contain sufficient titanium, aluminium or niobium to make the weld deposit harden if held within this temperature range, so that stress-relieving joints at 580–650°C will result in some degree of weld hardening. Such hardening is not usually harmful in a non-corrosive environment, but its potential effect must be considered (see Section 9.4.4). If a non-ageing deposit is required for nickel–chromium–iron alloys, an 80 Ni 20 Cr filler alloy may be used. Welding fully heat-treated age-hardened alloys is only possible under conditions of minimum restraint, and, to restore the full properties, solution treatment followed by ageing must be repeated after welding.

9.4.4 Corrosion resistance

Pure nickel and many of the nickel alloys are used for corrosion-resistant duties, as indicated in Table 9.1. Pure nickel has good resistance to caustic solutions, while the Ni–Mo and Ni–Cr–Mo alloys withstand some of the most severely corrosive environments encountered in chemical plant. These alloys are welded using the GMA or GTA processes with electrodes that produce a deposit of matching composition, modified where necessary by the addition of deoxidisers. The corrosion resistance of such weld metal is generally adequate, but the base metal must, for exposure to severe conditions, be formulated to avoid intergranular precipitation due to the weld thermal cycle.

Considering Ni–Cr–Fe alloys in general, the effect of increasing the Ni content is to reduce the susceptibility to transgranular SCC and to increase the susceptibility to intergranular attack. Figure 9.8 shows this effect in terms of weight loss in a standard IG test as a function of nickel content. By the same token it is necessary, as the Ni content increases, to reduce the carbon content to lower values in order to maintain IG corrosion resistance. It may also be necessary to add vanadium as a stabilising element (note the compositions of Hastelloys B2 and C276 in Table 9.1). Sensitisation is generally due to carbide precipitation, but in the more complex alloys and in those containing

Table 9.1 Nickel and nickel alloys

Designation	Ni	Cr	Co	Cu	Fe	Mn	Chemical composition*					Al	Ti	Mg	Typical use
							Mo	Si	W	C	S	P			
Nickel 200	99.2 min.	—	—	0.25	0.40	0.35	—	0.15	—	0.10	0.005	—	0.10	0.10	Caustic service
Low-C Nickel 201	99.0 min.	—	—	0.25	0.40	0.35	—	0.15	—	0.02	0.005	—	0.10	0.10	Caustic service over 316 °C
Monel 400	63.0–70.0	—	—	28.0–34.0	1.0–2.5	1.25	—	0.5	—	0.15	0.02	—	0.50	—	Sea water, chlorides, HCl, HF
Hastelloy B	Bal	1.0	2.5	—	4.0–7.0	—	26.0–30.0	—	—	0.05	—	—	—	—	HCl service
Hastelloy B2	Bal	1.0	1.0	—	2.0	1.0	26.0–30.0	0.10	—	0.02	0.03	0.04	—	—	HCl service, as-welded
Hastelloy C	Bal	14.5–16.5	2.5	—	4.0–7.0	—	15.0–17.0	—	3.0–4.5	0.08	—	—	—	—	Strong oxidisers, mineral acids, wet chlorine gas
Hastelloy C276	Bal	14.5–16.5	2.5	—	4.0–7.0	1.0	15.0–17.0	0.08	3.0–4.5	0.02	0.03	0.04	V	—	As above, as-welded
Incoloy 825	40.0–45.0	20.0–24.0	—	1.5–2.5	Bal	—	2.5–3.5	—	—	0.05	—	—	0.20	0.7–1.1	Resistance to chlorides and mineral acids
Inconel 600	72.0 min.	14.0–17.0	—	0.50	6.0–10.0	1.0	—	0.50	—	0.08	0.015	—	—	0.30	Oxidation resistance to 1175 °C. Resistance to SCC. Nuclear components
Incoloy 800	30.0–35.0	19.0–23.0	—	0.75	Bal	1.5	—	1.0	—	0.10	0.015	—	—	—	Petrochemical furnaces and piping. Oxidation resistant

* Maximum except where a range is indicated.

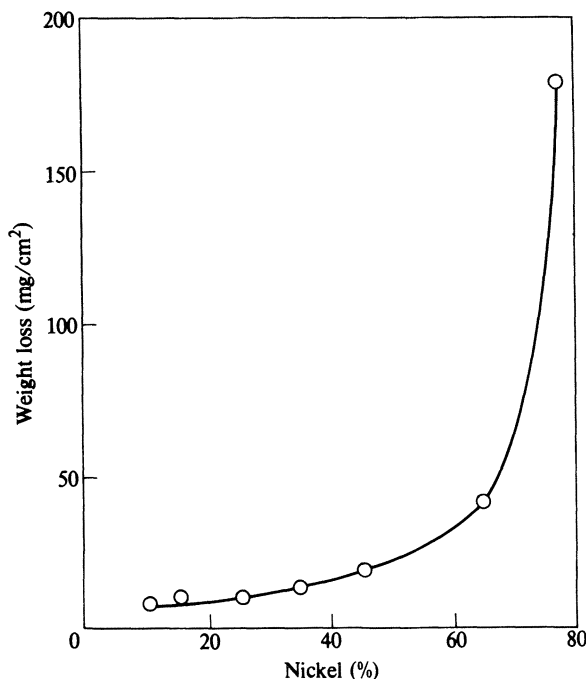


Figure 9.8 Influence of nickel content on intergranular corrosion of Ni–17Cr–Fe alloys. Tested 70 h in 5 M HNO₃ + 1 g/l Cr at 108 °C (Heathorne, M. Intergranular corrosion. In *Localised corrosion – cause of metal failure*. ASTM STP 516).

molybdenum intermetallic compounds or phases may also precipitate in the grain boundaries. Commercially pure nickel may also suffer weld decay and a low-carbon type (Nickel 201) is used for the more severe environments. IG attack of nickel-base alloys has been found in a number of acid media but it has also been observed in high temperature water and in alkaline solutions. The standard test solution for detecting sensitisation of these alloys is a mixture of sulphuric acid and ferric sulphate, as specified in ASTM A262.

Nickel-base filler metal is used for joining austenitic Cr–Ni steels to carbon and low-alloy steel, particularly when the joint is to be given a PWHT. Where a Cr–Ni filler (say type 309 or 310) is used for such joints they are likely to embrittle by sigma phase formation and by carbon migration from the ferritic steel into the weld deposit. Nickel-base weld metal does not suffer either of these two deficiencies. There is, however, the moderate hardening effect described earlier, and in most instances the weld metal will be sensitised, and may not be suitable for exposure to corrosive environments.

9.4.5 Oxidation and creep resistance

A number of nickel-base and cobalt-base alloys have useful oxidation-resistant and creep-resistant properties, and at the same time retain adequate ductility after periods of ageing at elevated temperature. They are used for gas-turbine parts and in high temperature furnaces for the petrochemical industry. Incoloy 800, for example, is specified for furnace tubes, headers and transfer lines in locations where there is a risk of thermal movement. Incoloy 800 behaves like a high-nickel steel when fusion welded in that a matching composition filler metal is too susceptible to solidification cracking for practical use. Nickel-base Ni–Cr–Fe filler alloys are therefore used to weld alloy 800, and the rupture strength of the weld metal is lower than that of the parent material. When this type of weldment is subject to strain in service, failure may occur in the form of creep cracking in the weld metal.

Problems associated with creep-resistant alloys are considered also in Section 8.6.

9.4.6 Alloys and welding procedures

Nickel and nickel-base alloys may be welded by nearly all the available welding processes. Those alloys that are employed for corrosion resistance (nickel, Monel, Hastelloy, for example) are normally joined using SMA or GTA welding. In GMA and SA welding it is necessary to restrict heat-input rates to avoid solidification cracking, particularly with the complex nickel alloys and with cobalt-base alloys. In some instances fusion welding is practicable in the flat position only. Gas-turbine alloys are welded by the GTA and EB processes and also by resistance welding.

9.5 THE REACTIVE AND REFRACTORY METALS – BERYLLIUM, TITANIUM, ZIRCONIUM, NIOBIUM, MOLYBDENUM, TANTALUM AND TUNGSTEN

The reactive metals present some difficult welding problems. They have in common a high affinity for oxygen and other elements, and welding processes that employ a flux, or that permit exposure of heated metal to the atmosphere, are inapplicable because of contamination and embrittlement of the joint. Likewise cleanliness is of special importance in welding reactive metals.

The processes that have been applied experimentally and in production are GTA (d.c. electrode-negative), electron beam, spot, seam and flash butt, pressure, ultrasonic and explosive welding. GTA welding without filler wire addition is the most generally successful and widely used technique. The problems chiefly encountered are embrittlement due to contamination, embrittlement due to recrystallisation, and porosity.

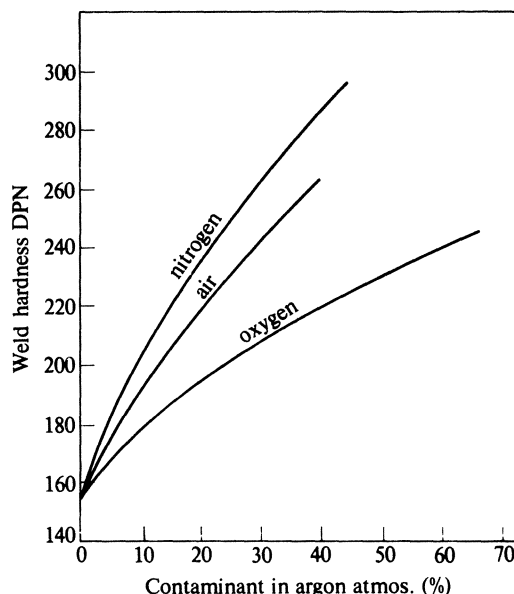


Figure 9.9 Effect of atmospheric contamination of hardness of weld in titanium (Borland, J. C. 1961. *Brit. Welding J.* 8, 64).

9.5.1 Embrittlement due to gas absorption

Beryllium, titanium, zirconium, niobium and tantalum react rapidly at temperatures well below the melting point with all the common gases except the inert gases. **Contamination** by dissolving oxygen and nitrogen from the atmosphere in the molten weld pool results in an increase in tensile strength and hardness and reduction in ductility (Figure 9.9). As a result, even welds which have been effectively shielded show some hardness increase across the fused zone, and with increasing hardness so the ductility of the joint is reduced (Figure 9.10). Thus the degree of ductility of the completed fusion weld depends upon the effectiveness of the gas shielding. To obtain the minimum degree of effective shielding, a blanket of inert gas is required both on the torch side and the underside of the joint, and various devices, including welding jigs having an argon-filled groove below the joint line, are used for this purpose. Welding with a standard type of GTA torch and with argon backing to the joint is practicable for titanium and zirconium. The other materials are best welded inside an argon-filled enclosure. Such enclosures are of two types – a **plastic tent** which can be flushed with argon, or a metal chamber fitted with glass ports for viewing the work and sometimes glove pockets for manipulation. The latter, after evacuation and when filled with purified argon or helium, provides the best available protection for tungsten-arc fusion welding.

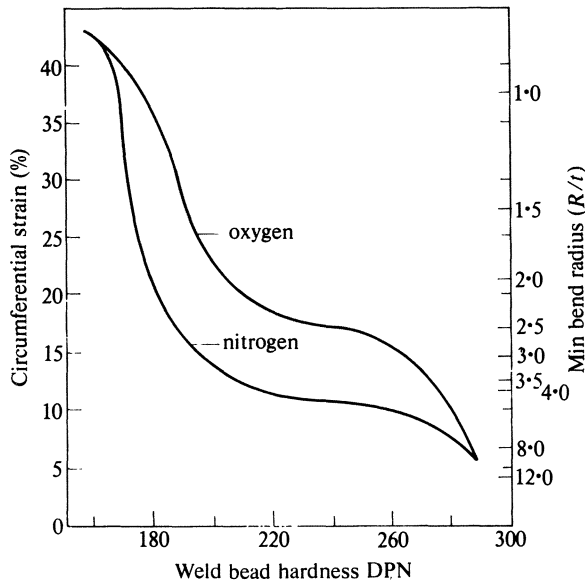


Figure 9.10 Relationship between weld hardness and ductility: titanium welds contaminated with oxygen or nitrogen (Borland, J. C. 1961. *Brit. Welding J.* 8, 65).

Electron beam welding avoids contamination problems entirely, since it is carried out in a vacuum. Resistance welds can normally be made in air because the time cycle is too short for any substantial degree of gas pickup.

Beryllium has a very low ductility at room temperature in the unwelded condition, and welds, even without contamination, are likewise brittle.

9.5.2 Embrittlement due to recrystallisation

Molybdenum and tungsten are body-centred cubic metals and behave like iron in that, above a certain temperature — the **transition** temperature — they are ductile, whereas below this temperature they are brittle. Tungsten, even when cold-worked to fine grain size, has a transition temperature well above room temperature (typically 200–250 °C), but molybdenum, which also has a high transition temperature in the ‘as-cast’ or recrystallised condition, may be cold-worked to give reasonable ductility at room temperature. Tantalum and niobium also have a body-centred cubic structure, but the transition temperature is well below room temperature and does not limit their usefulness.

When tungsten and molybdenum are joined by the GTA or resistance-spot or seam-welding processes, recrystallisation occurs in the heat-affected zone, so that the joint has a higher transition temperature than the parent metal. In the case of tungsten this is not of great consequence, because the parent metal

is in any event brittle at room temperature and the transition temperature is raised by only about 100 °C.

Molybdenums joints, however, may have some ductility, depending upon purity, alloy content and welding technique. The Mo–½Ti alloy is capable of deformation in a slow bend test if welded in a chamber with a preheat of 150 °C. Such welds are nevertheless brittle when subject to impact loading.

Brittleness may occur in spot-welded molybdenum. It may be minimised by inserting tantalum, zirconium, nickel or copper foil, or metal fibre between the surfaces to be spot welded.

9.5.3 Porosity

Porosity in titanium fusion welds was at one time thought to be due to entrapment of argon gas between the butting faces of the joint, but it is now attributed to hydrogenation from inadequate precleaning. Metal which is produced by powder metallurgy often contains entrapped or dissolved gas which can be liberated on fusion welding and this effect can cause porosity in molybdenum and tungsten welds. Titanium or zirconium produced by casting and rolling is, therefore, preferred for fusion-welded applications. Porosity may also result (for example in beryllium) from inadequate cleaning of the metal surface. Effective preweld cleaning is most important for all the reactive metals and is accomplished by machining, grit-blasting or grinding followed by degreasing, or by pickling. Given a clean metal surface, parent metal free from contamination and defects, and reasonable care in welding, porosity is not a serious problem with the metals under consideration.

9.5.4 Cracking

The unalloyed reactive metals are not prone to hot cracking, nor are the alloys that are commonly welded. The brittle metals beryllium, molybdenum and tungsten may crack at low temperature if welded under restraint, and joints are designed so as to minimise this hazard.

9.5.5 Tensile properties

The tensile strength of uncontaminated fusion welds made in the reactive metals in the annealed condition approximates to those of the parent metal. In cold-worked material the joint strength is reduced to a degree which depends upon the nature of the welding process; for example, GTA welds in cold-worked Mo–½Ti sheet have a joint efficiency of about 50% whereas that of electron-beam welds (which have narrower fusion and heat-affected zones) is about 70%. GTA welds usually have a tensile strength approximating to that of the annealed material.

Welds in heat-treatable alloys — for example, the duplex Ti–4 Al–4 Mn type — may have good strength but are deficient in ductility and impact resistance.

To restore adequate properties it is necessary to fully heat-treat after welding. Welding is usually restricted to the pure metals and non-heat-treatable alloys, and even in these materials ductility is frequently impaired by oxygen or nitrogen contamination, by recrystallisation, or by a combination of these factors.

9.5.6 Alloys and welding procedures

The most widely used of the reactive metals is titanium, which is employed for a number of aircraft applications and also for corrosion-resistant duties. The Ti-6 Al-5 Zr- $\frac{1}{2}$ Mo- $\frac{1}{4}$ Si alloy, which combines high creep resistance with good fracture toughness and weldability, has been used for a welded high-pressure gas-turbine case, but most aircraft applications are compressor discs, blades, and non-welded structural parts. In the chemical industry, likewise, the bulk use is for unwelded items such as heat-exchanger tubes and plates. However, a significant amount of titanium has been employed for pressure vessel manufacture, either as linings or in the solid form. Commercially pure titanium has exceptional resistance to chlorides and to oxidising acids, while for more reducing conditions titanium containing 0.15% palladium is better. Both these metals are welded by the GTA process, ensuring that the gas shield is adequate both on the top side and underside of the joint, and that there is no iron contamination of either the weld metal or the plate surface. Under corrosive conditions corrosion of the iron generates hydrogen, which in turn embrittles the titanium and causes localised cracking.

Zirconium is also used, but to a more limited extent, for corrosion-resistant linings for chemical process vessels, and much the same precautions are required as for titanium. A major use for zirconium is Zircaloy canisters for the containment of fissile material in nuclear reactors. The canisters are seal welded but this weld does not present serious difficulties. The most important processes for welding the reactive metals as a whole are GTA welding and resistance spot welding. Wherever possible the use of filler rod with GTA welding is avoided because it constitutes a potential source of contamination. The metals concerned are normally welded in the form of thin sheet or tube, and filler rod is not often needed. The more difficult and brittle metals are best joined, where possible, by means of edge welds since the degree of restraint is a minimum in this type of joint configuration. Brazing and diffusion bonding are also used as a method of joining. For high-temperature applications of metals such as molybdenum, the braze is made below the recrystallisation temperature, and the temperature of the joint is then raised to diffuse part or all of the brazing material into the parent metal.

There are difficulties with sticking of the electrode to the workpiece in spot welding molybdenum and other refractory metals. Insertion of a shim of foreign metal between the surfaces to be joined helps to overcome this problem.

9.6 THE LOW-MELTING METALS: LEAD AND ZINC

9.6.1 Lead

Although lead forms a notably protective oxide layer, it may readily be cleaned by scraping or scratch-brushing, and consequently is welded without flux. Gas welding is virtually the only method used for lead, and either the oxy-coal gas, oxy-hydrogen or oxy-acetylene torches are applicable.

Metallurgical problems associated with the welding of lead are rare, most of the difficulties being manipulative. Carbon-steel chemical vessels handling corrosive fluids are sometimes *homogeneously lined* with lead. The metal surface is cleaned by shot blasting or other means and then tinned with a lead-tin solder using zinc chloride flux. Lead is then melted directly on to the tinned surface in two or three successive coats. Careful inspection for pinholes must be made between coats. Vessels may also be lined with sheet lead.

9.6.2 Zinc

Zinc is fusion welded either by the oxy-acetylene welding process or by the GTA process. In gas welding the oxide layer must be removed by means of a flux consisting of equal parts of ammonium chloride and zinc or lithium chloride. This is applied as an aqueous paste on either side of the joint, and welding is carried out with a neutral or slightly reducing flame, adding filler rod if necessary. Welds may be hammered to improve their strength, but such treatment must be carried out between 100 and 150 °C; outside this temperature range the metal is too brittle.

Zinc-coated sheet is successfully spot and seam welded in spite of reduced electrode life due to zinc contamination. Galvanised steel may be fusion welded using coated electrodes but there is a risk of porosity and cracking, and for stressed joints the galvanising should be removed in the vicinity of the joint. Austenitic chromium-nickel weld metal will certainly crack if deposited on a galvanised or zinc-coated surface. Zinc-rich primers are often used for protecting steelwork before it is erected. Welds can be made through such primers if the paint thickness is not more than, say, 25 µm; with thicker layers there may be a reduction of impact properties of the weld metal.

Zinc-base die-castings commonly contain about 4% aluminium and, because of the oxide skin which forms on heating, are most difficult to weld. Heavy fluxing and careful manipulation are the only available means to success in this case.

In fusion-welding zinc and zinc-coated materials there is a danger that toxic concentrations of zinc fume may built up. Good ventilation is therefore essential.

9.7 THE PRECIOUS METALS: SILVER, GOLD, PLATINUM

9.7.1 Silver

In its welding characteristics silver resembles copper: it has high thermal conductivity and low chemical affinity for atmospheric gases. It is, however, capable of dissolving oxygen, and rejection of this gas during welding can give rise to porosity.

Pure silver or the silver–30% copper alloy is used as a sheet metal lining or in the form of clad plate for vessels in the chemical industry. Liners were formerly welded using oxy-acetylene torches (without flux), but modern practice is to weld with the GTA process, direct-current electrode-negative. Welds free of porosity may be obtained by using lithium-deoxidised parent metal and filler wire. In welding clad plate, care must be taken to avoid iron contamination; this, however, is less difficult than with most clad material, because silver does not alloy with iron and has a much lower melting point.

Silver may be pressure welded, and spot welding is possible in spite of the high electrical conductivity.

9.7.2 Gold

Gold in fabricated form is used almost entirely for jewellery and the problem of welding in bulk form does not arise. Oxy-coal gas welding of gold is practicable and is used by jewellers. Gold is also brazed and a series of gold brazing alloys are available.

Gold may be readily pressure welded.

9.7.3 Platinum

Platinum is used for catalysts, insoluble anodes, thermocouples, laboratory ware, electrical contacts, and jewellery. Welding is accomplished by the oxy-acetylene or GTA processes (for example, for joining thermocouples), and it may be joined by resistance welding and pressure welding.

9.7.4 Other platinum-group metals

Palladium may be welded in the same way as platinum, but the use of reducing atmospheres must be avoided; in oxy-acetylene welding a neutral or slightly oxidising flame is used. Rhodium, iridium, ruthenium and osmium may be joined by tungsten inert-gas welding, the latter two in a controlled atmosphere chamber.

FURTHER READING

- West, E. G. 1951. *The welding of non-ferrous metals*. London: Chapman & Hall.
- American Welding Society 1972. *Welding handbook*, 6th edn. Section 4: *Metals and their weldability*. Miami: AWS; London: Macmillan.
- Baker, R. G. (ed.) 1970. *Proceedings of the conference on weldable Al–Zn–Mg alloys*. Cambridge: The Welding Institute.
- Linnert, G. E. 1965. *Welding metallurgy*, vol. 1. Miami: American Welding Society.
- Linnert, G. E. 1967. *Welding metallurgy*, vol. 2. Miami: American Welding Society.

10 The behaviour of welds in service

10.1 RELIABILITY

One of the primary reasons for attempting to understand the complex physical and metallurgical processes that take place during the welding – particularly the fusion welding – of metals is to increase the *reliability* of welded joints by specifying the optimum materials, welding procedures and quality-control techniques. For example, in the boiler of a major power station there may be thousands of pipe welds, and the failure of only one of these welds may result in a plant shut-down. In structural work, deficiencies in a single weld may not have such serious effects; nevertheless, if a weld in a critical location fails, the structure as a whole may collapse or be condemned. By studying the reliability of welds in service it is possible to obtain a measure of the success or otherwise of the welding engineer in achieving sound joints.

Quantitatively, the reliability of a piece of equipment is the probability of it performing the required service duty for a specified period of time. Under steady operating conditions it often happens that failures occur at random intervals of time. Such failures are said to have an *exponential* distribution, and the reliability is given by:

$$R = e^{-\lambda t} \quad (10.1)$$

where λ is the **chance failure rate**: i.e. the number of failures in unit period of time. If, for example, the rate of failure of welds in an item of process equipment is 10^{-4} per hour and the interval between maintenance shut-downs is 300 days, the probability that the equipment will not fail during the interval between planned shut-downs is

$$R = e^{-300 \times 24 \times 10^{-4}} = 0.487$$

Likewise, the number of unscheduled shut-downs during the year is $300 \times 24 \times 10^{-4} = 0.7$. In other words, if there are ten identical items of such equipment operating in parallel, it is probable that seven will suffer an unscheduled shutdown.

Another method of treating failure records is to plot them on a **Weibull chart**. The vertical scale of such a chart records the cumulative percentage of failures, and the horizontal scale represents time. Figure 10.1 shows a Weibull plot of creep-rupture failures of welds in the tubes of a steam/methane reformer furnace. In this instance, the furnace tubes were made up of three lengths of

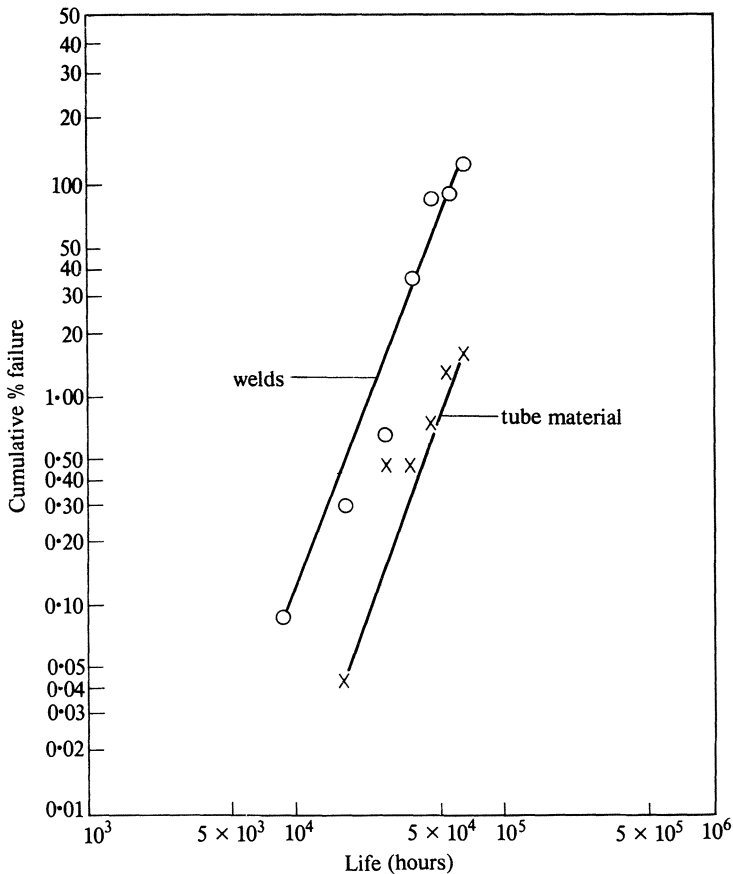


Figure 10.1 Weibull plot of catalyst tube failures in primary reformer furnaces.

centrifugally cast 0.4 C 25 Cr 20 Ni steel tubes welded circumferentially using matching coated electrodes. The creep-rupture strength of the weld metal was substantially lower than that of the parent metal, and this fact, combined with unanticipated longitudinal stress and other chance circumstances such as local overheating, led to intermittent failure. Such chance failures will generally be scattered around a straight line on a Weibull plot, and extrapolating this line makes it possible to predict when a given percentage of tubes will have failed. This in turn makes it possible to plan for replacement.

In practice reliability problems are not often as simple as the examples given. Nevertheless, a quantitative technique for recording such problems is of value both for planning and, when there are identical items of equipment with different failure rates, for diagnosing the environmental causes of breakdown.

10.2 SERVICE PROBLEMS ASSOCIATED WITH WELDING

Welding may generate both physical and metallurgical discontinuities in a structure and these in turn may adversely affect the service behaviour. The difference in properties between the weld and the parent metal is not very great with solid-phase welds made at elevated temperature, such as friction welds and hot pressure welds, but in the case of fusion welds the weld metal and/or HAZ may differ in various ways from the parent metal. Mechanical properties such as tensile and yield strength, hardness, impact properties, fatigue strength, creep-rupture strength and ductility, and resistance to slow or fast crack propagation may be affected. In addition, the resistance to various modes of corrosive attack may be modified; the weld or HAZ may be subject to selective wastage, and if the conditions are such as to generate stress corrosion cracking then the residual stresses caused by fusion welding are normally sufficient to propagate such cracks. In the absence of metallurgical effects, defects and discontinuities can give rise to various types of failure; for example, brittle fracture, accelerated fatigue failure, selective corrosion and stress corrosion cracking. These deficiencies will be discussed below but it will be convenient to start with fast crack propagation, since the technique for studying and quantifying this phenomenon is applicable to varying degrees in the case of other failure modes.

10.3 FAST CRACK GROWTH

10.3.1 General

Although fast crack propagation in welded structures is most commonly associated with the brittle fracture of carbon-steel plate, it can affect many other materials (including non-metals) and other product forms. There are three preconditions for such cracking:

- (a) a crack source, which will generally be a crack-like discontinuity;
- (b) a tensile stress, so oriented that it tends to open the discontinuity;
- (c) an energy source, such that during crack propagation the rate of release of energy available from the source is at least equal to the rate at which it is absorbed by the moving crack.

When crack growth has been initiated, and condition (c) applies, the crack is said to be *unstable*. Under carefully controlled laboratory conditions it is possible to equate the rates of release and absorption of energy, and obtain *stable* crack growth, such that the crack can be started or arrested at will. The energy source in laboratory tests is usually the elastic strain energy present in the test specimen due to applying a tensile force. Under practical conditions there may be additional contributory sources: for example, the strain energy contained in

surrounding structural members, or in pipe branches that are subject to bending due to steady loading or to impact. Impact loading generates up to twice the strain-energy content as compared with that due to a steady load of the same magnitude. The energy due to compressed gas or liquid in pressure vessels and piping can provide a major source for the propagation of fast fractures.

The fracture itself may be completely ductile, with a shear fracture face at 45° to the plate surface and a substantial amount of thinning around the crack. At the other extreme it may be completely brittle, with cleavage facets forming at right angles to the plate surface. Between these two extremes are **quasi-cleavage** fractures of which the face is likewise at right angles to the plate surface, but where the fracture mechanism is a mixture of cleavage and ductile tearing. Fast ductile failures are observed in gas transmission pipelines and in pressure vessels subject to a sudden overload; in both cases the energy source is primarily that due to compression of the gas. Such failures will not be considered further because their occurrence is unrelated to the presence of welds in the structure.

The nature of fracture in completely brittle substances is fairly well understood. If glass, for example, is subjected to sufficiently high tensile stress, a pre-existing microcrack extends slowly until it reaches a critical size, when the crack propagates rapidly and complete fracture takes place. During the rapid stage of crack propagation the energy required to create the fracture surfaces is supplied by the elastic strain present in the material ahead of the advancing crack. The crack is therefore **self-propagating**, and does not require the expenditure of work from any external source for its maintenance. The elastic strain at the crack tip is a function of the applied stress and the stress concentration factor due to the crack. Now the stress concentration factor increases as the crack length increases, and there is, for any given tensile stress, a **critical crack length** below which the rate of release of strain energy is lower than the absorption of energy by the formation of new surfaces. Equating the two energy terms gives the relation between critical crack length a , surface energy γ and tensile stress to propagate fracture

$$\sigma = \left(\frac{E\gamma}{\pi a} \right)^{1/2} \quad (10.2)$$

where E is Young's modulus. This equation, originally developed by Griffiths, has been verified for glass using values of γ determined independently.

In the case of metals in a brittle or quasi-brittle condition the value of γ as determined by experiment is several orders of magnitude higher than the true surface energy because some plastic deformation takes place even in an apparently brittle crack. Nevertheless, Equation 10.2 is qualitatively correct, and in particular the concept of a critical crack length for the initiation of fast fracture, which is inversely proportional to the square of the applied tensile stress times a factor that varies with the degree of embrittlement of the metal, remains valid. Methods of determining this factor have been the subject of much research. Tests that are applicable to elastic behaviour will be discussed below under the heading of **linear elastic-fracture mechanics**, while those appropriate to

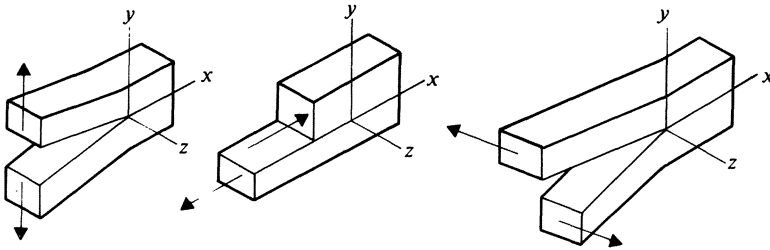


Figure 10.2 The basic modes of crack surface displacements (Paris, P. C. and G. C. Sih. Stress analysis of cracks. In *Fracture toughness testing*. ASTM STP 381).

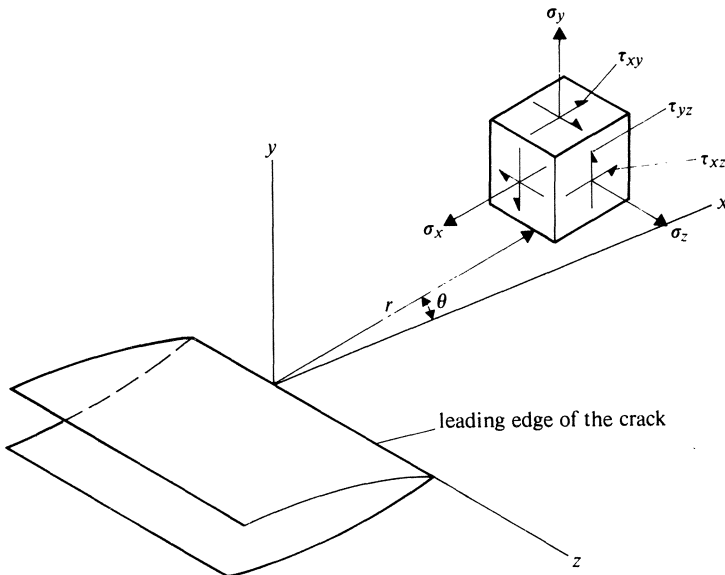


Figure 10.3 Co-ordinates measured from the leading edge of a crack and the stress components in the crack tip stress field (Paris, P. C. and G. C. Sih. Stress analysis of cracks. In *Fracture toughness testing*. ASTM STP 381).

elastic/plastic and plastic conditions are **crack-opening displacement** and **J-integral** tests.

10.3.2 Linear elastic-fracture mechanics (LEFM)

The basic concept of LEFM is that a crack will extend as a fast linear fracture when the intensity of the stress field at the crack tip reaches a critical level. In order to standardise and validate tests it is necessary to determine first, the distribution of elastic stress around the crack tip, and secondly, the conditions under which plasticity is so limited as to justify an assumption of elastic behaviour.

Figure 10.2 shows the three possible displacement modes for a running crack while Figure 10.3 shows the co-ordinate systems. Modes II and III are observed

with brittle non-metallic materials but for metals they are exceptional, and therefore the discussion will be confined to Mode I. Ignoring higher-order terms in r , the distribution of stress and displacement for Mode I (the opening mode) is given in terms of spherical polar co-ordinates (r, θ, ϕ) by Equations 10.3

$$\begin{aligned}\sigma_x &= \frac{K_I}{(2\pi r)^{1/2}} \cos \frac{\theta}{2} \left[1 - \sin \frac{\theta}{2} \sin \frac{3\theta}{2} \right] \\ \sigma_y &= \frac{K_I}{(2\pi r)^{1/2}} \cos \frac{\theta}{2} \left[1 + \sin \frac{\theta}{2} \sin \frac{3\theta}{2} \right] \\ \tau_{xy} &= \frac{K_I}{(2\pi r)^{1/2}} \sin \frac{\theta}{2} \cos \frac{\theta}{2} \cos \frac{3\theta}{2} \\ \sigma_z &= \nu(\sigma_x + \sigma_y), \quad \tau_{xz} = \tau_{yz} = 0 \\ u &= \frac{K_I}{G} [r/(2\pi)]^{1/2} \cos \frac{\theta}{2} \left[1 - 2\nu + \sin^2 \frac{\theta}{2} \right] \\ v &= \frac{K_I}{G} [r/(2\pi)]^{1/2} \sin \frac{\theta}{2} \left[2 - 2\nu - \cos^2 \frac{\theta}{2} \right] \\ w &= 0\end{aligned}\tag{10.3}$$

ν is Poisson's ratio, which for steel is about 0.3. G is the shear modulus. The principal stresses are σ_x , σ_y and σ_z , shear stresses τ_{xy} etc., and displacements u , v and w . K_I is the **stress intensity factor** and is given by

$$K_I = k(\pi a)^{1/2} \sigma\tag{10.4}$$

where a is the crack length and σ the applied tensile stress remote from the crack. The factor k varies with the geometry of the system: for a crack width $2a$ in the centre of an infinite plate $k = 1$, while for an edge crack of depth a in a semi-infinite plate, $k = 1.12$. For a centre crack the transverse stress along the x axis where $\theta = 0$ (i.e. along the line of the crack) is given by

$$\sigma_y = \left(\frac{a}{2r} \right)^{1/2} \sigma\tag{10.5}$$

Thus, the validity of ignoring the higher-order terms depends on the value of (a/r) . In other words, Equations 10.3 are sufficiently accurate close to the crack tip except in the case of very short cracks. These relationships apply to the **plane strain** condition; that is, where there is no displacement in the direction at right angles to the plate surface (in the z direction). This is the case where the plate is thick relative to the extent of the plastic zone. Figure 10.4 shows the theoretical form of the plastic zone in a thick plate. At the plate surface displacement in the z direction is possible and the **plane stress** condition governs locally. If the plate is thin enough, the plane stress zones merge and the elastic analysis is invalidated by the relatively large plastic region. When the plate thickness is

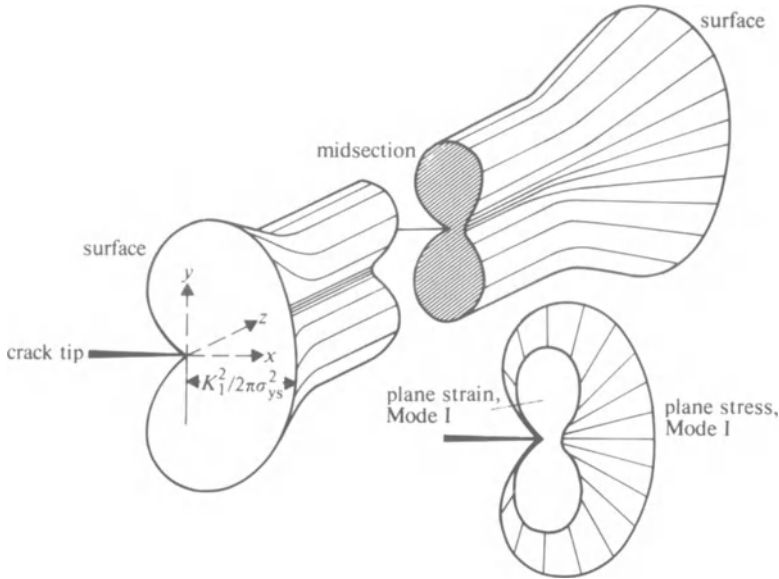


Figure 10.4 Formal representation of plastic zone at the front of a through-thickness crack in a plate (Srawley, J. E. 1969. Linear elastic fracture mechanics. In *Practical mechanics for structural steel*, R. W. Nichols (ed.). UKAEA.)

large compared with $(K_I/\sigma_{ys})^2$, where σ_{ys} is the yield stress, plane strain conditions prevail. K_I varies with crack length and applied stress and is a measure of the intensity of the stress field. Values of K_I are frequently given in imperial units as $\text{Ksi}\sqrt{\text{inches}}$. A convenient SI unit is $\text{N}/\text{mm}^{3/2}$; $1 \text{ Ksi}\sqrt{\text{in}} = 1.368 \text{ N}/\text{mm}^{3/2}$. When K_I reaches the value at which the crack starts to run it is designated K_{IC} , indicating that this is the critical value for crack extension. K_{IC} is the **fracture toughness** and is the measure of the resistance to fast crack propagation when the plate is thick enough, or the yield strength of the material high enough, for plane strain conditions to prevail. Hahn has proposed three categories of failure: (1) linear elastic, (2) non-linear elastic, and (3) plastic instability, and gives the dividing line between categories (1) and (2) as

$$\left(\frac{K_{IC}}{\sigma_{ys}}\right)^2 \frac{1}{a} = 1.2 \quad (10.6)$$

and between categories (2) and (3) as

$$\left(\frac{K_{IC}}{\sigma_{ys}}\right)^2 \frac{1}{a} = 7 \quad (10.7)$$

In practical terms, ductile engineering steels have fracture toughness values in the region of $100 \text{ N}/\text{mm}^{3/2}$, while material with a fracture toughness of about $10 \text{ N}/\text{mm}^{3/2}$ would be regarded as being in a notch-brittle condition.

The relationship between the fracture toughness and the strain-energy release

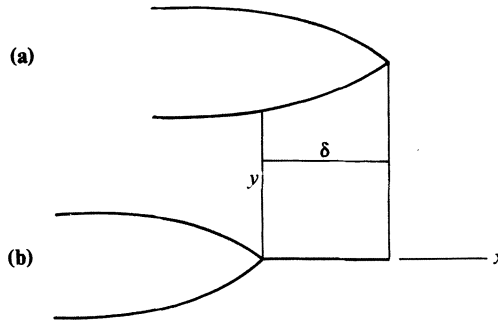


Figure 10.5 The tip of a crack (a) which has been pulled closed (b) along a segment adjacent to the tip (Paris, P. C. and G. C. Sih. Stress analysis of cracks. In *Fracture toughness testing*. ASTM STP 381).

rate (designated G , and sometimes called the **crack extension force**) can be obtained by calculating the work done to close a short length δ of the crack, as indicated in Figure 10.5. The required value is obtained by integrating the product of stress and displacement (the strain energy), obtained from Equations 10.3, over the length δ :

$$G_I = \lim_{\delta \rightarrow 0} \frac{2}{\delta} \int_0^\delta \left(\frac{\sigma_y v}{2} + \frac{\tau_{yx} u}{2} \right) dx \quad (10.8)$$

whence

$$G_I = \frac{(1 - \nu^2)}{E} K_I^2 \quad (10.9)$$

The factor $(1 - \nu^2) \simeq 1$ and is usually ignored. For the centre-cracked infinite plate $K_I^2 = \pi a \sigma^2$ and

$$\sigma = \left(\frac{EG_I}{\pi a} \right)^{1/2} \quad (10.10)$$

which is identical to the Griffiths relationship given in Equation 10.2. The dimensions of G are J/m^2 , as for surface energy. G_{IC} (equal to $(K_{IC})^2/E$) is the critical strain energy release rate for crack extension, and is a measure of the work done per unit area in forming the crack. Thus, G_{IC} is the metallic equivalent of the bonding energy of an adhesive joint γ_a , and the condition for brittle crack extension is similar to that given in Equation 6.10:

$$\partial U / \partial A \geq G_{IC} \quad (10.11)$$

where $\partial U / \partial A$ is the specific rate of release of energy due to relaxation of the strain in the surrounding metal. As pointed out earlier, there may be more than one source of strain energy in an actual structure.

G_{IC} is the effective surface energy of fracture. It varies with the amount of localised plastic strain associated with the fracture, with the proportion of cleavage in the fracture, with bulk mechanical strength of the steel and possibly

other factors. Although it may not be possible to define these contributions to G_{IC} in quantitative terms, it is clear that the effective surface energy of fracture is a material property with an identifiable physical meaning. K_{IC} does not have any such physical meaning and is simply the value of K_I at which a given crack will extend in an unstable manner. K_I in turn is the factor that determines the intensity of the stress field surrounding the crack tip, as defined by Equations 10.3. Nevertheless, the stress-intensity factor is complementary to G in assessing the failure risk. If there are sources of strain energy other than that in the stress field local to the crack tip, then the problem is best considered in terms of energy. If, on the other hand, there are additional sources of stress local to the crack then the stress-intensity factor is the more useful quantity. For example, it has been found experimentally that if there is a welding residual stress in the cracked region equal to σ_r then there is a stress-intensity factor associated with this residual stress.

$$K_r = k(\pi a)^{1/2} \sigma_r \quad (10.12)$$

and this stress intensity factor may be added to that associated with the membrane stress K_0 to given an effective stress intensity factor K_c

$$K_c = K_0 + K_r \quad (10.13)$$

Alternatively, the stresses may be summed:

$$K_c = k(\pi a)^{1/2} (\sigma_0 + \sigma_r) \quad (10.14)$$

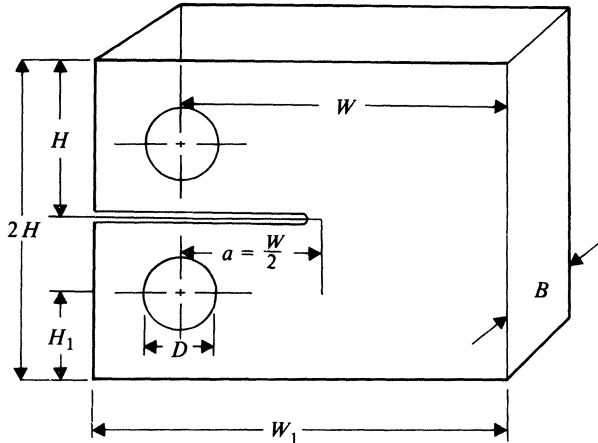
The primary interest of fracture mechanics in the welding field is to assess the potential risk due to the presence of weld defects. Knowing the fracture toughness of a steel it is possible to assess the risk of brittle fracture due to a crack-like defect of any given dimensions. Values for stress-intensity factors for various crack shapes and specimen geometries are given by Paris and Sih in ASTM STP 381 (see 'Further Reading' at the end of this chapter). For example, the factor for a circular crack of radius a lying at right angles to a uniform tensile stress σ in an infinite body is

$$K_I = 2\sigma \left(\frac{a}{\pi} \right)^{1/2} \quad (10.15)$$

Generally, the stress-intensity factor for a defect elongated in the direction of the weld and of depth a is about $(\pi a/2)^{1/2} \sigma$. Such formulae permit order-of-magnitude estimates of the hazard associated with defects by comparing the calculated K_I for the defect with K_{IC} for the material in question. In so doing, allowance must be made for the possible embrittlement of the material; in the case of steel, by strain-ageing, temper embrittlement, transformation, or the presence of dissolved hydrogen. Possibly the simplest method is to calculate the stress-intensity factor for the defect in question and to compare this with such K_{IC} values for embrittled steel as may be available in the literature.

It is also necessary to take account of the possibility of crack extension by fatigue loading, even in those cases where fatigue is not normally a design

consideration: for example, in the case of pressure vessels where loading and unloading take place at start-up and shut-down of the associated plant. Knowing the fatigue loading it is possible to use fatigue crack growth curves (see Section 10.4) for the material in question to adjust the crack size.



$$\begin{aligned} W &= 2.0 B & D &= 0.5 B \\ a &= 1.0 B & W_1 &= 2.5 B \\ H &= 1.2 B & H_1 &= 0.65 B \end{aligned}$$

Figure 10.6 ASTM compact tensile specimen for the measurement of K_{IC} (Wessel, E. T. 1969. Linear elastic fracture mechanics for thick-walled welded steel pressure vessels. In *Practical fracture mechanics for structural steel*, R. W. Nichols (ed.). UKAEA.).

Fracture toughness is measured using notched and precracked rectangular specimens, the dimensions of which are standardised in the relevant national standards, or by notched slow bend tests. Figure 10.6 shows the general configuration of a specimen according to ASTM E-24; precracked bend specimens similar to those used for crack opening displacement tests may also be employed. An important limitation is that for plane strain conditions both a and B (plate thickness) must be equal to or greater than $2.5 (K_{IC}/\sigma_{ys})^2$, and test results not conforming to this criterion are considered invalid. For unembrittled carbon and carbon-manganese steels the specimen dimensions required to meet the ASTM E-24 criterion are impracticably large; even for a steel with a yield stress of 500 MN/m^2 a specimen thickness of 300 mm is required. For lower-strength steels, and for cases where general yielding precedes fracture, other methods are used to determine fracture toughness, as discussed below.

10.3.3 Alternative means of estimating or measuring fracture toughness

Consider a centre crack of length $2a$ in an infinite plate and apply a uniform tensile stress at right angles to the crack. Under plastic conditions the crack

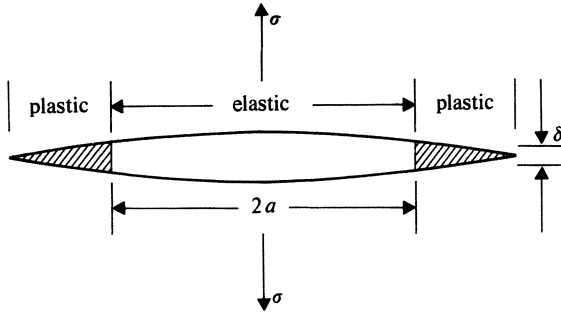


Figure 10.7 Assumed form of plastic deformation at the tip of a centre crack of length $2a$.

opens, and it is assumed that plastic wedges are formed at each end which prevent crack extension until a critical value of the plastic displacement at the crack tip is reached (Fig. 10.7). It may be shown that the displacement δ is given by

$$\delta = 8 \frac{\sigma_{ys}}{\pi E} a \ln \sec \left(\frac{\pi \sigma}{2\sigma_{ys}} \right) \quad (10.16)$$

Expanding the $\ln \sec$ term

$$\delta = \frac{8\sigma_{ys}}{\pi E} a \left[\frac{1}{2} \left(\frac{\pi \sigma}{2\sigma_{ys}} \right)^2 + \frac{1}{12} \left(\frac{\pi \sigma}{2\sigma_{ys}} \right)^4 + \frac{1}{45} \left(\frac{\pi \sigma}{2\sigma_{ys}} \right)^6 \dots \right] \quad (10.17)$$

Using the first term of the expansion only

$$\delta \simeq \frac{\pi \sigma^2 a}{E \sigma_{ys}} \quad (10.18)$$

But from Equation 10.10

$$G_I = \frac{\pi \sigma^2 a}{E}$$

Therefore, at the point of instability

$$G_{IC} = \sigma_{ys} \delta_C \quad (10.19)$$

where δ_C is the critical crack-opening displacement (critical COD). Thus, it is possible to obtain an estimate of the strain-energy release rate at fracture without reference to the elastic stress distribution at the crack tip, and under conditions where there may be general yielding. One disadvantage of this method is that it is not possible to derive analytical relationships between the critical COD for a centre-cracked plate and that for other geometries. However, it may reasonably be assumed that the same relationship applies as in the elastic case, and where this assumption has been tested by experiment it appears to hold quite well.

It is now thought that the yield stress σ_{ys} is not the value measured in a

uniaxial tensile test σ_y but the stress for yielding under the constraint that exists at the root of the notch. This will in general be higher than σ_y by a factor m (as indicated later in Equation 10.21). This factor has been computed as lying between about 1.0 and 3.0, and experimental results would appear to lie within this range.

Note also that Equation 10.18 becomes increasingly inaccurate as $(\pi\sigma/2\sigma_{ys})$ exceeds unity. The same is generally true for other approximations made in translating the results of fracture toughness tests in the elastic/plastic range into values of G or K ; on the other hand, the values of stress to which real structures are exposed is, except for localised regions, relatively small and therefore the equivalence of, say, δ and G is valid for cracks other than those situated in regions of above-yield stress. Crack-opening displacement tests are made using a full-plate thickness specimen containing a machined notch which is extended by fatigue cracking (Fig. 10.8).

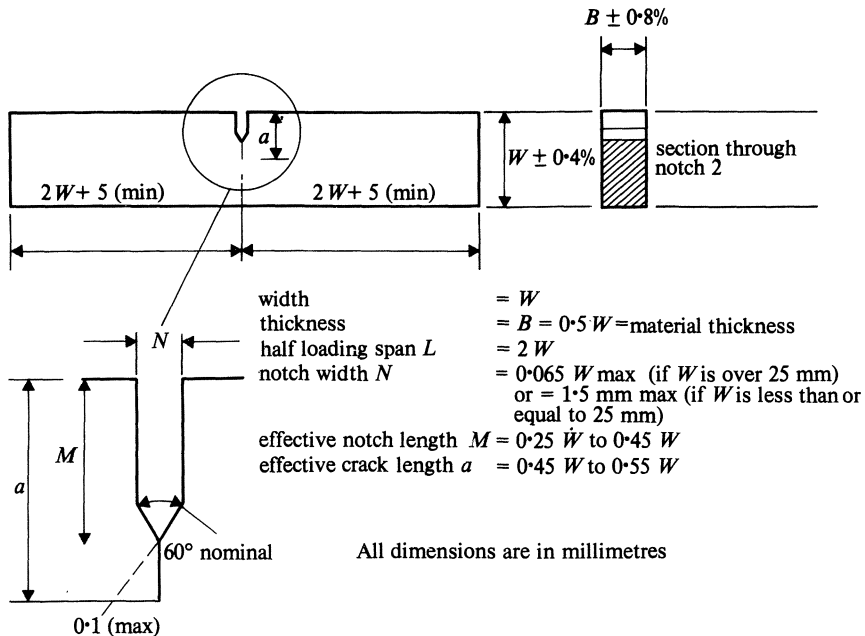


Figure 10.8 COD test specimen. The testpiece is bent in three-point loading and the displacement at the crack tip measured continuously to failure. There are no restrictions as to the validity of the test results.

A method of obtaining an equivalent to the stress-intensity factor for elastic/plastic conditions is to calculate the stresses and displacements for the configuration in question, and then integrate strain energy around a closed path that includes the crack tip. The result (designated J) is theoretically independent of the path taken, and it is related to the stress-intensity factor in the same way as G

$$J = \frac{K^2}{E} \quad (10.20)$$

One problem with this method is to assess strain energy in the plastic region. The integration is carried out numerically after dividing the section of the specimen into a suitable grid pattern. J is related to COD by

$$J = m\sigma_y\delta \quad (10.21)$$

where m is a factor that usually lies between 1 and 3.

A general correlation between Charpy V-notch test results and K_{IC} is not practicable. On theoretical grounds, it would be difficult to justify such a correlation because of the small size of the Charpy specimen, the lack of a sharp notch, and impact loading. Nevertheless empirical relationships have been established between C_v and K_{IC} for particular steels so that (apart from the wealth of practical experience in the use of impact testing) there is a justification for using the Charpy V test as a means of controlling fracture toughness.

10.4 SLOW CRACK PROPAGATION

There are a number of modes of slow cracking which may affect welds, including hydrogen cracking, reheat cracking, creep cracking, stress corrosion cracking, and fatigue. To some degree the concepts of LEFM can be used for the study and understanding of these phenomena, and indeed they have already been applied to hydrogen cracking in Section 7.5.3.5. Reheat and creep cracking both occur by the nucleation and growth of cavities along the grain boundaries or other interfaces, and LEFM is irrelevant. Nevertheless, it is found experimentally that where the test specimen contains a crack of length a , the crack growth rate is, in many instances, proportional to the n th power of the stress-intensity factor

$$\frac{\partial a}{\partial t} \propto (K)^n \quad (10.22)$$

The exponent n lies between 3 and 30, and for any given material has a value similar to the exponent for the rate of strain in secondary creep. In other cases the crack growth rate correlates better with the net section stress (load divided by uncracked sectional area). Justification for such correlations is possible using the techniques of non-linear fracture mechanics.

Reheat cracking occurs most frequently during PWHT, but may also occur in service. Reheat cracking in service is almost entirely confined to welds in $\frac{1}{2}$ Cr $\frac{1}{2}$ Mo $\frac{1}{4}$ V steel and is prevented either by using a different steel, such as $2\frac{1}{4}$ Cr 1 Mo, or by controlling the composition of the alloy to minimise the content of impurities that contribute to the high-temperature cracking. Creep-rupture cracking is avoided by using weld metal of improved rupture properties.

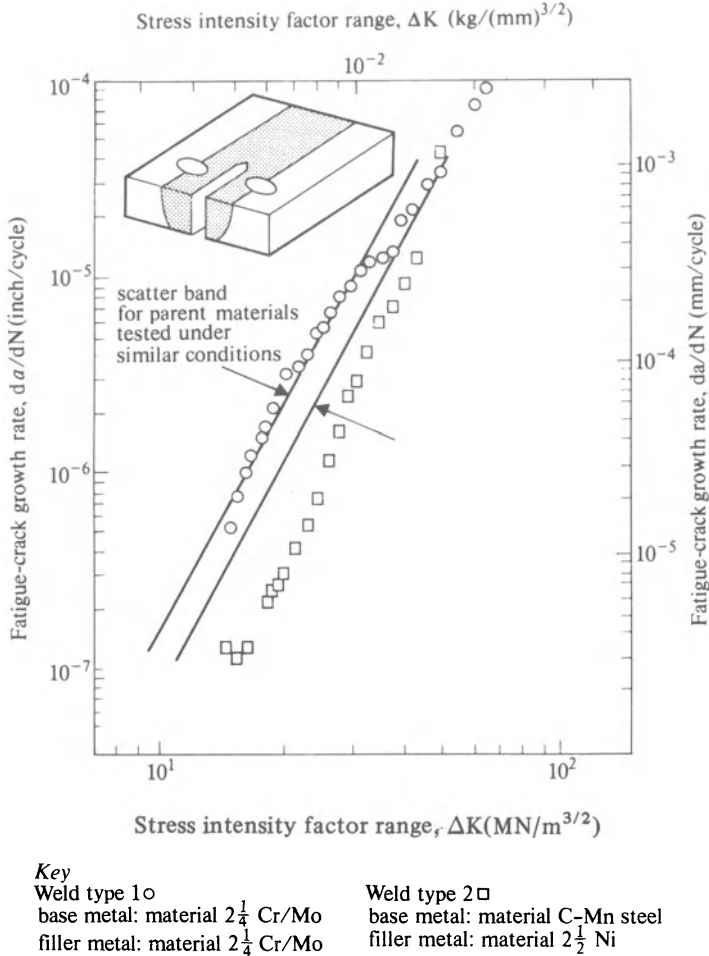


Figure 10.9 Fatigue-crack growth behaviour of pressure-vessel steel weldments tested in an air environment at 24 °C (James, L. A. 1977. *Welding J.* 56, 386–91).

In both cases the fracture mechanism is ductile, but it occurs along planes of weakness within the structure and is therefore crack-like.

The rate of growth of fatigue cracks, and of fatigue cracks in welds in particular, can be correlated with the stress-intensity range ΔK to which the specimen or structure is exposed. The crack growth rate is given by

$$\frac{da}{dN} = C_0 (\Delta K)^n \tag{10.23}$$

where C_0 is a constant and n varies in the range 2 to 30. Figure 10.9 shows a typical plot. In the case of fatigue there is no size effect and small laboratory

test specimens can be used to assess growth rates in large sections. Fatigue cracking is primarily of concern in structures exposed to fluctuating loads, such as bridges, but (as discussed earlier) may be a factor in the design of pressure vessels.

Stress corrosion cracking may also be studied using LEFM techniques. With certain combinations of metal and environment there is a value of K below which stress corrosion cracks do not propagate, this limit being designated K_{ISCC} . Such data are not, however, of much value for welds because the driving force for SCC of fusion welds is the residual stress, which is in the region of the yield stress and above most SCC threshold levels. This is not always the case; for example, stress corrosion cracking of steel by H_2S requires a relatively high level of absolute stress and can be avoided in pipework by limiting the weld hardness to 200 BHN. The same limit may be used for aqueous solutions of cyanides.

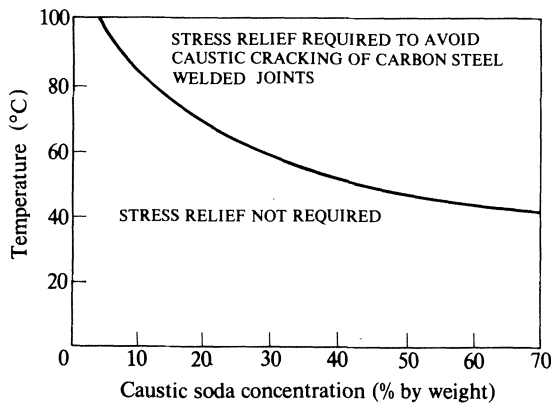


Figure 10.10 Conditions under which stress relief of welded joints in carbon steel is required in order to avoid stress corrosion cracking in caustic soda solution.

Caustic alkalis, sodium and potassium carbonate, and nitrate solutions may cause intergranular SCC of carbon and low-alloy steel. Figure 10.10 shows the concentration/temperature limit above which it is necessary to stress-relieve carbon steel welds in order to avoid caustic SSC. Stress corrosion cracking has also been observed where welds containing a pre-existing crack or crack-like defect are in contact with high purity boiler feed water at elevated temperature.

The stress corrosion cracking of austenitic chromium–nickel steel welds by chlorides has been mentioned in Chapter 8. In principle, chloride SCC of austenitic stainless steel may be avoided by stress relief at 850 °C to 900 °C. In so doing, it is necessary to support the joint adequately to avoid stress-rupture failure and also in the case of localised PWHT of pipe welds, to ensure that the temperature gradient at the edge of the heated zone is as low as practicable. In practice it is exceptional to attempt this PWHT. An alternative solution is to select a more resistant alloy. The molybdenum-bearing type 316

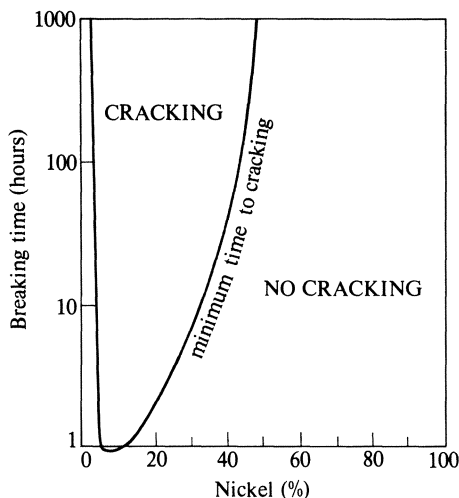


Figure 10.11 Effect of nickel on stress corrosion cracking (Copson, H. R. 1959. Effect of composition on stress corrosion cracking of some alloys containing nickel. In *Physical metallurgy of stress corrosion fracture*. New York: Interscience Publishers).

steel is significantly more resistant to SCC than types 304, 321 or 347. Reducing or increasing the nickel content may be beneficial. Figure 10.11 illustrates this possible approach. Higher nickel grades such as alloy 20 Cb 3 (with up to 35% Ni) are more resistant but also more costly. Lower nickel grades such as the 26 Cr 5 Ni $1\frac{1}{2}$ Mo are similar in price to type 316 but may present difficulties due to embrittlement in the HAZ of welds. Indeed, there is no generally satisfactory solution to the problem of SCC of austenitic chromium–nickel steel.

Table 10.1 lists alloy combinations that may be subject to SCC. This list is not exhaustive but is intended to include those cases where SCC of welded joints is possible.

10.5 CORROSION OF WELDS

Selective corrosion of welds is inevitable in certain environments due to differences in structure, segregation, or different alloy content as compared with the parent metal. Figure 10.12 shows the various modes of wastage to which welds may be subject. In some instances it is not easy to predict which mode will dominate. For example, carbon-steel welds exposed to sea water may corrode preferentially either in the weld metal or in the HAZ. In wet CO_2 corrosion is usually confined to the HAZ, forming a double groove on either side of the weld bead. One special case of selective corrosion of carbon-steel weld metal may occur in HF alkylation units, where the alkylation catalyst is dry HF. In the absence of water the mixture of HF and hydrocarbon is

Table 10.1 Alloy systems subject to stress corrosion cracking (adapted from 'The role of stainless steels in petroleum refining', American Iron and Steel Institute Publication SS 607-477-20M-HP, 1977)

<i>Alloy</i>	<i>Environment</i>
Aluminium base	Air Sea water Salt and chemical combinations
Magnesium base	Nitric acid Caustic HF solutions Salts Coastal atmospheres
Copper base	Primarily ammonia and ammonium hydroxide Amines Mercury
Carbon steel	Caustic Anhydrous ammonia Nitrate solutions CO/CO ₂ solutions H ₂ S and cyanides in aqueous solution
Martensitic and precipitation hardening stainless steels	Seawater Chlorides H ₂ S solutions
Austenitic stainless steels	Chlorides – inorganic and organic Caustic solutions Sulphurous and polythionic acids
Nickel base	Caustic above 600 °F (315 °C) Fused caustic Hydrofluoric acid
Titanium	Seawater Salt atmospheres Fused salt

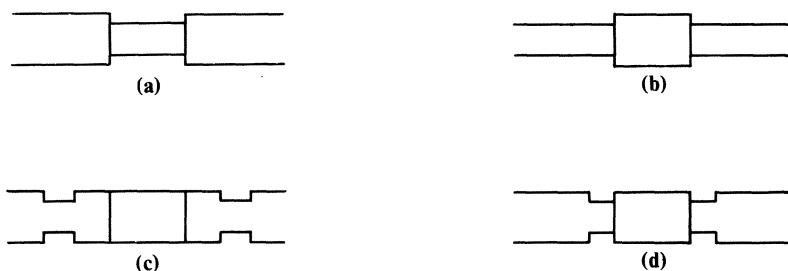


Figure 10.12 Selective corrosion of welds: (a) parent metal passive; (b) weld metal passive; (c) low temperature HAZ attack; (d) high temperature HAZ attack.

non-corrosive to carbon steel but will attack any slag inclusions present at the surface of the weld.

Austenitic chromium–nickel steels suffer preferential corrosion of the weld metal under various conditions. In acid chloride environments which are encountered in the food industry type 316 weld metal may be selectively attacked, and one solution to this problem is to raise the molybdenum content of the weld metal, say, 1% above that of the parent metal. In urea plants the urea reactor may be clad with type 316L stainless steel either by using roll-bonded plate or by weld deposit cladding. In either case, the weld metal is subject to selective attack if any substantial amount of ferrite is present, and it is usual to limit the ferrite content to 2% maximum. Selective attack on ferrite is also possible in hot mineral acids and other acid environments.

Intergranular attack adjacent to the weld (knife-line attack) and weld decay in the more remote part of the HAZ have been described in Chapter 8. This type of problem is avoided by using extra low carbon grades of stainless steel or, in the case of weld decay, stabilised grades. IG corrosion of ferritic chromium steel welds may occur in the weld and HAZ. In this case it results from the solution of carbides and nitrides at temperatures above 950 °C, followed by their reprecipitation on rapid cooling. Limitation of carbon and nitrogen to very low levels is necessary for immunity. Ferritic/austenitic steels behave more like austenitic steels in this respect.

Aluminium is a useful metal for handling strong nitric acid, but high-purity aluminium is required for the more severe conditions. In such conditions weld metal is selectively attacked, probably because of the inevitable segregation in the cast structure of the weld.

Under special conditions exposure to elevated temperature may cause deterioration of welds. Hot, hydrogen-rich gas may attack carbon and low-alloy steels at temperatures above 250 °C, as described in Section 7.5.3.1. The operating conditions (partial pressure and temperature of hydrogen) below which carbon steel and Cr–Mo steels may safely be exposed to hydrogen are given by the **Nelson chart**, published by the American Petroleum Institute (API Publ. 941). Normally equipment is designed to conform to this chart, but in exceptional circumstances hydrogen corrosion may take place and it is not uncommon for the HAZ of fusion welds to be preferentially attacked.

Under non-corrosive conditions carbon and carbon–manganese steel welds may lose strength due to **graphitisation**. If steel is held at temperatures above 450 °C for long periods of time the cementite may decompose, eventually forming nodules of graphite in a low-carbon iron matrix. The breakdown of cementite appears to be promoted by the addition of aluminium to the steel. Carbon and carbon– $\frac{1}{2}$ Mo steels are both susceptible to this defect; however, in carbon steel the graphite nodules tend to be scattered and do not form localised areas of weakness. In C– $\frac{1}{2}$ Mo steel, on the other hand, the graphite forms ‘eyebrows’ in the HAZ, and there have been isolated failures in steam lines from this cause. Cr–Mo steels do not suffer graphitisation since the carbides are more stable. For this reason, Cr–Mo material is often specified

for elevated temperature duties (particularly piping) where in other respects $C\frac{1}{2}$ Mo steel would be adequate. Alternatively, samples may be removed from the pipe from time to time and examined metallographically for evidence of graphitisation.

10.6 RISK ANALYSIS

There are various circumstances under which it is required to assess the failure risk associated with weld defects. Most frequently this is when a defect has been found in service; cracks or crack-like defects appearing during manufacture will normally be repaired in accordance with the requirement of the governing code.

The method of assessment is generally as follows:

- (a) Characterise the flaw (i.e. find the simple geometric form equivalent to the actual or postulated flaw).
- (b) Determine the steady stress.
- (c) Determine the cyclic load.
- (d) Estimate K_I and ΔK .
- (e) Measure or estimate K_{IC} .
- (f) From (d) and (e) estimate the time for the flaw to grow to critical size.

Formal methods of characterising flaws have been developed and are given in, for example, the ASME code Section XI. Note that the analysis does not apply to stress corrosion cracking or to cracks exposed to a potentially corrosive medium. However, it may be possible to measure the rate of growth of stress corrosion cracks ultrasonically and determine when they are likely to reach critical size. The stress analysis should consider all forms of stress, including pressure stresses, thermal stresses, discontinuity stresses and residual stress due to fabrication. Similarly, all cyclic loads must be considered. Having done this, it will be practicable to determine K_I and ΔK . Where flaws are in steel plate there may be a lower limit of stress intensity range ΔK below which no fatigue crack extension occurs. In welds, however, this is unlikely to be the case.

The technique outlined above applies specifically to those structures where the strain energy content is substantially equal to that of a plate subject to the various loadings under consideration. It may also be necessary to take into account external sources of strain energy such as pipe branches subject to a steady load, or impact loads due to collision or by the local failure of supports. Such an analysis may reinforce intuition by indicating the need for a design change: for example, the elimination of pipe branches on road tankers carrying inflammable or toxic liquids. A quantitative analysis may not always be practicable but order-of-magnitude estimates may be useful in indicating areas of potential risk.

Estimation of K_{IC} remains a potentially difficult task because for most steels used in welded structures valid measurements cannot be made. Therefore,

it is necessary to make estimates from COD or Charpy impact test values. Having done so, it is equally necessary to assess the risk of embrittlement, because generally it is only through some embrittlement mechanism that a real failure risk arises. An order-of-magnitude assessment at this stage will indicate, as a rule, whether a hazard exists and how far it will be necessary to refine the analysis. Finally, the risk assessment is completed by determining the time required for a critical-size crack to develop. Although this type of analysis is attended by numbers of uncertainties, it can often quantify the risk associated with the size of defect normally present in, say, pressure vessel welds and permit a rational decision as to future action.

FURTHER READING

Fracture toughness 1968. ISI Publications 120 and 121.

Fracture toughness testing 1965. ASTM STP 381.

Progress in flaw growth and fracture toughness testing 1973. ASTM STP 536.

The mechanics and physics of fracture 1975. London: The Metals Society and the Institute of Physics.

Bazovski, I. 1961. *Reliability theory and practice*. Englewood Cliffs, N.J.: Prentice-Hall.

Rolfe, S. T. and J. M. Basson 1977. *Fracture and fatigue control in structures*. Englewood Cliffs, N.J.: Prentice-Hall.

American Society for Metals 1975. *Metals handbook*, 8th edn, vol. 10.

Appendix 1 Symbols

		<i>Units</i> (<i>nd = non-dimensional</i>)
a	crack length, spherical radius	m
	acceleration	m/s ²
B	basicity index	nd
	magnetic flux density	N/m A
	specimen width	m
c	concentration	nd
C	constant	nd
C_p	specific heat at constant pressure	J/kg K
d	lateral separation, width, grain size	m
D	coefficient of diffusion	m ² /s
e	electronic charge	q (coulombs)
erf	error function	nd
E	modulus of elasticity	MN/m ²
F	force	N
g	acceleration due to gravity	m/s ²
G	crack extension force	J/m ²
	free energy of formation	J/mol
	shear modulus	MN/m ²
	solidification temperature gradient	K/m
h, H	vertical height	m
I	current	A
$I_n(z)$	modified Bessel function of the first kind of order n	nd
J	current density	A/m ²
k	any proportional factor	nd
	Boltzmann's constant	J/K
K	absolute temperature	K
	equilibrium constant of a chemical reaction	nd
	stress intensity factor	MN/m ^{3/2}
K_I	stress intensity factor in the opening mode (I)	MN/m ^{3/2}
K_{IC}	critical value of K_I for unstable crack extension	MN/m ^{3/2}
K_n	modified Bessel function of the second kind of order n	nd
ln	logarithm to base e	nd
log	logarithm to base 10	nd
l, L	length, distance	m
m	any integer	nd
M	any metal	nd

		Units
		(<i>nd</i> = non-dimensional)
n	any numerical factor	nd
P	pressure	N/m ²
Pr	Prandtl number $\eta C_p / \kappa$	nd
q	rate of heat/energy flow	W
	electric charge, coulombs	q
Q	quantity of heat/energy	J
r	radius	m
R	gas constant	J/mol K
R, R_0	outer radius of a cylinder	m
R	solidification rate	m/s
s	time in seconds	s
S	solubility (gas in metal)	ppm, g/tonne
T	temperature	K, °C
U	strain energy	J
V	voltage	V
w	thickness	m
W	work of cohesion	J/m ²
	rate of heat/energy flow	W
α	diffusivity of heat	m ² /s
	coefficient of thermal expansion	K ⁻¹
γ	surface tension	N/m
	surface energy	J/m ²
δ	longitudinal displacement	m
	crack opening displacement	m
δ_c	critical crack opening displacement	m
Δ	increment	nd
ϵ	radial displacement	m
η	viscosity	kg/sm
	arc efficiency	nd
θ	angle	nd
	absolute temperature	K
κ	thermal conductivity	W/mK
λ	wavelength	m
	chance failure rate	s ⁻¹
	cos θ	nd
μ	magnetic permeability	N/A ²
μ_0	permeability of free space	N/A ²
ν	kinematic viscosity	m ² /s
	Poisson's ratio	nd
ρ	mass density	kg/m ³
σ	stress	MN/m ²
	electrical conductivity	A/Vm
σ_u	ultimate stress	MN/m ²
σ_y	yield stress	MN/m ²
τ	non-dimensional time $(v^2/2\alpha)t$	nd
	shear stress	MN/m ²

		Units (<i>nd</i> = non-dimensional)
ϕ	angle	nd
	electron work function	J
Φ	viscous dissipation of energy	J/m ³
ψ	stream function	m ³ /s
ω	frequency	s ⁻¹
	inverse time constant for instability	s ⁻¹

VECTOR NOTATION

$$\mathbf{v} = i v_x + j v_y + k v_z$$

where i , j and k are unit vectors in the x , y and z directions respectively.

$$\nabla p = \text{grad } p = i \frac{\partial p}{\partial x} + j \frac{\partial p}{\partial y} + k \frac{\partial p}{\partial z}$$

$$\nabla \cdot \mathbf{v} = \text{div } v = \frac{\partial v_x}{\partial x} + \frac{\partial v_y}{\partial y} + \frac{\partial v_z}{\partial z}$$

$$\nabla \times \mathbf{v} = \text{curl } v = i \left(\frac{\partial v_z}{\partial y} - \frac{\partial v_y}{\partial z} \right) + j \left(\frac{\partial v_x}{\partial z} - \frac{\partial v_z}{\partial x} \right) + k \left(\frac{\partial v_y}{\partial x} - \frac{\partial v_x}{\partial y} \right)$$

$$\nabla^2 T = \frac{\partial^2 T}{\partial x^2} + \frac{\partial^2 T}{\partial y^2} + \frac{\partial^2 T}{\partial z^2}$$

$$\nabla^2 \mathbf{v} = i \left(\frac{\partial^2 v_x}{\partial x^2} + \frac{\partial^2 v_x}{\partial y^2} + \frac{\partial^2 v_x}{\partial z^2} \right) \quad \text{etc.}$$

$$(\mathbf{v} \cdot \nabla) T = v_x \frac{\partial T}{\partial x} + v_y \frac{\partial T}{\partial y} + v_z \frac{\partial T}{\partial z}$$

Appendix 2 Conversion factors

<i>To convert SI to A multiply by</i>	<i>A</i>	<i>SI</i>	<i>To convert A to SI multiply by</i>
1×10^{10}	Ångström unit	m	1×10^{-10}
$9.869\,2 \times 10^{-6}$	atmosphere	N/m ²	$1.013\,25 \times 10^5$
1×10^{-5}	bar	N/m ²	1×10^5
$9.478\,17 \times 10^{-4}$	BThU	J = N m	$1.055\,06 \times 10^3$
$5.265\,65 \times 10^{-4}$	BThU/°F	J/K	$1.899\,09 \times 10^3$
0.056 869	BThU/min	W = J/s	17.584 26
$4.299\,23 \times 10^{-4}$	BThU/pound	J/kg	2.326×10^3
0.316 998	BThU/ft ² /hr	W/m ²	3.154 59
0.577 8	BThU/ft ² /hr for a temperature gradient of 1 °F/foot	W/m K	1.730 73
0.238 846	calorie	J	4.186 8
$2.388\,46 \times 10^{-5}$	calorie/cm ² /sec	W/m ² s	$4.186\,8 \times 10^4$
$2.388\,46 \times 10^{-4}$	calorie/g	J/kg	$4.186\,8 \times 10^3$
$2.388\,46 \times 10^{-4}$	calorie/g/°C	J/kg K	$4.186\,8 \times 10^3$
$2.388\,9 \times 10^{-4}$	kg calorie/g-mol	J/mol	$4.186\,8 \times 10^3$
35.314 7	cubic foot	m ³	0.028 316 8
$6.102\,4 \times 10^4$	cubic inch	m ³	$1.638\,71 \times 10^{-5}$
1×10^5	dyne	N	1×10^{-5}
1×10^7	dyne cm	N m	1×10^{-7}
1×10^3	dyne/cm	N/m	1×10^{-3}
10	dyne/cm ²	N/m ²	0.1
1×10^7	erg	J	1×10^{-7}
1×10^3	erg/cm ²	J/m ²	1×10^{-3}
1×10^7	erg/sec	W	1×10^{-7}
3.280 84	foot	m	0.304 8
23.730 4	foot poundals	J	0.042 14
0.737 56	foot pound-force	J	1.355 82
$2.199\,69 \times 10^2$	gallon (UK)	m ³	$4.546\,09 \times 10^{-3}$
$2.641\,72 \times 10^2$	gallon (US)	m ³	$3.785\,41 \times 10^{-3}$
$1.543\,24 \times 10^4$	grain	kg	$6.479\,9 \times 10^{-5}$
1.0×10^{-3}	gram/cubic cm	kg m ⁻³	1.0×10^3
1.0	gram-mol (c.g.s.)	mol	1.0
1×10^{-7}	hectobar	N/m ²	1×10^7
$1.341\,02 \times 10^{-3}$	horsepower	W	745.7

<i>To convert SI to A multiply by</i>	<i>A</i>	<i>SI</i>	<i>To convert A to SI multiply by</i>
39.370 1	inch	m	2.54×10^{-2}
2.362 21	inches/min	mm/s	0.423 33
0.101 972	kilogramme-force	N	9.806 65
$1.019\,72 \times 10^{-5}$	kilogramme force per square centimetre	N/m ²	$9.806\,65 \times 10^4$
0.101 972	kilogramme force per square millimetre	MN m ⁻²	9.806 65
0.224 809	pound-force	N	4.448 221 6
$9.999\,72 \times 10^2$	litre	m ³	$1.000\,028 \times 10^{-3}$
0.039 370 1	mil (thou)	μ m (micron)	25.4
0.621 371	mile	km	1.609 344
10	poise (dyn s cm ⁻²)	Ns/m ²	0.1
7.233 01	poundal	N	0.138 255
0.204 809	pound-force	N	4.448 22
1.45038×10^{-4}	pound-force per square inch	N/m ²	$6.894\,76 \times 10^3$
$3.612\,73 \times 10^{-5}$	pound per cubic inch	kg m ⁻³	$2.767\,99 \times 10^4$
1.55×10^3	square inch	m ²	$6.451\,6 \times 10^{-4}$
10.763 9	square feet	m ²	0.092 903
0.386 100 6	square miles	km ²	2.589 998
1×10^4	stoke, cgs unit of diffusivity or thermal diffusivity (cm ² s ⁻¹)	m ² /s	1×10^{-4}
$9.842\,07 \times 10^{-4}$	ton (UK)	kg	$1.016\,05 \times 10^3$
$1.102\,31 \times 10^{-3}$	ton (short ton, US)	kg	907.185
0.100 361	UK ton-force	kN	9.964 02
0.064 749	UK ton-force per square inch	MN/m ²	15.444 3
$7.500\,62 \times 10^{-3}$	Torr (1 mm mercury)	N/m ²	133.322

Index

- adhesive bonding 91–2, 103–8, 205
- age-hardening
 - aluminium alloys 203, 204
 - nickel alloys 213
 - stainless steels 195–6
- aluminium
 - adhesive bonding 205
 - fracture toughness of steel and 132, 164
 - graphitisation of steel and 241
 - as deoxidant in steel 112
 - as grain-refiner of steel 122, 132, 164
 - welding and brazing of 197–8
- aluminium bronze 210
- antimony in solder 96
- arc
 - as welding heat source 32–9
 - efficiency 13, 34–5
- austenite
 - solidification cracking and 116–17, 182–4
 - forming elements 179–80
 - in carbon steel welds 118, 121–5
- bainite
 - effect on HAZ toughness 132
 - in carbon steel weld metal 122
 - in HAZ 124, 126, 132
 - structure 132
- basicity of SAW flux 114–15
- beryllium 218–19
- bismuth 209
- bonding mechanisms 74–6, 87–91
- boron 94, 98–9
- brass 207
- brazing 93–5, 97–103, 198
- bronze welding 102
- buttering 58, 156–7, 162
- calcium 70, 112
- cap copper 209, 210
- carbide
 - intergranular 174, 181, 182
 - intragranular 186
 - precipitation 174, 180–2
 - solution treatment 182
- carbon
 - effect on hydrogen cracking 145
 - effect on solidification cracking
 - carbon steel 116–18
 - austenitic Cr–Ni steel 183–4
 - equivalent 129–31, 149, 164
 - porosity in welds 53–5, 111–12, 198–9, 208, 213
- carbon steel welds
 - corrosion of 241–2
 - gas content 140–4
 - grain size 121–4, 127–8
 - macrostructure 123
 - mechanical properties 126–35
 - microstructure 120–6
 - porosity 111–12
 - slag–metal reactions 112–16
 - solidification cracking 116–18
- cast iron, welding of 160–3
- catastrophic oxidation 194–5
- caustic soda 238
- Charpy impact test 133, 236
- chevron cracking 116, 152–4
- clad plate 193–4
- cleavage strength 74–5
- coated electrodes
 - coating types 15, 140–4, 128–9
 - moisture content 15, 141–3
- coherence temperature 64, 200
- cohesion 74–6, 88
- cold pressure welding 83
- conservation laws 19–20
- continuous cooling transformation (CCT)
 - 120, 124–5, 146, 165–6
- controlled thermal severity (CTS) test
 - 147–8
- cooling rate
 - effect on hydrogen-induced cracking 131–2, 143, 152
 - effect on microstructure 59–63
 - heat input rate and 13, 43–4, 47–8
 - measurements 47–8
 - theoretical 43–4
- copper 207–11
- corrosion of welds
 - austenitic Cr–Ni steel 187–93, 241
 - carbon steel 239–41
 - hydrogen 136
 - intergranular 187–90
 - knife-line attack 187–9
 - modes 239–40
 - preferential 191–2, 239–41
 - stress corrosion 190–1, 240
 - weld decay 187
- crack extension force 231–2
- crack growth 226–8, 236–9
- cracking modes
 - carbon and 116–18
 - chevron 152–4
 - cold 63
 - delayed 147
 - ductility dip 69, 154, 184
 - HAZ 13, 139–40, 185–7
 - hot 13, 63, 185–6, 209, 241
 - hydrogen 13, 138–52

- intergranular 64–6, 139, 154, 157, 183, 184, 186, 191
- lamellar tearing 155–6
- liquation 170, 199, 202
- macro 63, 64–7
- micro 63, 64–7
- nickel content and 117
- reheat 156–60, 186–7
- shrinkage 66
- solidification 66–7, 116–18, 182–4, 199–202, 206, 209
- stress-corrosion 190–1, 199, 238, 240
- subsolidus 63, 67
- supersolidus 63, 64–7
- weld boundary 185
- weld metal 66, 139–40, 182–4
- crack-opening displacement tests 235
- theory 233–5
- cupronickel 210–11
- delayed fracture 136–7, 147
- deoxidation and deoxidants
 - aluminium 112, 198, 208, 212
 - calcium 70, 112
 - carbon steel 110–12
 - coated electrodes 15, 111
 - copper 208–9
 - GMA welding 111–12
 - GTA welding 111
 - lithium 222
 - manganese 112, 208
 - phosphorus 208
 - porosity and 54–5
 - silicon 112, 208
 - titanium 112, 208, 211, 212
 - zirconium 70, 112
- dew point 99, 101
- diffusion 56–9
- diffusion bonding 79, 80, 82, 103
- dilution 58–9
- dispersion equation 24
- dispersion forces 75, 88
- dissimilar metal joints 81, 82, 84, 193–4, 207
- dissociation
 - gases 35, 37, 99–101
 - metal oxides 53–4, 98–101, 114
 - pressure of oxides 99
- ductility dip cracking 69, 154, 184
- edge preparation 16–17
- electron beam welding 11, 12, 16, 42
- electron work function 33, 36
- electroslag welding
 - cracking 66
 - cooling rate 68
 - grain size 62, 68, 123
 - macrostructure 123, 128
 - process 8
- elevated temperature properties 129, 172–3, 194–5
- embrittlement
 - by PWHT 129, 134, 165
 - ductility dip 69–70
 - fusion welds 68–70
 - gas absorption 217–18
 - HAZ 68–9
 - hydrogen 134–9
 - recrystallisation 218–19
 - secondary hardening 134, 165
 - sigma phase 180
 - steam reaction 208
 - strain-age 124, 133, 134
 - temper 69, 129, 134, 139, 176
 - transformation 121–4, 131–2
- epitaxial grain growth 59
- explosive welding 81, 84–6
- fatigue properties
 - carbon steel welds 126–7
 - crack growth rate 236–8
 - weld profile and 126
- ferrite
 - acicular 120, 127–8
 - forming elements 179–80
 - grain size 127
 - pro-eutectoid 120, 124, 127, 128
- flash-butt welding 79, 80
- flowability 95
- flux
 - acid 15, 114
 - active 114
 - as a shielding agent 14, 15
 - basic 15, 114, 128
 - basicity 114–15
 - neutral 15, 114
 - types 115
- forge welding 1
- fracture mechanics
 - application to hydrogen cracking 146–7
 - measurement of K_{IC} 233–6
 - theory 228–32
- fracture toughness
 - definition 230
 - of HAZ in steel 131–4
 - measurement of 233–6
- free energy of formation 53–5, 98–101
- free-machining steel 183
- freezing time 60
- friction welding 81, 83–4
- full penetration welding 16
- fusion welding 6–7
- fusion zone 6–7
- gas metal arc welding (GMA)
 - current density 22, 29
 - efficiency 23–5
 - metal transfer 21, 22
 - of aluminium 197

- cast iron 162
- copper 207–8, 210
- nickel 213, 216
- steel 111, 127, 151, 159, 167, 170, 174–5
- process 8
- Gas tungsten arc welding (GTA)
 - a.c. 197
 - current density 34–5
 - efficiency 33–5
 - of aluminium 197
 - copper 207–8, 210
 - low-melting metals 221
 - magnesium 206
 - nickel 216
 - precious metals 222
 - reactive welds 210, 216–17, 219
 - steel 127, 170, 176
 - process 9
 - gas welding 2–3, 9
- gases in weld metal
 - absorption 52–3
 - diffusion 56–8
 - evolution 55–8, 198–9
 - reactions 51–3, 110–12, 208
 - solubility 52–3, 198
- glove box 217
- gold 222
- grain coarsening temperature 122, 123
- grain size
 - aluminium and 123
 - austenitic 124, 127
 - cooling rate and 68
 - fracture toughness and 127
 - HAZ 13–14, 67–8, 121–6, 127
 - titanium and 131–4
 - weld metal 127–8
- graphitisation 241
- hammer welding 2
- hardness
 - HAZ 129–31
 - weld metal 128
- hardness traverse 131
- heat affected zone (HAZ)
 - embrittlement of 131–4
 - fracture toughness 131–4
 - grain growth in 13–14, 62, 67–8, 121–6, 127, 173–4
 - hardness 129–31, 145
 - hydrogen cracking in 139–40
 - mechanical properties 129–34, 202–4
 - microstructure 121–6
 - softening of 202–5, 209
 - strain ageing in 124, 133
 - weld metal in 121, 124
 - width 123
- heat flow 39–49
- heat sources 7, 12–13, 31–2, 42–4
- helium shielding 9–11, 197, 208
- homogeneous linings 221
- honeycomb structure 108
- hot pressure welding 78–82
- hot tears 66
- hydrogen
 - absorption of 51–3, 136–8
 - attack 136
 - blistering 139
 - cold cracking and 135–52
 - content of weld metal 137–43
 - diffusible 137
 - diffusivity in steel 57
 - embrittlement 134–9
 - notched tensile strength and 136
 - porosity 55–6, 198–9, 208–9, 212–13, 219
 - reactions in liquid metal 51–3, 111–12, 208–9
 - total 137
 - traps 58, 136, 137
 - water content of flux and 141–4
- hydrogen-controlled electrodes 140–4
- impact properties
 - HAZ 133
 - weld metal 128
- implant test 148–9
- instabilities
 - flute 26–9
 - kink 26–9
 - pinch 22–6
- intergranular
 - corrosion 187–190
 - fracture 64–6, 139, 154, 157, 183, 184, 186
 - precipitation 174, 180–2, 213, 214
- intragranular precipitation 186–7
- ionisation potential 33
- iron–carbon constitution diagram 116, 118
- joint clearance 95
- lamellar tearing 155–6
- laser welding 11, 12
- lead
 - homogeneous linings of 221
 - in solder 96
 - welding 221
 - wetting of steel 94
- Lehigh slit groove test 147–8
- liquation
 - cracking 124, 147, 183, 199, 202
 - in HAZ 124, 202
 - of brazing solders 95
- lithium 222
- low-hydrogen consumables 140–4
- magnesium 205–7
- manganese
 - as deoxidant 112

- cracking and 116–118
- slag–metal reactions 112–16
- manganese/sulphur ratio in
 - austenitic Cr–Ni steel 183
 - carbon steel 117
- martensite
 - carbon content and 131
 - hydrogen cracking and 145
 - in carbon steel welds 120–2, 124–5, 131–2, 133
 - in carbon–manganese steel 163
 - in cast iron 161
 - in ferritic alloy steel welds 166, 170, 173, 176
 - in high-alloy steel welds 195–6
- mass flow
 - electrode to workpiece 21–9
 - general 20–1
 - in the arc column 37–9
 - in the weld pool 29–31
- metal inert gas (MIG) welding
 - see gas metal arc welding (GMA)
- metal transfer in arc welding
 - dip transfer 15, 22
 - modes 21
 - short-arc 22
 - short-circuiting 15
- molybdenum
 - in austenitic Cr–Ni steels 179, 184, 192, 193
 - in ferritic steels 165, 167, 168–9, 170–7
 - welding of 216, 220
- moisture content of flux, control of 140–2
- monel 212–16
- nickel
 - fracture toughness of welds and 129, 133
 - solidification cracking of steel and 117
 - welding of 211–16
- nil-ductility temperature 64, 200
- niobium
 - as carbide stabiliser 181
 - as grain refiner 132, 165
 - in steel 166–70, 174–5
 - reheat cracking and 185–7
 - structure of HAZ and 132–3
- nitrogen
 - as shielding gas 53, 207
 - content of steel 163
 - embrittlement by 14, 163
 - porosity 55, 112
 - reaction with liquid metals 14, 55
- notch-ductility
 - HAZ 131–4
 - weld metal 128
- notched tensile test 136–7, 145
- OFHC copper 209–10
- orbital welding 167
- overlay weld cladding 193–4
- oxyacetylene welding 9, 197, 207
- oxygen
 - content of weld metal 111–14, 216–18
 - effect on microstructure 121
 - embrittlement by 216–18
 - porosity in silver 222
 - potential 99
 - reaction with liquid metals 53–5, 110–12
- parent metal 6
- partial penetration weld 16
- peritectic reaction 116–17
- phosphorus
 - as deoxidant 208
 - embrittlement 98
 - solidification cracking 117
 - subsolidus cracking 70
- plasma jet 37–9
- plastic instability 74
- plastic tent 217
- platinum metals 222
- polar bonding 88
- porosity
 - aluminium 198–9
 - copper 208–9
 - general 51–6, 110–12
 - hydrogen 52–3, 112, 198–9
 - nickel 212–13
 - nucleation 55
 - reactive metals 219
 - steel 110–12
 - strength and 199
 - tunnelling 199, 208
- positional welding 17
- post welding heat treatment (PWHT)
 - cast iron 161–2
 - dissimilar metal joints 194
 - embrittlement by 129, 134, 165
 - fracture toughness and 129, 133–4
 - nickel alloy steels 172
 - normalising 164
 - reheat cracking and 156–60, 172
- precipitation hardening
 - aluminium 203–4
 - carbon steel 165, 170
 - nickel welds 213
 - stainless steels 196
- preheat
 - carbon steel 163
 - cast iron 161
 - copper 207
 - cooling rate and 146
 - heat flow and 45
 - hydrogen cracking and 151–2
 - lamellar tearing and 156
 - microstructure and 126
- rail steel 164

- redox process 108
- reheat cracking 156–60
- reinforcing bar 164
- reliability 224–5
- residence time 47–9, 68
- residual stress 70–2
- resistance welding
 - aluminium 198
 - copper alloys 207
 - nickel alloys 216
 - processes 11, 80
 - reactive metals 218, 219, 220
- restraint
 - hydrogen cracking and 143–4
 - intensity factor 151
 - RRC test 149–51
- roll bonding 82
- RPI test 149–50
- Schaeffler diagram 180
- secondary hardening 134, 165
- sigma phase 180
- silicon
 - as deoxidant 112
 - cracking and 183–4
 - slag–metal reactions 112–16
- silicon bronze 211
- silver 222
- single-pass welds 13
- slag–metal reactions 112–16
- soldering 1, 93–7
- solders 91, 95, 96, 197
- solid phase welding
 - aluminium 81, 198
 - copper 81
 - dissimilar metals 81
 - iron and steel 1–2, 80–1
 - nickel 80
 - processes 2, 6–7, 74–86
- solidification
 - modes 59–61
 - parameter 59
 - structure 61–3
- steam reaction 208
- steel, austenitic Cr–Ni
 - brazing 102, 191
 - carbide precipitation in 180–2, 188, 190
 - constitution 178–9
 - corrosion of welds in 191–2
 - grades 192
 - hardenable 195–6
 - heat-resisting 194–5
 - soldering 97
 - solidification cracking 182–4
 - stabilisation 187–90
 - stress-corrosion cracking 190–1, 238–9, 240
 - subsolidus cracking 185–7
- steel, ferritic
 - acicular ferrite 166
 - aluminium-treated 122, 123, 132, 163–4
 - balanced 163
 - Bessemer 163
 - carbon–manganese 163–4
 - corrosion-resistant 172–7
 - electric furnace 163
 - ferritic stainless 173–7
 - heat resistant 172–3
 - HSLA 164–7
 - killed 163
 - line pipe 165–7
 - low-alloy 167–73
 - low-temperature (cryogenic) 172
 - maraging 170
 - microalloyed 164–7
 - normalised and tempered 167, 170
 - open–hearth 163
 - oxygen converter 163
 - pearlite–reduced 166
 - quenched and tempered 170
 - reinforcing bar 164
 - rail 164
 - running 163
 - semi-killed 163
 - strain ageing 124, 133, 134
 - strain energy release rate 230–2
 - stress concentration factor 134
 - stress-corrosion cracking 90–1, 238–9, 240
 - stress intensity factor 228–33
 - stress relief heat treatment 72
 - studding 162–3
 - submerged arc welding (SAW)
 - chevron cracking in 152–4
 - cooling rate 45–9
 - flow in weld pool 30–1
 - flux
 - basicity 114, 152–4
 - moisture in 140–2
 - reactions 114–16
 - types 115
 - gas content of weld metal 114
 - grain size 128
 - mechanical properties 127
 - metal transfer 21
 - process 8
 - residual stress 71–2
 - sulphur, effect on
 - hardenability of steel 138
 - hydrogen embrittlement and cracking 138, 150–1
 - lamellar tearing 155–6
 - line pipe steel 165
 - liquation cracking 170
 - nickel 211–12
 - solidification cracking 64, 65, 116–17
 - upper shelf Charpy level 165
 - weldability of cast iron 160
 - surface energy
 - bonding and 88–91

fracture of adhesive joints and 92–3
 surface tension 89, 90

tantalum 217

tensile strength

adhesive joints 88, 104
 alloy steel, notched 136, 137
 aluminium welds 202–4
 brazed and soldered joints 88, 95–6,
 97–8

carbon steel welds 127, 129–31

copper welds 208–9

ferritic alloy steel welds 129

high-alloy steel 195–6

nickel welds 213

reactive metal welds 219–20

solid-phase welds 76–7

thermal cycle 19, 41–9

thermal cycle, effect on

contraction and residual stress 70–3

embrittlement in HAZ 68–70

gas–metal reactions 51–8

grain size 13–14, 62, 68

weld cracking 63–7

weld pool solidification 59–63

thermal severity number 147

thermit welding

austenitic Cr–Ni steel 193

copper 210

process 11

rails 164

tin

deposition from flux 94

in solder 94, 96

tin bronze 207

titanium

as carbide stabiliser 174

as deoxidant 112, 180–2

as grain refiner 62

in microalloyed steel 164–6

welding of 216–20

toe crack 140

tough pitch copper 209–10

transformation products, steel 119

transition, brittle–ductile

curve 128

in reactive metals 218–19

temperature 127

tungsten

as cathode material 34

embrittlement 218

welding 218–19

tunnelling 199, 208

ultrasonic welding 76, 83

underbead crack 140

uniformity of weld metal 58–9

Van der Waal's forces 75, 88, 103

vibratory stress relief 73

Weibull chart 224–5

weld decay

austenitic Cr–Ni steels 187–90

nickel-base alloys 213–15

weld pool

heat flow 41

mass flow 29–31

solidification 59–64

temperature 41

wetting

angle 66

brazing and soldering in 89

solid by liquid 90–1

solidification cracking and 64–5

zinc 221

zirconium

as deoxidant 70, 112

cracking of austenitic Cr–Ni welds and
 183–4

welding 216–20